Woodhead Publishing Series in Civil and Structural Engineering

Rehabilitation of Pipelines Using Fiber-reinforced Polymer (FRP) Composites

Edited by Vistasp M. Karbhari

WP
WOODHEAD PUBLISHING

Rehabilitation of Pipelines Using Fiber-reinforced Polymer (FRP) Composites

Related titles

Structural health monitoring of civil infrastructure systems

(ISBN 978-1-84569-392-3)

Strengthening and rehabilitation of civil infrastructures using fibre-reinforced polymer (FRP) composites

(ISBN 978-1-84569-448-7)

Rehabilitation of metallic infrastructure using fibre reinforced polymer composites

(ISBN 978-0-85709-653-1)

Woodhead Publishing Series in Civil and Structural Engineering: Number 52

Rehabilitation of Pipelines Using Fiber-reinforced Polymer (FRP) Composites

Edited by

Vistasp M. Karbhari

AMSTERDAM • BOSTON • CAMBRIDGE • HEIDELBERG
LONDON • NEW YORK • OXFORD • PARIS • SAN DIEGO
SAN FRANCISCO • SINGAPORE • SYDNEY • TOKYO
Woodhead Publishing is an imprint of Elsevier

Woodhead Publishing is an imprint of Elsevier
80 High Street, Sawston, Cambridge, CB22 3HJ, UK
225 Wyman Street, Waltham, MA 02451, USA
Langford Lane, Kidlington, OX5 1GB, UK

British Library Cataloguing-in-Publication Data
A catalogue record for this book is available from the British Library

Library of Congress Control Number: 2015932739

ISBN: 978-0-85709-684-5 (print)
ISBN: 978-0-85709-692-0 (online)

Contents

List of contributors

S. Banerjee University of Southern Queensland, Toowoomba, QLD, Australia

W.A. Bruce Det Norske Veritas (USA), Inc., Dublin, OH, USA

P.H. Chan University of Nottingham, Semenyih, Malaysia

L. Deaton Neptune Research, Inc., Lake Park, FL, USA

L.P. Djukic Advanced Composite Structures Australia Pty Ltd, Port Melbourne, VIC, Australia; Cooperative Research Centre for Advanced Composite Structures Ltd, Port Melbourne, VIC, Australia

M. Ehsani QuakeWrap, Inc., Tucson, AZ, USA

H. Estrada University of the Pacific, Stockton, CA, USA

A.G. Gibson Newcastle University, Newcastle-upon-Tyne, UK

M. Johnson University of Nottingham, Nottingham, UK

W. Karunasena University of Southern Queensland, Toowoomba, QLD, Australia

C.C. Lam University of Macau, Macau, China

L.S. Lee University of the Pacific, Stockton, CA, USA

K.H. Leong PETRONAS Research, Kajang, Selangor, Malaysia

D.S. Lesmana Country Manager and Representatives (Indonesia), Clock Spring Company L.P., Houston, TX, USA

S. Li University of Nottingham, Nottingham, UK

A.C. Manalo University of Southern Queensland, Toowoomba, QLD, Australia; Cooperative Research Centre for Advanced Composite Structures, Port Melbourne, VIC, Australia

L. McGarva Cooperative Research Centre for Advanced Composite Structures, Port Melbourne, VIC, Australia; Advanced Composite Structures Australia Pty Ltd, Port Melbourne, VIC, Australia

R.P. Ojdrovic Simpson Gumpertz & Heger, Waltham, MA, USA

A.B. Pridmore Structural Technologies, Columbia, MD, USA

H.R. Ronagh The University of Queensland, Brisbane, QLD, Australia

N. Saeed The University of Queensland, Brisbane, QLD, Australia; Cooperative Research Centre for Advanced Composite Structures, Port Melbourne, VIC, Australia

C.S. Sirimanna University of Southern Queensland, Toowoomba, QLD, Australia; Cooperative Research Centre for Advanced Composite Structures, Port Melbourne, VIC, Australia

W.S. Sum PETRONAS Research, Kajang, Selangor, Malaysia

K.Y. Tshai University of Nottingham, Semenyih, Malaysia

A.S. Virk Griffith University, Gold Coast, QLD, Australia

Woodhead Publishing Series in Civil and Structural Engineering

1 **Finite element techniques in structural mechanics**
C. T. F. Ross
2 **Finite element programs in structural engineering and continuum mechanics**
C. T. F. Ross
3 **Macro-engineering**
F. P. Davidson, E. G. Frankl and C. L. Meador
4 **Macro-engineering and the earth**
U. W. Kitzinger and E. G. Frankel
5 **Strengthening of reinforced concrete structures**
Edited by L. C. Hollaway and M. Leeming
6 **Analysis of engineering structures**
B. Bedenik and C. B. Besant
7 **Mechanics of solids**
C. T. F. Ross
8 **Plasticity for engineers**
C. R. Calladine
9 **Elastic beams and frames**
J. D. Renton
10 **Introduction to structures**
W. R. Spillers
11 **Applied elasticity**
J. D. Renton
12 **Durability of engineering structures**
J. Bijen
13 **Advanced polymer composites for structural applications in construction**
Edited by L. C. Hollaway
14 **Corrosion in reinforced concrete structures**
Edited by H. Böhni
15 **The deformation and processing of structural materials**
Edited by Z. X. Guo
16 **Inspection and monitoring techniques for bridges and civil structures**
Edited by G. Fu
17 **Advanced civil infrastructure materials**
Edited by H. Wu
18 **Analysis and design of plated structures Volume 1: Stability**
Edited by E. Shanmugam and C. M. Wang

19 **Analysis and design of plated structures Volume 2: Dynamics**
Edited by E. Shanmugam and C. M. Wang
20 **Multiscale materials modelling**
Edited by Z. X. Guo
21 **Durability of concrete and cement composites**
Edited by C. L. Page and M. M. Page
22 **Durability of composites for civil structural applications**
Edited by V. M. Karbhari
23 **Design and optimization of metal structures**
J. Farkas and K. Jarmai
24 **Developments in the formulation and reinforcement of concrete**
Edited by S. Mindess
25 **Strengthening and rehabilitation of civil infrastructures using fibre-reinforced polymer (FRP) composites**
Edited by L. C. Hollaway and J. C. Teng
26 **Condition assessment of aged structures**
Edited by J. K. Paik and R. M. Melchers
27 **Sustainability of construction materials**
J. Khatib
28 **Structural dynamics of earthquake engineering**
S. Rajasekaran
29 **Geopolymers: Structures, processing, properties and industrial applications**
Edited by J. L. Provis and J. S. J. van Deventer
30 **Structural health monitoring of civil infrastructure systems**
Edited by V. M. Karbhari and F. Ansari
31 **Architectural glass to resist seismic and extreme climatic events**
Edited by R. A. Behr
32 **Failure, distress and repair of concrete structures**
Edited by N. Delatte
33 **Blast protection of civil infrastructures and vehicles using composites**
Edited by N. Uddin
34 **Non-destructive evaluation of reinforced concrete structures Volume 1: Deterioration processes**
Edited by C. Maierhofer, H.-W. Reinhardt and G. Dobmann
35 **Non-destructive evaluation of reinforced concrete structures Volume 2: Non-destructive testing methods**
Edited by C. Maierhofer, H.-W. Reinhardt and G. Dobmann
36 **Service life estimation and extension of civil engineering structures**
Edited by V. M. Karbhari and L. S. Lee
37 **Building decorative materials**
Edited by Y. Li and S. Ren
38 **Building materials in civil engineering**
Edited by H. Zhang
39 **Polymer modified bitumen**
Edited by T. McNally
40 **Understanding the rheology of concrete**
Edited by N. Roussel

41 **Toxicity of building materials**
Edited by F. Pacheco-Torgal, S. Jalali and A. Fucic
42 **Eco-efficient concrete**
Edited by F. Pacheco-Torgal, S. Jalali, J. Labrincha and V. M. John
43 **Nanotechnology in eco-efficient construction**
Edited by F. Pacheco-Torgal, M. V. Diamanti, A. Nazari and C. Goran-Granqvist
44 **Handbook of seismic risk analysis and management of civil infrastructure systems**
Edited by F. Tesfamariam and K. Goda
45 **Developments in fiber-reinforced polymer (FRP) composites for civil engineering**
Edited by N. Uddin
46 **Advanced fibre-reinforced polymer (FRP) composites for structural applications**
Edited by J. Bai
47 **Handbook of recycled concrete and demolition waste**
Edited by F. Pacheco-Torgal, V. W. Y. Tam, J. A. Labrincha, Y. Ding and J. de Brito
48 **Understanding the tensile properties of concrete**
Edited by J. Weerheijm
49 **Eco-efficient construction and building materials: Life cycle assessment (LCA), eco-labelling and case studies**
Edited by F. Pacheco-Torgal, L. F. Cabeza, J. Labrincha and A. de Magalhães
50 **Advanced composites in bridge construction and repair**
Edited by Y. J. Kim
51 **Rehabilitation of metallic civil infrastructure using fiber-reinforced polymer (FRP) composites**
Edited by V. Karbhari
52 **Rehabilitation of pipelines using fiber-reinforced polymer (FRP) composites**
Edited by V. Karbhari
53 **Transport properties of concrete: Measurement and applications**
P. A. Claisse
54 **Handbook of alkali-activated cements, mortars and concretes**
F. Pacheco-Torgal, J. A. Labrincha, C. Leonelli, A. Palomo and P. Chindaprasirt
55 **Eco-efficient masonry bricks and blocks: Design, properties and durability**
F. Pacheco-Torgal, P.B. Lourenço, J. A. Labrincha, S. Kumar and P. Chindaprasirt
56 **Advances in asphalt materials: Road and pavement construction**
Edited by Shin-Che Huang and Hervé Di Benedetto
57 **Acoustic Emission (AE) and Related Non-destructive Evaluation (NDE) Techniques in the Fracture Mechanics of Concrete: Fundamentals and Applications**
Edited by Masayasu Ohtsu

This page intentionally left blank

Types of pipe repaired with composites: water supply and sewage pipelines

1

A.B. Pridmore[1], R.P. Ojdrovic[2]
[1]Structural Technologies, Columbia, MD, USA; [2]Simpson Gumpertz & Heger, Waltham, MA, USA

1.1 Introduction

It is well documented that the water and sewage pipeline infrastructure in the US is aging and deteriorating at a rapid rate. The latest ASCE report card (ASCE, 2013) states the following regarding drinking water and wastewater infrastructure:

> ***Drinking water****: The grade for drinking water improved slightly to a D. At the dawn of the 21st century, much of our drinking water infrastructure is nearing the end of its useful life. There are an estimated 240,000 water main breaks per year in the United States. Assuming every pipe would need to be replaced, the cost over the coming decades could reach more than $1 trillion, according to the American Water Works Association (AWWA). The quality of drinking water in the United States remains universally high, however. Even though pipes and mains are frequently more than 100 years old and in need of replacement, outbreaks of disease attributable to drinking water are rare.*

> ***Wastewater****: The grade for wastewater improved slightly to a D. Capital investment needs for the nation's wastewater and stormwater systems are estimated to total $298 billion over the next 20 years. Pipes represent the largest capital need, comprising three quarters of total needs. Fixing and expanding the pipes will address sanitary sewer overflows, combined sewer overflows, and other pipe-related issues. In recent years, capital needs for the treatment plants comprise about 15–20% of total needs, but will likely increase due to new regulatory requirements. Stormwater needs, while growing, are still small compared with sanitary pipes and treatment plants. Since 2007, the federal government has required cities to invest more than $15 billion in new pipes, plants, and equipment to eliminate combined sewer overflows.*

As supported by the "D" grades given to both sets of pipeline infrastructure, hardly a day goes by without a newsworthy pipe rupture somewhere in the US. While most of these ruptures occur in small-diameter pipelines, large-diameter water or sewer main breaks are increasingly more common occurrences, leaving a sinkhole in the ground (Figure 1.1), causing millions of dollars in damage and in extreme cases significant risk of human injuries.

Rehabilitation of Pipelines Using Fiber-reinforced Polymer (FRP) Composites. http://dx.doi.org/10.1016/B978-0-85709-684-5.00001-1

Figure 1.1 Large-diameter water main break.

Pipeline systems are comprised of short pieces, which typically range from 8 to 30 ft (244−914 cm), depending on the pipe type, joined to form a continuous conduit. Large-diameter pressure pipelines, 24 in. (60 cm) or more, are typically made of cast and ductile iron, steel, reinforced concrete, and prestressed concrete. In many cases, these pipes are now between 50 and 100 years old. In the past several decades, utility agencies nationwide have been developing and implementing pipeline asset management programs with increased intensity.

Over the last decade, as part of these asset management programs, water and sewage pipeline owners have began widespread use of fiber-reinforced polymer (FRP) composites, particularly carbon fiber-reinforced polymer composites (CFRP), as valuable tools for pipeline rehabilitation and repair. There is a wide range of rehabilitation options available for gravity-fed sewer mains; however, there are a limited number of solutions available for pressurized water mains or sewer force mains. For sewer force mains, over 50% of the pipeline inventory is comprised of prestressed concrete cylinder pipes (PCCP) or concrete cylinder pipes (WERF, 2009) which lend themselves particularly well to FRP repairs. For this reason, FRP composites are used primarily for repair of pressurized water mains or sewer force mains. Because the use of FRP composites for pipelines involves manual application of the materials, this technology is primarily applicable for targeted internal repair and strengthening of 36 in. (91 cm) and larger buried pipelines which allow for entry into the pipeline. External strengthening of pipelines using FRP has primarily been utilized for above-ground water and wastewater pipelines which cannot be taken out of service.

1.2 Pipeline asset management

The primary goal of an asset management program is to maintain a desired reliability of the pipelines at an acceptable cost. As discussed earlier in Section 1.1, pipe rupture has potentially severe life safety, property damage and water loss consequences at the failure site, and service interruption consequences downstream. The cost of a pipe

rupture can vary greatly depending on location and collateral damage and is typically in the range of hundreds of thousands to millions of dollars. For large-diameter pipelines, where the consequences of failure is higher, the most cost-effective approach to maintaining pipeline reliability is to identify and repair individual distressed pipes, or pipe segments, before a rupture occurs.

Most major urban utilities typically have several large-diameter pipelines of different ages, installed in soils of varying corrosivity, operated and pressurized to different levels, possibly overloaded and deteriorated to unknown levels. Many of the records about the pipelines in major urban areas are either difficult to find or lost over the years, and are often not readily available. Proactive utilities are beginning to compile the data and create databases with basic pipeline information, for example, age, material, pipeline plan and profile drawings, etc., and potential consequences of pipe failure at various locations in the system.

1.2.1 Pipeline criticality and inspection priority

Condition assessment of all pipelines in a system may take years because of operational constraints, logistical issues, and cost. It is therefore important to determine priority, sequence, and long-term schedules for pipeline inspection. These decisions are usually driven by potential consequences of failure and perceived pipeline condition based on the history of performance and other pipeline risk factors. There are two important components in determining the risk associated with a pipeline and therefore the pipeline criticality and inspection priority: (1) the likelihood of pipe failure and (2) the consequence of failure, should it occur on a given pipeline (Zarghamee et al., 2012).

Determining the likelihood of pipe failure involves understanding pipe failure modes and mechanisms of deterioration and performing the necessary structural analysis to calculate the probability of failure of individual pipe pieces under current conditions. These design conditions include the working pressures, pipe and water weight, soil load, and live loads. In addition, soil corrosivity analysis through a conductivity survey, chemical analysis, and testing of soil can identify potentially more corrosive areas in the system.

Establishing the consequences of failure for a given pipeline involves understanding the level of redundancy in a pipeline, the surrounding environment, and how pipeline customers and surrounding environments may be impacted by a pipe rupture. For example, pipelines which run adjacent to or under a school or busy roadway have a higher consequence of failure than a pipeline running through an open field in a rural area. Certain pipelines also have no redundancy, so a single pipe which services a hospital or a power plant's circulating water line could cause significant consequences if the pipe abruptly ceases to function.

1.2.2 Inspection and condition assessment

Pipeline inspection tools depend on the type of pipe and the level of details which the owner chooses to budget for during the inspection. One of the most cost-effective

methods for large-diameter pipelines which can be taken out of service is a visual and sounding inspection by a professional experienced with pipeline degradation mechanisms. A proper visual and sounding inspection can identify segments with severe distress, damaged pipe joints, areas with severe pipe ovality, or concrete spalling. For metallic pipes that are more likely to degrade gradually through corrosion and pitting resulting in wall thinning, pinholes, and leaks, leak detection technologies provide a relatively cost-effective approach to pinpointing distress zones. Leak detection tools which are inserted into the pipeline and allowed to travel along the length of the pipeline can also be used for detecting gas pockets in sewer force mains, which often lead to localized degradation of the pipeline in regions near these gas pockets. More in-depth inspection methods for metallic pipelines involve measurement of the wall thickness of the pipe by either capturing average wall thickness data over the length between inspection points or using an array of sensors that can capture more localized thickness information.

The state-of-the-art inspection tools for PCCP use the electromagnetic Remote Field Eddy Current/Transformer Coupling method for detecting broken prestressing wires and acoustic methods for detecting leaks and wire breakage (Zarghamee et al., 2012). The most important feature of these nondestructive methods is their ability to identify individual deteriorated pipe pieces, thus enabling utilities to evaluate the risk of failure and prioritize repairs of individual pipe spool pieces. Historical data indicate that on the average only about 3−4% of PCCP have broken prestressing wires (Higgins et al., 2012), and only a small fraction of pipes with broken wires may be at a high risk of failure and require repairs within the next 5 years. The cost savings of a pipeline inspection program combined with risk analysis and repair of individual pipe pieces to maintain the overall pipeline reliability are significant as compared with repair or replacement of entire pipeline systems.

1.2.3 Failure risk and repair priority for pipelines

PCCP has been manufactured and installed since the early 1940s. PCCP is designed to resist circumferential bending moments and thrusts resulting from prestress, internal pressure, pipe and fluid weights, and earth load. Design requirements are based on serviceability, elastic, and strength limit states for concrete core, mortar coating, steel cylinder, and prestressing wires specified in AWWA C304 Standard. Over time, prestressing wires may corrode and break and the concrete core may lose prestress. The loss of prestress in the pipe wall leads to cracking of the concrete core and mortar coating, mortar coating delamination, accelerated corrosion, and breakage of prestressing wires, corrosion and/or yielding of the steel cylinder, and ultimately pipe rupture. A pressure pipe will typically rupture when a finite number of prestressing wires is broken along the pipe length. Individual distressed pipe pieces with broken wires may be identified through an internal inspection, such as visual inspection, sounding, electromagnetic inspection, or others. Repairs of pipes may be prioritized based on the risk of failure of pipe calculated for the extent of prestress loss, maximum internal pressure, and pipe design and installation condition. A sample risk analysis (Figure 1.2) shows serviceability, structural

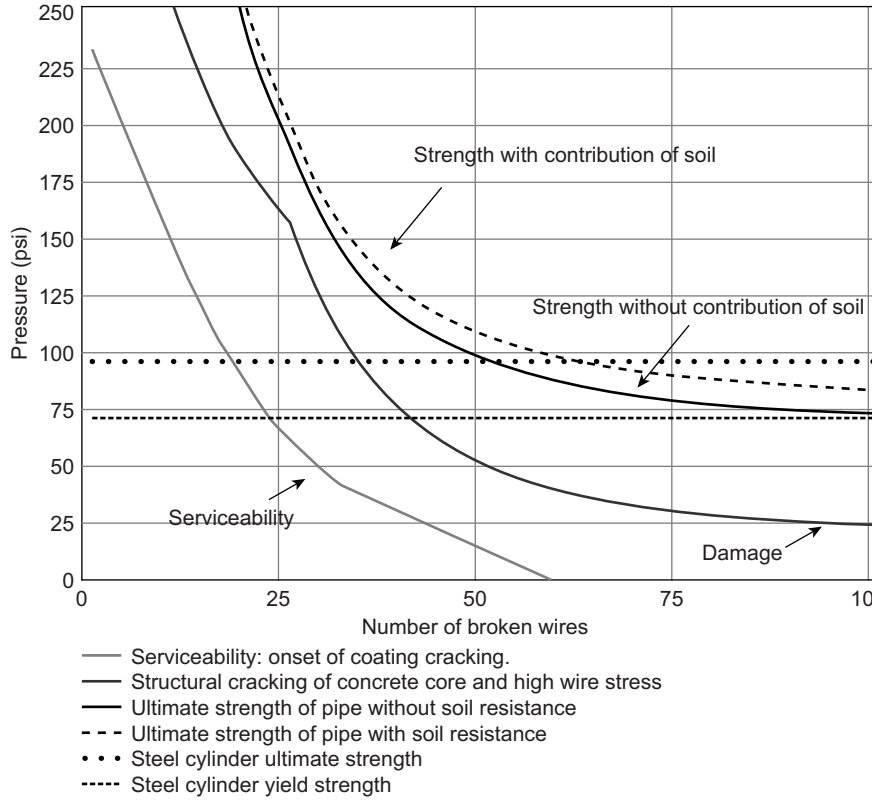

Figure 1.2 Example of risk curve for a specific ECP type PCCP design (Zarghamee et al., 2012).

damage, and strength limit states used to assess the risk of failure of a pipe with broken prestressing wires and to recommend time interval to repair individual pipes with broken wires.

Risk curves and models for likelihood of failure can also be developed to address other types of pipe, such as steel, ductile iron, fiberglass, etc., utilizing relevant structural performance data such as remaining pipe wall thickness or other structural parameters. Prioritization of repairs involves reassessing the risk associated with a pipeline caused by the likelihood and consequence of failure, as described above.

1.3 Rehabilitation options for large-diameter pipelines

After a condition assessment has been performed and regions of a large-diameter pressure pipeline are identified for structural rehabilitation, there are several different methods available for pipeline rehabilitation. For pipelines with sufficient redundancy and easy access for excavation, removal and replacement of distressed sections of pipeline is an effective approach. Individual distressed pipes may be externally

repaired by post-tensioning or installation of steel couplings or sleeves. If longer stretches of the large-diameter pressure pipeline need to be rehabilitated, one alternative repair method is steel slip lining. Steel slip lining involves excavation of a localized region of the pipeline and removal of a section of pipe to allow for a smaller diameter steel pipe to be inserted in the host pipe. The pipe sections are welded together in place and inserted from the access pit in one or both directions away from the access pit. The annular space between the steel pipe and the host pipe is grouted and mortar lining or other types of corrosion protection are applied on the interior of the steel slip line. Because steel slip lining typically reduces the internal diameter of the pipeline by approximately 6 in. (15 cm) and has difficulty navigating through bends in a pipeline, this process is most appropriate for longer straight runs of pipe where the original pipe is oversized for its intended use.

Many large-diameter pipelines owned by public utilities, power generation facilities, and industrial sites are located in areas where any excavation is challenging or undesirable. For these types of limited access pipes, and especially in cases where targeted repairs of distressed pipes are to take place, the use of carbon fiber-reinforced polymer (CFRP) lining becomes the most cost-effective and efficient repair or upgrade solution.

1.3.1 CFRP liner construction

Prior to finalizing CFRP as the selected repair option, an extensive technical effort is undertaken to confirm applicability and constructability. Upon selection of CFRP as the desired repair method, and approval of the technical submittal, the installation crew mobilizes to the jobsite to begin installation. An intensive preplanning process, including safety protocol, has already taken place prior to mobilization.

The application of a CFRP lining system to a pipeline is a bond critical application, so the surface of the pipeline must be prepared sufficiently to ensure proper adhesion. Concrete surfaces are profiled using abrasive or water blasting to a minimum International Concrete Repair Institute (ICRI) concrete surface preparation CSP 3, as shown in Figure 1.3, whereas a metallic surface will be prepared using abrasive blasting to a near white metal surface profile. Surface contaminants (laitance, carbonated and weak concrete, cracked and spalled concrete) are removed and the substrate is repaired as necessary. The work requires the pipe surface to be thoroughly cleaned, dried, and dehumidified.

CFRP liners are applied to the inside of the pipe in layers, with the specific number of sheets of unidirectional carbon fiber fabric in the longitudinal and circumferential directions designed on a per-pipe basis to meet the design requirements. The carbon fiber fabric is impregnated with a two-part epoxy resin system outside of the pipeline and is then carried through the pipeline and applied to the interior of the pipe by hand lay-up. Since the fabric is flexible prior to curing, all materials can be passed through the existing manhole access as part of the fully trenchless method. The end product (Figure 1.4) is a low-profile liner adhered to the inside of the pipe, typically $^{3}/_{4}$ in. (1.9 cm) thick or less. The material is flexible and customizable designs are created for bends and fittings. The liner is top coated with the appropriate material, given

Figure 1.3 Prepared surface on inside of pipeline.
Photo credit: Mr Hector Posada from Tucson.

Figure 1.4 Completed CFRP liner.
Courtesy of Mr Hector Posada of Tucson Water.

environmental exposure, and the final surface is smooth and corrosion resistant. Constituent system components include the following:

Primer*: The concrete substrate is primed with an epoxy material, which penetrates the pore structure of the substrate. The primer is a 100% solid, low-viscosity epoxy material. Primers are specifically designed for moist concrete surface application.*

Fibers*: High strength unidirectional carbon fiber fabrics provide structural integrity. Glass fiber fabrics are utilized in direct contact with any metallic substrate to serve as a dielectric barrier between any carbon fiber layers and the metallic substrate.*

***Saturating epoxy**: The carbon fibers are bonded to the pipe substrate and encapsulated in a 100% solid, low-viscosity epoxy material.*

***Protective coating**: The FRP system is top coated with a protective coating layer.*

CFRP liners are typically applied as proprietary systems consisting of all associated fiber reinforcement and polymer adhesives/epoxies. For potable water applications, all the polymer adhesives/epoxies need to be certified by NSF International (ANSI/NSF 61).

One additional note on construction is that all work is performed within a confined space—access, ventilation, egress, and all other OSHA regulations in confined spaces must be observed to ensure worker safety during construction.

1.4 Motivation for repairing pipes with CFRP composites

Because of the relatively high cost of the CFRP rehabilitation techniques as compared to more conventional construction methods, the use of these materials is primarily for targeted structural repairs and upgrades following pipeline condition assessment.

1.4.1 Proactive upgrade of aging pipelines

Over the past decade, municipalities throughout the US have increasingly utilized CFRP liners, and this repair option has become a part of their overall asset management programs. Several owners with significant inventory of PCCP have programs which focus on electromagnetic inspection to determine pipes with broken prestressed wires, and as these segments are identified and evaluated, CFRP upgrades are then implemented (Moncrief et al., 2001; Alkhrdaji and Thomas, 2003; Ojdrovic and LaBonte, 2008; Terrero et al., 2012; Gipsov and Pridmore, 2012; Ambroziak et al., 2012). These programs are systematized in a manner which creates an inspection cycle and rapid identification of segments designated for CFRP repair. The typical cycle includes several miles of pipe inspected at regular intervals, followed by evaluation of distress levels, if any, in each pipe segment. Typically less than 1% of the inspected pipeline(s) are repaired with CFRP liners, resulting in the cost of inspection and targeted proactive upgrades far less than systematic replacement of an entire pipeline.

For the upgrade of large-diameter pipelines, another approach involves proactive continuous repair of deteriorated segments with CFRP lining or pipeline renewal. This approach has been used by Orange County Sanitation District (OCSD) for a pressurized wastewater effluent main operating in a critical treatment plant (Hay et al., 2011). OCSD had concerns about the overall structural integrity of this pipeline and found that in the congested plant environment, a CFRP liner was the

most effective solution. For this steel pipeline the CFRP liner was designed as a stand-alone system, able to resist all loads and load combinations. As this was a steel pipeline, and because CFRP lining has the potential for electrical conductivity, a layer of glass fiber-reinforced polymer composites (GFRP) was utilized in direct contact with the metallic substrate to provide a dielectric barrier for the CFRP system. While there was redundancy in the system which allowed the pipe to be taken out of service, contingencies were in place to allow for emergency reinstatement of the line in a matter of hours if the alternate system were to lose functionality. Along with being the preferred trenchless method, no other repair scenario would have easily been able to accommodate such contingency measures.

In addition to municipal pipeline owners, power generation facilities have increasingly used a comparable approach for assessing and proactively addressing their large diameter circulating water pipeline systems (Cribb and Pridmore, 2012; Ojdrovic and LaBonte, 2008). The pipeline systems in power generation facilities typically have minimal, or no, redundancy and their rupture causes loss of revenue and significant impact to the public, should there be a high demand for power at the time of pipe failure. Several plants in the US have ongoing programs which address identified distressed pipeline segments during each plant outage. Beyond just pipes showing distress, certain power plant owners elect wholesale installation of CFRP liners across 100% of their critical pipeline infrastructure with the upgrade work performed during limited plant outages (Bologna et al., 2011).

1.4.2 Contractor initiated defects

A growing problem with underground infrastructure is the coordination of buried assets among multiple owners such as the water and sewer municipalities with oil and gas companies and power companies, who are often sharing limited underground real estate. There is often some uncertainty in the precise location of all buried infrastructure and sometimes this information has not been properly researched by contractors prior to performing work. Several recent CFRP repair projects resulted from contractor initiated defects.

During a 2013 inspection of their 48-in. PCCP water main, the city of Phoenix discovered an interior patch which had been placed on the inside of their main by a contractor, as shown in Figure 1.5. It was determined that this pipeline segment had been previously damaged during construction of adjacent utilities. Although it was patched, the pipeline segment was determined to be at risk. Given the location of this potentially distressed pipeline segment, and the targeted nature of the repair needed, a CFRP liner was selected as the appropriate method. A was installed over the damaged region, then the surface was rendered flush with the interior pipe substrate, as shown in Figure 1.6. The CFRP liner was then installed to strengthen the deteriorated pipe segment (Figure 1.7 shows installation of the initial longitudinal layer of CFRP onto the distressed pipeline).

Another recent example took place in a midwestern US city where a horizontal directional driller punctured a 48 in. pipe segment (Bueno, 2012; Bass et al., 2012). The horizontal directional drilling (HDD) mishap created a 4 in. circular hole in a

Figure 1.5 Corrosion of steel cylinder.
Courtesy of Mr Michael Ambroziak of CPM.

Figure 1.6 Rendered surface.
Courtesy of Mr Michael Ambroziak of CPM.

critical pressure pipeline. To complicate matters further, the pipe segment was located next to a creek and bridge structure, in an environmentally sensitive area. The local utility explored several options, but due to the factors listed above, a CFRP liner was the only viable option. Other options would have required rerouting or damming of the creek water and potential disruption to traffic patterns in the area. In this case, the CFRP liner was installed in a single-pipe segment on a 60° vertical slope.

In both of the cases above, where contractor initiated defects occurred, the defect area was first repaired using patch and weld methods, followed by installation of a stand-alone CFRP liner. The CFRP pipeline upgrade was designed to resist all internal pressure and external loads, among various other criteria.

Figure 1.7 Internal application of CFRP.
Courtesy of Mr Michael Ambroziak of CPM.

1.4.3 Longitudinal distress in the pipeline

One unique application for CFRP liners which has become more prevalent in the past several years is the correction and reinforcement of specific pipe segments found to have inadequate thrust restraint. This condition has been identified during the inspection and evaluation of leaks occurring at bend areas as well as through analysis of existing pipelines installed prior to code changes addressing thrust design (Zarghamee et al., 2004; Shumaker, 2012; Hutson et al., 2012).

North Texas Municipal Water District performed an evaluation on a 72-in. pipeline and found over 20 segments at bend areas which were determined to be insufficiently designed to handle the required forces at these bends (Hutson et al., 2012). The original pipeline design, to code at the time, was not up to current code, which takes into account more load scenarios. The current code pays particular attention to thrust loading. Several of the 20 segments were addressed externally using conventional construction methods, as they were in easily accessible areas. The remaining segments, with more challenging access issues, were addressed using a CFRP liner. The CFRP system was designed as a composite system which interacted with the host pipe to withstand all loading, including thrust, thereby extending the life of the affected pipeline segments.

Tucson Water has had an active asset management program in place for many years, as they have several large-diameter PCCP mains within their pipeline inventory. Tucson regularly utilizes the electromagnetic inspection tools described above and is able to identify pipeline areas, or segments, for precision repairs. During a recent inspection of a designated pipeline system, an 84-in. water main, a leak was discovered at a joint located at a horizontal bend in the pipe. The location and nature of this leak indicated that longitudinal forces were the cause. Other than the joint issues, the pipeline segment inspected did not display any other distress symptoms indicative of wire breaks (Acosta and Pridmore, 2014).

A CFRP liner was selected specifically because it could be installed rapidly, allowing the pipe to be put back in service within a very short time window. In this case, the use of CFRP was preplanned so the repair could be completed as an emergency. The planning, notifications, and construction window for the replacement of the pipe segment made that option infeasible. The CFRP liner utilized to address this longitudinal weakness was designed to specifically provide primary reinforcement in the longitudinal direction.

1.4.4 External rehabilitation of pipelines with CFRP

External repair and upgrade of pipelines using CFRP has primarily been utilized for above-ground water and wastewater pipelines which cannot be taken out of service. External repairs of buried pipelines with CFRP are not typical because once a pipe segment has been excavated, replacement, post-tensioning, or other external repairs are the preferred alternatives. The design and installation process for external repairs is similar to internal lining; however, construction complexities are eased due to the work not taking place in a confined space. The design process often includes taking into account support structures which are part of above-ground pipeline systems. These designs must address connection detailing and load transfer through the pipe support structure. In addition, if corrosion and/or degradation are originating at the interior portion of the pipeline, the support structure will need to be fully encapsulated with CFRP as part of the design. Another distinction of external repairs is that best practices include the use of a UV-resistant topcoat.

A recent project where external CFRP repair methods were advantageous was for an aerial sewer located in an environmentally sensitive area (Bian et al., 2011). The sewer pipeline, owned by DC Water, traversed over a creek located on US National Park property. The 46 lineal ft section was an 18-in. terra cotta sewer pipe with a 30-in. by 30-in. concrete encasement. The pipe was supported by concrete columns and footings which were also degrading. The erosion caused by the creek undermined the concrete footings such that the designed spans between supports doubled in length, placing the pipeline in jeopardy, as shown in Figure 1.8. Other rehabilitation options were considered and rejected due to the high invasiveness of construction methods using traditional repair techniques. The CFRP lining was selected specifically because of the low impact of the installation process on the surrounding environment. The design process included some unique aspects; additional reinforcement was needed

Figure 1.8 Original condition of aerial sewer crossing (Bian et al., 2011).

Figure 1.9 Aerial sewer crossing (Bian et al., 2011).

to provide flexural reinforcement to accommodate the spans between the footings, connection details were needed to tie the CFRP rehabilitation into the abutments, and a fire-resistant external finish was required to match aesthetics of the surrounding environment. The completed repair is shown in Figure 1.9.

External repair of pipelines using CFRP lining has many advantages, such as the case with DC Water, and is a viable option for all types of distressed above-ground pipelines.

1.5 Conclusions

Pipeline asset management programs may be implemented to maintain overall pipeline reliability at an acceptable level by identifying individual distressed pipe pieces or segments, determining their risk of failure, prioritizing repairs, and repairing pipes that are at a high risk of failure. The condition of a pipeline is assessed followed by targeted structural rehabilitation using carbon fiber on the deteriorated pipe segments which are difficult to address using conventional construction methods. A CFRP liner is a viable repair option, provided that repairs are designed and implemented appropriately.

Acknowledgements

The authors would like to acknowledge Mr Paul Acosta, Mr Britt Klein, and Mr Hector Posada from Tucson Water as well as Mr Michael Ambroziak from CPM and Ms. Amy Conroy from the City of Phoenix for their contributions of photos and case history insight to this chapter. The authors would also like thank Mr Mark Geraghty of Structural Technologies for his time and efforts contributed to editing this work.

References

Acosta, P., Pridmore, A.B., 2014. Tucson water's strengthening approach to address thrust restraint for PCCP. In: ASCE Pipelines Conference 2014, Portland, OR.

Alkhrdaji, T., Thomas, J., 2003. Carbon FRP strengthening of PCCP aqueducts. In: ASCE Pipelines Conference 2003, Baltimore, MD, pp. 892−901.

Ambroziak, M., Conroy, A., McDonald, B., 2012. Redeveloping Phoenix's PCCP assessment program: a pragmatic approach. In: ASCE Pipelines Conference 2012, Miami, FL, pp. 1223−1232.

ANSI/NSF 61, 2013. Drinking Water System Components−Health Effects. NSF International/ANSI. http://www.nsf.org/certified/PwsComponents/.

ASCE (American Society of Civil Engineers), 2013. Report Card for America's Infrastructure. http://www.infrastructurereportcard.org, 2013.

Bass, B.J., Ojdrovic, R.P., Haemmerle, B.M., 2012. Repair of a punctured 48 in diameter prestressed concrete cylinder pipe on a sixty degree slope. In: ASCE Pipelines Conference 2012, Miami, FL, pp. 816−826.

Bologna, G., Pridmore, A.B., Geraghty, M., Alexander, J., 2011. Power generation case study: feasibility of carbon fiber and alternate repair methods. In: ASCE Pipelines Conference, July 23−27, 2011, Seattle, WA.

Bueno, S.M., March 09, 2012. Carbon Fiber Lining Successfully Repairs Water Main in Columbus. Online. Ohio Trenchless Technology.

Bian, S., Pridmore, A.B., Loera, R., Marshall, J., 2011. Pipeline rehabilitation amidst environmentally sensitive location. In: ASCE Pipelines Conference 2011; Seattle, Washington.

Cribb, M., Pridmore, A.B., 2012. Proactive upgrade of steel pipelines during scheduled outages. In: ASCE Pipelines Annual Conference, August 21, 2012, Miami, FL.

Gipsov, M., Pridmore, A.B., 2012. WSSC's systematic approach to the CFRP liner installation process. In: ASCE Pipelines Conference 2012, Miami, FL.

Hay, J., Titus, H., Koester, P., Francis, V., French, J., Wurst, D., 2011. Assessing the condition of OCSD's 20-year old ocean outfall piping system using state of the nondestructive testing techniques. In: WEFTEC Conference 2011, Los Angeles, CA.

Higgins, H.S., Stroebele, A., Zahidi, S., 2012. Numbers don't lie, PCCP performance and deterioration based on a statistical review of a decade of condition assessment data. In: ASCE Pipelines Conference 2012, Miami, FL.

Hutson, A., Long, S., Payne, J., Zarghamee, M.S., 2012. Can it handle the pressure? Condition assessment, structural evaluation, and repair of an existing 72 inch PCCP pipeline. In: ASCE Pipelines Conference 2012, Miami, FL, pp. 1203−1213.

Moncreif, W.J., Kendall, D.R., Mulligan, S.B., Blake, R.C., Watkins, C.M., 2001. Rehabilitation of 78-inch PCCP with carbon fiber reinforced composite material. In: ASCE Pipelines Conference 2001; Reston, VA.

Ojdrovic, R.P., LaBonte, G., 2008. Inspection, failure risk analysis, and repair of cooling-water lines in one outage. In: ASCE Pipelines Conference 2008, Atlanta, GA, pp. 1−10.

Shumaker, S., 2012. Progress toward a unified thrust restraint Design—An update. In: ASCE Pipelines Conference 2012, Miami, FL, pp. 1438−1449.

Terrero, R.A., Coates, R., Aguiar, L., Pridmore, A.B., Alexander, J., 2012. Miami-Dade case study: managing and minimizing pipeline outages through the use of carbon fiber. In: ASCE Pipelines Annual Conference 2012, Miami, FL.

Water Environment Research Foundation (WERF), 2009. Guidelines for the Inspection of Force Mains (Draft). 04-CTS-6UR, Alexandria, VA.

Zarghamee, M.S., Eggers, D.W., Ojdrovic, R.P., Valentine, D.P., 2004. Thrust restraint design of concrete pressure pipe. Journal of Structural Engineering 130 (1), 95−107.

Zarghamee, M.S., Ojdrovic, R.P., Nardini, P.D., 2012. Best practices manual for prestressed concrete pipe condition assessment: What works? What doesn't? What's next? Water Research Foundation.

Abbreviations

ASCE	American Society of Civil Engineers
AWWA	American Water Works Association
CFRP	Carbon fiber-reinforced polymer
GFRP	Glass fiber-reinforced polymer
ICRI	International Concrete Repair Institute
PCCP	Prestressed concrete cylinder pipe

This page intentionally left blank

Trenchless repair of concrete pipelines using fiber-reinforced polymer composites

2

A.B. Pridmore[1], *R.P. Ojdrovic*[2]
[1]Structural Technologies, Columbia, MD, USA; [2]Simpson Gumpertz & Heger, Waltham, MA, USA

2.1 Introduction

This chapter will discuss the history of the use of fiber-reinforced polymer (FRP) composites for internal repair of concrete pipelines, with a focus on the design, materials, installation, and quality control for this trenchless pipeline repair and upgrade method.

Carbon fiber-reinforced polymer (CFRP) lining systems have been used increasingly for internal rehabilitation of water and wastewater pipelines since the mid-1990s. The primary motivation for use of CFRP linings as a rehabilitation technology is minimizing disruption to the surrounding environment, particularly for distressed pipelines with difficult access to the exterior of the pipeline.

Advancements in inspection methods, failure risk analysis, and repair prioritization for prestressed concrete cylinder pipe (PCCP) caused an increase in the demand for targeted-rehabilitation technologies by providing utility owners with critical information regarding the exact location of distressed pipes. Based on this repair prioritization information, utilities have taken proactive steps in advance of failure to replace or repair the distressed pipes with an unacceptably high risk of failure. There are several repair options for concrete pressure pipes, which include encasing the degraded pipe in a reinforced concrete block, posttensioning by wrapping tendons around the pipe, or relining the pipeline. Relining is typically performed by utilizing CFRP or by steel slip-lining.

CFRP was first used in the United States for the internal rehabilitation and strengthening of large-diameter underground PCCP in the late 1990s. Large diameter, for the purposes of establishing limitations, is defined as 24-in. (760 mm) diameter and above for CFRP repairs because personnel entry is required into the pipeline for manual application of the CFRP materials. Following these initial installations, various municipal utilities and power-generation facilities began the widespread use of CFRP lining for PCCP. By the mid-to-late 2000s, with the increase in demand driven by routine inspections, installation of CFRP inside degraded or weak PCCP had become an acceptable repair-and-strengthening system for PCCP.

Rehabilitation of Pipelines Using Fiber-reinforced Polymer (FRP) Composites. http://dx.doi.org/10.1016/B978-0-85709-684-5.00002-3

2.2 Background

2.2.1 Overview of large-diameter concrete pipe use in the United States

In the United States alone, there are more than 1.4 million miles of buried pipelines for water and wastewater municipal infrastructure (General Accounting Office, 2004). According to a recent study commissioned by the American Water Works Association (AWWA) (AWWA, 2011), approximately 25% of water mains greater than 10 in (25 cm) are made of reinforced concrete or PCCP, with over $10 billion of PCCP assets in the United States alone. CFRP linings are primarily used for targeted strengthening of large-diameter pressure pipe, pipelines greater than 24 in (760 mm), which has led to a primary focus on PCCP for use of CFRP linings.

PCCP has had a long and diverse history since its earliest application in the United States in 1942, with many changes in standards and materials over the years (Romer et al., 2008). There are two types of PCCP: (1) prestressed concrete with a lined cylinder (LCP), consisting of a steel cylinder with cast concrete core, wrapped with steel prestressing wire directly over the steel cylinder; and (2) prestressed concrete with an embedded cylinder (ECP) as shown in Figure 2.1. ECP has been constructed

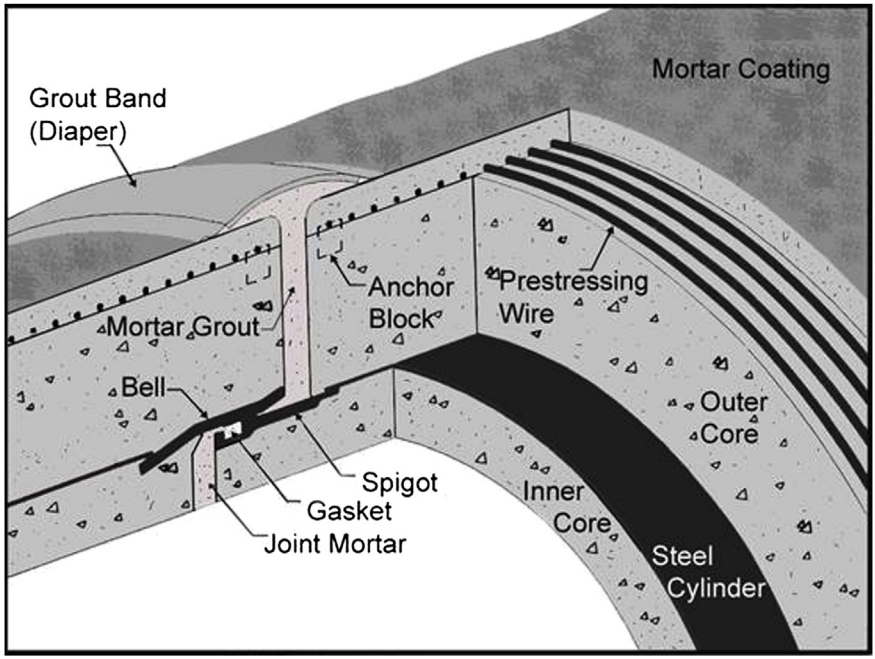

Figure 2.1 Cross-section of a prestressed concrete cylinder pipe, ECP-type Ojdrovic, 2013.

as large as 252 in. in diameter. Both types of PCCP are designed for the specific combination of internal pressure and external load in accordance with the procedures outlined in ANSI/AWWA C304, Standard for Design of Prestressed Concrete Cylinder Pipe.

The utilization of large-diameter PCCP became increasingly popular in the 1960s for municipal water supply and sewer systems as well as for circulating water systems at power plants. Like any type of pipeline system, as the use of PCCP increased, maintenance issues emerged. In addition to typical maintenance issues, there was a problematic type of wire used on certain vintages of PCCP in the 1970s time frame (Romer et al., 2008). In the early 1990s, a group of municipalities that owned PCCP began collaborating and sharing best practices on how to inspect and repair their PCCP water mains. This group, referred to informally as PCCP Users Group, began holding meetings on a regular basis. The results of this group's efforts led to a heightened focus on development of inspection technologies to identify localized damage within PCCP and failure risk analysis. These results also made development of targeted repair methods to restore the structural integrity of the pipeline segments a priority, including CFRP repair.

PCCP is composed of an inner concrete core, a steel cylinder, an outer concrete core, prestressed wires that are wrapped around the outer core under tension, and an exterior mortar coating protecting prestressing wires from the environment (Figure 2.1). PCCP is designed for combined loads including internal working and transient pressure, pipe and water weight, soil load, and life load. The current analysis and design procedure is based on checking certain serviceability, damage, and strengthen limit states by calculating stresses and strains in the concrete core, mortar coating, steel cylinder, and prestressing wires (AWWA C304).

There are various failure mechanisms for PCCP; however, a typical failure mechanism involves breakage of the prestressing wires on individual sections of pipe (Romer et al., 2008). When prestressed wires on an individual section of pipe break, the structural integrity of that pipe is compromised and the risk of a failure in the line may be significantly increased, particularly if a pressure surge occurs in the line.

In the late 1990s, electromagnetic technologies were developed to structurally assess the integrity of the prestressed wires on PCCP (Zarghamee et al., 2012). These inspections are able to isolate the location of broken prestressed wires with an accuracy that allows pipeline owners to identify individual pieces of pipe that have been structurally compromised. Based on more than 2 million feet of PCCP electromagnetically inspected to date, the distress rate in PCCP is approximately 3.9%, with only a fraction of the distressed pipes having a significant number of broken wires (Higgins et al., 2012). Once distressed pipe sections have been identified for rehabilitation, either replacement or a structural repair is selected based on various constraints typically related to accessibility to excavate, downtime, and cost. Failure risk of pipes with broken wires can be performed and repairs can be prioritized (Zarghamee and Ojdrovic, 2001).

2.2.2 Pipe repair options

Pipe repair options include (1) external repairs, such as circumferential posttensioning, replacement, external steel or CFRP bands, or encasement of the distressed pipe, or (2) internal repairs, such as installing a steel liner or slip-lining with fiberglass or steel pipes, or lining with hand lay-up CFRP. Selecting the best option depends on access, acceptable duration of construction, impact on operation, the expected cost of repair, and reliability of the repaired pipeline.

In most cases, if excavating is a viable option, external posttensioning repairs or pipe segment replacement are the most cost-effective and expeditious repairs. However, internal repair is the preferred alternative in cases where excavation is costly due to high soil cover height and presence of other underground or aboveground structures that impede access to the outside of the pipe. Internal repair of several adjacent distressed pipe pieces may be performed by slip-lining distressed pieces with either steel pipe or fiberglass pipe sections. An advantage of a slip-lining repair is that an extended deteriorated portion of the pipe can be addressed without excavating all of the distressed pipe. However, this method reduces pipe diameter (typically a minimum of 6 in (154 mm) diameter loss), requires an installation pit, and has a longer lead time and down time.

Alternatively, an individual pipe segment or groups of pipes may be repaired internally using wet lay-up CFRP applied by hand to the walls of the pipeline. Figure 2.2 shows a completed CFRP lining system. CFRP repairs have the following advantages:

- Access through existing or new manholes. No need for excavation and pipe removal.
- Materials are flexible and easy to transport through the pipeline until applied and cured.
- Work can be conducted on a tight schedule; work can be performed by multiple crews along the pipeline.

Figure 2.2 Completed CFRP-lined section.
Courtesy of Mr Hector Posada of Tucson Water.

- Short lead time, readily available for emergency repairs.
- Minimum impact to traffic as relatively small staging area is required.
- Does not adversely affect flow; a typical CFRP liner is between 3/8 in (9.5 mm) and 3/4 in (19 mm), and its surface profile is smoother than the existing inner concrete core. The resulting hydraulic capacity of the pipeline remains relatively unchanged, if not slightly improved.
- CFRP is corrosion resistant.

Disadvantages of CFRP lining include lack of a published design standard and limited performance history in pipeline applications, although CFRP has been used extensively in other civil infrastructure upgrade scenarios for many years, and there is an AWWA standard on CFRP renewal and strengthening of PCCP currently in development.

2.3 CFRP liner design

The design principles for CFRP lining systems have evolved since the first repairs took place in the 1990s, and through testing and in-service experience, improvements in design concepts have led to an increase in the long-term performance expectations for CFRP systems (McReynolds et al., 2013). Currently, there is no standard for design of CFRP lining repairs of pipes; however, there is an AWWA subcommittee that is developing a standard that addresses design, materials, installation, and quality control for CFRP renewal and strengthening of PCCP (ANSI/AWWA CFRP). The design principles described herein are inline with the concepts being implemented into the standard.

The circumferential design of a CFRP liner is based on the combined effects of gravity loads and internal pressures consisting of pipe and fluid weights and earth load that will be imparted to the lined pipe as the host pipe continues to deteriorate and experiences loss of prestress in PCCP, cracking of concrete core, corrosion of steel cylinder, and additional deformation. For a distressed or degraded PCCP, the CFRP liner can be designed as a composite system with the PCCP inner concrete core or as a stand-alone system that does not rely on the host pipe for resisting any of the design loads.

2.3.1 Distress state of host pipe

Depending upon the level of degradation or distress within the host pipe at the time of repair, the CFRP liner is designed to resist the design loads through either composite action with a part of the pipe wall or as a stand-alone system. Levels of degradation of host pipe for CFRP rehabilitation and strengthening of PCCP are as follows:

- *Nondegraded pipe*. The CFRP liner for a nondegraded pipe, requiring strengthening due to increased load (e.g., pressure, earth load, live load), is designed by considering the composite action of the CFRP with the entire pipe wall thickness.
- *Degraded pipe*. A degraded pipe consists of PCCP with some broken wires but with an inner core that is circular and may have some minor cracking that can be repaired.

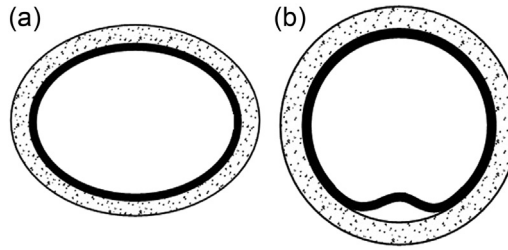

Figure 2.3 (a) Ovality and (b) waviness imperfections.
Courtesy of Simpson Gumpertz & Heger.

For PCCP, embedded-cylinder type (ECP), the outer concrete core may be cracked and softened and the steel cylinder may be corroded and even perforated, allowing ground water into the pipe. For PCCP, lined-cylinder type (LCP), coating may be cracked and delaminated, the wires may be broken, and the steel cylinder may be corroded and even perforated. The CFRP repair of degraded pipe shall be based on either composite action of concrete inner core reinforced with CFRP laminate or stand-alone CFRP liner. A degraded pipe is expected to experience additional wire breakage, core cracking, deformation, and corrosion of steel cylinder with time after the repair. The CFRP will be subjected to high stresses during the continued deterioration of PCCP.

- *Severely degraded pipe*. Severely degraded pipe consists of PCCP with broken wires, multiple wide cracks in the concrete core, as well as a significantly deformed and uneven internal surface with ovality or waviness as illustrated in Figure 2.3.

CFRP repair of degraded PCCP provides strength, durability, and reliability throughout the service life of the repaired pipe when the pipeline is subjected to long-term and short-term loads. The CFRP system is designed to have adequate strength to eliminate failure of the CFRP system by rupture or buckling. The CFRP system is also designed to have adequate durability to prevent failure of the CFRP system during the service life as both the CFRP and the PCCP continue to degrade with time.

The CFRP system is designed to have adequate reliability such that the probability of failure of the repaired pipe resulting from the variations of loads and resistance is similar to the probability of failure associated with the use of more conventional structural repair materials. The CFRP repair design is to allow the service life of the repairs to be in the range of 5−50 years.

2.2.2 Structural behavior of the CFRP liner for degraded PCCP

While applied loads do not change significantly over time, the moment capacity of the pipe reduces as the repaired pipe degrades due to broken prestressing wires and cracking of the core. The moment demand in excess of capacity at the pipe spring line redistributes to the invert and crown of the repaired pipe. This moment redistribution increases the moment demand at the invert of the repaired pipe and hence the tension demand in the liner. The structural system of the pipe changes from a relatively rigid pipe at the time of internal repair to a more flexible, fully deteriorated pipe

resulting in increased deflections and pipe ovaling. The CFRP system has to be capable of accommodating such deformations.

During the degradation process, there will be localized wire breaks (in the form of bands) that cause differences in stiffness along the length of the pipe. The design of the CFRP liner is based on the loss of all prestressing wires, which results in a flexible pipe design for the liner. In addition, the design accounts for the bending of the CFRP lining due to differential stiffness along the length of the pipe encountered during the degradation process.

The CFRP liner relies on the stiffness of the soil to resist the external loads. Adequate geotechnical data at the site are needed to support selection of the constrained soil modulus for design of the CFRP liner (AWWA M45).

2.3.3 Design limit states

As part of the process of CFRP lining design, multiple limit states must be addressed. For a stand-alone CFRP liner design, the limit states addressed are as follows:

- Rupture of CFRP circumferential and longitudinal laminate in tension, compression, flexure, or shear.
- Circumferential or longitudinal buckling of the CFRP laminate.

When the inner concrete core is taken into account in the CFRP design, as part of a compositely designed system, the following additional limit states are addressed:

- Rupture of the CFRP laminate in tension or combined tension and bending.
- Buckling of the CFRP laminate bonded to the concrete inner core.
- Debonding of CFRP from the concrete inner core under one of the following circumstances:
  - Shear between the CFRP and the concrete inner core.
  - Excessive radial tension.
  - Concrete core crushing from gravity loads, in absence of internal pressure.

2.4 Material selection

A typical CFRP liner system consists of primers, thickened resins, resins, reinforcing fabric, and topcoat. The most effective resin systems for long-term civil infrastructure rehabilitation applications, such as rehabilitation of PCCP lines, are ambient-cure thermoset epoxy systems. In order to minimize environmental hazards present inside the pipeline during application of the materials, epoxy systems that are made of 100% solids and are VOC compliant are utilized.

The primer layer of epoxy applied to the pipe consists of a low-viscosity epoxy that penetrates into the concrete substrate, providing an adhesive bond for the thickened epoxy filler and saturating layers as well as subsequent layers of the CFRP system.

The thickened epoxy filler system consists of the saturating resin and silica fume that have been mixed together in accordance with the manufacturer's recommended procedure in order to provide a smooth surface for application of the carbon fiber material. The thickened epoxy filler is used to fill voids and even out the concrete substrate; it is also used in between layers of CFRP to ensure intimate contact of the CFRP system at all locations within the CFRP liner.

The topcoat of the CFRP is typically thickened epoxy, either with or without a pigment added for ease of inspection. In wastewater or industrial environments where high concentrations of H_2S or aggressive chemicals are anticipated, a topcoat that is formulated for heightened chemical resistance is often used. In circumstances where the CFRP system is applied to the outside of the pipe, a UV-resistant topcoat is utilized.

In any applications where potable water is conveyed by the pipeline system, industry standard is that all materials utilized in the CFRP liner repair are to have been tested to be in compliance with ANSI/NSF 61, which is the nationally recognized health-effects standard for all components, devices, and materials that come in contact with drinking water (http://www.nsf.org/certified/PwsComponents/).

2.4.1 Types of FRP composites used

There is a wide variety of reinforcing fabrics available in other industries; however, for internal repair of pipelines, best practices include only the use of unidirectional carbon fiber fabric as the structural reinforcement. In order to resist all of the design loads acting on the pipeline, separate sheets of epoxy-saturated carbon fiber—reinforcing fabric are applied inside the pipeline with the direction of the fibers oriented in either the longitudinal or the circumferential direction to provide the necessary strength.

Carbon fibers have the potential for electrical conductivity; therefore, to avoid galvanic corrosion of steel in proximity to carbon fibers, a glass-fiber fabric is used for isolation of any steel substrate from the CFRP system. Fiber sizing and coupling agent shall be compatible with the resin system used to impregnate the fibers.

2.4.2 Material performance requirements

CFRP liner systems are typically specified to be functional and made with durable CFRP materials based on performance-based specification. Like with other construction materials, inappropriate and unsuitable FRP materials may lead to a substantial reduction in the service life of CFRP repairs.

One industry certification that can aid owners and engineers is the inclusion of a valid International Code Council (ICC) Evaluation Service Report (ESR) as a requirement for FRP materials. The ICC developed a set of minimum durability and performance criteria for CFRP materials that must be adhered to in order to receive ICC approval and a valid ICC report. ICC's Acceptance Criteria 125 (AC125) and AC178 establish the minimum acceptable durability criteria, structural

performance, and inspection criteria for any CFRP liner system to be considered suitable for structural rehabilitation applications. To obtain a valid ICC report, materials must maintain minimum percent retention of properties when they are tested after 1000, 3000, and 10,000 h exposure to various aggressive environments including water at different temperatures, saltwater, alkali solutions, and dry heat (ICC 125, 2010 and ICC 178, 2010). Specifications that protect owners and engineers, ensuring properly tested CFRP materials are installed, require a valid ICC report as part of the bid submission.

More extensive durability testing beyond the 10,000-h exposure tests required by ICC AC125 is available for selected CFRP materials. For instance, a recently released study highlights an 8-year durability study completed by the Metropolitan Water District (MWD) of Southern California (Sleeper et al., 2010). In this study, an inspection of CFRP-lined PCCP was performed approximately 8 years after the installation of the CFRP lining system. The visual and sounding inspection indicated no damage in the form for delaminations, bubbles, cracks, or edge lifting. Observations from the same inspectors who were present during the initial CFRP lining installation noted that the CFRP was in comparable condition to the originally installed system. In addition to the results of the in-service CFRP inspection, coupons made from the same CFRP system installed in MWD's pipeline were tensile tested after 8 years of exposure to tap water in environmental chambers. The tensile test results indicated a minimal change in the structural performance of the CFRP system, as measured through tensile strength, tensile modulus, and breakage strain, after being continuously immersed in tap water for a period of more than 8 years (Sleeper et al., 2010). The results of this durability study indicate strong potential for the CFRP lining system to perform well as a long-term solution for pipeline rehabilitation.

2.5 Methods of repair

2.5.1 Preconstruction

CFRP repair of large-diameter PCCP lines requires a great deal of planning, especially in municipal areas where traffic control and other complications persist. Access to pipeline segments to be repaired and dewatering of the pipeline are typically coordinated by the owner. Prior to the pipeline shutdown period, crews arrive at the site; set up fencing and material, equipment, and storage areas, temporary office facilities as necessary, lay-down areas, and saturator and material mixing areas; and have all required materials and equipment staged at the pipeline work locations.

Safety is an important aspect of these projects, given that the work takes place in a confined space with limited available access and egress. Ensuring that crews within the pipe have adequate air supply is one portion of the safety approach. Dehumidification air-blowing units are installed at the appropriate locations to ensure a constant supply of clean, dry air for ventilation purposes and also to assist in drying the segments to be strengthened following the surface-preparation operation.

Upon initial entry of each pipe repair area, inspectors walk the entire length of the pipe from the access point to the location of air supply and note the presence of any leaks and the amount of residual water. Then, pumps and other water-removal equipment are started and removal of the residual water commences. Crews typically construct temporary bulkheads as necessary to create beneficial airflow within the work space and promote drying of the repair pipe segments. Crews also convey water as needed to points of discharge and construct temporary weirs to control continuously flowing nuisance water.

2.5.2 Overview of installation procedure

General work activities associated with the PCCP-strengthening-system installation that occur outside of the pipe include the preparation and mixing of the epoxy system and the saturation of glass- and carbon-fabric sheets prior to mobilizing the saturated sheets into the pipe for technician installation. General work activities associated with the CFRP system installation that will occur inside of the pipe include joint preparation, surface preparation of the inner core, installation of the CFRP system, and installation of the end terminations. Details for each procedure are provided in the following sections.

This subsection will include an overview of installation methods with particular focus on wet lay-up and the various components that lead to successful CFRP system installations. Wet lay-up is the procedure considered best practice as an installation method. As detailed below, this includes the saturation of the fiber system through a mechanical saturator. Other installation methods, such as dry lay-up, may lead to inadequate fiber saturation and delamination of the CFRP system. Dry lay-up is the application of dry fiber sheet and in situ application of the epoxy to the fiber at the point of application. This is deemed to be an unreliable installation method. Detailed steps of the wet lay-up process follow.

2.5.3 Surface preparation

Surface preparation is one of the most important aspects of the CFRP installation process. Concrete surfaces are to be prepared to an ICRI profile of CSP-3 or greater to create an open-pore structure and to remove all protrusions, sharp edges, and surface contaminants. Surface residue resulting from surface preparation is to be collected from within the construction area and removed from the pipe.

Joint areas are also prepared during surface preparation. For instance, with bell-and-spigot-type PCCP, the inner concrete is first demolished to expose the steel liner at both the bell and spigot ends. The extent of the demolition depends on the thickness of the inner-core concrete and the required bond length at CFRP terminations. Adequate area is to be demolished to allow for the type of transition called for in the design. The steel surfaces at termination detail areas are also prepared to at least a near-white metal finish.

Surface preparation typically takes place concurrently with joint termination demolition. Surface preparation can be performed by ultra-high-pressure water blasting, abrasive blasting, or pneumatic sponge blasting.

If water blasting is selected, it is recommended that 40,000 psi (275 MPa) equipment, operating at 30,000−36,000 psi (207−248 MPa), is utilized to ensure proper profiling of the concrete substrate. As water flows from this type of water-blasting equipment are low, the conveyance of blasting water and debris can be facilitated from the surface-preparation area. Abrasive blasting is another effective method for surface preparation and standard techniques apply to the specified surface profile. Special precautions are taken for this type of blasting in a confined space.

An alternative method of abrasive blasting with environmental benefit is sponge blasting. Sponge media is an open-celled, water-based polyurethane impregnated with abrasives. On impact with the surface, the sponge particles compress and slide across the surface, producing a scrubbing action, more similar to a sanding effect but eliminating the harsher and dusty negative effects associated with conventional grit blasting. The abrasive particles remove the desired surface profile and the media rebounds at quite low velocity as the media converts the majority of its energy into work at the surface. The sponge-blast media generates less than 10% of the airborne-dust levels normally experienced with conventional grit-blasting media, allowing for improved safety during surface preparation.

Following surface preparation, the transition between the inner concrete surface of the pipe and the steel liner will be filled with a thickened epoxy mortar extended with sand at a ratio of approximately one part epoxy to five parts sand. The thickened epoxy is created in the field by extending the epoxy with silica. The thickened epoxy mortar is used to create a transition slope at the end details as needed to meet design requirements. As surface preparation is completed, a low-viscosity primer coat of epoxy is applied to all concrete surfaces as shown in Figure 2.4.

Figure 2.4 Application of epoxy primer.
Courtesy of Mr Hector Posada of Tucson Water.

2.5.4 Saturation of the carbon- and glass-fiber systems

Saturation is the process of impregnating epoxy resin into the fiber fabric at the proper ratio for installation. Critical design properties are ensured through proper saturation of the material. All resin components are mixed from preportioned and prepackaged containers until there is a uniform and complete mixing of components. The mixing procedure for each resin system should be in accordance with the manufacturer's recommendations.

Proper saturation of glass- and carbon-fabric sheets prior to installation is typically performed using a "top-feeding"-type saturating machine as shown in Figure 2.5. The fabric is fed on a roller through a gap between multiple drum rollers, which is gauged to provide the appropriate ratio of fabric to resin per manufacturer's instructions. The gap between rollers is to be periodically calibrated and verified. The fabric-to-resin weight ratio is to be verified at the beginning of each work shift by performing a weigh test, where a piece of reinforcing fabric is weighed before and after saturation. Use of the mechanical saturator is critical for ensuring consistency in saturation of the reinforcing fabric and is an important part of the quality assurance/quality control (QA/QC) process.

2.5.5 Installation of saturated–carbon fiber lamina

The installation process includes the steps after the fiber fabric is saturated, covered for protection, and transported to the CFRP repair segment of PCCP. Following the surface preparation and prior to CFRP installation, portable scaffolding is erected, as needed, spanning the pipe section to be lined. This is to give the crew the ability to apply the CFRP liner to all areas of the pipe section without the need to walk on the pipe. Best industry practice to ensure a successful installation is that the application takes place continuously in a manner that avoids contact with the CFRP after installation and until cured.

Figure 2.5 Saturation of carbon-fiber fabric of epoxy primer.
Courtesy of Structural Technologies, LLC.

Figure 2.6 Installation of the circumferential layer of CFRP (Gipsov et al., 2012).

The saturated carbon fiber is applied to the inside surface of the host pipe in a wet lay-up process as shown in Figure 2.6. The wet-out fabric is pressed to the inside surface of the host pipe to achieve intimate contact. Any entrapped air between layers is to be released or rolled out without wrinkling of carbon fibers. Fabric kinks, folds, or severe waviness are not acceptable conditions.

When the CFRP is not properly aligned, the affected layer of the CFRP system needs to be removed and replaced prior to curing. If the CFRP layer cannot be removed without affecting the integrity of the surrounding carbon fiber, an additional layer is overlaid onto the off-axis fibers to restore the laminate structure to its intended axial-strength requirements.

2.5.6 Termination requirements

The termination points of the CFRP liner are designed such that internal water pressure is not able to migrate behind the inner core. This is critical because the PCCP may continue to degrade and the adjacent pipes may also become degraded. This results in longitudinal cracks in the outer core that diminishes the outer-core stiffness against radial movement of the pipe wall and results in separation of the cylinder from the inner core. If the CFRP is not properly sealed at termination points and pressure is allowed to build up behind the inner core, the inner core will be stress free and structurally ineffective. Designs that include termination details with the CFRP extended into the next pipe section will allow water pressure to build up behind the inner core when the adjacent pipe degrades, and hence this termination detail is not used.

The length of the bond between CFRP laminate and the steel joint rings plus steel cylinder is a minimum of 3 in and long enough so that the maximum axial force in the CFRP in the longitudinal direction from all loading conditions will not cause shear-bond failure or tension failure. The surface of steel substrate over the bond length is prepared to at least near-white-metal condition and is primed to promote adhesion.

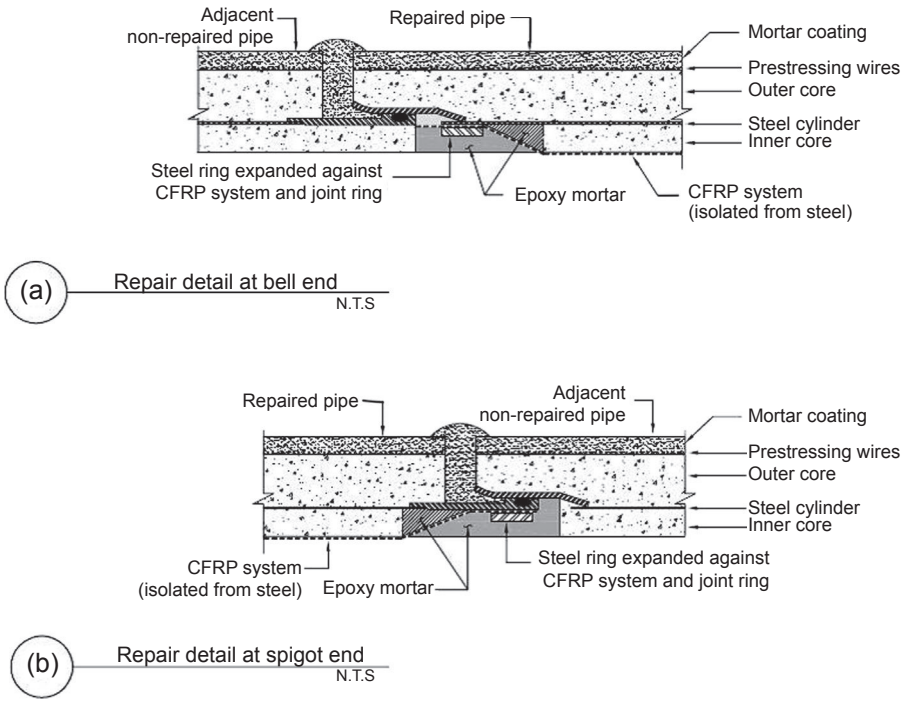

Figure 2.7 Generic representation of termination details at (a) bell and (b) spigot ends (ANSI/AWWA CFRP).
Courtesy of Simpson Gumpertz & Heger.

To prevent galvanic corrosion, the CFRP is constructed on GFRP applied to steel surface. The procedure used for preparation of termination detail must avoid damage to the steel cylinder. Any damage, including gouges and punctures, needs to be repaired prior to CFRP system installation.

Epoxy mortar is used to construct the transition areas as shown in Figure 2.7. The epoxy mortar must be applied carefully in order to avoid contaminating the bond region of CFRP and steel cylinder and joint ring surfaces through smearing of epoxy mortar on this bond region. Installation of glass layer as the dielectric barrier between the steel and carbon fibers is applied to the substrate starting from the bare-steel end to avoid epoxy-mortar contamination of the bonding surface. Following this, steel expansion rings are installed at both ends of each repair region at least 24 h after CFRP installation. The rings are expanded to achieve minimum 100 psi (689 kPa) interface pressure.

2.5.7 Finish and topcoat requirements

Following installation of the CFRP system, a topcoat is applied to provide an abrasion wear layer and friction surface. Some owners opt for installation of a white or bright-colored topcoat to facilitate future inspections.

The topcoat needs to completely encapsulate the CFRP system with no fiber strands exposed and needs to be applied within the manufacturer-specified application time window to ensure appropriate adhesion to the reinforcing fabric and to prevent amine blush. If conditions prevent the application of the topcoat within the manufacturer's specified application window, a solvent wipe, as recommended by the manufacturer, is to be applied to the surface of the structural laminate to remove all amine blush. Localized and small blisters are to be removed and sanded, and the topcoat material reapplied as per the manufacturer's recommendations. The topcoat is to be inspected periodically and maintained as specified by the manufacturer to ensure its effectiveness.

2.5.8 Fittings and specials on the pipe segment

The CFRP liner for pipe with an inlet or an outlet is designed in the same manner as for the pipe without an inlet or an outlet. Additional strengthening of the CFRP liner at an inlet or an outlet is equivalent to at least 100% of the fibers interrupted in the direction of such fibers. The additional strengthening shall be applied around the inlet or outlet, extending beyond the opening.

In addition to strengthening of the CFRP liner, transitional CFRP laminate needs to be applied to the interior of the inlet or outlet pipe. If there are any bare-steel surfaces, a GFRP insulation layer is utilized prior to installation of the CFRP layers to prevent galvanic corrosion. The transitional CFRP laminate is bonded to the insulating GFRP layer of the inlet or outlet and is cut radially in strips that are bent and adhered to the GFRP layer as shown in Figure 2.8. The transitional CFRP needs to be designed and constructed in such a way that internal water pressure is not allowed to get behind the inner core in the future as the host pipe continues to degrade.

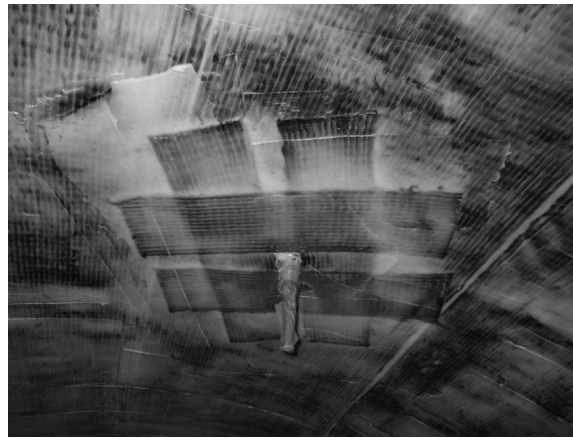

Figure 2.8 Typical inlet additional CFRP for strengthening and transition (ANSI/AWWA CFRP).
Courtesy of Simpson Gumpertz & Heger.

2.5.9 Defect repair requirements

After the CFRP system has reached a gel state, but prior to the system achieving full cure, the CFRP system is inspected to identify defects to be corrected prior to cure. Entrapped air must be released to establish intimate contact between the CFRP laminate and the inner core. Where possible, the inspections must be performed early in the process so that they can be corrected without requiring patching or filling. Air voids or bubbles are detected by holding a light against the surface of the laminate and illuminating the surface parallel to pipe. Once the system has cured, a visual inspection of the entire surface is performed. Where air voids have been detected, they need to be repaired in accordance with the manufacturer's requirements. At a minimum, air voids greater than 1 in (25 mm) in diameter are to be injected with resin. This may be accomplished by drilling small holes in the laminate at the top and bottom of the air void and filling the void space with the thickened epoxy.

At a minimum, any defect requiring a patch is to be addressed with an equivalent number of layers that the defect penetrates. Dry lay-up is not appropriate and should not be permitted for patch repair. Patches are to extend in accordance with the development length stated as per the design.

2.5.10 Installation environment requirements

The atmospheric conditions during the time of application are to be within the limits set forth by the material manufacturer's technical data sheets. Dehumidifying and raising the temperature of the air is an acceptable means of improving the environment.

The ambient temperature conditions dictate the rate of cure for the resins used in the system. The air is to be dehumidified to avoid moisture present on the substrate during installation. The ambient air temperature during the time of application cannot be below 40 °F or above 100 °F. The CFRP system is to have a minimum of 85% cure before the pipe is returned to service. Durability of CFRP is affected by the degree of cure of the CFRP. CFRP curing time varies between products, and is shortened significantly by application of heated air.

2.6 Quality control measures

The overall quality of CFRP liner repairs is governed by quality of design, quality of materials used, experience of workers and supervisors involved in installation, and quality of installation (Engindeniz et al., 2011). Quality of installation is ensured by CFRP installation inspection and inspection of the finished product performed by the design engineer or owner's inspector. A trained field supervisor needs to observe all aspects of the on-site preparation and material application including surface preparation, epoxy-component mixing, application of primers, application of epoxies, placement of fiber fabrics, curing of composite, and application of protective coatings. Inspection of cured CFRP laminates includes sounding and bond-strength testing. Tapping with a hammer or metal rod is common and impact echo has been used to detect voids and delaminations in CFRP. The size of delaminations determines the

appropriate repair method ranging from low-pressure epoxy injection to removal of affected area and reapplication of CFRP layers.

Bond-strength testing includes a direct pull-off test based on ASTM D4541-09-1 that is used to test the bond between the cured CFRP laminas and between the laminate and the concrete substrate at representative locations. Surface-preparation bond-strength tests may be performed on small areas of adjacent pipes prepared similarly to the repair pipe, and on the repair pipe.

The CFRP installer should provide for inspection hold points to allow inspection of the workmanship of in-process construction. Inspection hold points are critical breaks in activities to inspect the workmanship of in-process construction. It should be noted that the hold point inspections do not relieve the owner's inspector from performing continuous in-process inspections during construction activities. The owner's inspector (design engineer) should anticipate the timing of the hold points and be on site for inspection. Delays in activities may impact the quality of the work. The owner's inspector's approval of the work as satisfactory at the hold points should be a requirement for the construction work to proceed. The owner's inspector should also document the inspection at the hold point and his or her approval.

The owner's inspector should examine the surface for cleanliness after the pipe segment(s) have been cleaned and the surface has been broom cleaned, vacuumed, or otherwise rendered free of dust, debris, and moisture.

The owner's inspector inspects the concrete inner core and steel substrate to which CFRP will be adhered after the surfaces have been prepared in order to establish that the surface profile conforms to the project specification and Section. 3.5.2, and that the prepared surface extends beyond the limits of construction for the pipe segment(s) being strengthened. To ensure a high-quality installation, surface preparation should continue until the requirements for surfaces have been met.

The owner's inspector verifies that the carbon fiber is being saturated in accordance with manufacturer's technical data. The inspector should witness the quality control procedure of verifying the resin-to-fabric ratio and document the results in the project inspection log.

The owner's inspector inspects the layout lines for the starts and stops of carbon fiber fabric to ensure that the layout conforms to the approved plans. Particular attention should be paid to longitudinal layout so that the fabric starts on axis and to the radial layout so that the overlaps at the ends are within specification.

Upon completion of the fabric lay-up, the owner's inspector inspects the installed carbon fiber strengthening system for cuts, folds, end curls, bubbles, and any other apparent defect, and immediately brings it to the attention of the CFRP system installer for additional tooling and repair. Once the material has enough time to gel but before the material has fully cured, the owner's inspector examines the installation for air voids that may have formed during the curing process and direct the CFRP system installer to release the air and work the fabric back into the surface.

This is accomplished by holding a light adjacent to the laminate surface with the beam pointing down the length of the pipe parallel to the surface and verified using a detection tap test. The tap test method consists of running a quarter or tapping with a ball-peen hammer over the surface and listening for the difference in tone.

Where an air void is suspected, the change in tone provides confirmation of a hollow spot. Once the system has cured or hardened enough to walk on, the owner's inspector performs a visual inspection of the entire CFRP surface, bringing to the attention of the installer any defects requiring repair.

2.6.1 Adhesion testing

In order to validate the adequacy of the surface preparation and the adhesion strength of the carbon fiber–strengthening system, the installer has to perform adhesion tests on the prepared concrete substrate adjacent to repair pipes as directed by the engineer and witnessed by the owner's inspector. The owner's inspector designates the areas for trial adhesion tests prior to the surface-preparation activities. These areas are to be cleaned, prepared, and covered with two-ply CFRP system test patches with minimum dimensions of 2 × 2 ft (60 × 60 cm). The patch consists of two orthogonal layers of CFRP.

Adhesion tests are then performed and reported in accordance with ASTM D4541-09-1. Three adhesion tests are performed on each test patch. The remaining adhesion test panels are finish coated and remain in place for future testing purposes. The installer is to log the location of the adhesion test and report the test results to the owner.

2.6.2 Tensile testing

In order to verify that the material properties of the field-applied CFRP system are inline with the properties used in the design, tensile tests are performed in accordance with ASTM D3039-14 on test panels that are field fabricated using the carbon-fiber fabric, resins, and saturation equipment used in the production runs for the field-installed CFRP lining system. These panels are made with typical minimum dimensions of 12 × 12 in (30 × 30 cm) and are prepared on a smooth, flat surface overlaid with plastic (polyethylene or vinyl) sheeting.

Saturating resin is used to prime the surface, followed by the saturated CFRP system, and finally topped with more saturating resin. A cover of plastic sheeting is placed over the panel and the panel squeegeed to remove any bubbles and other surface irregularities to ensure a smooth flat surface. The panel is labeled with time, date, sample panel number, fabric lot numbers, and resin batch numbers. It is then stored in a dry place to cure. Two test panels are typically fabricated per day of installation of the CFRP system in the field. A minimum of 10% of all fabricated samples are typically tested at an independent testing laboratory. The test lab will perform tensile tests with the fibers oriented in the strong direction for each tensile test panel in accordance with ASTM D3039-14 and provide test results for tensile strength, tensile modulus, and percent elongation.

2.7 Future trends

One of the reasons for the use of carbon-fiber lining systems primarily as a targeted structural repair, rather than a continuous lining system, is the relatively high

cost of this installation. Proper installation of a carbon-fiber lining system is labor intensive and utilizes expensive materials as well. Recent advancements of composite lining systems have attempted to reduce overall project costs so that this type of structural system can be used for repair or renewal of extended runs of pipe.

One concept often explored to reduce the costs has been the automation of the installation process. In recent years, several attempts have been made at robotic automation of the CFRP lining process as well as implementation of CFRP materials into the cured in-place pipe process. However, at the time of this writing, these systems are still in early development phases.

One recently developed solution involves use of high-strength steel wire in place of carbon fiber composites in the hoop direction, with glass and carbon fibers still utilized to provide longitudinal reinforcement. The spirally wound hoop steel reinforcement is embedded into a thickened epoxy putty, and the steel-reinforced polymer composite is sandwiched between layers of glass fiber-reinforced polymer composites. The glass fiber layers on either side of the steel serve as electrical isolation for the steel wires as well as longitudinal reinforcement. Additional layers of longitudinal glass and/or carbon fiber longitudinal layers are utilized as needed for reinforcement as shown in Figure 2.9. This modified composite lining system helps to reduce both labor and material costs, thereby allowing composite linings to be a viable option for longer runs of pipeline repair.

Due to limitations in the geometry of the robotics, this type of system is most applicable for 42-in and larger diameter pipelines. When the repaired pipe section has bends or laterals as part of a continuous repair, laterals and bends are addressed using conventional carbon-fiber composites prior to transitioning back to the hybrid FRP steel system.

Full-scale testing has been successfully performed on the hybrid FRP system (Alkhrdaji et al., 2013), and multiple installations have taken place to date (Rocca et al., 2013). Additional research and development are taking place to further expand the capabilities of this pipeline strengthening system.

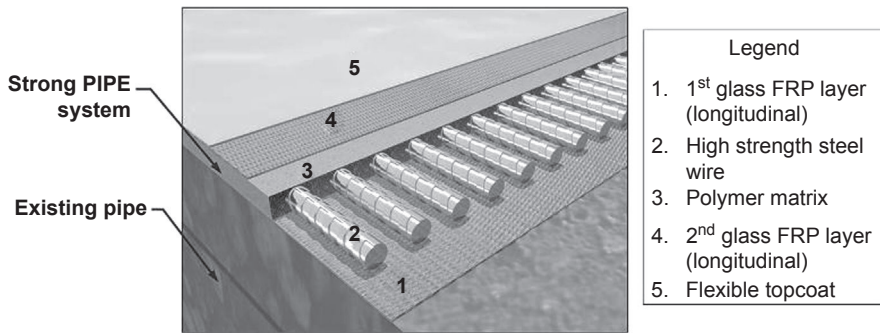

Figure 2.9 Hybrid steel–FRP system.
Courtesy of Structural Technologies, LLC.

2.8 Further sources of information

This section provides further information on research, publications, and current developments related to PCCP and the use of CFRP lining systems for internal repair of concrete pressure pipes.

For background on prestressed concrete pipe design code variations and failure mechanisms of PCCP, the authors recommend WRF Report #91214, *Failure of Prestressed Concrete Cylinder Pipe* (Romer et al., 2008). The designs of PCCP have varied significantly over the past 65 years, and it is important to understand the original design of the pipeline as the pipeline is being evaluated for potential rehabilitation. A thorough review of condition assessment technologies relevant to PCCP is provided by Zarghamee et al. (2012) titled *Best Practices Manual for Prestressed Concrete Pipe Condition Assessment: What Works? What Doesn't? What's Next?* This report provides an overview of available technologies for condition assessment, monitoring, and failure margin/remaining service life analysis of PCCP as well as a summary of best practices for selecting appropriate technologies for condition assessment of a pipeline system.

As of now, AWWA is nearing publication of a standard on "CFRP Renewal and Strengthening of Prestressed Concrete Cylinder Pipe (PCCP)" (now designated as ANSI/AWWA CFRP). This standard has been in development since late 2009 and is intended to provide a consensus document that reflects the state of technology for material selection, design, installation, and QA/QC of the CFRP renewal and strengthening of PCCP.

In support of establishing technical guidelines, AWWA Research Foundation (AWWARF) and the US Environmental Protection Agency (USEPA) have funded research being performed by Simpson Gumpertz & Heger on the use of CFRP for the structural renewal of PCCP. AWWARF Project No. 4352, *CFRP Renewal of Prestressed Cylinder Concrete Pipe*, investigates factors that should be considered when designing, testing, and performing CFRP lining projects. This program includes several sets of component- and full-scale testing to support the technical development of the standards for CFRP renewal of PCCP pipelines (Zarghamee et al., 2013).

Acknowledgements

The authors would like to acknowledge Dr Mehdi Zarghamee for his leadership on development of the AWWA standard for CFRP renewal and strengthening of PCCP as well as his technical leadership in the AWWA Research Foundation project. These efforts have contributed significantly to the content of this chapter. The authors would like to thank Mark Geraghty of Structural Technologies, LLC for his time and efforts.

References

Alkhdraji, T., Rocca, S., Galati, N., 2013. PCCP rehabilitation using advanced hybrid FRP composite liner. In: ASCE Pipelines Conference 2013, Fort Worth, TX.

ANSI/AWWA C304-07, 2007. Standard for Design of Prestressed Concrete Cylinder Pipe. American Water Works Association (AWWA).

ANSI/AWWA CFRP, in preparation. Standard for CFRP Renewal and Strengthening of PCCP: Fiberglass Pipe Design Manual, American Water Works Association (AWWA).

ANSI/NSF 61, 2013. Drinking Water System Components—Health Effects. NSF International/ANSI. http://www.nsf.org/certified/PwsComponents/.

ASTM D3039-14, Standard test method for tensile properties of polymer matrix composite materials, Book of Standards Vol. 15.03. American Standard for Testing and Materials (ASTM).

ASTM D4541-09-1, Standard test method for pull-off strength of coatings using portable adhesion, Book of Standards Vol. 06.02. American Standard for Testing and Materials (ASTM).

AWWA M45, 2005. Fiberglass Pipe Design Manual. American Water Works Association (AWWA).

AWWA, 2011. Buried No Longer—Confronting America's Water Infrastructure Challenge. American Water Works Association.

AWWARF, 2013 draft, Project No. 4352, CFRP Renewal of Prestressed Cylinder Concrete Pipe. American Water Works Association Research Foundation.

Engindeniz, M., Ojdrovic, R.P., Zarghamee, M.S., 2011. Quality assurance procedures for repair of concrete pressure pipes with CFRP composites. In: ASCE Pipelines 2011 Conference, Seattle, WA, 23−27 July 2011.

General Accounting Office, 2004. GAO 04-461, Water Infrastructure: Comprehensive Asset Management Has Potential to Help Utilities Better Identify Needs and Plan Future Investments, p. 14.

Gipsov, M., Pridmore, A.B., 2012. WSSC's systematic approach to the CFRP liner installation process. In: ASCE Pipelines Conference 2012, Miami, FL.

Higgins, H.S., Stroebele, A., Zahidi, S., 2012. Numbers don't lie, PCCP performance and deterioration based on a statistical review of a decade of condition assessment data. In: ASCE Pipelines Conference 2012. Miami, FL.

ICRI Guideline No. 310.2, Selecting and Specifying Concrete Surface Preparation for Sealers, Coatings, and Polymer Overlays. International Concrete Repair Institute (ICRI).

McReynolds, M., Sleeper, B., Zarghamee, M.S., Pridmore, A.B., 2013. Retrofit of CFRP installation to meet current design standards. In: ASCE Pipelines 2013, Fort Worth, TX.

Ojdrovic, R.P., 2013. Asset Management and Repair Prioritization of Prestressed Concrete Cylinder Pipe (PCCP) Lines. In: AWWA Distributions Systems Symposium, September 2013.

Rocca, S., Alkhrdaji, T., Frye, M., 2013. Rehabilitation of 120 inch PCCP at a New Mexico power plant using FRP and hybrid FRP systems—a comparative study. In: ASCE Pipelines 2013, Fort Worth, TX.

Romer, A.E., Ellison, D., Bell, G.E.C., Clark, B., 2008. Failure of Prestressed Concrete Cylinder Pipe. American Water Works Association Research Foundation, Report #91214. AWWA, Denver, Colorado.

Sleeper, W., Arnold, S., Pridmore, A.B., Carr, H., 2010. Carbon fiber as a long term repair solution. In: ASCE Pipelines Conference 2010, Keystone, Colorado.

Zarghamee, M.S., Engindeniz, M., Wang, N., 2013. CFRP Renewal of Prestressed Concrete Cylinder Pipe. Water Research Foundation. Report #4352.

Zarghamee, M.S., Ojdrovic, R.P., 2001. Risk assessment and repair priority of PCCP with broken wires. In: ASCE Pipelines Conference 2001, San Diego, California.

Zarghamee, M.S., Ojdrovic, R.P., Nardini, P.D., 2012. Best Practices Manual for Prestressed Concrete Pipe Condition Assessment: What Works? What Doesn't? What's Next? Water Research Foundation.

Abbreviations

ASTM	American Standard for Testing and Materials
AWWA	American Water Works Association
AWWARF	AWWA Research Foundation
CFRP	Carbon fiber-reinforced polymer
LRFD	Load and resistance factor design
PCCP	Prestressed concrete cylinder pipe
USEPA	US Environmental Protection Agency

Repair of corroded/damaged metallic pipelines using fiber-reinforced polymer composites

3

M. Ehsani
QuakeWrap, Inc., Tucson, AZ, USA

The versatility of metallic pipes has resulted in their widespread use in a large number of industries. The ability to resist high pressure makes these pipes an ideal candidate for industrial applications to convey high-pressure fluids and gases. While copper, aluminum, and brass pipes are available, by far the majority of metallic pipes are made of steel or iron. These pipes have been used extensively to carry oil and gas as well as water and sewer. In most such applications, the interior surface of the pipe is coated with a polymer or cementitious mortar lining to improve the chemical resistance of the pipe. The exterior of the pipe can also be coated or protected against corrosion using cathodic protection. Steel pipes in the form of corrugated metal pipe (CMP) have also been widely used as culverts.

With the passage of time, environmental factors both inside and outside the pipe lead to gradual corrosion and loss of strength in the pipe. In the early stages, this deterioration is visible as surface corrosion and pitting on the pipe, which may be relatively easy to fix. However, if unattended to, the corrosion could result in severe section loss that could not only cause leakage in and out of the pipe but could jeopardize the overall stability of the pipe in resisting external gravity loads. The latter is particularly common in deteriorated CMP culverts where the corrosion of steel in the invert of the pipe can lead to partial collapse of the culvert.

In many cases, the replacement of the deteriorated pipe with a new one is cost prohibitive and a time-consuming effort that cannot be easily accommodated. Fiber-reinforced polymer (FRP) products offer solutions that can often be installed in a trenchless manner that requires little or no digging of the pipe. The high-tensile strength, lightweight, and noncorroding attributes of FRP make these materials a viable repair system for steel pipes.

Various repair techniques with FRP products will be presented in this chapter. These include the use of fabrics referred to as the wet lay-up method, which was the earliest approach and until now has been the most widely used method for pipe repair. Also discussed are two new recently developed FRP systems that offer advantages over the wet lay-up method (Ehsani, 2012a,b).

Rehabilitation of Pipelines Using Fiber-reinforced Polymer (FRP) Composites. http://dx.doi.org/10.1016/B978-0-85709-684-5.00003-5

3.1 Wet lay-up

Most of the steel pipes in use can be categorized as operating under moderate to high pressure. Corrosion of steel results in the reduction of wall thickness whereby the strength and pressure rating of the pipe are compromised. FRP can be used to create a pressure vessel inside the pipe that can resist all or a portion of the total internal pressure of the pipe.

The wet lay-up is the most basic method for repair of pipes. As with all repair techniques, the surface of the pipe must be cleaned and prepared. Most designs assume that after the repair is completed the stresses in the pipe will be resisted jointly by the steel pipe and the FRP liner. This requires proper bonding between the FRP and the host pipe. A typical surface preparation for such pipes includes sandblasting of the pipe to white metal condition. The surface of the pipe must be cleaned by air pressure to remove any loose materials. If the resin system is moisture sensitive, care must be taken to avoid moisture buildup on the pipe surface. In most cases, forced airflow will provide ventilation for the crew working inside the pipe. The temperature of this air can be adjusted to ensure a dry pipe surface during the repair.

Prior to application of the FRP, any sections with significant deterioration or small holes can be patched. Smaller holes (around 30 mm) can be repaired with extra layers of FRP. For larger holes, it may be necessary to weld a steel plate over the deteriorated area. Some steel pipes may have protrusions due to rivets or welded seams. Care must be taken to smooth these areas. The most common practice is to apply a coating of a high-viscosity epoxy over those areas. The same resin that is used to saturate the fabrics can be thickened in the field with fumed silica (e.g., Cabosil) for this application.

Carbon and steel are dissimilar metals and when they come in contact, galvanic corrosion can ensue. The best way to prevent this is to provide a dielectric barrier between the carbon fibers and steel pipe. While the epoxy resin in the FRP does cover all the fibers, the thin layer of resin is not considered by many to be a proper long-term insulating shield to prevent this contact. The most widely accepted practice in the industry is to apply a layer of glass fabric as the first layer for any repairs in steel pipes (Figure 3.1). If the glass fabric is not intended to provide any strength for the pipe,

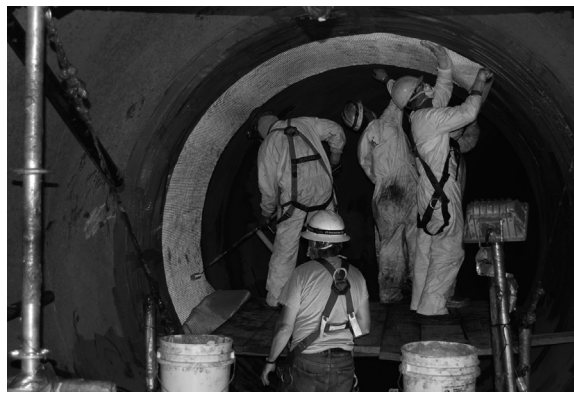

Figure 3.1 Glass fabric installed on a steel pipe serves as a dielectric barrier between the steel and carbon fabric.

a light fabric weighing approximately 10 oz per square yard (330 g/m^2) or less can be used for such applications.

Saturation of the fabric can be performed with saturating machines that use two rollers to force the resin into the dry fabric. The gap between the two rollers must be set properly to ensure that the saturated fabric has the correct resin-to-fiber ratio. Most manufacturers require an approximately equal volumetric ratio of resin to the fabric. The saturated fabric is automatically wound around a PVC tube, which is delivered to the crew for installation on the pipe surface. Depending on the diameter of the pipe, length of the repair and its proximity to the access ports, the operation for fabric saturation may be set up outside or inside the pipe. Some contractors have collapsible saturating equipment that can be partially taken apart to pass through a 24-in access port (Figure 3.2); once inside the pipe, the equipment is quickly reassembled.

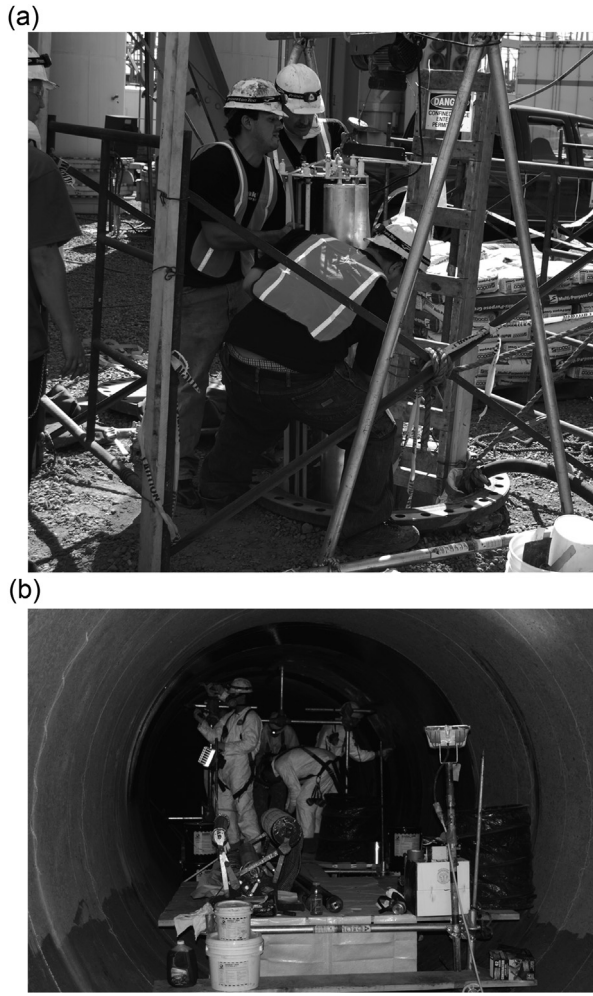

Figure 3.2 (a) Collapsible saturator machine is lowered into the pipe through a 24-in (610-mm) access port and (b) it is reassembled inside the 120-in (3-m) pipe.

FRP products are anisotropic since their strength depends on the orientation and amount of fiber in each direction. This is a unique advantage in repair of pipelines where most of the stresses from internal pressure are in the hoop direction. Thus, a larger portion of the fibers will be oriented in the hoop direction. Curves and change of direction also result in thrusts along the length of the pipe. If required, these stresses will be resisted with fibers that are aligned along the axis of the pipe. As part of the design, the number of layers of fabric and orientation of the fibers are specified.

Carbon fabrics can be manufactured as unidirectional or bidirectional and are supplied in rolls 12−50 in (300−1300 mm) wide and 200−300 ft (60−90 m) long. In unidirectional fabrics, the bulk of the fibers is positioned in a single direction, normally along the length of the fabric. There may be a small amount of fibers in the transverse direction to hold the longitudinal fibers together, but the limited strength of these fibers is often ignored in design. If necessary, one or more layers of fabric will be applied in the longitudinal direction to provide strength in that direction. These strips will be several meters long, and adjacent bands of fabric can be butt jointed around the circumference of the pipe to cover the entire pipe circumference. The ends of these strips must be overlapped along the length of pipe to ensure development of the full strength of the fibers in that direction. The fabrics to be applied in the hoop direction are typically cut in lengths equal to the circumference of the pipe plus the necessary overlap length for development of the forces in the fibers. Each strip is applied in the hoop direction, and adjacent strips can be butt jointed along the length of the pipe. However, the final layer of the fabric that is applied in the hoop direction must include overlaps between adjacent strips of fabric. These overlaps in the hoop direction must be positioned in the direction of the flow and act as shingles to ensure that water flow under high pressure will not be able to get behind the fabric and potentially cause separation of the fabric from the pipe (Figure 3.3).

Figure 3.3 Worker installing 24-in (610-mm) wide strips of carbon fabric in a curved section of a 42-in (1065-mm) steel pipe with overlapping joints in the direction of flow.

Biaxial fabrics can be manufactured with different amounts of fibers oriented in the longitudinal and transverse directions. Economical considerations require these fabrics to be supplied in wider rolls, closer to 50 in (1300 mm). These fabrics are typically applied in bands in the hoop direction with sufficient overlap in both the hoop and longitudinal directions. In this case, the overlap length along the length of the pipe is not only required to provide the aforementioned shingle effect but also to ensure that the strength of the fibers along the length of the pipe is fully developed.

In the above applications, care must be taken during the installation process to ensure that the fibers are properly oriented (in the hoop or longitudinal direction). Misaligned or loosely placed fibers lower the strength and stiffness of the lining system. The flexibility of the fabrics in wet lay-up application allows accommodation of curves and bends in pipes (Figures 3.3 and 3.4). Additional layers of thickened epoxy may be necessary on the upper half of the pipe between the fabric layers to make sure that the saturated fabrics stay in position while the epoxy cures. The crew must also ensure that no air is entrapped between the fabric layers. Design specifications provide solutions for repair of air bubbles that depend on the size and frequency of such occurrence. In addition, witness panels of the saturated carbon fabric are periodically produced on the job site and saved for future testing to make sure that the materials used on site meet the project specifications. These tests must be timed to ensure that the results become available before the project is completed in case any remedial action is necessary.

As described earlier, one of the concerns about repair of pipelines with FRP is the potential for the fluids to get between the FRP and the host pipe, which could cause separation of the FRP from the pipe. For the most part, this can be prevented by providing a small overlap between adjacent strips of fabric in the direction of the flow, similar to roof shingles. However, this method leaves one of the edges of the most upstream strip of fabric unprotected. For concrete pipes or steel pipes where a cementitious lining is present, a circumferential joint can be cut into the cement lining and the edge of the fabric can be pressed against the steel pipe; the joint is then filled with a mix of thickened epoxy and sand to provide a smooth finish that will hide the leading edge of the fabric. When no mortar lining is present, a mechanical seal can be

Figure 3.4 Application of top coat to a large-diameter pipe.

used to protect the free end of the fabric and press it tightly against the host pipe. Products such as WEKO-SEAL perform well for such applications.

Many projects may include the application of a final topcoat of epoxy to the finished installation (Figure 3.4). This coating is often supplied in a lighter color and provides further chemical protection for the FRP system, covering any pinholes that may have been left during fabric installation.

3.2 FRP laminates

The wet lay-up system described above has been the primary technique for repair of structures and pipelines with FRP for over two decades. However, recently, a new generation of FRP laminates has been introduced that offers major advantages in certain applications (Ehsani, 2010); these products are available under the trademark PipeMedic®. The FRP laminates are constructed with specially designed equipment. Sheets of carbon or glass fabric up to 60 in (1.5 m) wide are saturated with resin and passed through a press that applies uniform heat and pressure to produce the PipeMedic® laminates (Figures 3.5 and 3.6). These laminates offer several major advantages compared to fabrics and other narrower laminate strips that have been available to date:

1. Using a combination of unidirectional and/or biaxial fabrics, the laminates provide strength in both longitudinal and transverse directions. The range of the tensile strength of PipeMedic® laminates is 60−155 ksi (415−1070 MPa).
2. The laminates are much thinner than conventional laminate strips; with a thickness as small as 0.01 in (0.25 mm), they can be easily coiled to fit a pipe with a diameter of 3 in (75 mm).
3. The laminates are manufactured in plants under high-quality control standards, which improves the quality of the finished construction.
4. The repairs can be completed much faster in the field.
5. The strength of the laminates can be tested *prior* to installation; in contrast, when the wet lay-up method is used, samples are made daily in the field for future testing and any defective material will not be revealed for several days until the samples are tested; this makes remedial measures difficult to implement.
6. The number and pattern of the layers of fabrics in PipeMedic® laminates can be adjusted to produce an endless array of customized products that can significantly save construction time and money.

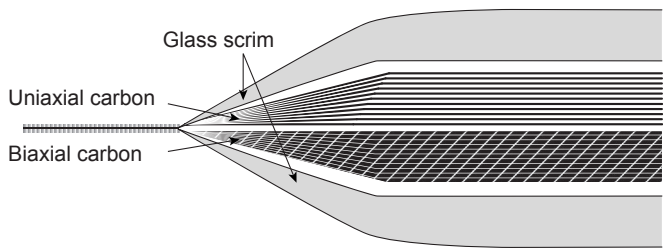

Figure 3.5 PipeMedic® laminates may be constructed with multiple layers of unidirectional or biaxial fabrics.

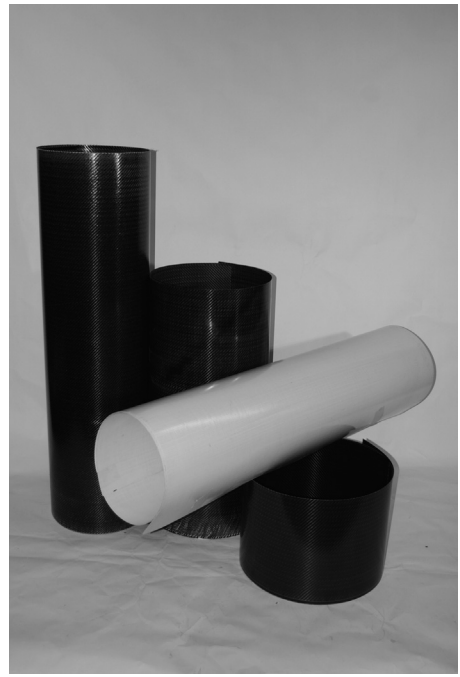

Figure 3.6 PipeMedic® glass and carbon laminate sheets are up to 60 in (1.5 m) wide and are flexible for insertion in small-diameter pipes.

As an example, the strength requirements for a steel pipe may require a layer of unidirectional carbon fabric along the length of the pipe and two layers of unidirectional carbon fabric in the hoop direction. At the same time, to prevent galvanic corrosion an additional layer of glass fabric must be applied as a dielectric barrier. Using PipeMedic® laminates, this is accomplished by sandwiching the carbon fabrics between the two thin layers of glass scrim. Thus, in this example, a single layer of FRP laminate can address both the structural (i.e., strength) requirements and the durability considerations of the project. In contrast, wet lay-up FRP would require installation of four layers in the field: one layer of glass fabric and three layers of unidirectional carbon fabric.

The laminates are particularly suited for repair of smaller pipes where man entry is not possible. Such pipes operating under high pressure are frequently found in the oil and gas industries. The first field application of PipeMedic® laminates to repair a gas pipe received the 2011 Trenchless Technology Project of the Year Award (Bueno, 2011). The design considerations and applications of these laminates are best described by introducing the reader to this unique project.

As gas utilities try to limit leakage and improve flow in their transmission lines, they have turned to lining the pipes with very thin liners. At times, operational requirements for these companies call for abandoning a drip pot or a T-connection in a transmission line. When these pipes are lined with a nonstructural liner, the pressure of the gas

passing through the liner causes failure of the liner over the abandoned T-connections or drip pots. In other words, the nonstructural liner can only be installed if it is fully supported by a structural pipe along its entire length. In many cases, these abandoned T's or drip pots are located under developed areas or buildings that make access very difficult, and the option of digging and replacing the pipe is not a viable solution.

Recently, faced with a similar problem, Public Service Electric and Gas (PSE&G) of New Jersey chose to evaluate FRP laminate as a possible solution for this problem. An exact replica of the field condition was constructed by placing two sections of 16-in (400-mm)-diameter steel pipes a distance of 24 in (610 mm) apart (Figure 3.7(a)).

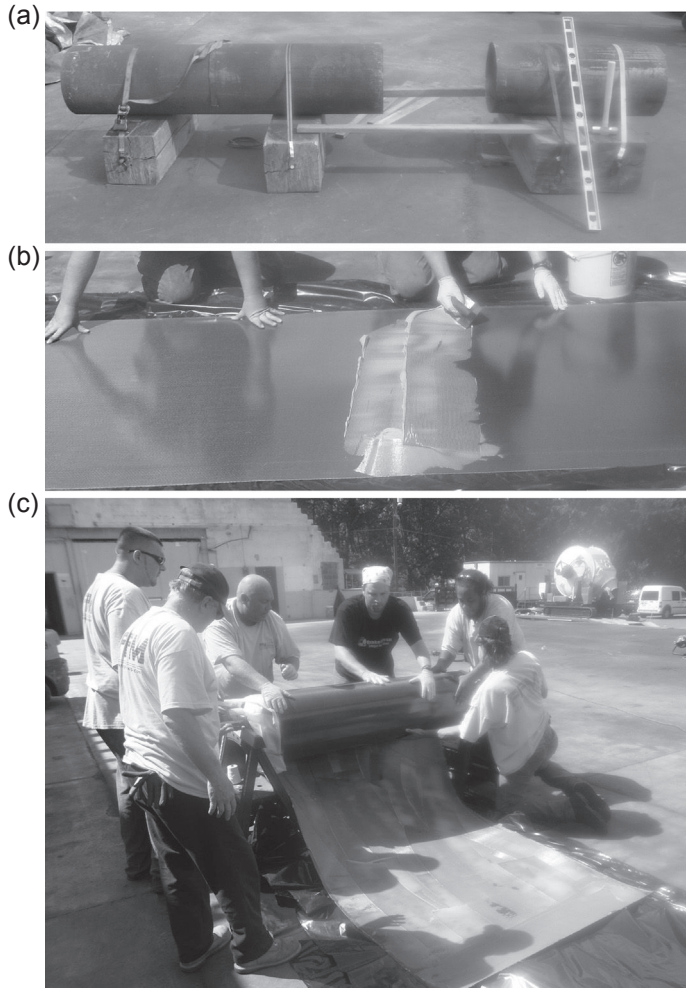

Figure 3.7 Preparation of test pipe: (a) 16-in pipes with 24-in gap, (b) applying resin to fiber-reinforced polymer laminate, (c) wrapping it around a packer, (d) inserting packer into the pipe and guiding it to position, (e) inflating packer, and (f) finished sample.

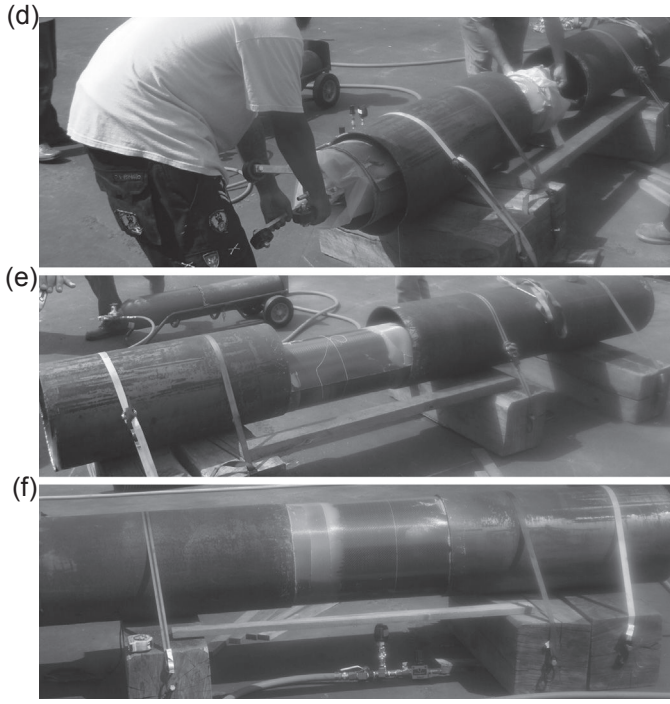

Figure 3.7 Continued.

The 24 in (610 mm) of separation represents the width of an existing drip pot that was to be abandoned and bridged over. A piece of a carbon PipeMedic® laminate 4 ft wide × 13.25 ft long (1.2 × 4 m) was cut; this length was long enough to create a 3-ply shell inside the 16-in pipe with an 8-in (200 mm) overlap beyond the starting point. The overlapping portions of the laminate were coated with a special epoxy paste, and the laminate was coiled around a packer (Figure 3.7(c)) in an approximately 13−14-in (350-mm) cylinder. Packers are commonly used in pipe repair projects; they are inflatable bladders that can be used to transport and deliver the repair material to the repair point inside the pipe. The three wheels at each end make sure that the packer remains centered in the pipe and that the epoxy on the outer surface of the laminate does not come in contact with the pipe en route to the repair point. A video of this installation is available on http://goo.gl/Dqix74.

The packer was inserted into the pipe from one end (Figure 3.7(d)) and guided to the repair position (Figure 3.7(e)). At that point the bladder was inflated allowing the super laminate to unravel and seat tightly against the host pipe; the epoxy applied to the super laminate acts as a lubricant that allows the layers of laminate to slide against each other. This resulted in a 48-in (1.2-m)-long three-ply tube (or pipe) that was supported only by the host steel pipe over a 12-in (300-mm) length at each end. After the epoxy was cured, the packer was deflated and removed from the pipe.

The design of the laminate for such a unique application was challenging, and the product had to meet the following criteria:

1. Because the host pipe was made of steel, to avoid galvanic corrosion the pipe first had to be lined with a glass fabric. This was satisfied by including very thin glass scrims on both faces of the FRP laminate.
2. During service, the internal pressure of the pipe causes both hoop stresses and stresses along the 24-in span of the liner. Thus, a laminate with strength in two directions (biaxial) was required.
3. During the installation process, the laminate must be stiff enough not to deform under the pressure of the packer. An FRP fabric such as a wet lay-up application could not be used in this arrangement because during the installation process, as the packer is inflated the FRP fabric would expand with the packer, creating a bulging bubble over the 24-in gap!

The combination of these design requirements could only be satisfied with a specially designed biaxial PipeMedic® carbon laminate. Independent testing of the repaired pipe was carried out by the Gas Technology Institute (GTI). The requirements for the lining system as specified in ASTM F2207 (2006) include performing a test at a pressure not less than twice the certified maximum allowable operating pressure (MAOP) of the pipeline for a minimum of 1 h without leakage. For these gas mains, MAOP is 60 psig (4.1 bar). The ends of the test pipe shown in Figure 3.7 were capped, and the pipe was subjected to hydrostatic pressure that was increased every 2 h by 50 psi up to the maximum pressure of 250 psi (17.2 bar), more than four times the MAOP (Figure 3.8). The measured strain in the FRP laminate was less than 25% of its tensile strength at this pressure (Farrag, 2011), so the repair system could resist a pressure of nearly 1000 psi (69 bar). As noted in Figure 3.8, significant strain was recorded in the longitudinal direction as well. This clearly points to the need for a biaxial laminate capable of resisting stresses in both longitudinal and hoop directions.

GTI also constructed and tested samples for 6- and 12-in (150 and 300 mm)-diameter steel pipes that are shown in Figure 3.8. These pipes were repaired with a more flexible biaxial glass PipeMedic® laminate that could be inserted in these smaller pipes. All of those tests were also successful; the results are available to GTI-affiliate member organizations for potential similar applications worldwide.

The first field application of this technique involved creating an FRP laminate bridge across a steel pipe that was buried under a railroad track. An access pit was created in a convenient location in a nearby parking lot, and a section of the pipe was cut and removed. The cleaning and repair procedure were carried out remotely from this location while the railroad remained fully operational (Carbone et al., 2012). The various stages of repair are shown in Figure 3.9. For this particular application, a robotic cutting tool had to be launched to cut the standpipe that was in the middle of the drip pot to provide clear access through the pipe. The three-ply installed laminate as shown in Figure 3.9(e) is about 0.1 in (2.5 mm) thick and barely visible after the nonstructural liner was installed (Figure 3.9(f)). Following the first installation, more than thirty similar repairs have been successfully completed.

The potential for using these laminates to repair steel pipes where man entry is not possible is tremendous. The September 9, 2010, explosion of the 30-in (750-mm)-diameter gas pipe in San Bruno, California, that resulted in eight dead and many more casualties and loss of property is a recent reminder of the devastating results of such failures. A detailed investigation by the National Transportation Safety Board noted brittle

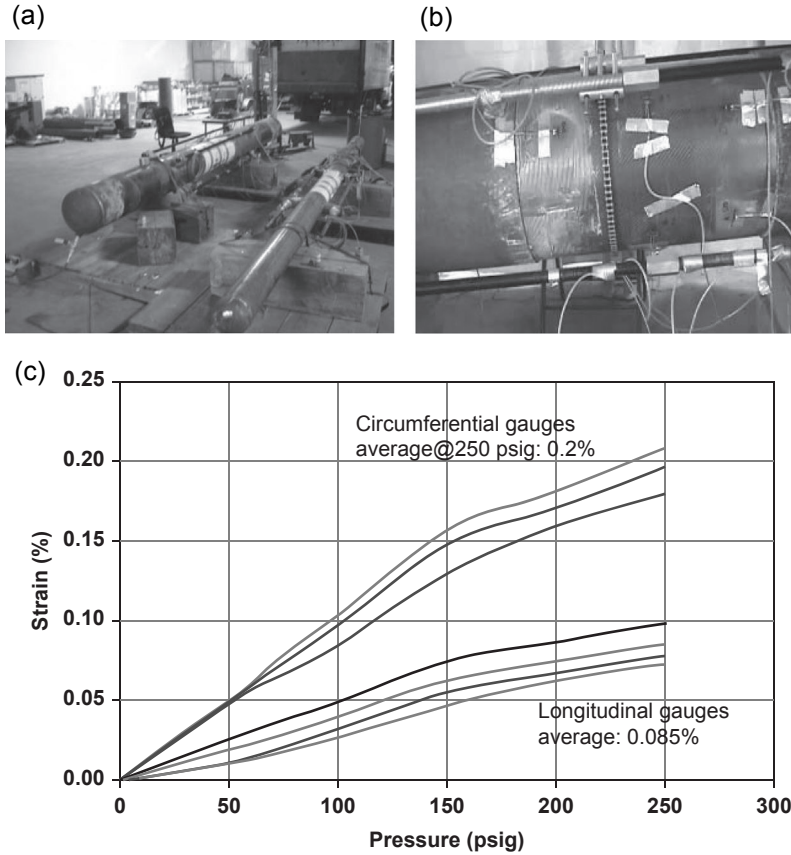

Figure 3.8 (a) Test setup, (b) close-up view of instrumentation, and (c) measured strains for a steel pipe retrofitted with PipeMedic® laminate and tested at Gas Technology Institute.

pipes, old welds, corrosion, or widening of cracks as potential causes of failure (NTSB, 2011). As reported by the *San Francisco Chronicle*, Pacific Gas and Electric estimated the cost of complying with the mandated repair of its pipes in California alone to exceed $11 billion (Van Derbeken, 2012).

The GTI tests have demonstrated the effectiveness of the FRP laminates in a significantly more critical application where an entire section of the pipe was missing and had to be bridged. Clearly, those same laminates can easily provide the necessary strength for a pipe weakened by small cracks or defective welds. The strength of the laminates for such repairs has already been verified by the GTI. Improved delivery systems are required to repair the thousands of miles of such pipes in a timely manner. One possibility is the development of robots that could install these laminates in a continuous helical manner inside the pipe. The PipeMedic® laminates could incorporate adhesives on one face that is covered by a protective film. The robot can remove the film before pressing the carbon laminate against the pipe surface. This will simplify the installation significantly by eliminating the need for transporting and applying epoxies inside the pipe.

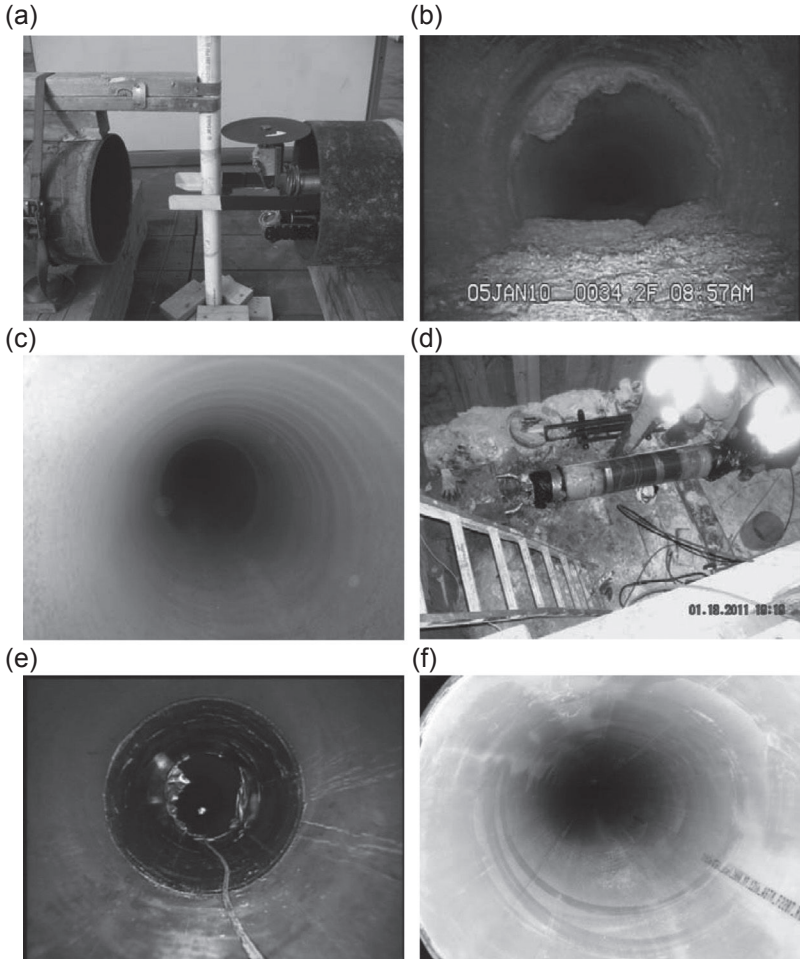

Figure 3.9 Field installation: (a) robot to cut the standpipe, (b) debris-laden pipe, (c) cleaned pipe, (d) laminate and packer assembly, (e) laminate installed across the drip pot, and (f) completed installation.

3.3 Sandwich composite pipe

In recent years, there has been a tendency toward designing liners where the liner not only resists the internal pressure of the pipe but also the traffic and soil pressure. The latter assumes that at some point in the future the host pipe will fully disintegrate. While this may pose an extremely conservative view, it essentially requires building a new pipe inside the old pipe that could resist all internal and external loads independently of the host pipe.

The design of such pipes is controlled by buckling of the liner (Moser and Folkman, 2008). The compressive strength of FRP products is lower than their tensile strength,

and the thin FRP sheets have little stiffness. That leads to installing layer after layer of carbon fabric inside a pressure pipe to create a thick enough liner with adequate stiffness. For such repairs, it is common to see designs calling for 10 or more layers of carbon FRP. Both the high cost of repair and the long installation time required to accomplish the repair are major shortcomings of this system. It is emphasized that many of these repairs must be performed under very tight shutdown schedules. Therefore, shortening the repair time is of extreme value to the owners of these pipes.

The other option for repair of pressure pipes is to slip-line them with a new steel pipe. In this case, a section of the host pipe is removed to allow a segment of a new pipe to be inserted into the pipe. Next, an additional segment of pipe is welded in the field to the first segment and the two are pushed together into the pipe, using special rigs to push or pull the heavy pipe assemblies. The process continues as long as the pipe is running straight; bends in the pipe must be handled differently and may require cutting a new trench for access. Once the new pipe is in place, the annular space between that and the host pipe is filled with grout. A major shortcoming of this technique is that the new pipe is often one size (e.g., 6-in diameter) smaller than the host pipe, and this leads to a significant loss of capacity compared to the original pipe. The new steel liner must also be protected against corrosion.

To overcome the above shortcomings, a new honeycomb-FRP pipe has been developed (Ehsani, 2012b) that is marketed under the trade name StifPipe® (Figure 3.10). For these applications, the structure of a pipe or liner must offer two primary attributes: (1) sufficient strength and stiffness so it can be handled during installation and resist gravity loads safely and (2) adequate strength to resist the internal fluid pressure. These can be separately addressed in StifPipe® that uses the more costly carbon or glass FRP materials as the skin and the relatively inexpensive lightweight polypropylene honeycomb panels as the core. In this case, the carbon FRP fabric applied to the interior surface of StifPipe® will resist hoop and thrust loads, similar to the wet lay-up application described earlier. The lightweight honeycomb core will be used as a filler material, like the web of an I-beam, and additional layer(s) of glass or carbon FRP will be used as the outer skin of the pipe (Figure 3.10).

As shown in Figure 3.11, when a 0.1-in (2.5-mm)-thick carbon FRP is sandwiched between a 0.3-in (7.5-mm)-thick honeycomb (making the total thickness 0.4 in (10 mm)), the stiffness of the panel is increased 37 times while there is only a 9%

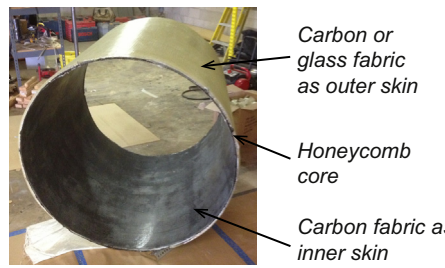

Figure 3.10 Different layers comprising the wall of the honeycomb-FRP (fiber-reinforced polymer) pipe.

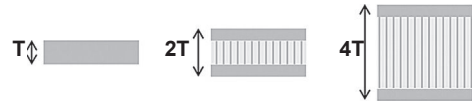

Relative stiffness	1	7	37
weight (pounds/ft^2)	0.910	0.978	0.994

Figure 3.11 Comparison of stiffness of carbon fiber-reinforced polymer (FRP) with carbon FRP applied as skin reinforcement to a lightweight polypropylene honeycomb core.

increase in weight! This principle forms the basis of the design of the newly developed StifPipe®. The pipe can be designed for virtually any internal pressure by adding additional layers of carbon FRP on the inner surface of the pipe. The lightweight and inexpensive polypropylene honeycomb provides the stiffness of the pipe. A more economical glass fabric can also be used as the outer skin to provide rigidity for the pipe.

A typical honeycomb pipe weighs 10−15% of a conventional fiberglass pipe, and is significantly lighter when compared to a steel or concrete pipe. All of the aforementioned factors contribute to the low cost of this pipe. The sections of this pipe will be built in advance and will be used to slip-line the existing deteriorated steel pipe in the field.

In its simplest form, the construction of a honeycomb-FRP pipe begins by building a mandrel of the desired size and shape; in Figure 3.12, a CMP is used as the mandrel.

Figure 3.12 Steps in the construction of StifPipe®: (a) corrugated metal pipe used as mandrel, (b) carbon fabric wrapped around mandrel, and (c) pipe allowed to cure in ambient condition.

Alternatively, a collapsible mandrel can be designed to allow easy removal of the finished pipe. The mandrel is covered with a nonbonding release material (Figure 3.12(a)). Depending on the design requirements for the internal pressure rating of the pipe, one or more layers of carbon fabric saturated with resin are wrapped around the mandrel (Figure 3.12(b)). These fabrics typically have a thickness of less than 0.05 in (1.3 mm) per layer. Next, the honeycomb sheet is coated with epoxy and wrapped around the carbon fabric; the thickness of the honeycomb typically varies between 0.5 and 1.5 in (13−38 mm), which is determined based on the overall stiffness requirements for the pipe. Additional layers of carbon or glass fabric saturated with epoxy are wrapped on the outside of the honeycomb. The pipe section is cured under ambient conditions before it is removed from the mandrel (Figure 3.12(c)). If necessary, the curing process can be accelerated by heating the assembly to a moderate temperature, for example, 150 °F (65 °C).

Honeycomb-FRP pipes can be installed using the slip-lining approach. The pipe segments will be constructed offsite and delivered to the job site before the scheduled repair begins. The length of the StifPipe® segments will be dependent on the allowable size of the access pit, and the pipe cross-section will be slightly smaller than the host pipe. As shown in Figure 3.13(a), a 4-ft (1220 mm)-long, 46-in (1170-mm)-diameter pipe section weighs only 50 pounds (22.7 kg) and can be easily lifted by

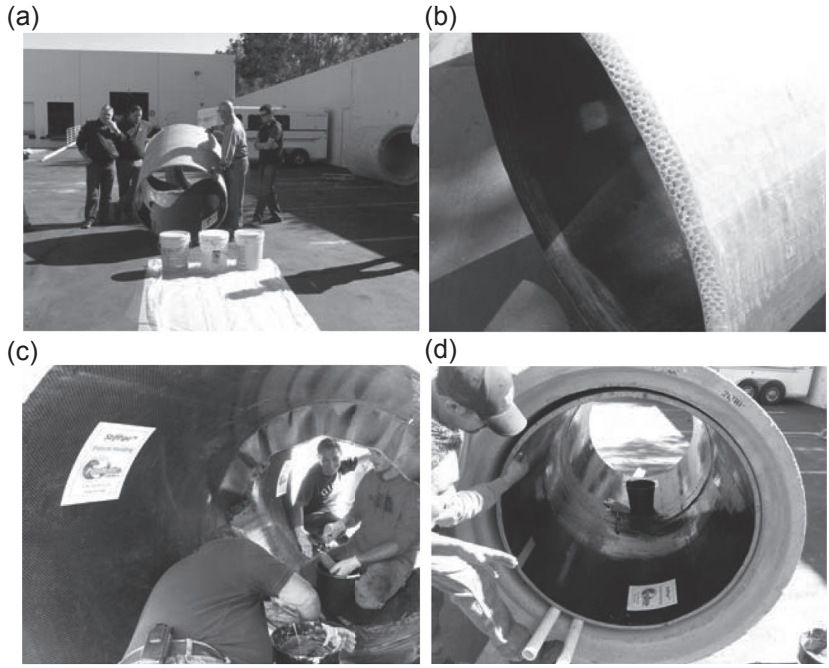

Figure 3.13 Installation steps: (a) lightweight pipe is hand-carried into the host pipe, (b) beveled end, (c) fabric band is saturated to complete the joint, and (d) small annular space between the liner and host pipe can be grouted.

hand and carried into the host pipe. The segments will be positioned sequentially along the pipe (Figure 3.13(c)), and adjacent segments will be connected together with a special detail described below to create a long continuous pipe (Figure 3.13(d)). The small annular space between the liner and the host pipe will be filled with resin or grout to join the two pipes together.

The ends of StifPipe® sections can be connected in a number of ways. One such detail includes a beveled edge shown in Figures 3.13(b) and 3.14(a). One end of the pipe has a 2-in cured FRP tab on the exterior face and a 6-in dry carbon fabric on the interior face (Figure 3.12(c)). Once the two beveled ends of the pipe are mated together in the field, the dry fabric is saturated with resin and bonded to the adjacent pipe section to create a smooth overlapping joint in the direction of the flow

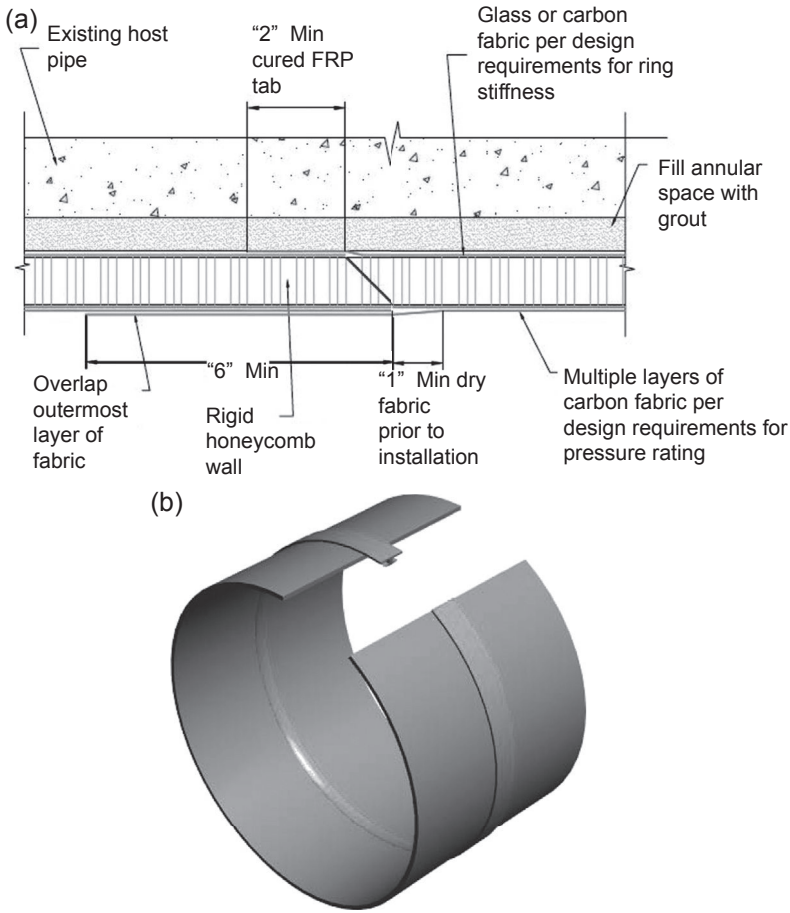

Figure 3.14 Connection details at ends of StifPipe®: (a) wet lay-up and (b) rubber gasket.

(Figure 3.13(c) and (d)). The 2-in (50-mm)-cured FRP tab on the outside prevents the grout from getting into the pipe.

This connection is good for pipes large enough to allow man entry. Other gasket connections (Figure 3.14(b)) can be used for smaller diameter pipes or when man entry is not desirable.

For repair of smaller diameter pipes and culverts, the connection between pipe segments can be made by using a slightly larger size StifPipe® (Figure 3.15(a)) that can be cut into short segments and used as a sleeve connection in the field. The light segments of StifPipe® can be pushed into the culvert with no need for special equipment (Figure 3.15(b)). This type of connection allows for installation when there is standing or flowing water in the pipe.

CMP culverts are widely used in the construction of roadways. Many of these pipes are deteriorated and replacement will cause significant traffic disruption. Because the majority of these pipes have an oval-shaped cross-section (Figure 3.16), slip-lining of these culverts with standard cylindrical pipes leads to a significant loss of cross-section and flow. A possible alternative is to use a custom-made honeycomb-FRP pipe that matches the shape of the culvert. These lightweight sections can be inserted in the host culvert and the annular space can be filled with grout to provide a new structural pipe. A video of a recently completed project using this technology is available online (http://goo.gl/XfQCV).

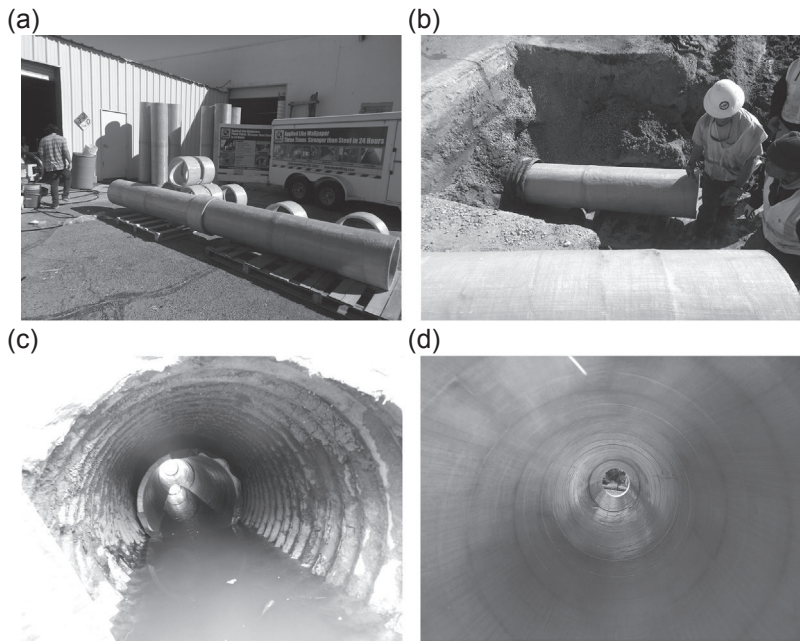

Figure 3.15 StifPipe™ used to repair a deteriorated corrugated metal pipe culvert: (a) pipe sections and sleeve connections, (b) pipe being inserted into culvert, (c) standing water in pipe during installation, and (d) inside view of installed pipe.

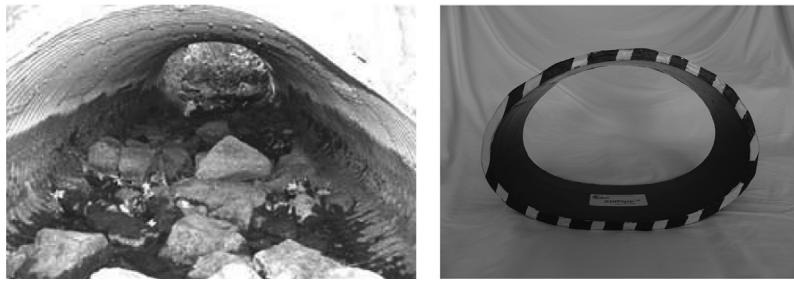

Figure 3.16 (a) A corroded oval-shaped corrugated metal pipe culvert requiring repair and (b) a custom-made honeycomb-FRP (fiber-reinforced polymer) pipe can match the shape of the culvert to minimize the loss of flow.

3.4 Supported penstocks

A category of steel pipes and penstocks that are supported at discrete points along their length may require special considerations (ASCE-79, 1993). These penstocks typically consist of very large-diameter steel pipes that were manufactured on site by either welding or riveting steel plates together. The penstocks are usually supported on saddles or ring girders. The saddles support only a fraction of the full perimeter of the penstock, generally between 90° and 180°, while the ring girders support the full perimeter. The main function of these supports is to provide stiffness for the penstock and support for the pipe as a multispan beam. Ring girders allow the penstock to span fairly long distances (100 ft (30 m) or more) compared to saddle-type supports (40 ft (12 m) or less). The presence of these supports and the loading condition introduce unique stresses that are beyond the scope of this writing. ASCE-79 (1993) provides a comprehensive treatment of these pipes.

In general, there are very high stress concentrations at or near the supports, which demand an unusually large amount of FRP. In a recent project where the retrofit of an 18-ft (5.5-m)-diameter penstock was being considered, these regions required as many as 30 layers of carbon FRP to achieve the required strength. An alternative economical approach for this project was considered whereby a layer of gunite could be sprayed on the inside of the pipe. Shear studs were designed to provide full composite action between the steel pipe and the concrete. This combination of steel-concrete composite section could resist the stresses in the vicinity of the support saddles. To provide resistance against internal pressure of the pipe, three layers of carbon FRP was found to be sufficient. In addition to providing hoop strength, the carbon FRP layers provide a barrier against moisture intrusion and will significantly reduce future corrosion of the steel pipe from inside.

3.5 Repair costs

Many engineers assume that the cost of repair of pipes with carbon FRP is very high and therefore they may not consider such repair as an alternative. The fact is that when

all attributes of this system are considered, including short repair time, little or no digging of trenches, the versatility of the materials that allows them to be used on pipes of any shape and size, the FRP option can be quite attractive. Depending on the size and complexity of the project, carbon FRP fabric can be installed in most industrial settings for about $25−$30 per square foot per layer of fabric. This cost does not include any surface cleaning or other repairs that may be necessary before the fabric is applied. A major factor influencing this cost is the number of access points to the pipes and their proximity to the repair location. For smaller diameter pipes with few access points, the time required to deliver the saturated fabric to the installing crew can reduce the production rate and therefore increase the repair cost.

As the required number of layers of fabric increases, it is obvious that the cost of such multilayered FRP systems could make the use of the wet lay-up system less attractive. This may be the case, for example, when several layers of carbon FRP are required to create a free-standing pipe that could resist all internal and external gravity loads. In such instances, other FRP systems such as StifPipe® that was discussed earlier may be more suitable. To demonstrate this point, a recent case study follows.

A recent project for rehabilitation of over 5800 ft (1770 m) of a 36-in (910-mm)-diameter pipe required two layers of carbon fabric to resist the internal pressure. However, the client's requirement to design the liner as a "stand-alone" Class IV liner capable of resisting both internal and external (gravity) loads resulted in six layers of carbon fabric. To compare the effectiveness of the honeycomb-FRP pipe with the wet lay-up option, two samples of a 36-in pipe were constructed. The first sample followed the conventional wet lay-up repair and consisted of six layers of unidirectional carbon fabric applied on top of one another, resulting in a liner thickness of 0.30 in (7.6 mm). The second sample consisted of a single layer of honeycomb core sandwiched between two layers of glass fabric, one on each face. This liner had an average thickness of 0.71 in (18 mm) (Figure 3.17(a)). The StifPipe® was conservatively constructed with glass fabric that has a stiffness nearly one-third that of the carbon fabric.

The standard test for determining stiffness of liners is provided by ASTM D2412 (2002). Figure 3.17(b) shows the setup for such tests. The load vs deflection results for both pipe liners are presented in Figure 3.17(c). As can be seen, the honeycomb-FRP pipe has a stiffness that is 2.1 times that of the conventional CFRP system with six layers of carbon fabric.

The actual StifPipe® for this project will include a single layer of glass on the outside. However, on the inside, two layers of carbon fabric will be used to meet the design requirements for resisting the internal pressure of the pipe. This will increase the stiffness of the honeycomb pipe even beyond what is shown in these tests with little change in the thickness of the pipe.

The honeycomb-FRP pipe will reduce the pipe diameter by a slight amount over the wet lay-up system. However, considering all the other significant advantages that are detailed below, the honeycomb-FRP pipe can be the preferred option for repair of many pressurized pipes.

As shown in Table 1, the use of honeycomb-FRP pipe for this project would result in over 75% cost savings and 38 fewer days to complete the repair. For nearly all

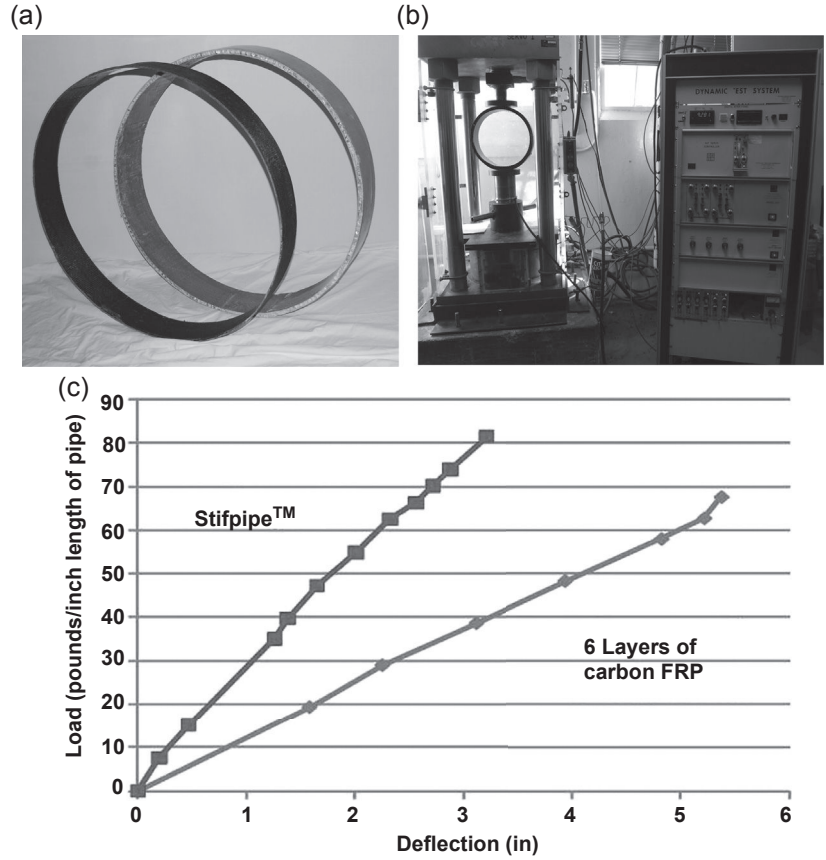

Figure 3.17 Comparison of 36-in diameter carbon fiber-reinforced polymer (FRP) pipe with honeycomb-FRP pipe: (a) samples, (b) test setup, and (c) load versus deflection.

Table 3.1 Comparison of time and cost to repair a pipe with wet layup fabric vs. honeycomb-FRP

	Wet layup	Honeycomb-FRP
Layers of fabric	6 Carbon	2 Carbon + honeycomb core + 1 glass
Work is performed	All inside the pipe	Off-site; assembled inside the pipe
Man-hours to complete	20,500[a]	3,500[b]
Days the pipeline will be out of service for repairs	45[a]	15[b]
Estimated total cost	$6,500,000	$2,500,000

[a]All work hours must be performed during the complete shut-down of pipe.
[b]Most of the work hour are performed outside of the shut-down window of pipe.

clients, the shorter repair time is of great value for which they are usually willing to pay a premium.

The above calculations account for the time that is needed to cut trenches for accessing the pipe and repair of those trenches. A further advantage of the honeycomb-FRP solution is that the working conditions for building the pipe segments are significantly superior compared to that for the wet lay-up repair. This results in a higher quality product. Furthermore, the actual pipe sections can be tested in advance to make sure that they meet the specifications before they are installed.

References

ASCE-79, 1993. Steel Penstocks. American Society of Civil Engineers, 467 pp.

ASTM D2412, 2002. Standard Test Method for Determination of External Loading Characteristics of Plastic Pipe by Parallel-Plate Loading. American Society for Testing of Materials.

ASTM F2207, 2006. Standard Specification for Cured-in-Place Lining System for Rehabilitation of Metallic Gas Pipe. American Society for Testing of Materials.

Bueno, S., 2011. Rehab winner: CIPP of leaking high-pressure cast iron main. Trenchless Technology 20 (11), 22−24.

Carbone, M., Ehsani, M., Ragula, G., 2012. Winter Wonderland Does Wonders to CIPP Renewal of a High Pressure Gas Main in NJ. North American Society for Trenchless Technology, No-Dig Show, Nashville, TN.

Ehsani, M., March 2010. FRP super laminates: transforming the future of repair and retrofit with FRP. Concrete International, ACI 32 (03), 49−53.

Ehsani, M., 2012a. A new generation of FRP laminates for repair of pipelines in gas industry. In: ASCE Pipelines Conference, Miami, FL, August 2012.

Ehsani, M., 2012b. Introducing a new honeycomb-FRP pipe. In: ASCE Pipelines Conference, Miami, FL, August 2012.

Farrag, K., June 2011. Testing of PipeMedic™ Fiber Reinforced Polymer for Rehabilitation of Steel Pipes. Final Report. Gas Technology Institute, 16 pp.

Moser, A.P., Folkman, S., 2008. Buried Pipe Design, third ed. McGraw Hill. 601 pp.

National Transportation Safety Board, 2011. Pipeline Accident Report: Pacific Gas and Electric Company Natural Gas Transmission Pipeline Rupture and Fire, San Bruno, California, September 9, 2010. Report No. NTSB/PAR-11/01. NTSB, Washington, DC, 153 pp.

Van Derbeken, J., March 20, 2012. PG&E: Pipeline Upgrade Could Top $11 Billion. San Francisco Chronicle.

This page intentionally left blank

Comparison of fiber-reinforced polymer wrapping versus steel sleeves for repair of pipelines

4

W.A. Bruce
Det Norske Veritas (USA), Inc., Dublin, OH, USA

4.1 Introduction

When areas of corrosion or other damage on operating pipelines are identified, there are often significant economic and environmental incentives for performing repair without removing the pipeline from service. From an economic viewpoint, a shutdown involves revenue loss from the loss of pipeline throughput. In addition, for gas transmission pipelines, a shutdown typically involves a significant quantity of gas that is lost to the atmosphere. Since methane is a so-called "greenhouse gas," there are also environmental incentives for avoiding the venting of large quantities of gas into the atmosphere.

When faced with the need to repair an operating pipeline, there are often a variety of in-service repair strategies available to pipeline operators for a given repair situation. While the use of nonmetallic composite materials to repair damage has increased in recent years, the predominant method of reinforcing damage in cross-country pipelines is to install a full-encirclement steel sleeve. The use of steel sleeves, which is a mature technology, has some advantages over the use of composite materials for many applications, in terms of both performance and cost.

4.2 Background

The use of full-encirclement steel sleeves for pipeline repair was developed during work led by Kiefner at Battelle Laboratories in the early 1970s (Kiefner and Duffy, 1974; Kiefner et al., 1978). There are two basic types of full-encirclement steel sleeves: Type A and Type B (Figures 4.1–4.3).

Type A sleeves simply encircle the pipeline and provide structural reinforcement of the defective area. To do this, they do not require sleeve-end fillet welds. Type B sleeves also encircle the pipeline and provide structural reinforcement, but since the ends are fillet welded to the pipeline, they can also contain pressure in the event that the defect is leaking or will eventually leak in subsequent service. The results of work at Battelle showed that steel sleeve repairs are capable of restoring the strength of a damaged pipeline to a pressure level in excess of a pressure that corresponds to 100% of the specified minimum yield strength of the line pipe steel. The results of this work led to the widespread use of full-encirclement steel sleeves for pipeline

Rehabilitation of Pipelines Using Fiber-reinforced Polymer (FRP) Composites. http://dx.doi.org/10.1016/B978-0-85709-684-5.00004-7

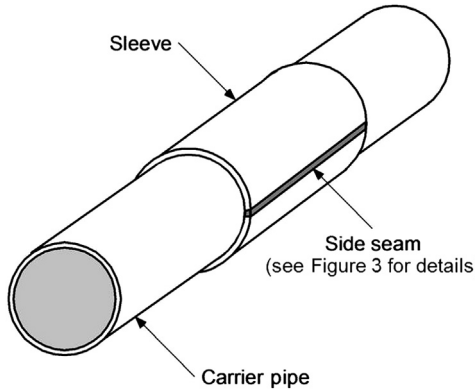

Figure 4.1 Type A full-encirclement repair sleeve: structural reinforcement.

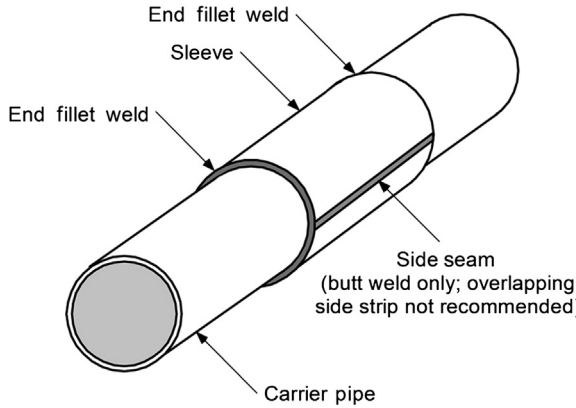

Figure 4.2 Type B full-encirclement repair sleeve: structural reinforcement and pressure containment.

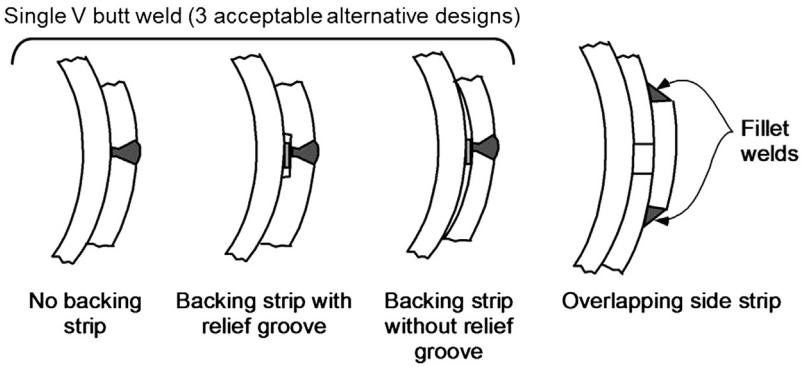

Figure 4.3 Longitudinal seam weld options.

repair. Prior to this, repair by cutting out and replacing the damaged segment was common.

The use of fiber-reinforced composite materials for pipeline repairs was developed during work at Southwest Research Institute and Battelle in the late 1980s (Fawley, 1994; Stephens and Kilinski, 1994). There are two basic types of composite repair systems: preformed (composite sleeves) and wet lay-up (composite wraps). The first commercially available system was Clock Spring®, which consists of an E-glass/polyester resin-based composite material preformed into a multilayer coil that is installed using an adhesive (Figure 4.4).

The use of wet lay-up systems for pipeline repair began in the early 1990s. These wet lay-up systems use either a resin-impregnated cloth that is activated by water in the field or a cloth that is saturated with epoxy resin in the field (Figure 4.5). The early

Figure 4.4 Installation of preformed composite sleeve (Clock Spring®).

Figure 4.5 Installation of wet lay-up composite wrap (Armor Plate® pipe wrap).

composite systems all use E-glass as the fiber material. The use of carbon fiber composite material as a substitute for E-glass for pipeline repair was introduced in the late 1990s (Alexander and Francini, 2006).

4.3 Principle of operation

The early work at Battelle showed that steel sleeves are effective because they restrain bulging, or accumulation of strain, in the defective area. Steel sleeves accomplish this while absorbing only 15–20% of the hoop stress in the carrier pipe. Steel sleeves are effective because the stiffness (elastic modulus) of the sleeve material is equivalent to that of the line pipe steel.

The mechanism by which composite materials reinforce areas of damage on operating pipelines is much more complex than that for steel sleeves because the tensile properties of composite materials are much different from those of steel (Figure 4.6). While the strength of composite materials is similar to that of line pipe steel, the elastic modulus—or stiffness—is significantly lower (Leewis and Laughlin, 2010). Steel has an elastic modulus (i.e., slope of the stress–strain curve in the elastic region) of approximately 30×10^6 psi (207 GPa), whereas E-glass-based composite materials typically have an elastic modulus of $2.5–6 \times 10^6$ psi (17–41 GPa). Carbon fiber–based composite materials typically have an elastic modulus that is approximately twice that of E-glass-based composites but still significantly less than that of steel. In addition, composite materials that consist of woven cloth initially have a lower modulus than composites composed of uniaxial fibers because the curved fibers in woven cloth must straighten upon loading (small arrows in Figure 4.6).

Because of the significantly reduced stiffness compared to steel, composite materials must experience a significantly greater amount of strain (elongation) before a

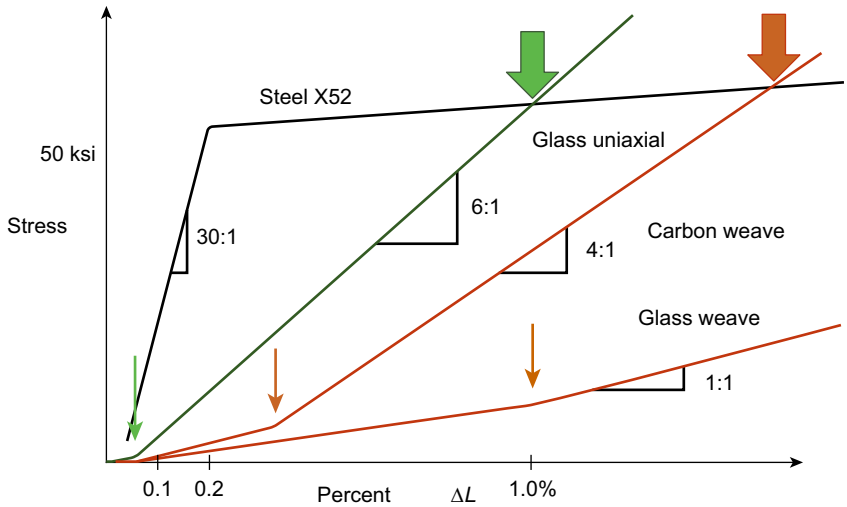

Figure 4.6 Tensile properties of composite materials compared to steel.

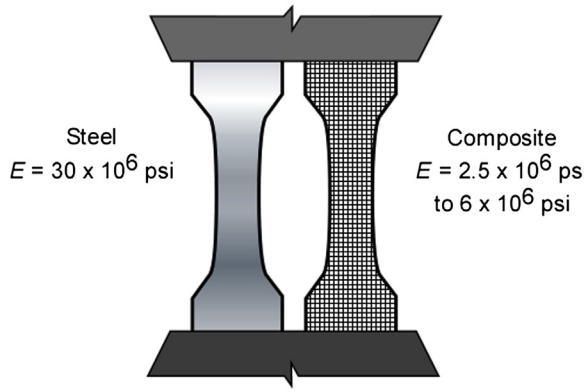

Figure 4.7 Steel and composite material tensile test specimens.

load equivalent to that of steel can be carried. When installed over steel, the composite is constrained by the steel and cannot carry a significant portion of the load until the steel begins to yield (large arrows in Figure 4.6). To illustrate this point, imagine two identically sized tensile test specimens, one composed of steel and the other composed of a fiber-reinforced composite material. When a given load is applied to each specimen separately, the specimen composed of fiber-reinforced composite material will elongate much more than the specimen composed of steel. Now imagine that both specimens are clamped in a tensile test machine side by side (Figure 4.7). It is easy to see that as a load is applied, the steel, which is much stiffer than the composite material, initially carries the majority of the load. The high stiffness of the steel specimen prevents the composite specimen from straining sufficiently to carry any significant portion of the load until the steel begins to yield.

For a composite material to prevent a defect in a pipeline from rupturing, the defect must typically plastically deform in the process of the load being transferred to the composite material. This concept may not be well understood by many users of composite repair materials for pipeline repair. Defects in brittle pipe material or brittle seam welds may only be able to tolerate a very small amount of plastic strain, which composite repairs are unable to protect against, before the defect grows and fails.

For both steel sleeves and composite repairs, a high-compressive strength filler material is used to fill defect areas so that load is effectively transferred to the repair material.

4.4 Comparison of capabilities

Composite repairs are often compared to Type B steel sleeves. As will be shown in this section, the applicability of composite repairs is most similar to that of Type A sleeves, whereas Type B sleeves have additional applicability over both composite repairs and Type A sleeves.

Table 4.1 is an excerpt from the Pipeline Research Council International (PRCI) *Pipeline Repair Manual* (Jaske et al., 2006), which provides an overview of pipeline

Table 4.1 Applicability of steel sleeves and composite repairs

Repair option for various types of defects			
Type of defect	**Type A sleeves**	**Composite repairs**	**Type B sleeves**
1. Leak (from any cause) or defect $> 0.8t$	No	No	Yes
2. External corrosion			
2a. Shallow-to-moderate pitting $< 0.8t$	Yes	Yes	Yes
2b. Deep pitting $\geq 0.8t$	No	No	Yes
2c. Selective seam attack	No	No	Yes[a]
3. Internal defect corrosion	Yes[b]	Yes[b]	Yes
4. Gouge of other metal loss on pipe body	Yes[c]	Yes[c]	Yes[d]
5. Arc burn, inclusion, or lamination	Yes	Yes[c]	Yes
6. Hard spot	Yes	No	Yes
7. Dent			
7a. Smooth dent	Yes[e]	Yes[e]	Yes
7b. Dent with stress concentrator on seam weld or pipe body	Yes[c,e,f]	Yes[c,e,f]	Yes
7c. Dent with stress concentrator on girth weld	No	No	Yes
8. Crack or cracking			
8a. Shallow cracking $< 0.4t$	Yes[c]	Yes[c]	Yes[a]
8b. Deep crack $> 0.4t$ and not more than $0.8t$	Yes[c]	Yes[c]	Yes[a]
9. Seam weld defect			
9a. Volumetric defect	Yes[c]	Yes[c]	Yes

Table 4.1 Continued

Repair option for various types of defects			
Type of defect	**Type A sleeves**	**Composite repairs**	**Type B sleeves**
9b. Linear defect	Yes[c]	Yes[c]	Yes[a]
9c. Defect in or near an ERW seam	No	No	Yes[a]
10. Girth weld defect	No	No	Yes
11. Wrinkle bend, buckle, or coupling	No	No	Yes[g]
12. Blisters, hydrogen-induced cracking	Yes	No	Yes

[a]Make sure defect length is subcritical or pressurize sleeve.
[b]Make sure that internal defect or corrosion does not continue to grow beyond acceptable limits.
[c]Repair may be used for defects less than 0.8t deep, provided that damaged material has been removed by grinding and removal has been verified by inspection.
[d]It is recommended that the damaged material be removed with removal verified by inspection or that the carrier pipe be tapped for this repair.
[e]Use of filler material in dent and engineering assessment of fatigue are recommended.
[f]Code and regulatory restrictions on maximum dent size should be followed.
[g]Sleeve should be designed and fabricated to special "pumpkin" configuration.

repair methods that can typically be applied to various types of defects. The first column in Table 4.1 lists 12 types of pipeline defects to which repairs are typically applied. The remaining columns provide information regarding the applicability of steel sleeves (Type A and Type B) and composite repairs.

The notation used in Table 4.1 is as follows:

- "Yes" indicates a repair method that typically can be used to permanently repair the type of defect. In some cases, a footnote(s) is added to indicate qualifying conditions for the method to be considered permanent.
- "No" indicates a repair method that typically is not recommended for repair of the type of defect. These are shaded in Table 4.1 for quick recognition.

Table 4.1 indicates that with very few exceptions the applicability of Type A sleeves and composite repairs is similar. The two exceptions are (1) repair of arc burns, where Type A sleeves can be used without complete removal of metallurgically altered material, whereas composite repairs cannot; and (2) repair of hydrogen-induced cracking and blistering, where Type A sleeves can be used and composite repairs cannot. Both of these exceptions are the result of composite materials having an elastic modulus that is significantly lower than that of steel. As a result of the lower elastic modulus and the susceptibility of these defects to grow upon the application of comparatively small amounts of strain, the composite repairs allow these defects to strain sufficiently to cause them to fail or grow by fatigue.

Table 4.1 also indicates that Type B sleeves can be used to repair a wide variety of defects for which composite repairs cannot. For example, a leak imposes significant limitations on the choice of repair method. In general, only a Type B sleeve is appropriate.[1]

Rows 2a, 2b, and 2c of Table 4.1 highlight methods applicable for the repair of external corrosion including the consideration of maximum pit depth. All three repair methods listed in Table 4.1 are acceptable for relatively shallow to moderately deep external corrosion (less than 80% deep). Very deep external corrosion (80% deep or greater) should be repaired only using methods that are appropriate for leaks (i.e., Type B sleeves).

4.5 Advantages and disadvantages

In the previous section, it was shown that the applicability of Type A sleeves and composite repairs is similar and that Type B sleeves can be used where Type A sleeves and composite repairs cannot.

One of the claimed advantages of composite repairs over steel sleeves is that their installation requires no welding to an in-service pipeline. It is clear from the previous discussion that the installation of Type A sleeves, which can serve the same purpose as composite repairs, also requires no welding to an in-service pipeline. Welds that do not contact the carrier pipe are not considered to be "in-service" welds according to Appendix B of API 1104 (API Standard 1104, 2005), even though longitudinal seam welds are made while the pipeline is in service.

Another claimed advantage of composite repairs is that their installation is simpler than steel sleeves. While this may be the case for Type B sleeves where welding to an in-service pipeline using specially qualified welding procedures and specially qualified welders is required, this is certainly not the case for Type A sleeves. Type A sleeves require no in-service welding, can have fillet-welded overlapping side strips (Figure 4.8), and are very simple to fabricate and install. They can be supplied with the side strips fillet welded to the bottom half of the sleeve so that the only welds required in the field are the fillet welds on the top of the side strips. These welds can be readily made by welders without special training or in-service welding qualification. The raw materials required to make Type A sleeves are significantly less expensive than composite materials. Type A sleeves can be fabricated in the field by simply splitting a length of pipe of equal diameter wall thickness and grade as the line pipe material.

Unlike composite materials, steel sleeves have no finite "shelf life." The shelf life of composite repair kits must be tracked, and kits that are not used prior to the expiration date must be discarded. Because of their high stiffness, steel sleeves are less sensitive to pressure reduction during installation than composite repairs. Composite

[1] When using a steel sleeve to repair a leaking defect, venting of the leak using a small branch pipe with a valve over a hole in one of the sleeve halves may be required.

Figure 4.8 Type A encirclement repair sleeve with fillet-welded overlapping side strips.

repairs that are installed without pressure reduction serve little purpose because the defect may grow or fail upon the application of comparatively small amounts of strain. In contrast, hydraulic clamps can be used to preload steel sleeves during installation (Figure 4.9), which has the same effect as a pressure reduction during installation. Thermal contraction of the longitudinal seam welds acts to further preload steel sleeves. Finally, the long-term performance of Type A sleeves is equivalent to that of line pipe steel.

Federal regulations in the United States require pipeline operators to repair pipelines using methods that have been shown to *permanently* restore the serviceability of the pipeline. While there is some subjectivity in determining what constitutes "permanent," this seems to imply that the expected life of the repair should be equal to the expected life of the pipeline. While the long-term performance of steel is well established, the long-term performance of composite materials on buried pipelines beyond about 20−25 years has not yet been demonstrated. Unlike steel, the

Figure 4.9 Hydraulic clamps being used to preload a steel sleeve during installation.

mechanical properties of composite materials are known to degrade over time. Steel sleeves do not have to be overdesigned initially to compensate for this degradation over time, as do composite repairs.

The significantly reduced stiffness of composite materials compared to steel makes the use of composite repairs questionable for applications on pipelines that experience cyclic pressure fluctuations. Cyclic strains in the defect area may cause the defect to grow and eventually fail in subsequent service. Work is currently being conducted to better define the long-term performance of composite repairs (Alexander, 2009; Alexander and Bedoya, 2010). Until this is better understood, considering composite repairs to be permanent, particularly for pipelines that experience cyclic pressure fluctuations, is questionable.

Both Type A sleeves and composite sleeves rely upon the use of an effective sealer to keep potentially corrosive fluids (e.g., groundwater) from entering the crevice area between the carrier pipe and the repair. Corrosion under Type A sleeves can be prevented by using either an elastomeric (i.e., caulk-like) sealant or a hardenable sealant (Figure 4.10). Examples of hardenable sealants include epoxy splash zone compounds that are similar to those used to adhere some composite sleeves in place or to fill areas of metal loss or denting. Some of the sealing compounds cure effectively on wet surfaces. Cure time is typically a function of the pipe temperature, with curing occurring more quickly on warmer surfaces.

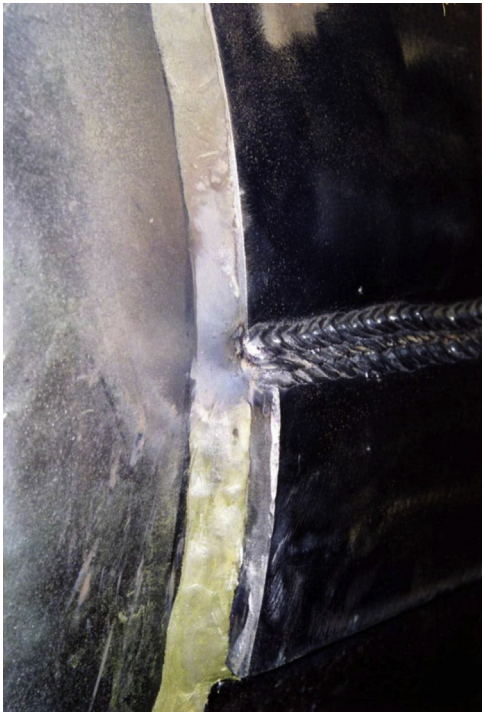

Figure 4.10 Type A sleeve end with hardenable sealant.

Figure 4.11 Installation of Type B full-encirclement repair sleeve.

While Type B sleeves have to be fillet welded to the pipeline (Figure 4.11), they can be used where composite repairs cannot, such as for repair of defects that are 80% deep or greater, circumferentially oriented defects, leaking defects or for defects that will eventually leak (e.g., internal corrosion), and cracks. The raw materials required to make Type B sleeves are significantly less expensive than composite materials, and the stiffness and long-term performance of Type B sleeves are equivalent to that of line pipe steel.

When considering the cost of various repair options, both material cost and cost of installation need to be considered. Mobilization cost and the application cost of steel sleeves may be highly variable, depending upon the availability and labor rates for welding personnel. While the mobilization cost for composite repair installation may be less in some cases, the materials are more expensive. Composite sleeves or wet lay-up composite repair kits are typically designed for a standard, fixed length (e.g., Clock Springs® are 12 in (305 mm) long). If the length of the area requiring repair is longer than that which can be repaired by a single composite sleeve, the use of steel sleeves may be significantly less expensive than composite repairs.

4.6 Welding onto an in-service pipeline

While there are concerns that need to be considered when welding a Type B sleeve onto an in-service pipeline, this can be relatively straightforward provided that well-established guidance is followed. The first of these concerns is for "burn-through," where the welding arc causes the wall of thin-wall pipe to be penetrated. The second concern is for hydrogen cracking, since welds made in service tend to cool at an accelerated rate as the result of the flowing contents' ability to remove heat from the pipe wall.

A burn-through, or blowout as it is sometimes called, will occur when welding onto a pressurized pipe if the unmelted area beneath the weld pool has insufficient strength to contain the internal pressure of the pipe. A photograph of a typical burn-through is shown in Figure 4.12. A burn-through typically results in a small pinhole in the bottom

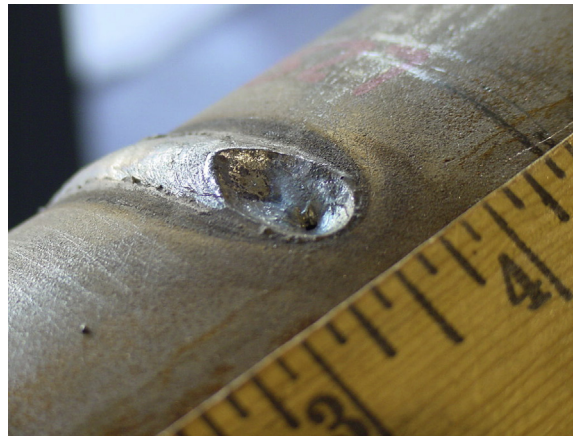

Figure 4.12 Typical burn-through on 0.125-in (3.2-mm)-thick pipe.

of what was the weld pool. The risk of burn-through will increase as the pipe wall thickness decreases and the weld penetration increases.

Welds made onto in-service pipelines tend to cool at an accelerated rate as the result of the ability of the flowing contents to remove heat from the pipe wall. Accelerated cooling rates promote the formation of hard-weld microstructures that are susceptible to hydrogen cracking. A photomicrograph of a typical hydrogen crack is shown in Figure 4.13. Hydrogen cracking requires that three primary, independent conditions be satisfied simultaneously: (1) hydrogen must be present in the weld, (2) there must be a susceptible weld microstructure, and (3) tensile stresses must be acting on the weld.

Simple guidance has been developed and is available elsewhere for preventing both burn-through and hydrogen when welding onto an in-service pipeline (Bruce, 2009). This simple guidance is summarized below.

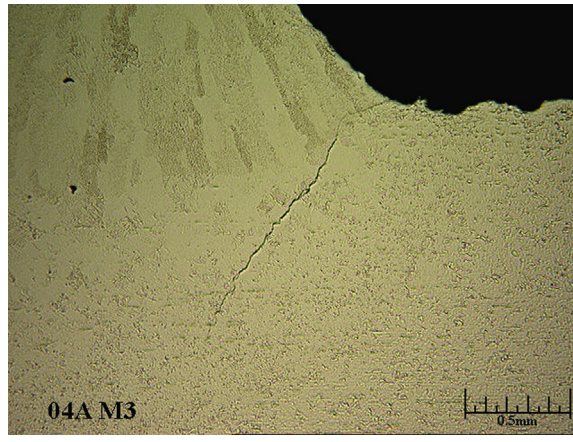

Figure 4.13 Micrograph of typical hydrogen crack at toe of fillet weld of full-encirclement sleeve.

4.7 Preventing burn-through

A well-established rule of thumb indicates that penetrating the pipe wall with the welding arc (i.e., burning through) is unlikely if the wall thickness is 0.250 in (6.4 mm) or greater, provided that low-hydrogen electrodes and normal welding practices are used. This rule of thumb seems to have been lost by some companies, who have requirements for maintaining flow and/or reducing pressure even when the wall thickness is 0.250 in (6.4 mm) or greater. If the wall thickness is 0.250 in (6.4 mm) or greater, the primary in-service welding concern should be for hydrogen cracking and not for burn-through.

If the wall thickness is less than 0.250 in (6.4 mm), there may be a need to take special precautions to minimize the risk of burn-through. These precautions include minimizing the penetration of the arc into the pipe wall by using small-diameter, low-hydrogen electrodes and a procedure that limits heat input.

The most useful tool for evaluating the risk of burn-through is thermal analysis computer modeling using either the Battelle model (Bubenik et al., 1991; Cola et al., 1992) or the PRCI model (Bruce et al., 2001). These computer models predict inside-surface temperatures, which must be kept below 1800 °F (982 °C) to minimize the risk of burn-through, as a function of the welding parameters (current, voltage, and travel speed), geometric parameters (wall thickness, etc.), and the operating conditions (contents, pressure, flow rate, etc.). The risk of burn-through for a given application can be evaluated or the limiting welding parameters for a given set of operating conditions can be determined.

There are several common misconceptions pertaining to operating practices required to prevent burn-through. One is that some level of flow must always be maintained to prevent burn-through and another is that the operating pressure must always be reduced. While maintaining flow does result in lower inside-surface temperatures, it can be shown that inside-surface temperatures are often less than 1800 °F (982 °C) due to the thermal mass of the pipe wall itself and the thermal properties of the contents, even at little or no flow. While a pressure reduction may be justified to prevent a defect from rupturing during repair on the basis of protecting the repair crew, or to further improve the tightness of the installed sleeve, previous work concluded that stress level in the pipe wall has a relatively small effect on the risk of burn-through (Kiefner and Fischer, 1988). The reason for this is that the size of the heated area by the welding arc is small and the stress in the pipe wall can redistribute itself around the heated area, as it does around a small corrosion pit. Pressure reductions are, therefore, relatively ineffective at preventing burn-through and are often unnecessary.

4.8 Preventing hydrogen cracking

To prevent hydrogen cracking, at least one of the three conditions necessary for its occurrence must be eliminated or reduced to below a threshold level. A significant amount of residual tensile stress acting on the weld cannot be avoided and must always be assumed. The first step taken by many companies toward avoiding hydrogen

cracking in welds made onto in-service pipelines is to minimize the hydrogen level by using low-hydrogen electrodes or a low-hydrogen welding process. As added assurance against hydrogen cracking, many companies have developed and follow procedures that minimize the formation of crack-susceptible microstructures and follow an installation sequence that minimizes welding residual stresses.

Much of the recent research-and-development work has been directed at predicting weld cooling rates, or more specifically, at predicting the required welding parameters to prevent the formation of crack-susceptible microstructures. Attention to this may have obscured the most important aspect of preventing hydrogen cracking, which is limiting the amount of hydrogen that enters the weld. The results of recent work show that close control of hydrogen level allows HAZ hardness in excess of 350 HV to be tolerated (Bruce and Boring, 2005).

4.8.1 Control of weld hydrogen levels

The first line of protection against hydrogen cracking for welds made onto in-service pipelines should be to strictly limit the amount of hydrogen that is allowed to enter the weld. Storage and handling of low-hydrogen electrodes is an inexact science at best, even though general guidelines for their use are available (Unknown a,b; AWS D1.1, 2004; WTIA Technical Note 3, 1994). The hydrogen level of welds made using low-hydrogen electrodes can vary widely depending on a range of factors. These include the manufacturer, classification/supplemental designation, packaging, storage conditions, handling, atmospheric exposure, and drying/reconditioning practices.

Many of the potential problems associated with minimizing hydrogen levels for welds made onto in-service pipelines, and thus preventing hydrogen cracking in these welds, can be addressed at the electrode procurement stage. Supplementary designators are now available that allow a specific maximum-allowable hydrogen level to be specified. In AWS A5.1 (AWS A5.1-91, 1991), these designators are H4, H8, and H16, where "H" indicates hydrogen and "4, 8, and 16" refer to the average maximum-allowable hydrogen level in mL/100 g of deposited weld metal in the "as-received" condition. In other parts of the world, a similar system is used, although the hydrogen levels are H5, H10, and H15. In addition, AWS has introduced an "R" designator that allows a moisture-resistant coating to be specified. The R designator indicates that the electrodes have passed an absorbed moisture test after exposure to an environment of 80 °F (26.7 °C) and 80% relative humidity for a period of not less than 9 h. Electrodes that meet this requirement have coating-moisture limits that are lower than their nonmoisture-resistant counterparts (i.e., the electrodes are initially drier).

For in-service welding applications, operators should specify electrodes with the H4R designator (e.g., E7018-H4R). These are becoming more common and, while there may be a price premium, this is negligible compared to the cost for remedial action that would be required following the discovery or failure of an in-service weld with hydrogen cracks.

For in-service welding applications, the use of electrodes that are packaged in hermetically sealed cans (i.e., appropriate for use in the as-received condition) should

Figure 4.14 E7018-H4R electrodes in 10-lb (4.5-kg) hermetically sealed can.

be specified. If electrodes packaged in plastic-wrapped cardboard cartons are used, care must be taken to ensure that drying is not required by the manufacturer prior to their use in the as-received condition. If the electrodes are intended to be used in the as-received condition and they are packaged in plastic-sealed cardboard containers, care should be taken to ensure that the plastic wrap is not damaged. If drying is required, care must be taken to ensure that the drying is carried out properly.

For in-service welding applications, low-hydrogen electrodes in smaller quantities (e.g., 10-lb (4.5-kg) cans) (Figure 4.14) should be specified. This is particularly true for smaller jobs (e.g., small-diameter lines) where it would be difficult to use an entire 50-lb (22.7-kg) can. However, there may also be a price premium for this type of packaging.

Low-hydrogen electrodes with the H4R supplemental designator (e.g., E7018-H4R), packaged in small quantities hermetically sealed cans are ideally suited for in-service welding.

4.8.2 Development and qualification of procedures

Thermal analysis models are useful for determining welding parameters that minimize the formation of crack-susceptible microstructures for specific applications, but their

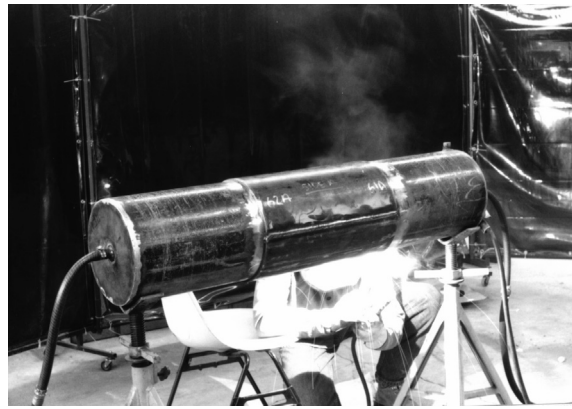

Figure 4.15 Setup for procedure qualification under simulated in-service conditions.

use is not always necessary. In fact, even if thermal analysis models are used, a welding procedure should be qualified under simulated in-service conditions to demonstrate that the predicted parameters are practical under field conditions and that sound, crack-free welds are produced.

Simple methods have been developed for qualifying welding procedures under thermal conditions that simulate those experienced when welding onto an actual in-service pipeline (i.e., conditions that result in realistic weld cooling rates and solidification characteristics). Filling a pipe section with water and letting water flow through the pipe section while the procedure qualification welds are deposited (Figure 4.15) has been shown to be more severe with respect to the resulting weld cooling rates than with most hydrocarbon liquids and high-pressure gases (Bruce and Threadgill, 1994). A water flow rate that is attainable from a garden hose (e.g., 10 gal/min (37.8 L/min)) is sufficient. The thermal conductivity of water more than compensates for the lack of a representative flow rate.

A standard set of procedures can be qualified that covers a range of conditions, and then simple guidelines can be developed so that the simplest procedure can be selected for a specific application. The results of previous work (Bruce, 2001) indicate that provided that hydrogen levels are closely controlled, under worst-case conditions (flowing water), a procedure that relies on a heat input of at least 25 kJ/in (1.0 kJ/mm) is suitable for pipe materials with carbon equivalent (CE_{IIW}) levels up to 0.35. A procedure that relies on a heat input of at least 40 kJ/in (1.6 kJ/mm) is suitable for pipe materials with CE_{IIW} up to 0.42. A procedure that relies on a properly developed temper bead deposition sequence is suitable for pipe materials with CE_{IIW} up to 0.50. Temper bead procedures are also useful for welding onto thin-wall pipe where the use of a high heat-input level represents a risk of burn-through. These three procedures cover a wide range of conditions. There may be some conservatism associated with this approach, as not all in-service welds cool as quickly as welds made using flowing water.

4.9 Summary and conclusions

The use of full-encirclement steel sleeves for pipeline repair is a relatively mature technology. As a result, relatively little is written about the use of steel sleeves compared to the use of composites where new products are continually introduced.

The applicability of Type A sleeves is nearly identical to that for composite repairs and their installation involves no welding to an in-service pipeline. Type B sleeves can be used where composite repairs cannot, such as for repair of defects that are 80% deep or greater, circumferentially oriented defects, leaking defects or for defects that will eventually leak (e.g., internal corrosion), and cracks. For both types of full-encirclement steel sleeve, the raw materials are relatively inexpensive, and the stiffness and long-term performance are equivalent to that of line pipe steel.

The installation of Type B sleeves does involve the need to weld to an in-service pipeline. Adherence to the simple guidance summarized here will minimize the potential concerns associated with welding to an in-service pipeline.

References

AWS D1.1, 2004. Structural Welding Code—Steel. American Welding Society, Miami, FL.

AWS A5.1-91, 1991. Specification for Carbon Steel Electrodes for Shielded Metal Arc Welding. American Welding Society, Miami, FL.

Alexander, C., Francini, B., State of the art assessment of composite systems used to repair transmission pipelines. Stress Engineering Services, Inc. and Kiefner & Associates, Inc., Proceedings of IPC2006, 6th International Pipeline Conference, IPC2006−10484, Calgary, Alberta, Canada, September 25−29, 2006.

Alexander, C., Overview and recent advances in application of composite materials for repair of transmission pipelines: evaluation of test results and ongoing research. Stress Engineering Services, Inc., Evaluation and Rehabilitation of Pipelines Conference, Pittsburgh, October 2009.

Alexander, C., Bedoya, J., Repair of dents subjected to cyclic pressure service using composite materials. Stress Engineering Services, Inc., Proceedings of the 8th International Pipeline Conference IPC2010, Calgary, September 27−October 1, 2010.

Bruce, W.A., A simple approach to hot tap and repair sleeve welding. Evaluation and Rehabilitation of Pipelines, Clarion Technical Conferences and Scientific Surveys Ltd, Pittsburgh, Pennsylvania, October 19−22, 2009.

Bubenik, T.A., Fischer, R.D., Whitacre, G.R., Jones, D.J., Kiefner, J.F., Cola, M.J., Bruce, W.A., December 1991. Investigation and prediction of cooling rates during pipeline maintenance welding. In: Final Report to American Petroleum Institute.

Bruce, W.A., Li, V., Citterberg, R., Wang, Y.-Y., Chen, Y., July 2001. Improved Cooling Rate Model for Welding on In-service Pipelines. PRCI Contract No. PR-185−9633, EWI Project No. 42508CAP. Edison Welding Institute, Columbus, OH.

Bruce, W.A., Boring, M.A., January 2005. Realistic Hardness Limits for In-service Welding. Draft Final Report for PRCI Contract No. GRI-8758, EWI Project No. 46344CAP. Edison Welding Institute, Columbus, OH.

Bruce, W.A., Threadgill, P.L., July 21, 1994. Effect of procedure qualification variables for welding onto in-service pipelines. In: Final Report to A.G.A. Welding Supervisory Committee, Project PR-185-9329, EWI, Columbus, OH.

Bruce, W.A., March 2001. Selecting an appropriate procedure for welding onto in-service pipelines. In: International Conference on Pipeline Repairs. Welding Technology Institute of Australia, Wollongong, Australia.

Cola, M.J., Kiefner, J.F., Fischer, R.D., Jones, D.J., Bruce, W.A., July 1992. Development of simplified weld cooling rate models for in-service gas pipelines. In: Project Report No. J7134 to A.G.A. Pipeline Research Committee. Edison Welding Institute, Kiefner and Associates and Battelle Columbus Division, Columbus, OH.

Fawley, N.C., March 1994. Development of fiberglass composite systems for natural gas pipeline service. In: Final Report GRI-94/0072.

Jaske, C.E., Hart, B.O., Bruce, W.A., August 8, 2006. Pipeline repair manual. In: Final Report to Pipeline Research Council International, Inc., Contract PR-186−0324. DNV/CC Technologies, Inc. and Edison Welding Institute.

Kiefner, J.F., Duffy, A.R., October 31, 1974. A Study of Two Methods for Repairing Defects in Line Pipe. Battelle Columbus Laboratories. NG-18 Report No. 32, PRCI Catalog No. L22275.

Kiefner, J.F., Whitacre, G.R., Eiber, R.J., March 2, 1978. Further Studies of Two Methods for Repairing Defects in Line Pipe. Battelle Columbus Laboratories. NG-18 Report No. 112.

Kiefner, J.F., Fischer, R.D., 1987. Repair and hot tap welding on pressurized pipelines. In: Symposium during 11th Annual Energy Sources Technology Conference and Exhibition, New Orleans, LA, January 10−13, 1988, PD-vol. 14. American Society of Mechanical Engineers, New York, NY, pp. 1−10.

Leewis, K., Laughlin, S., Understanding strain performance considerations in the composite repair of dents and SCC. Proceedings of IPC2010, 8th International Pipeline Conference, IPC2010−31586, Calgary, Alberta, Canada, September 27−October 1, 2010.

Stephens, D.R., Kilinski, T., March 1994. Field validation of composite repair of gas transmission pipelines. In: GRI Annual Report GRI-94/0139.

API Standard 1104, November 2005. Welding of Pipelines and Related Facilities, 20th ed. American Petroleum Institute, Washington, DC.

Unknown a, Storing and Re-drying Electrodes, The Lincoln Electric Company, Cleveland, OH, http://lincolnelectric.com/knowledge/articles/content/storing.asp.

Unknown b, Recommendations for the Storage, Re-drying and Handling of ESAB Consumables, ESAB AB, Göteborg, Sweden, http://esabsp.esab.net/templates/docOpen.asp?file=files/Handbooks/Welding%20Consumables/XA00097020.pdf.

WTIA Technical Note 3, 1994. Care and Conditioning of Arc Welding Consumables. WTIA TN-3-94. Welding Technology Institute of Australia, Silverwater, NSW.

Time-dependent probability analysis of fiber-reinforced polymer rehabilitated pipes

5

L.S. Lee, H. Estrada
University of the Pacific, Stockton, CA, USA

5.1 Introduction

Research and interest in management of infrastructure is of great importance to municipalities, private companies, and researchers because of deterioration of existing systems and components, occurrence of catastrophic failures, and continued maintenance deferment due to limits on financial resources. The decreasing reliability of an aging civil infrastructure has amplified the need to better evaluate and monitor the condition of new and existing infrastructure systems and components. In particular, the vast network of underground and aboveground pipelines serves as the "arteries" for a functioning modern society. Piping systems are relied upon for the delivery of oil, gas, water, wastewater, and other liquids to and from residences and businesses. It is estimated that there are more than 2.5 million miles of pipeline in the United States used to deliver liquid petroleum products, and globally, pipelines represent the primary means of energy transportation due to their efficiency and reliability.

Given our complex modern society's dependence on these systems for conveying energy (oil and gas for production of electric power and transportation) as well as conveyance of water, aging infrastructure poses a real threat to our current way of life (Cagno et al., 2011). Pipelines are particularly susceptible to maintenance neglect because of their low visibility and low instances of catastrophic failure; however, piping systems are subject to material degradation, corrosion, environmental attack, impact damage, and increased demands in internal pressure and surface traffic, which can lead to reductions in service life or failure (Amirat et al., 2006; Najafi, 2011). Limited financial resources have forced many industries to extend the service life of piping systems well beyond their design life, which has resulted in the need for innovative repair solutions that can extend the service life of these systems and provide a managed solution to system restoration or replacement. One potential solution to the rehabilitation of piping components and systems is the application of fiber-reinforced polymer (FRP) composites to strengthen and seal deficient pipes.

Pipeline rehabilitation and retrofit with FRP composites were introduced in the early 1990s as an alternative to using steel sleeves (Alexander, 2007, 2009). FRP composites can provide a wide range of performance options for pipeline components due to their lightweight, high specific stiffness, high specific strength, ease of fabrication,

Rehabilitation of Pipelines Using Fiber-reinforced Polymer (FRP) Composites. http://dx.doi.org/10.1016/B978-0-85709-684-5.00005-9

and a higher degree of design flexibility (Karbhari and Zhao, 2000; Hastak et al., 2003). Although the advantages of FRP composites are well documented in literature, the long-term performance of FRP composites in pipeline repair, particularly issues related to durability, quality of construction, and design, has only recently begun to be investigated. This chapter summarizes these recent developments.

The use of FRP composites in civil infrastructure is extensive, and numerous techniques are widely available to integrate FRP composites for purposes of restoration and renewal of aging infrastructure; however, many of the design procedures involve the use of deterministic equations that use conservative safety factors to account for uncertainty in as-built material parameters and durability effects. Probabilistic analysis provides a more accurate means to evaluate the effectiveness of structural systems or components by accounting for uncertainties in design parameters and quantifying the impact of manufacturing quality of a repair on performance as opposed to traditional deterministic methods that utilize fixed values and point estimates (Sadiq et al., 2004). The goal of this chapter is to provide and to demonstrate a framework for evaluating the long-term performance of FRP composite rehabilitated piping components using probabilistic modeling. In order to achieve this goal, the following objectives will be accomplished. First, a framework for infrastructure management is described in terms of integrating service life estimation and decision-making processes with probabilistic analysis. Then, we provide an overview of the basic reliability problem and the application of Monte Carlo simulation to estimate the time-dependent failure probability of a structural component. Next, the variables of FRP composites that are influenced by quality of construction and by durability considerations, which ultimately influence the failure probability of a repaired piping component, are discussed. Finally, an evaluation of the time-dependent failure probability of an FRP composite repaired steel pipe is demonstrated along with discussion on the influence of fabrication quality on overall performance of FRP-rehabilitated pipes.

5.1.1 FRP composites in pipe rehabilitation

Failure in piping components and systems depends on the type of material, physical design, age, functionality, and external and internal environment (Najafi, 2011). These and other deficiencies in piping systems can be classified as as-built or long-term defects. For pipes that are laid underground or underwater, adverse deterioration due to corrosion, cracking, dents, wearing, buckling, gouging, spalling, leaks, and rupture can occur, and all can lead to failure over time (Shamsuddoha et al., 2013; Alexander and Francini, 2006). For instance, in energy transmission pipelines, which are predominantly constructed of steel, failure as a result of sulfate and subsequent stress corrosion cracking is of particular concern. Traditional repair methods for steel pipes include replacing segments of the damaged pipe, cutting out the damaged region, and welding a steel plate to cover the cutout area, and installation of steel repair sleeves; however, the difficulties of welding and clamping bulky, heavy steel sleeves in underground or underwater applications are difficult to implement and costly (Shamsuddoha et al., 2013). Consequently, application of FRP composites for pipeline retrofit and repair has become well established.

Two types of FRP construction techniques that are common in pipeline rehabilitation are wet lay-up and pre-cured layered systems (Shamsuddoha et al., 2013; Alexander and Francini, 2006). In the wet lay-up process, fiber reinforcement is impregnated with resin and bonded to the entire internal or external surface of the pipe. A wet lay-up system is advantageous because it has the ability to cover a range of geometries including tees, elbows, bends, and valves and has been shown to be effective in restoring strength to pipe components with part wall defects and corrosion (Shamuddoha et al., 2013; Alexander and Francini, 2006). On the other hand, wet lay-up fabricated composites are limited to medium-to-low pressure applications and the manual nature of the fabrication process makes it susceptible to defects and variations in geometry and material properties. In a layered system, pre-cured composite layers are bonded to the outside diameter of the pipe using an adhesive. While the layered system is typically restricted to straight sections of the pipe, the prefabricated nature of the composite results in improved composite mechanical properties with increasing fiber volume fractions. In both systems, the majority of fibers are oriented in the hoop direction in order to restore or increase the structural integrity of the damaged pipe section.

In addition to rehabilitation of steel pipes, glass- and carbon-fiber composites have been incorporated in cast-in-place polymer liners in the rehabilitation of sewer lines, low-pressure water lines, wastewater, and air ducts and in the repair of large-diameter piping components (Black, 2005; Bethel et al., 2006; Toutanji and Dempsey, 2001; Duell et al., 2008). Despite the increased application of FRP composites in piping networks, the selection of rehabilitation methods and materials suitable for underground infrastructure remains uninformed because of a lack of understanding of the capabilities of various proposed rehabilitation methods as well as limited available data on the effectiveness and long-term performance of these methods.

5.2 Infrastructure management

The selection of FRP composite materials for pipeline repair depends on accessibility, location, performance, and cost requirements associated with the required piping system. For proper cost comparisons between composite and traditional materials for repair, a life cycle cost analysis is most appropriate since FRP composites are often associated with a high initial start-up cost (Hastak et al., 2003; Kawahara et al., 2012). Consequently, it is necessary to predict the life of FRP materials under service operating conditions. One way to predict the life of composite materials in operation is by predicting the reduction in their load-carrying capacity over time, which is a function of viscoelastic behavior of polymers, temperature, permeability of protective coatings on both polymers and fibers, exposure to depredating environments including moisture, and the permeability of the main composite constituents to moisture and harsh chemicals. This reduction in strength and stiffness caused by these variables as a function of time is the primary focus of the work presented in this chapter. Given that the use of composites is relatively new compared to traditional infrastructure materials, in order to obtain the aged properties of composites

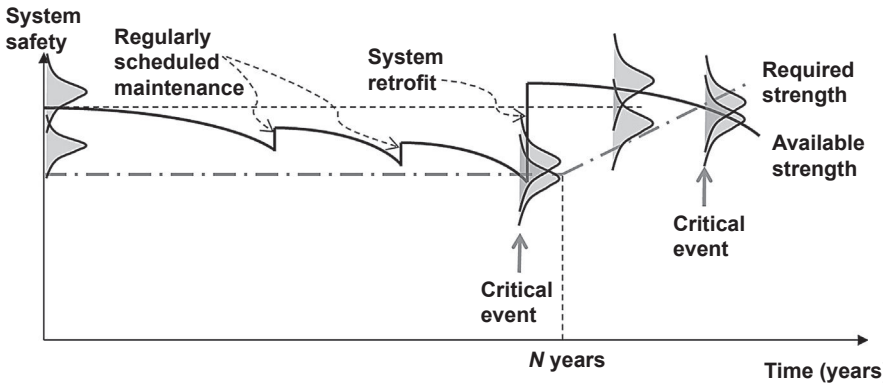

Figure 5.1 System safety concept over the design life cycle.

it is common to immerse samples in water at elevated temperatures to accelerate material degradation—in effect, acquiring long-term properties by short-term degradation measurements, which can then be used to extrapolate the expected life of a structure.

Figure 5.1 depicts a model of the service life of a structural system over its design life cycle. Most structural systems are designed to have available strength that exceeds the required strength obtained from critical loads expected to act on the system at some point in time over the useful life of the system. Given the number of uncertainties in the design process, engineers use a margin of safety—the difference between the dashed line (initially on top) and the dash-dot line (initially on the bottom) in Figure 5.1. The bell-shape distributions outlined on the sketch indicate that there is statistical variability associated with required and available strengths; any overlap in the distributions indicates failure of the system. Notice that initially the overlap area is relatively small but over time as the available strength degrades, the overlap area increases. The required strength is expected to remain constant for the duration of the expected life or N years as shown in Figure 5.1. After the life expectancy of the system, the probability of a larger design load increases because the returned period is extended (we do not take this into account here). The available strength meanwhile decreases due to deterioration processes and cannot be greater than the initial strength unless the system is retrofitted. The regularly scheduled maintenance events only yield a small recovery of the initial available strength, indicated by the jumps in the green line.

With the ever-aging infrastructure in the United States and the ever-increasing deferment of maintenance of structural systems, it is important to develop rapid and inexpensive retrofit techniques that can extend the useful life of these systems. At the core of infrastructure management is the ability to estimate the time-dependent performance of a structural system or component in the presence of uncertainty. A time-dependent measure of system or component safety (e.g., reliability or failure probability) provides valuable insight for design and maintenance decisions that ultimately alter the life cycle cost of a system. In the following sections, a process for evaluating the time-dependent failure probability of an infrastructure component is described.

5.2.1 Reliability analysis

The primary objective of a reliability analysis, or an estimate of failure probability, is to quantify the safety of a structural system accounting for uncertainty and variability. Structural reliability methods are used to estimate the failure probability based on the materials and configuration of a structure (Atadero et al., 2005). In an FRP-rehabilitated component, uncertainties in the FRP composite, in the structure's existing material and as-built condition, in deterioration, in analytical models, and in loading often result in excessive knockdown factors associated with specific service lives, whereas probabilistic analysis methods provide an opportunity to integrate uncertainty, deterioration models, and different service lives in analysis and design.

The basic reliability formulation considers a performance function, $g(\overrightarrow{\mathbf{X}})$, to describe a limit state (a condition where a system or component fails to perform its intended function) within a structural component, where $\overrightarrow{\mathbf{X}}$ represents a vector of random variables. A failure event or violation of the limit state equation occurs when $g(\overrightarrow{\mathbf{X}}) \leq 0$. The likelihood of a failure event is then determined as follows:

$$p_f = P\left[g\left(\overrightarrow{\mathbf{X}}\right) \leq 0\right] = \int_{g\left(\overrightarrow{\mathbf{X}}\right)\leq 0} f_{\overrightarrow{\mathbf{X}}}(\overrightarrow{\mathbf{x}})\mathrm{d}\overrightarrow{\mathbf{x}} \tag{5.1}$$

where $f_{\overrightarrow{\mathbf{X}}}(\overrightarrow{\mathbf{x}})$ is the joint probability distribution of random variables, $\overrightarrow{\mathbf{X}}$. This integral is the key operation in reliability analysis; however, evaluating it can be rather difficult. For this reason, a number of approximate analytical solution methods have been developed, including the first-order reliability method and the second-order reliability method (Ditlevson and Madsen, 1996; Melchers, 1999). On the other hand, numerical simulation techniques, such as Monte Carlo simulation, are often needed for more complex combinations of random variables, such as where products or quotients of several random variables are involved and multiple probability distributions are used to characterize different random variables. In these instances analytical determination of the joint probability density function is complex, if not impossible (Ang and Tang, 2007; Melchers, 2011).

5.2.2 Monte Carlo simulation

Because analytical evaluation of component or system failure probabilities (or reliabilities) is rather complicated for cases with multiple random variables, multiple probability distribution types, or complex limit state functions, we must employ numerical methods to solve this complex problem. Numerical methods for solving probabilistic problems in engineering applications have proven practical and efficient (Ang and Tang, 2007). These numerical methods, often identified as Monte Carlo methods, provide a simple approach to evaluating the failure probability of a given limit state function. Monte Carlo simulation involves the generation of random numbers for each random variable according to its respective probability distribution. A number of commercial software packages, such as Matlab and MathCAD, include

random number generators suitable for a numerical solution. In order to describe the basic Monte Carlo simulation method to estimate failure probability, consider a limit state function with random variables for resistance, $R(T)$, and demand, $S(T)$, which vary with time, T:

$$g(R,S,T) = R(T) - S(T) \tag{5.2}$$

For a specific instance of time, a Monte Carlo simulation is conducted by generating random numbers for variables R and S with respect to specified probability distribution functions for each random variable. Time dependence allows for nonstationary loads in demand variables and deterioration processes associated with resistance variables (Melchers, 2011).

Generated random numbers are then substituted into the performance function or limit state equation to determine if an instance of failure has occurred. For each evaluation of the performance function, the occurrence of $g(R,S,T) \leq 0$ is counted. The total number of failure events, n_f, are determined after N samples have been generated. The probability of failure, p_f, at time, T, is then estimated as

$$p_f(T) = \frac{n_f}{N} \tag{5.3}$$

For each interval of time, a Monte Carlo simulation is performed to generate failure probability as a function of time. Figure 5.2 shows a representative plot of the failure

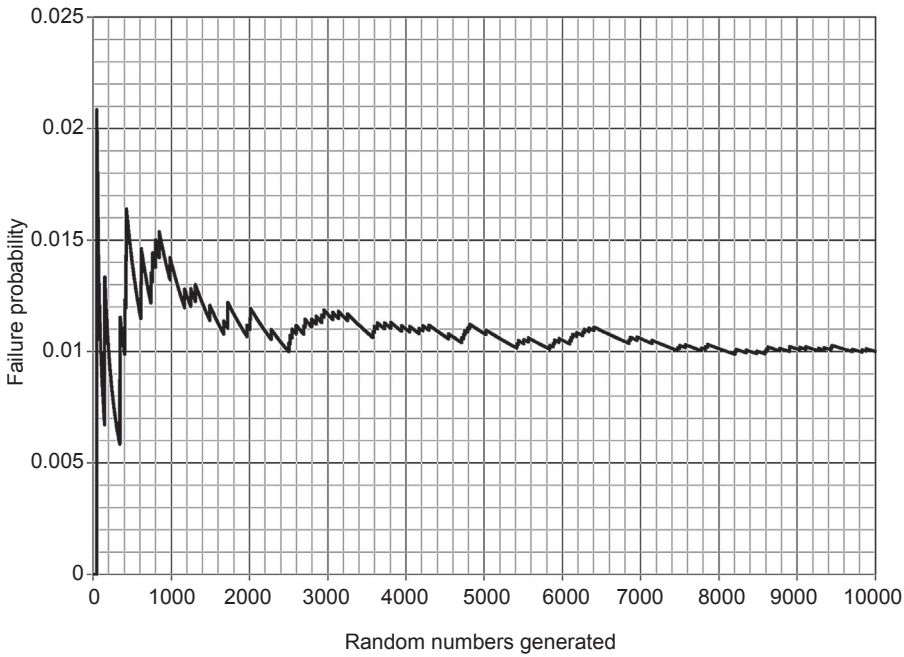

Figure 5.2 Failure probability versus sample size in a Monte Carlo simulation.

probability as a function of sample size for single simulation, at one instance of time. As the number of samples approaches 10,000, the failure probability is observed to converge. The primary disadvantage associated with Monte Carlo simulation is the intensive computational effort that is required when the failure probability is very low. It can be shown that the coefficient of variation (COV) of the average failure probability in a basic Monte Carlo simulation is proportional to $1/\sqrt{N}$, which implies that for a failure probability of 10^{-4}, a sample size of $N \approx 10^6$ would be required to obtain a COV of 10%. Monte Carlo simulation is generally efficient for mid-range failure probabilities and typically becomes unfeasible for very small failure probabilities (e.g., $p_f \leq 10^{-4}$).

5.3 Material considerations

Material selection, quality of fabrication, and durability issues are primary factors in as-built and long-term performance of FRP-rehabilitated structural components. Material selection involves design choices related to the combination of constituent materials used to fabricate a composite. The quality of fabrication of a composite material is generally associated with its fiber, matrix, and void volume fractions, which directly impact the mechanical behavior of composites. Depending on the manufacturing method and environment during construction, the fiber volume fraction of a composite is likely to vary. For instance, wet lay-up of FRP composites can result in fiber volume fractions between 20% and 30% (Astrom, 1997), while fiber volume fractions of 35−60% can be attained in FRP composites manufactured via the pultrusion process. For further discussion regarding FRP-composite manufacturing, see Astrom (1997).

The probabilistic analysis presented in this chapter is not restricted to a specific fabrication approach but rather presents results as a function of the fiber volume fraction and can be applied to a wide range of pipe rehabilitation methods. The time-dependent failure probability analysis is illustrated for specific fiber volume fractions and can be repeated for any fiber volume fraction depending on the manufacturing process of interest. Typical fiber volume fractions of 30% and 40% are selected conservatively for example probability analysis conducted in the chapter. Recent efforts to measure fiber volume fractions used in composite pipe applications report fiber volume fraction values ranging from 47.6% to 54% for filament-wound composite pipes (Abdalla et al., 2008), and Chin and Lee (2005) measured volume fractions of 47% for unidirectional laminates manufactured via resin transfer molding in a trenchless rehabilitation scheme.

5.3.1 Durability characterization of FRP composites

Time-dependent and predictive component behavior is directly attributed to models based on durability tests at the material level. Bank et al. (1995) summarize predictive models for a particular material characteristic of FRP composites, including mechanics-based, chemical-based, accelerated-aging and long-term verification models. Of these, accelerated-aging models are the most commonly used for predictive modeling.

Accelerated-aging tests typically involve the exposure of the composite material to elevated temperatures and moisture, where the elevated temperature acts as a forcing function in a time−temperature superposition approach (Gentry et al., 2002; Karbhari and Abanilla, 2007). An Arrhenius relationship has been used by investigators to predict long-term performance of polymer-based composites where moisture diffusion is assumed Fickian. This method relates the material performance to temperature in an inverse logarithmic form over time, that is, time−temperature superposition. The prediction of material properties using an Arrhenius method results in equations of the following form (Karbhari and Abanilla, 2007):

$$P(t) = \frac{P_o}{100}[A \ln(T) + B] \quad \text{for } T > 0 \tag{5.4}$$

where $P(t)$ and P_o are performance attributes or material properties at time t and 0, respectively; A is a constant denoting degradation rate, and B is a constant reflecting the early effects of post-cure. This is a semiempirical, mechanism-based modeling approach. The model uses relevant, known, and observed phenomena to capture the first-order effects of interest through parameters A and B, which are obtained using a battery of short-term accelerated tests. To accelerate these tests, an environmental chamber is typically used, where the specimens can be subjected to changing moisture and temperature as a function of time.

While FRP composites are the primary focus in this durability discussion, it should be noted that degradation models for other materials within a component can be included in the framework for service life prediction (i.e., loss of area due to steel corrosion) in order to asses combined effects. The selection of material degradation models or inclusion of empirical data should reflect the environment where the rehabilitation is to take effect. For instance, where combinations of high temperature and high humidity are anticipated, prediction models developed from moisture and elevated temperatures would be considered most appropriate for the constituent materials selected in the rehabilitation.

5.4 Evaluation of pipe rehabilitation

A piping rehabilitation can be subjected to a number of potential limit states when considering all possible loading combinations and environments, for example, soil loads, traffic loads, bending of pipe, frost action, internal corrosion, etc. (Najafi, 2011). These potential limit states can be categorized into local and global performance functions. In this section, a time-dependent failure probability analysis is performed in order to predict long-term performance of FRP-rehabilitated piping components as described in Section 5.2. The analysis utilizes a stress-based performance function in the hoop direction, including the effects of overburden soil, traffic loads, and internal pressure. It is possible to consider multiple limit states, such as localized defects, in the probability analysis with another performance function and as statistical properties of critical variables become known.

For this example application, the objective is to evaluate the long-term performance of FRP rehabilitation on a fully deteriorated, pressurized pipe in terms of likelihood of failure. In particular, the effects of manufacturing quality on failure probability of the as-built and service life are considered, including

1. Fiber selection and fiber volume fraction.
2. Deterioration of mechanical properties of the composite.
3. Composite thickness variation resulting from fabrication quality.

The FRP composite is expected to resist both internal and external pressures without any contribution to the structural integrity of the system from the host pipe. It is also assumed that the pipe component is uniformly loaded and supported along its length, and the circumferential stresses are considered more critical than axial stresses (Ahmmad and Melchers, 1994; Toutanji and Dempsey, 2001; Sadiq et al., 2004). Furthermore, it is assumed that the pipe will remain at constant and uniform temperature. The total circumferential stress in the pipe wall includes the bending stresses induced by soil pressure and vehicular traffic as well as the hoop stress produced by internal fluid pressure. The total circumferential stress in the pipe wall due to loading, σ_θ, is given as follows (Ahmaad and Melchers, 1994; Amirat et al., 2006):

$$\sigma_\theta = \sigma_f + \sigma_s + \sigma_\tau \tag{5.5}$$

where σ_f is the circumferential (hoop) stress due to internal fluid pressure and evaluated according to Eqn (5.6); σ_s is the circumferential stress due to soil pressure and evaluated according to Eqn (5.7); σ_t is the circumferential stress induced by traffic loading and evaluated according to Eqn (5.8) (Ahmaad and Melchers, 1994; Amirat et al., 2006).

$$\sigma_f = \frac{pr}{t} \tag{5.6}$$

where it is assumed that wall thickness, t, is much smaller than the pipe radius, r, and p is the internal fluid pressure.

$$\sigma_s = \frac{6k_m C_d \gamma B_d^2 Etr}{Et^3 + 24k_d pr^3} \tag{5.7}$$

where C_d is the calculation coefficient for earth load, γ denotes unit weight of soil backfill, B_d is the width of the ditch coincident with the top of pipe, E is the modulus of elasticity of the metal pipe, and k_m is the bending moment coefficient dependent on the distribution of vertical load and reaction.

$$\sigma_\tau = \frac{6k_m I_c C_t FEtr}{A(Et^3 + 24k_d pr^3)} \tag{5.8}$$

where I_c is the impact factor, C_t is the surface load coefficient, F is the wheel load on the surface, and A is the effective length of a pipe on which load is computed.

5.4.1 Performance function

In this analysis a Monte Carlo simulation is conducted, where random numbers are generated for each identified random variable according to its respective probability distribution. The limit state function or performance equation for circumferential stress in FRP-composite pipes is provided as follows:

$$g(\vec{\mathbf{X}}) = \sigma_{\mathrm{ULT}} - \sigma_{\theta} \tag{5.9}$$

Failure in the hoop direction of the pipe is defined as the event when $g(\vec{\mathbf{X}}) \leq 0$. σ_{ULT} is the ultimate tensile strength of the FRP composite in the hoop direction and represents the resistance parameter in the performance function. σ_{θ} is the circumferential stress due to externally applied loading and represents the demand in this limit state equation and is given by Eqn (5.5). Table 5.1 summarizes the random variables used in this analysis, their distribution types, means, and COVs. The data for variables in Eqns (5.2)−(5.4) are uncertain, with the most significant being the surface wheel load, F, and the importance factor, I_c. Other coefficients (C_t, C_d, k_m, and k_d) in Table 5.1 are uncertain because they are chosen on the basis of limited information (Ahmmad and Melchers, 1994). The approach here is to generate random numbers for each random variable according to its respective probability density function and determine if a failure event has occurred in the performance function.

5.4.2 FRP composite properties

The mechanical, thermal, and hygrothermal properties of FRP composites are a function of selected constituent materials, namely fiber and matrix, and the fiber, matrix, and void volume fractions that are a result of the manufacturing process. In this analysis, the influence of fiber volume fraction on the failure probability of FRP-rehabilitated piping components is also examined. Procedures for micromechanical and macromechanical analysis of lamina (i.e., determination of lamina elastic moduli and strength properties) from basic constituent properties are well established and readily available in standard texts (Kaw, 2006). Table 5.2 summarizes the constituent properties of carbon fiber, glass fiber, and epoxy matrix utilized in the reliability analyses presented in this chapter. These standard properties were obtained from Kaw (2006).

An epoxy matrix is assumed for the FRP composite, although properties of polyester, vinylester, or other common matrices can be substituted. The distribution type and COVs for as-built composite modulus and ultimate tensile strength are given in Table 5.3. Mean values for ultimate tensile strength and modulus of elasticity of a lamina are calculated for a set of constituent materials for a specific fiber volume fraction assuming a 5% void volume fraction; other statistical properties were obtained from Atadero et al. (2005) for wet lay-up, field-manufactured composites, in order to emulate the possible variation in properties of FRP composites cured under ambient conditions.

Tables 5.4 and 5.5 list calculated modulus of elasticity and ultimate tensile strength in the hoop direction of a pipe rehabilitated with carbon/epoxy and glass/epoxy

Table 5.1 Description of random variables

Symbol	Description	Type	Mean	Units	COV	SD
p	Internal fluid pressure	Normal	6.205	MPa	0.2	1.241
r	Pipe radius	Normal	228.6	mm	0.05	11.43
t	FRP liner thickness	Normal	4.35	mm	0.1	0.435
F	Wheel-load traffic	Normal	267,000	N	0.25	66,750
A	Pipe effective length	Normal	914	mm	0.2	182.8
γ	Unit weight of soil	Normal	1.89E-05	N/mm^3	0.1	1.89E-06
B_d	Width of ditch	Normal	762	mm	0.15	114.3
I_c	Impact factor	Normal	1.5	–	0.25	0.375
k_d	Deflection coefficient	Lognormal	0.108	–	0.2	0.0216
C_t	Surface-load coefficient	Lognormal	0.12	–	0.2	0.024
k_m	Bending-moment coefficient	Lognormal	0.235	–	0.2	0.047
C_d	Calculation coefficient	Lognormal	1.32	–	0.2	0.264

Table 5.2 Fiber and matrix properties

Material description	Axial modulus (GPa)	Transverse modulus (GPa)	Axial tensile strength (MPa)	Ultimate tensile strain (%)	Transverse tensile strength (MPa)	Shear strength (MPa)
Carbon fiber	230	22	2067	0.9	77	36
Glass fiber	85	85	1550	1.8	1550	35
Epoxy matrix	3.4	3.4	72	–	72	34

Table 5.3 Statistical description of fiber-reinforced polymer-composite properties

Symbol	Description	Distribution type	COV (%)
E	Modulus of elasticity in the hoop direction	Lognormal	9.5
σ_{ULT}	Ultimate strength in the hoop direction	Weibull	12.2

Table 5.4 Mechanical properties and instantaneous failure probability for a carbon fiber-reinforced polymer

V_f	V_m	E (GPa)	σ_{ULT} (MPa)	$p_f(0)$ (%)
0.1	0.85	25.89	232.672	93.1
0.2	0.75	48.55	436.317	17.9
0.3	0.65	71.21	639.961	1.04
0.4	0.55	93.87	843.606	0.089
0.5	0.45	116.53	1047.250	0.014

Table 5.5 Mechanical properties and instantaneous failure probability for a glass fiber-reinforced polymer

V_f	V_m	E (GPa)	σ_{ULT} (MPa)	$p_f(0)$ (%)
0.1	0.85	11.39	207.700	95.8
0.2	0.75	19.55	356.500	40.4
0.3	0.65	27.71	505.300	5.46
0.4	0.55	35.87	654.100	0.624
0.5	0.45	44.03	802.900	0.156

composites, respectively; V_f and V_m denote the fiber volume and matrix volume fractions, respectively; E and σ_{ULT} are the modulus of elasticity and ultimate tensile strength, respectively, in the fiber direction of the lamina. It is assumed that fibers are oriented along the hoop direction of the pipe.

5.4.3 Instantaneous failure probability

The instantaneous failure probabilities at time $T = 0$, of a fully deteriorated pipe rehabilitated with carbon-FRP (CFRP) and glass-FRP (GFRP) composites versus

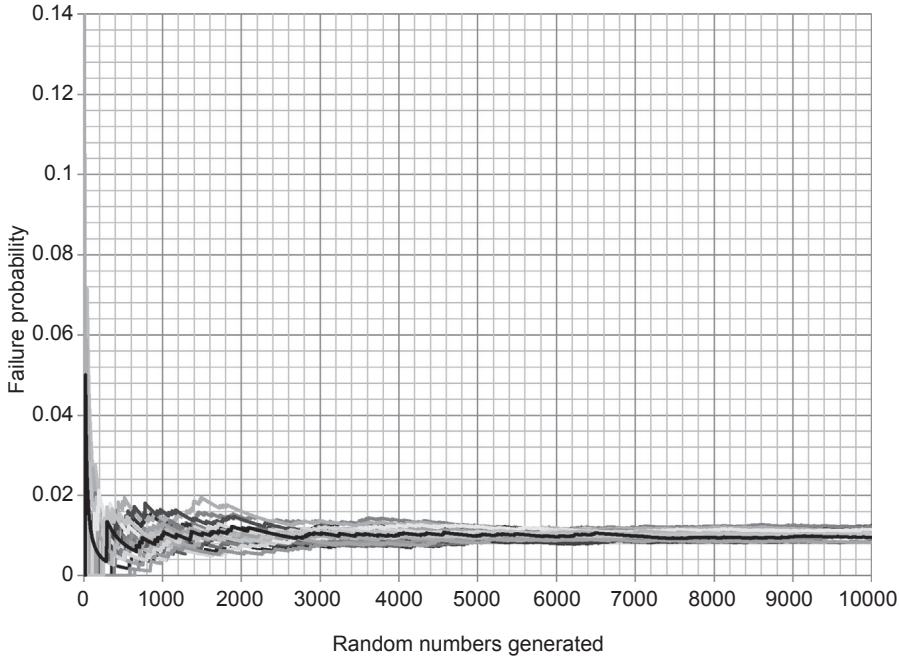

Figure 5.3 Failure probability versus sample size for 30 Monte Carlo simulations at time $T = 0$.

fiber volume fraction, V_f, are shown in Tables 5.4 and 5.5, respectively. Each of the failure probabilities listed in these tables is an average of 30 Monte Carlo simulations at time $T = 0$ for the hoop stress limit state function calculated using Eqn (5.5). Figure 5.3 shows the converging failure probability versus number of samples for all 30 Monte Carlo simulations for a CFRP-composite rehabilitation at time $T = 0$ and V_f of 30%.

A V_f of 30%, which is characteristic of wet lay-up manufactured composites (Astrom, 1997), results in failure probabilities of 1.04% and 5.46% for CFRP- and GFRP-composite rehabilitations, respectively. For comparison purposes, the failure probability of a steel pipe (mean values and distributions of tensile strength, modulus of elasticity, and thickness listed in Table 5.6) is also evaluated using Monte Carlo

Table 5.6 Random variables for steel pipe evaluation

Symbol	Description	Type	Mean	Units	COV
E	Modulus of elasticity of steel	Normal	207	GPa	0.05
σ_{ULT}	Ultimate tensile strength of steel	Normal	450	MPa	0.10
t	Thickness of steel pipe	Normal	8.73	mm	0.05

simulation. Following 30 iterations, an instantaneous average failure probability of 2.85% is determined. At a V_f of 30% and a void volume fraction, V_v, of 5%, the CFRP composite is able to attain a failure probability lower than that of the steel pipe; however, the GFRP rehabilitation has a higher failure probability as compared to the steel pipe alone. For a fabrication process that yields a composite with V_f of 40%, the failure probabilities with CFRP and GFRP composites decrease to 0.089% and 0.624%, respectively, and would both attain as-built failure probabilities lower than an as-built steel pipe.

While the examination of the as-built condition of an FRP-rehabilitated pipe is useful in targeting manufacturing techniques or establishing quality control standards, the analysis at a single instance of time yields limited information regarding the impact of deterioration processes; these deterioration processes adversely impact the service life of an FRP rehabilitation. In the following section, long-term material durability models are incorporated into the Monte Carlo simulation to generate a time-dependent failure probability.

5.4.4 Time-dependent failure probability

For the purposes of the current investigation, durability of FRP composites is characterized by the results of accelerated aging experiments. Predictions for FRP-composite tensile modulus and tensile strength for both CFRP and GFRP composites in this analysis are modeled with an Arrhenius rate relationship derived from results for wet lay-up CFRP composites immersed in deionized water at 23 °C for approximately 2 years (Karbhari and Abanilla, 2007). The time-dependent functions for tensile modulus and tensile strength for FRP composites are as follows:

$$E(T) = \frac{E_0}{100\left[-0.4182\cdot\ln\left(T\cdot 365\,\frac{\text{days}}{\text{year}}\right)+100\right]} \tag{5.10}$$

$$\sigma_{\text{ULT}}(T) = \frac{\sigma_0}{100\left[-3.366\cdot\ln\left(T\cdot 365\,\frac{\text{days}}{\text{year}}\right)+100\right]} \tag{5.11}$$

where subscript "0" indicates initial values or as-built properties, $E(T)$ and $\sigma_{\text{ULT}}(T)$ are time-dependent FRP-composite tensile modulus and tensile strength, respectively. The retention results conservatively neglect the early effects of post-cure by specifying the material constant term as 100 in Eqns (5.10) and (5.11) (see Karbhari and Abanilla, 2007).

The application of Eqns (5.10) and (5.11) allows for the calculation of mean values of FRP-composite tensile modulus and tensile strength as a function of time, T, and can be used to determine the corresponding failure probability at a given point in time. Similarly, for steel piping, degradation can be included as a function of time by including the decrease in pipe wall thickness caused by corrosion. For steel pipes,

pipe wall thickness, t, subject to corrosion is modeled by a power law in this analysis (Ahmmad and Melchers, 1994):

$$t = t_o - kT^n \tag{5.12}$$

where k is a multiplying constant characterized by a normal distribution with a mean value of 0.3 and COV of 9%; n is an exponential constant characterized by a normal distribution with a mean value of 0.6 and COV of 12%; and t_o is the as-built pipe thickness.

With all time-dependent parameters defined, the performance function is evaluated as a function of time as follows:

$$g\left(\vec{\mathbf{X}}, T\right) = \sigma_{\mathrm{ULT}}(T) - \sigma_\theta(T) \tag{5.13}$$

Figures 5.4 and 5.5 show the time-dependent failure probability of CFRP- and GFRP-rehabilitated piping components, respectively. Each point on the graph represents the average failure probability of 30 Monte Carlo simulations at each time interval. The plots indicate that a CFRP-composite rehabilitation with a V_f of 40% is more reliable than a steel pipe subject to corrosion over a 30-year period. In fact, a V_f of 40%

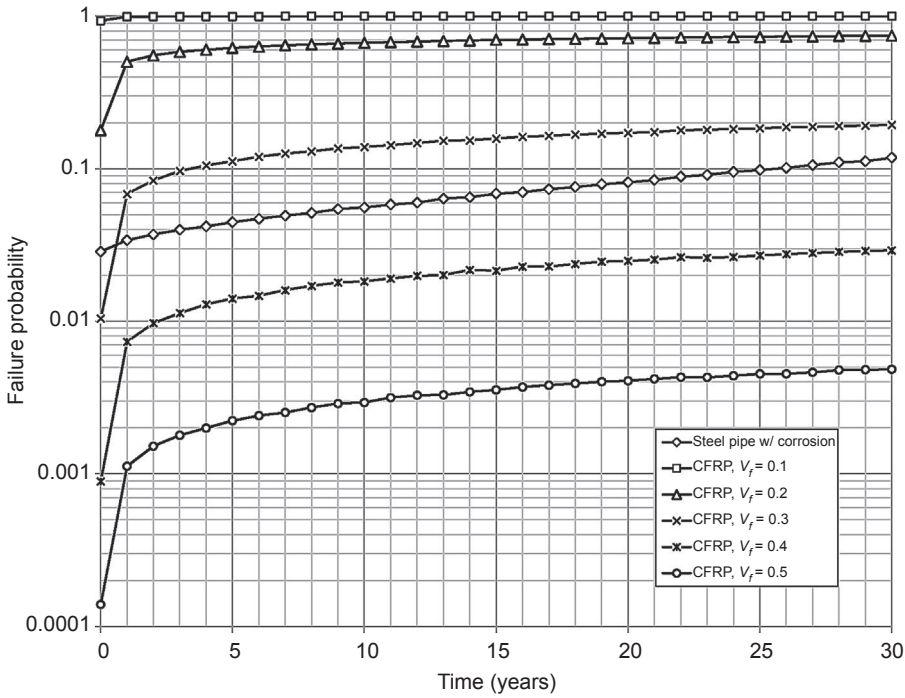

Figure 5.4 Failure probability of carbon fiber-reinforced polymer (CFRP)-composite pipe rehabilitation versus time.

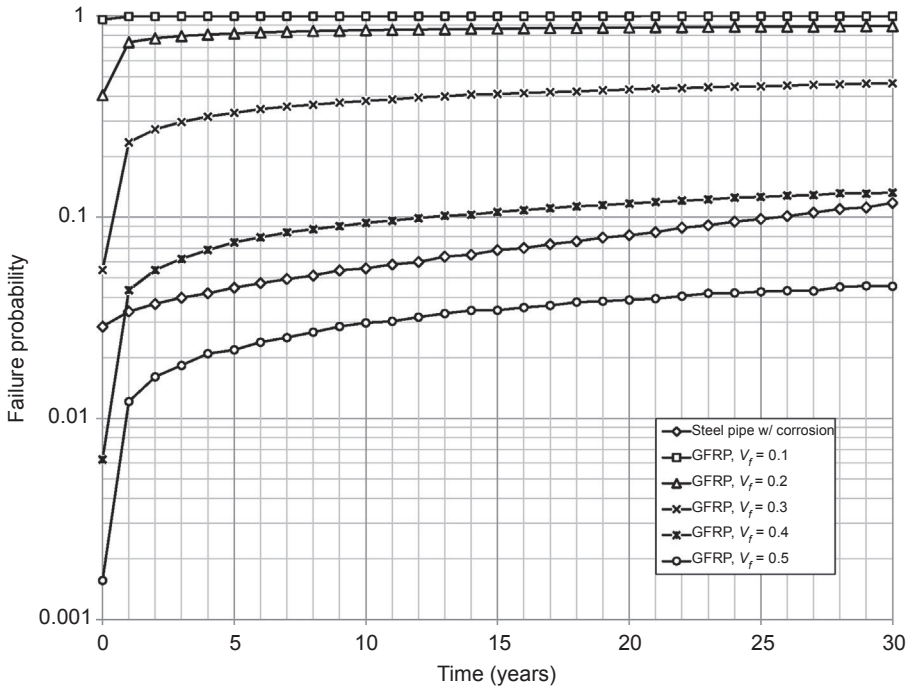

Figure 5.5 Failure probability of glass fiber-reinforced polymer (GFRP)-composite pipe rehabilitation versus time.

would be equally or more reliable than an as-built steel pipe without corrosion over the 30-year period. To provide the same level of reliability in a GFRP-composite rehabilitation as compared to a steel pipe with corrosion over a 30-year period, a V_f of 50% is needed. It is important to note that these predictions are based on composite durability models where the composite materials were fully immersed in water. Furthermore, time-dependent failure probability plots (Figures 5.4 and 5.5) indicate that volume fractions less than 20% for CFRP rehabilitation or 30% for GFRP rehabilitation are unable to provide strengthening at any instance of time.

Time-dependent failure probability results can also be used to develop design curves for the selection of constituent materials and manufacturing processes for a maximum-allowable failure probability criteria and desired service life as shown in Figures 5.6 and 5.7. For instance, in order to maintain a failure probability less than 3% (or reliability of 97%) for 10 years, a CFRP-composite rehabilitation needs to attain $V_f = 37.5\%$ at the time of construction, using materials described in this analysis.

5.4.5 Effect of composite thickness

While it is unlikely that a wet lay-up process can achieve fiber volume fractions of 50%, it must be noted that the average thickness specified in this analysis is

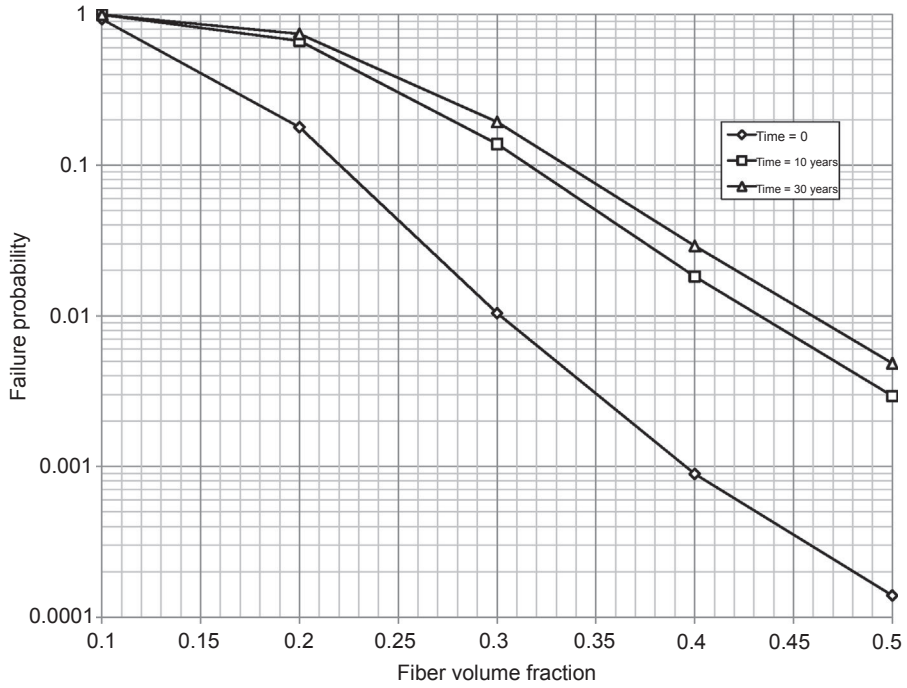

Figure 5.6 Carbon fiber-reinforced polymer-composite failure probability versus fiber volume fraction.

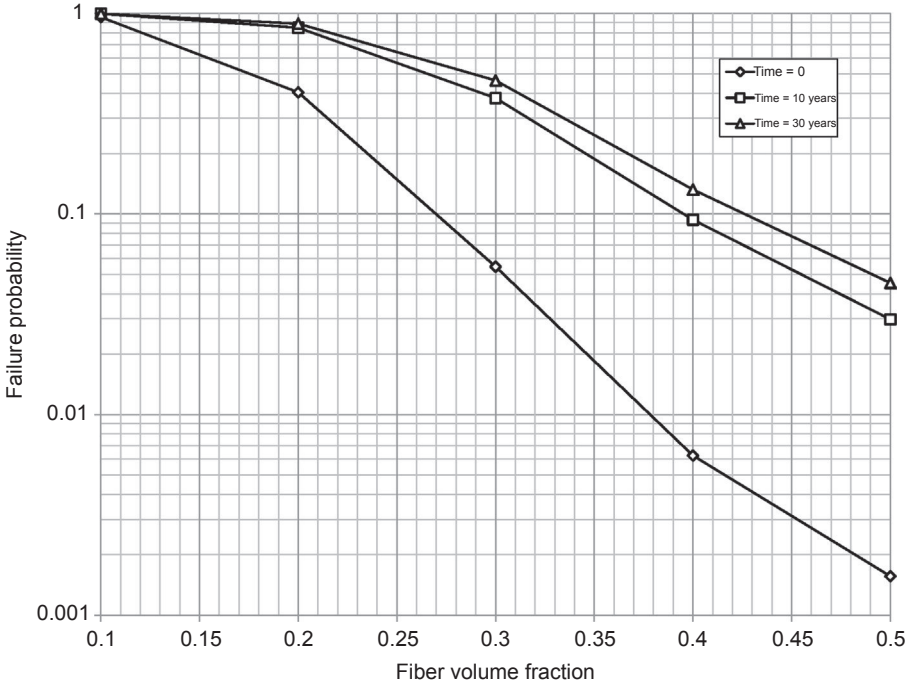

Figure 5.7 Glass fiber-reinforced polymer-composite failure probability versus fiber volume fraction.

4.35 mm versus a thickness of 8.73 mm for the steel pipe. The performance of FRP-rehabilitated piping components is sensitive to the thickness of the composite and can vary in manufacturing quality depending on the experience of the builder. For instance, Law and Moore (2007) conducted field observations of sewer liners with as-built liners measured for thickness at multiple locations. Multiple sections of liner samples displayed a mean thickness of 4.35 mm with COV of approximately 35%. All prior analyses discussed in this paper utilized a composite thickness of 4.35 mm with a COV of 10%.

Figure 5.8 shows the average failure probability results of a Monte Carlo simulation at time $T = 0$ as a function of the average thickness of CFRP- and GFRP-composite pipe rehabilitations with a thickness COV of 10%. Increasing the thickness of the composite can result in a decrease in the failure probability of an as-built rehabilitation from 2% with 4-mm thickness to 0.09% with 6-mm thickness in a CFRP-composite pipe. For a GFRP-composite pipe rehabilitation, increasing the average thickness from 4 to 6 mm results in a decrease in failure probability from 10% to 0.3%. However, as average thicknesses are increased in a wet lay-up composite, the COV of the thickness is likely to increase as well. Figure 5.9 displays the failure probability of CFRP- and GFRP-composite rehabilitations with a thickness of 4.35 mm as a function of COV. As expected, if the quality of fabrication

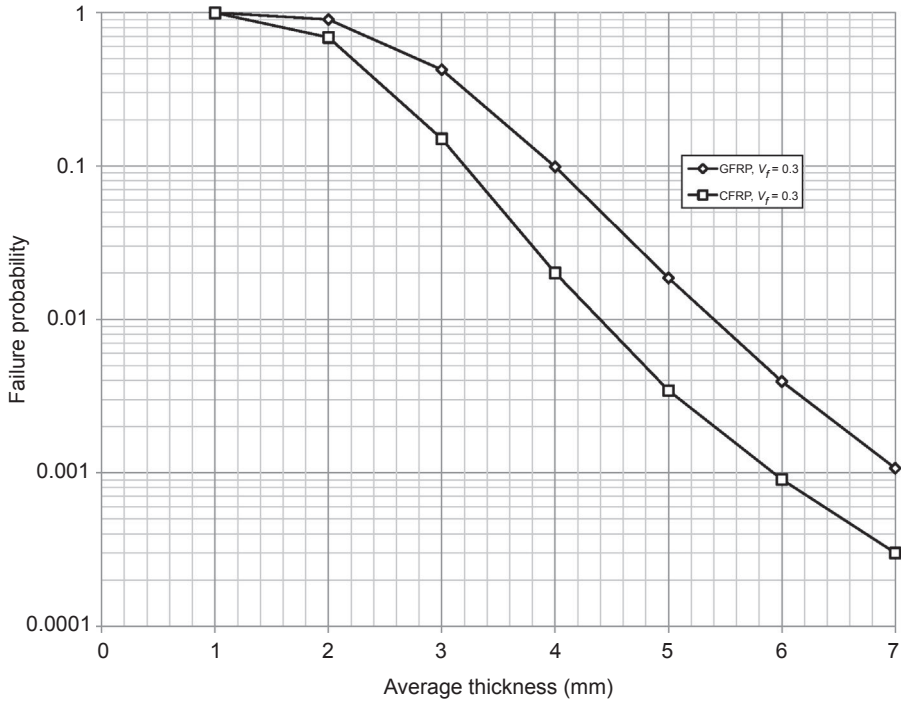

Figure 5.8 Failure probability versus average thickness of fiber-reinforced polymer-rehabilitated pipe.

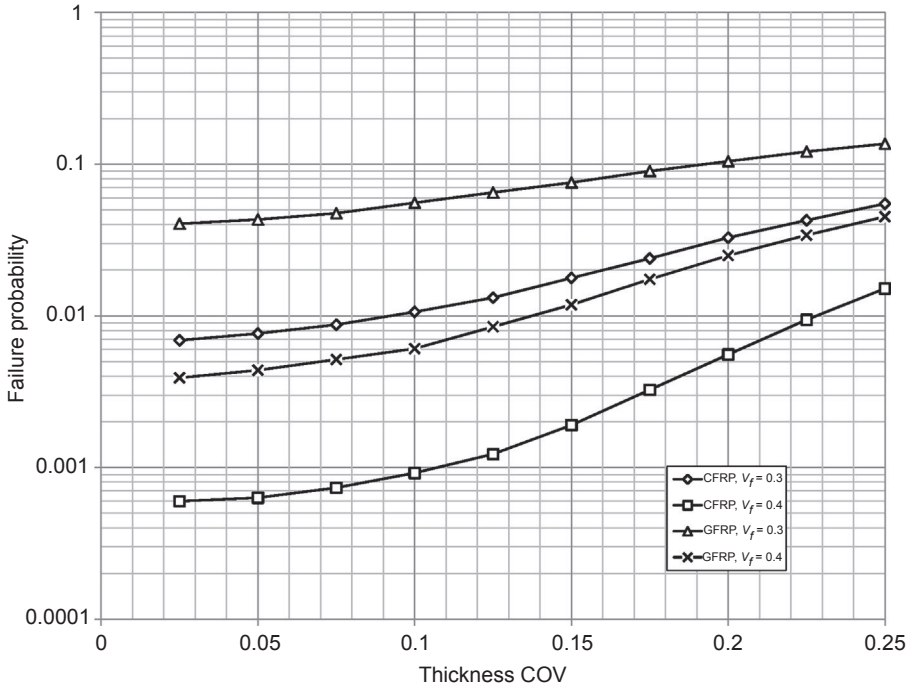

Figure 5.9 Failure probability versus thickness coefficients of variation (COVs) of fiber-reinforced polymer-rehabilitated pipe.

is improved as measured by a decreasing COV, then the failure probability of the component decreases and vice versa. The thickness analysis demonstrates the value of probabilistic analysis in establishing performance requirements for as-built geometry and characteristics of the composite (i.e., thickness, thickness variation, and fiber volume fraction) for FRP-rehabilitated pipes.

5.5 Conclusions

This chapter presents the use of probabilistic analysis of FRP-rehabilitated piping components using Monte Carlo simulation methods as part of an infrastructure management framework. At the core of this framework is the ability to incorporate material deterioration processes and uncertainty in order to estimate time-dependent performance and remaining service lives of these structural systems. FRP composites in pipe rehabilitation are capable of matching the safety and quality of new steel piping components; however, considerations such as materials selection, durability characterization, and manufacturing quality must be integrated with a design process in order to ensure long-term safety and reliability of infrastructure pipe networks.

The following observations were made with respect to the analysis of durability, fiber volume fraction, and thickness variation in FRP rehabilitation of piping components:

- In order to maintain a failure probability less than or equal to that of a steel pipe without corrosion, an FRP-rehabilitation scheme would require the use of CFRP composites with a fiber volume fraction greater than 40%.
- Evaluating the time-dependent performance of FRP-rehabilitation designs prior to selection and construction provides a valuable resource for owners to conduct cost−benefit analyses and prioritize locations within a piping network.
- The effect of composite thickness in a pipe rehabilitation can significantly impact the failure probability of an as-built rehabilitation (for a constant COV); in fact, incremental increases in thickness result in significant reductions in failure probability.
- Plots of failure probability versus fabrication criteria such as fiber volume fraction or thickness COV allow engineers to establish quality measures during construction that can predict long-term structural performance.

References

Abdalla, F.H., Megat, M.H., Sapaun, M.S., Shahari, B.B., 2008. Determination of volume fraction values of filament wound glass and carbon fiber reinforced composites. APRN Journal of Engineering and Applied Sciences 3 (4), 7−11.

Ahmmad, M., Melchers, R.E., 1994. Probabilistic analysis of underground pipelines subject to combined stresses and corrosion. Engineering Structures 19 (12), 988−994.

Alexander, C., 2007. Guidelines for repairing damaged pipelines using composite materials. In: Proceedings of Corrosion 2007, March 11−15, 2007. NACE International, Nashville, TN.

Alexander, C.R., July 2009. Advances in repair of pipelines using composite materials. In: Pipeline & Gas Technology Magazine. Hart Energy Publishing, LP.

Alexander, C., Francini, B., 2006. State of the art assessment of composite systems used to repair transmission pipelines. In: Proceedings of the Sixth International Pipline Conference, September 25−29, 2006, Calgary, Alberta, Canada.

Amirat, A., Mohamed-Chateauneuf, A., Chaoui, K., 2006. Reliaibility assessment of underground pipelines under the combined effect of active corrosion and residual stress. International Journal of Pressure Vessels and Piping 83, 107−117.

Ang, A.H.-S., Tang, W.H., 2007. Probability Concepts in Engineering − Emphasis on Applications to Civil and Environmental Engineering, second ed. John Wiley & Sons, Hoboken, NJ, USA.

Astrom, B.T., 1997. Manufacturing of Polymer Composites, first ed. Chapman & Hall, London, UK.

Atadero, R., Lee, L., Karbhari, V.M., 2005. Consideration of material variability in reliability analysis of FRP strengthened bridge decks. Composite Structures 70, 430−443.

Bank, L.C., Gentry, T.L., Barkatt, A.R., 1995. Accelerated test methods to determine the long-term behavior of FRP composite structures: environmental effects. Journal of Reinforced Plastics and Composites 14, 559−587.

Bethel, K., Catha, S.C., Kanninen, M.F., Stonesifer, R.B., Charbonneau, K., Ekelund, A., Mandich, I., Mc Intosh, R., Stringfellow, W.D., September 2006. The design, development, and validation of an innovative high strength, self monitoring, composite pipe liner for the

restoration of energy transmission pipelines. In: Proceedings of the Sixth International Pipeline Conference, Calgary, Alberta, Canada, September 25−29, 2006.

Black, S., June 1, 2005. Repair of infrastructure with composites: composites prove their mettle in large, demoing repairs and rehab. Composites Technology. http://www.compositesworld.com/articles/repair-of-infrastructure-with-composites.

Cagno, E., De Ambroggi, M., Grande, O., Trucco, P., 2011. Risk analysis of underground infrastructures in urban areas. Reliability Engineering and System Safety 96, 139−148.

Chin, W.S., Lee, D.G., 2005. Development of the trenchless rehabilitation process for underground pipes based on RTM. Composite Structures 68, 267−283.

Duell, J.M., Wilson, J.M., Kessler, M.R., 2008. Analysis of carbon composite overwrap pipeline repair system. International Journal of Pressure Vessels and Piping 85, 782−788.

Ditlevson, O., Madsen, H.O., 1996. Structural Reliability Methods, first ed. John Wiley & Sons, Chichester, England.

Gentry, T.R., Bank, L.C., Thompson, B.P., Russell, J.S., 2002. An accelerated-test-based specification for fiber reinforced plastics for structural systems. In: Proceedings of the Second International Conference on Durability of Fiber Reinforced Polymer (FRP) Composites for Construction, Montreal, Canada, May 29−31, 12 pp.

Hastak, M., Mirmiran, A., Deepak, R., 2003. A framework for life-cycle costs assessment of composites in construction. Journal of Reinforced Plastics and Composites 22 (15), 1409−1430.

Karbhari, V.M., Abanilla, A., 2007. Design factors, reliability, and durability prediction of wet lay-up carbon/epoxy used in external strengthening. Composites Part B 38, 10−23.

Karbhari, V.M., Zhao, L., 2000. Use of composites for 21st century civil infrastructure. Computer Methods in Applied Mechanics and Engineering. 135, 433−454.

Kaw, A.K., 2006. Mechanics of Composite Materials, second ed. CRC Press, Taylor & Francis Group, Boca Raton, FL.

Kawahara, B., Estrada, H., Lee, L.S., 2012. Chapter 12: life-cycle cost comparison for steel reinforced Concrete and fiber reinforced polymer bridge decks. In: Jain, R., Lee, L.S. (Eds.), Fiber Reinforced Polymer (FRP) Composites for Infrastructure Applications. Springer Science + Business Media, Dordrecht, The Netherlands, ISBN 978-94-007-2356-6.

Law, T.C.M., Moore, I.D., 2007. Installed geometry of cast-in-place polymer sewer liners. Journal of Performance of Constructed Facilities 21 (2), 172−176.

Melchers, R.E., 1999. Structural Reliability Analysis and Prediction, second ed. John Wiley & Sons, Chichester, England.

Melchers, R.E., 2011. Chapter 6 − probabilistic methods for service life estimation of civil engineering structures. In: Karbhari, V.M., Lee, L.S. (Eds.), Service Life Estimation and Extension of Civil Engineering Structures. Woodhead Publishing Ltd, Cambridge, England, ISBN 978-1-84569-398-5.

Najafi, M., 2011. Chapter 10 − pipeline rehabilitation systems for service life extension. In: Karbhari, V.M., Lee, L.S. (Eds.), Service Life Estimation and Extension of Civil Engineering Structures. Woodhead Publishing Ltd, Cambridge, England, ISBN 978-1-84569-398-5.

Sadiq, R., Rajani, B., Kleiner, Y., 2004. Probabilistic risk analysis of corrosion associated failures in cast iron water mains. Reliability Engineering and System Safety 86 (1), 1−10.

Shamsuddoha, M., Islam, M.M., Aravinthan, T., Manalo, A., Lau, K., 2013. Effectiveness of using fibre-reinforced polymer composites for underwater steel pipeline repairs. Composite Structures 100, 40−54.

Toutanji, H., Dempsey, S., 2001. Stress modeling of pipelines strengthened with advanced composite materials. Thin-Walled Structures 39, 153−165.

Use of Clock Spring® as a permanent means of pipeline repair

6

D.S. Lesmana
Country Manager and Representatives (Indonesia), Clock Spring Company L.P., Houston, TX, USA

6.1 The history of Clock Spring®

Maintaining a pipeline can be costly but can pale in comparison to the cost of a failure. Pipeline operators must balance maintenance costs with pipeline integrity. The purpose is not to save money but to attain a level of safety that is acceptable to the company and the public at a cost the company can afford. The public, however, is gaining an ever-increasing voice in where the integrity level is set (Porter, 2000).

Clock Spring® Company L.P. pioneered the use of composite technology for repairing blunt defects in high-pressure pipelines. This technology is now an accepted permanent repair technique and is used routinely throughout the world. There are more than one million Clock Spring® repairs in place and to date there have been no reports of material failure or deficiencies. Clock Spring® has an impressive record and an equally impressive history.

Clock Spring® was recognized by the US Department of Transportation (DOT) as an effective permanent repair for blunt defects in high-pressure pipelines. Several waivers were granted to various companies to allow the use of Clock Spring® in their rehabilitation programs. This recognition and approval was based on the extensive research, development, and testing conducted during product development. This development was supported by the pipeline industry through Gas Research Institute (GRI) and performed by some of the most prestigious laboratories in the United States, including Battelle, Southwest Research Institute, Kiefner and Associates, and Stress Engineering, to name just a few. Clock Spring® has met all of the requirements imposed by reasonable and prudent engineering.

The Code of Federal Regulations has adopted a performance-based standard. This means that each pipeline company can choose a repair method and use it as long as that method or technique is based on reasonable and prudent engineering judgment. This performance-based code allows for, and actually encourages, innovation. Clock Spring® supports this type of regulatory progress and applauds the Research and Special Programs Administration of the Department of Transportation for adopting this progressive approach. Performance-based codes put additional responsibility on pipeline operators. They must be sure of the techniques they adopt for pipeline repair and

Rehabilitation of Pipelines Using Fiber-reinforced Polymer (FRP) Composites. http://dx.doi.org/10.1016/B978-0-85709-684-5.00006-0

must have confidence that the system has been adequately tested and has the performance information to ensure durability.

The distinctions between different types of composites used for pipeline repair are important and must be understood to ensure the composite repair selected will meet the rigorous specifications demanded by sound engineering, testing, and analysis.

An extensive field validation program is required by the DOT. This requirement was added to verify the laboratory results and to provide and to validate the real world behavior on actual pipelines.

Clock Spring® design required a safety factor of 2 based on a maximum anticipated load of 10 ksi (69 MPa). The composite was designed to withstand 20 ksi (138 MPa) loads at 50 years of exposure to worst case operating conditions. Based on this equation the Clock Spring® 20 ksi (138 MPa) design life is 67 years. This equation shows the minimum; new ($t = 1$) tensile strength of the composite should exceed 42 ksi (290 MPa) (GRI, 1998).

The GRI program from the 1990s established a safety factor of 2, as a prudent engineering parameter. The design stress was established at twice the level that the composite would experience. Data were collected for several years as a prudent data set for extrapolation to longer time periods. The 50 years' design lifetime was established as the time period for "permanent." The lower bound line was chosen as the appropriate conservative consideration.

The accelerated testing for Clock Spring® conducted by GRI is shown in Figure 6.1.

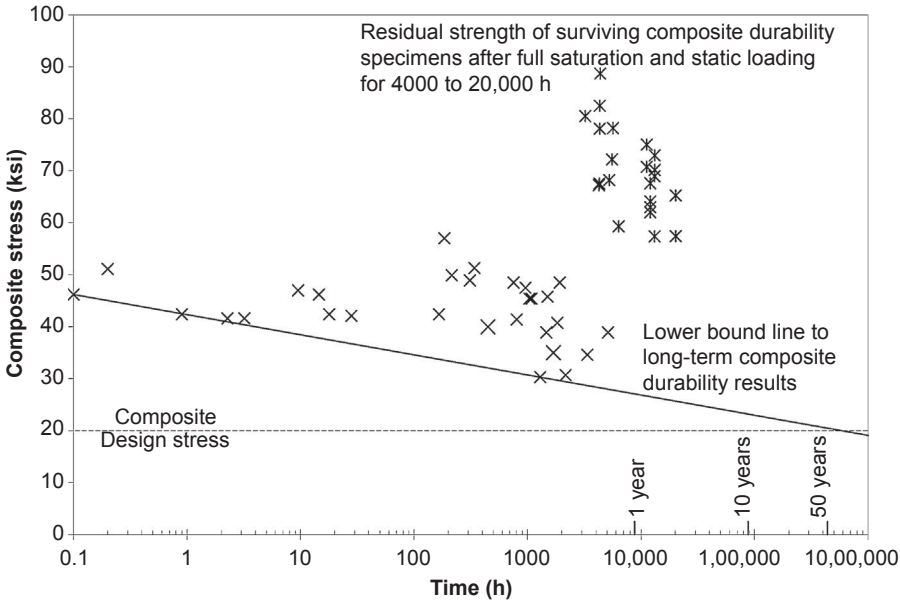

Figure 6.1 Accelerated testing of Clock Spring® specimens.
Courtesy of GRI-98/0032 (1998) *"Field Validation of Composite Repair of Gas Transmission Pipelines"* −Final Report−Gas Technology Institute, DesPlaines, IL.

Over two decades of time has passed since the GRI established the first steering committee of industry experts to design the scope and methods of the investigations. More than one million Clock Spring® composite sleeve repairs have since been made. Units have been installed in scores of countries and in almost all conceivable environmental conditions (onshore, offshore, subsea, tropical, desert, tundra, etc.) (Laughlin, 2011).

6.2 The Clock Spring® repair system

The composite sleeve repair consists of three parts: a full cured composite sleeve of unidirectional E-glass fibers and a polymer base (the strength member) manufactured to suit the specific pipe diameter; an adhesive to secure the repair; and a load transferring material to transfer the load from the defect to the composite sleeve (Figure 6.2).

A typical repair consists of locating and cleaning the defect area. The defect area and other voids under the repair are filled with a high compressive strength material to transfer the loads from the pipe to the externally applied composite sleeve.

A starter pad is applied to the pipe to secure the inner edge of the composite sleeve. Adhesive is used to secure the sleeve to the pipeline. The composite sleeve is then wrapped around the pipe, typically eight layers, while applying adhesive between each layer.

The unit is tightened onto the pipe. Excess adhesive and filler will extrude out the edge of the unit ensuring a fully filled, tight fit. The adhesive will cure in about 2 h and the repair area can be recoated and backfilled. The entire installation takes only about 30 min.

6.3 Pre-cured composite sleeve manufacturing

Composite can be completely manufactured in a factory (e.g., pulltruded such as Clock Spring®) or fiber and resin can be combined on site. Regardless of the manufacturing

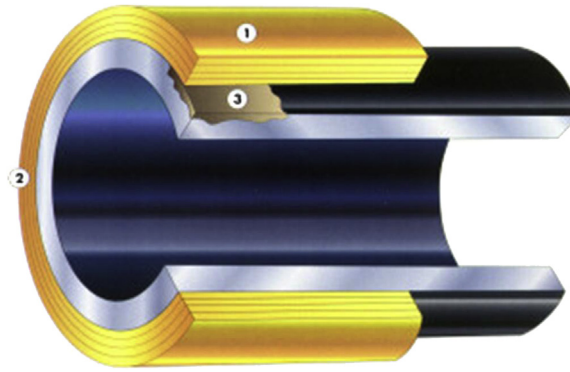

Figure 6.2 The Clock Spring® repair system.
Courtesy of Clock Spring® Company L.P.

process and its location, a quality composite requires that the reinforcement be completely saturated with the resin. The composite must also be compacted to squeeze out air bubbles and excess resin and be fully cured prior to carrying loads. In a factory environment quality control procedures will ensure more consistent properties in the finished product.

The Clock Spring® used today is manufactured by encapsulating tows of continuous E-glass fibers in an isophthalic polyester resin matrix. This is then bonded to the pipe and to itself with a methyl methacrylate adhesive. Before applying the Clock Spring® the defect area is filled with a high compressive strength filler material to transfer the load from the pipe to the Clock Spring®. This repair system is a result of *evolution* rather than *revolution*. Many other embodiments of composite technology were investigated and rejected for solid engineering reasons.

6.3.1 The nature of E-glass fibers

Most glass fibers consist of E-glass, a term which once stood for electrical grade glass, as is used in electrical insulators and capacitors. This glass is a supercooled mixture of metallic oxides. It is brittle and transparent but has very high tensile strength, 3400 MPa (500 ksi). Glasses in bulk form tend to have relatively low strength levels because of the presence of microscopic surface flaws that act as sites for crack propagation. Glass in fibrous form can be much stronger if the surface of the fibers is protected at all times against damage. Glass is produced in a furnace at about 1200 °C (2192 °F) and spun into fibers by allowing it to drain under its own weight through many heated bushings. Molten glass is quite corrosive, and the bushings must be made from platinum to avoid damage and protect the glass from contamination. Each bushing contains many hundreds of holes through which the molten glass must pass before forming fibers of approximately 10 microns (4×10^{-4} in.) in diameter.

The secret of the strength of glass fibers, and of their ability to bond to polymeric matrices, is the "size" which is applied to the surface of the fibers in the form of an aqueous solution shortly after the fibers emerge from the bushings. The size contains a polymeric binder which coats the glass surface to protect it and lightly binds together the individual fibers in each fiber tow to prevent them from rubbing against one another during subsequent handling and processing. The size also contains a coupling agent—a reactive component, usually an organo-silane—which is a multifunctional molecule. The silane part of the molecule bonds tightly to the surface of the glass while the organic part is designed to attach itself to the polymer matrix. When purchasing glass fiber it is necessary to stipulate the type of resin matrix to be used, since some coupling agents are specifically chosen to be compatible with particular resins. The size also contains a film former to enable it to spread over the glass surface and lubricants to facilitate processing without damage.

Despite the presence of the size, every processing or handling operation introduces flaws and reduces the strength of the glass. By the time it has been incorporated into the composite, the effective tensile strength is generally about 1700 MPa (246 ksi), which is lower than its strength immediately after leaving the bushing (3400 MPa) (500 ksi).

After spinning, the glass fiber tows, referred to as rovings, are wound at high speed onto cylindrical packages, or cheeses, and placed in a drying oven where the water in the size coating is removed. (Note: A tow is a bundle of filaments and rovings are bundles of tows but they are sometimes used interchangeably.) These cylindrical packages are the basic intermediate from which a wide variety of glass reinforcing products are manufactured.

Three characteristics must be considered when designing fiber reinforcement: fiber type (glass, carbon, or aramid); fiber form (typically roving, tow, mat, or woven fabric); and fiber orientation or architecture. Reinforcement can be oriented longitudinally in a structural element or transverse to the longitudinal direction or in any direction desired by the designer. Fiber direction can be so varied that virtually isotropic material can be produced. The most common structural elements are designed with greater strength in the direction subjected to the greatest load.

Unidirectional rovings can be used directly in composite manufacture, or they can be converted to other intermediate products. Direct applications include the unidirectional rovings used in processes such as spray lay up, filament winding, and pultrusion. Pultrusion is the process in which glass rovings or tows, in a preselected orientation, are saturated with resin and pulled through a heated die, where the part is formed and cured.

Pultrusion is the technique used in the manufacture of Clock Spring®. Alternatively, the glass strands may be chopped, usually to a length of 50 mm (2 in.), and sprinkled onto a moving belt to make chopped strand mat (CSM), the most widely used reinforcing product for both boat building and other general purpose GRP products. CSM contains randomly oriented glass strands, held together by the application of a small amount of polymeric binder (Figure 6.3).

Continuous strand mat or swirl mat is similar in some respects to CSM, except that the fibers are continuous. Swirl mat is used in pultrusion, where the reinforcement is required to have sufficient integrity to allow it to be pulled through the process under tension. The glass can also be woven to form a glass cloth with various weaves such as plain, satin, or twill.

For high-pressure pipeline repair applications, unidirectional alignment of the reinforcing glass and the pultrusion process has clear advantages.

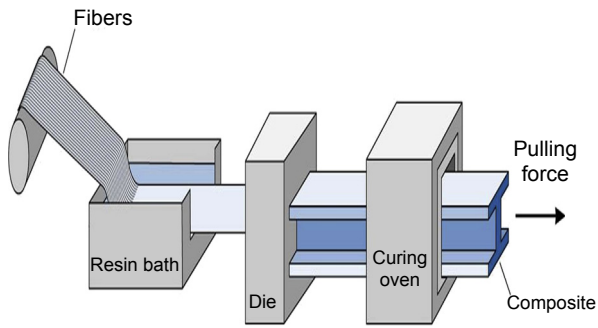

Figure 6.3 Producing composite shapes by pultrusion.
Courtesy of Brooks Cole a division of Thomson Learning Inc.

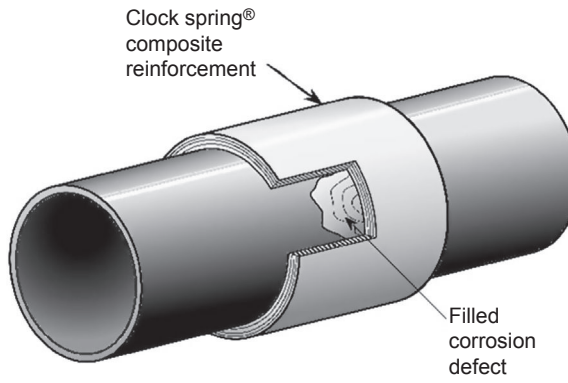

Figure 6.4 Clock Spring® repair application.
Courtesy of Clock Spring® Company L.P.

6.3.2 Full cure application

The composite sleeve is manufactured under controlled conditions. The ratio of glass to resin is accurately controlled and monitored. The unidirectional glass strands are carefully positioned and aligned to maximize strength in the hoop direction. The composite is squeezed, dried, heat-treated and cured, and shipped as a completed unit to the repair location. All design variables are controlled. The mechanical properties of the composite are consistent and well defined. Clock Spring® eliminates all of the variables of the wet wrap process.

The Clock Spring® composite laminate layers are nominally 0.065 in. thick and have a glass fiber content ranging from 60 to 70 percent by weight (45 to 55 percent by volume). The Clock Spring® composite material exhibits linear elastic behavior up to the point of failure in tension, typically 1.5−2% strain. Typical values of the elastic modulus are 5×10^6 psi in the fiber direction and 1.4×10^6 psi in the transverse direction. Tensile strength is typically 75 to 100 ksi. The coefficient of thermal expansion is 6.0×10^{-6} in./in./°F in the fiber direction and 3.2×10^{-5} in./in./°F in the transverse direction (see [4] in sources of further information).

It is because these variables are well controlled that the performance of the Clock Spring® repair can be predicted. Without this predictable performance, long-term durability would be questionable (Figure 6.4).

6.4 Case study of repair application

6.4.1 High-pressure gas transmission lines repair

Composite repairs have been utilized within the transmission pipeline industry for the past 20 years for the permanent repair and reinforcement of sections of the pipe wall which have been weakened due to corrosion.

Most internationally recognized repair codes such as ASME B31.4 and B31.8 accept the use of composites for this repair function. Most oil and gas pipeline operators are familiar with composites and the health, safety, technical, and commercial

benefits they provide. In this section, we will present several case studies of Clock Spring® repair application within the high-pressure gas transmission line repairs.

6.4.1.1 Case study no. 1: mechanical damage repair

During a routine excavation the excavator accidentally hit a 28-in. main gas transmission line situated in the middle of the Perawang jungle in Pekanbaru, Riau, Indonesia. The excavator had "caught" the pipeline causing a significant mechanical defect with 3 m of the pipeline being damaged. As the pipeline is the main supply to a local power station and also to Singapore, it was critical that it remained in operation. It was midsummer with temperatures in excess of 39 °C and a peak period for electricity supply (Figure 6.5).

The Clock Spring® repairs for the 28-in. API 5L X65 pipe were installed within 3 days on site without interrupting the pipeline operations (Figure 6.6).

A large number of studies have been conducted concerning the suitability of full cure laminate composite sleeves for the permanent repair of mechanical damage and

Figure 6.5 Mechanical damage defect on the 28-in. gas line.

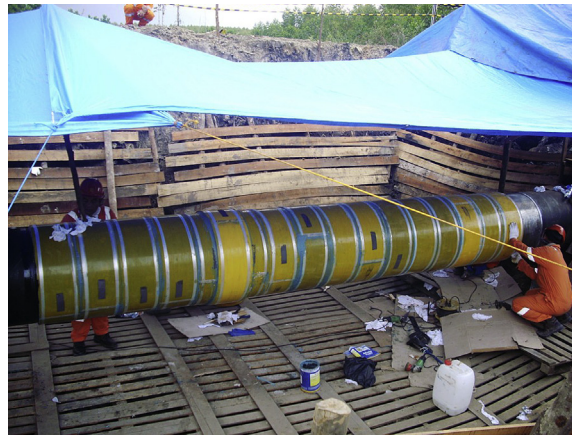

Figure 6.6 Installation of repair sleeves on the 28-in. gas transmission line.

third party interference. The results of these studies have shown that Clock Spring® composite repairs are acceptable (Lesmana, 2010).

6.4.1.2 Case study no. 2: mechanical damage repair

An external defect suspected to have been caused by mechanical damage from a backhoe loader during a pipeline installation was found after an ILI inspection for a main 32-in. gas transmission line supplying gas from Sumatra to Java Island in Indonesia (Figure 6.7).

A composite repair sleeve was applied to reinforce the damaged area, following excavation and manual surface preparations in accordance with industry standard guidelines (Figure 6.8).

The repair was completed under the supervision of a Clock Spring® installer within 1 day.

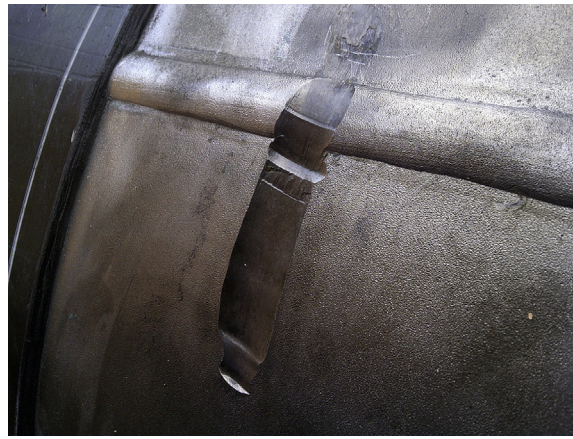

Figure 6.7 Defect in the 32-in. pipeline also affecting the seam weld.

Figure 6.8 Installation of the 32-in. seam sleeve.

6.4.1.3 Case study no. 3: alkaline soil erosion defect

An external defect suspected to have been caused by alkaline soil erosion resulted in significant mechanical and corrosion damage to the 28-in. main high-pressure gas transmission pipeline supplying gas to the Duri field in Riau, Indonesia (Figure 6.9).

For this repair four corrosion sleeves were needed and the repair was completed within 1 day under the guidance of a trained and qualified supervisor (Figure 6.10).

Figure 6.9 The alkaline soil erosion type defect.

Figure 6.10 Completed 28-in. repair sleeve installation.

6.4.2 Offshore riser and caisson repair

With the region (Asia Pacific Region) experiencing aging offshore oil and gas infrastructure, composites technology is a relatively recent innovation when it comes to repairing piping and pipelines, with an increasing number of applications now in service. This section will introduce the benefits of using composite materials as a methodology for permanently repairing pipe work and pipelines within the offshore area.

Figure 6.11 Sample of CUI defect.

Figure 6.12 Completed high-temperature composite sleeve repair.

6.4.2.1 Case study no. 1: CUI repair

An external defect due to corrosion under insulation (CUI) and hot atmospheric conditions (+80 C) was identified on a high pressure and high temperature riser in Mahakam Delta, East Kalimantan (Figure 6.11).

Following surface preparation by sand blasting, a high-temperature repair sleeve was applied to reinforce the weak area.

The installation was completed by a man crew of two under the supervision of a trained supervisor within 1 day with no need to shut in the riser and no hot work or specialized installation equipment (Figure 6.12).

6.4.2.2 Case study no. 2: external corrosion and leaking defect

External corrosion due to a harsh sea environment caused a corrosion and leaking defect on a 42-in. skim pileat the splash zone area. The platform is in the Natuna Block, South China Sea.

Following grit blasting and surface preparation in accordance to industry standard guidelines, a Snap Wrap full cured laminate repair was applied to seal the leak and reinforce the general corrosion area. The repair was completed within 1 day without interrupting the operation of the platform (Figure 6.13).

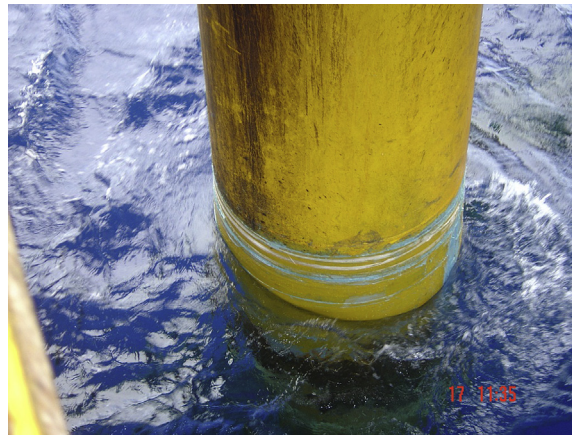

Figure 6.13 Completed 42-in. Skim Pile repair.

6.4.2.3 Case study no. 3: splash zone repair

A 36-in. sump caisson was leaking in one of the offshore oil and gas platforms in the Natuna Sea. Due to the allowable window of shutdown during the repair, a Snap Wrap was chosen to repair these sections and return the integrity of the caisson.

After surface preparation by sand blasting, the Clock Spring® Snap Wrap was applied for 1 m of total length to restore the capability of the operating caisson. The repair was made within 2 days with a man crew of only four.

The repair provided significant cost savings due to its efficiency, speed, and ease of installation (Figure 6.14).

Figure 6.14 Sample of completed sump caisson repair.

6.4.3 Onshore pipeline repair

Onshore pipeline operators must balance cost and safety but must never err on the side of just cost. Significant time and money is spent trying to determine the minimum repair cost that will provide acceptable safety. Dig up an external corrosion defect that is 30% of the wall and 1-in. long. The code says you can recoat and backfill. Is that the right thing to do? What if the pipeline is subjected to an abnormal operating condition and it fails? Most pipeline failures occur under unusual operating conditions. You have already spent money digging, cleaning, measuring, and analyzing the defect. Why not just fix it? Composites allow this option. Two men and 30 min will restore the pipe to an "as new" condition. Composite repairs may not be the right repair option every time, but they are an important alternative that can be very effective in most repair cases.

In this section, we will present several case studies of Clock Spring® repair applications within the onshore pipeline repairs.

6.4.3.1 Case study no. 1: girth weld repair

Significant external corrosion, up to 74% metal loss, adjacent to and affecting the circumferential girthweld, was located within an onshore LPG gas terminal in Samarinda, Kalimantan, Indonesia.

Figure 6.15 Completed girth weld repair.

A standard bridging technique for the full cured laminate repair sleeves was applied utilizing three complete 8-layer repair kits to support and bridge over the girth weld.

The repair was installed by a two-man crew within 3 h and with pipeline in operation and no hot work (Figure 6.15).

Within the US and Eastern Europe a number of test programs were instigated to confirm the suitability of composite repairs for this application. Tests were conducted on a number of pipe sections removed from operating gas lines where defects had been located in the girth welds which were of a serious enough nature to preclude continual operation of the pipelines at their MAOP.

Composite repairs were installed on the other available test pieces and subjected to a series of fatigue and pressure tests. In all instances failure of the pipe occurred outside of the repair area (Figures 6.16 and 6.17) in the main wall of the pipe and at pressures significantly higher than the pipeline MAOP (Patrick, 2004).

Figure 6.16 Photo of burst test section of girth weld repair.
Courtesy of University of Miskolc, Hungary (2001). Final report on experimental work accomplished in 2001 under the framework contract entitled "Testing and assessment of pipes, welded joints and repairs of transmission pipelines" (Appendix 4/2001 to the contract) based on the commission of MOL Hungarian Oil and Gas Plc.

Figure 6.17 Failure of the pipe occurred outside of the repair area.
Courtesy of University of Miskolc, Hungary (2001). Final report on experimental work accomplished in 2001 under the framework contract entitled "Testing and assessment of pipes, welded joints and repairs of transmission pipelines" (Appendix 4/2001 to the contract) based on the commission of MOL Hungarian Oil and Gas Plc.

6.4.3.2 Case study no. 2: CUI repair

An external defect due to CUI and hot atmospheric conditions was found after Long Range UT testing was conducted on a main hot water injection line to the main oil wells in Duri, Riau, Indonesia (Figure 6.18).

Following manual surface preparation in accordance to industry standard (NACE) guidelines, composite repair sleeves were applied to reinforce the corroded area. In total 16 repair kits were installed by a four-man crew within 3 days (Figure 6.19).

Figure 6.18 Sample of the CUI defect.

Figure 6.19 Completed high-temperature repair.

6.4.3.3 Case study no. 3: crack arrestor installation

A 12-in. gas pipeline in South Sumatra, Indonesia was found to be cracked and leaking and in need of urgent repair. A composite repair sleeve was considered to provide structural integrity and to prevent a running fracture from the longitudinal crack within the maximum operating pressure of 1200 psi (83 bars).

Due to the crack nature of the defect and to prevent expansion/bulging and failure of the pipe on either side of the leak repair clamp, it was recommended to install within 1 m on either side of the clamp 12-in. crack arrestors. This will not prevent the pipe from continuing to crack, but if it does it will prevent rupture. It is very important that this region of the pipe is restrained as it will greatly help the complete function of the total repair (Lesmana, 2011) (Figure 6.20).

The ease of installation makes the composite sleeve crack arrestor system effective. These units can be installed on the pipeline without the need to cut the pipe or for any

Figure 6.20 Completed crack arrestor repair.

heavy equipment or skilled labor. The installation was completed by a five-man crew within 1 day.

6.4.4 Plant and refinery repair

When considering a repair for piping and pipelines within the plant and refinery areas, a composite repair may be one of the engineer repairs of choice. This technology can be a cost-effective method of improving safety while keeping maintenance costs down, allowing plant and refinery operators to respond quickly to their repair requirements. Since they require no "hot" work or heavy equipment, they are also the safest repair alternative.

In this section, we will present several case studies of Clock Spring® repair applications within the plant and refinery operations.

6.4.4.1 Case study no. 1: external corrosion defect

A corrosion cell can find its way to a pipeline not only through the ground, but also by air. Recently, a refinery in southeast Houston, Texas found how corrosive an "airborne" drift from a cooling tower can be. An above ground pipeline had corrosion spots spanning over 900 ft running parallel to a cooling tower.

A conventional solution to this problem would have encountered serious challenges, such as additional work permits required from various divisions and companies and safety hazards due to the close proximity of process equipment and other product lines; this project under traditional scenarios would have been an arduous and expensive task. The Clock Spring® Snap Wrap composite sleeve reinforcement system was the logical alternative choice as no hot work, down time, or line reductions were necessary.

Nine hundred and three units were installed at the rate of approximately 75−100 ft per day. As a cleaning crew prepped the pipe, three installation crews applied the Clock Spring® Snap Wrap kits by a hand spool method since the pipes were within 3 in. of other hazardous product lines. The repairs also included 90° and 45° fittings.

Clock Spring® not only provided reinforcement to the damaged areas along the pipe but also permanent protection from suspension chemicals found in the drift of vapor off the cooling towers. The projected life of the repair exceeds the life of the plant (Figure 6.21).

Figure 6.21 Installation of Clock Spring® at a refinery.

6.4.4.2 Case study no. 2: galvanic and crevice corrosion

An onshore refinery operator in Far East Asia operates a vast amount of refineries in a complex measuring 10 km by 5 km. The majority of the refineries in this complex maze utilize the same common pipe rack. These gas racks are extremely compact and can be as wide as 8 m and as high as 6 stories.

The complex design of these gas racks means that conducting maintenance is a huge challenge as the pipes are located close to each other and mostly in hard to reach places, often at height. Conducting maintenance at these gas racks usually requires scaffolding to be built, and this entails additional costs to the operator even for a normal painting job.

Clock Spring® has been chosen by the owner of these refineries to be their preferred repair solution for their vast amount of pipes. Utilizing Clock Spring® to repair corroded pipes allows the operator to only build scaffolding for personnel to scale the piping instead of building the scaffolding along the length of the piping meant for repair.

A 12-in. diameter pipe located along a gas rack was experiencing severe corrosion due to a combination of galvanic corrosion and crevice corrosion.

This pipe needed reinforcement at its pipe support area for the total length of 150 m due to active galvanic and crevice corrosion. This is a very common problem with racked piping. The lines are subject to movement and wear away their coatings at the contact point with the pipe rack. Recoating is impossible without lifting the pipe. Water collects in these areas, speeding up the crevice corrosion.

This pipe is located 4 stories above ground and to build scaffolding this high runnig along the entire length of 150 m would certainly be costly.

A total of 20 pipe supports were repaired, each having a defect length ranging from 0.3 to 1.2 m. The Clock Spring® installations for these areas totalled 20 locations with more than 41 coils. A team of 10 contractors lead by one Clock Spring® installer completed the whole line in a 14-h shift in 1 day. The pipeline was in operation throughout the whole period of time (Figures 6.22 and 6.23).

As shown, composite repairs have proven to be a cost-effective repair alternative which allows pipeline operators to respond quickly and without the need to shut down the operations to meet their repair requirements.

Figure 6.22 The corroded pipe support area.

Figure 6.23 Completed installation of Clock Spring®.

Selecting the appropriate repair technique is an important decision which requires an understanding of the risks and rewards associated with each composite repair alternative and material architecture. Safety, permanency, and effectiveness are the primary drivers of this decision, but cost can also become an important issue.

Composites, like Clock Spring®, compete with older, more widely accepted welded repair techniques. These new repair options offer advantages over the more traditional repairs and are both more cost-effective and also the safest repair alternative.

Defects found in pipeline and piping systems both on- and offshore can be permanently repaired safely, quickly, and economically by using composite technology.

6.5 Sources of further information and advice

The following references have a wealth of information regarding the Clock Spring® composite sleeve repair system:

1. GRI-02/0165: Long-Term Lap−Shear Testing of Clock Spring® High Temperature Adhesive. Report: The Clock Spring® repair system is used as a reinforcement for pipelines with corrosion defects and/or mechanical damage, 2002.
2. GRI-98/0151: Evaluation of Plexus MA440™ Adhesive and Typical Pipeline Rehabilitation Coatings for Use with the Clock Spring® System. Report: The Clock Spring® system allows repair of pipeline defects without the need for welding and without taking the pipeline out of service, 1998.
3. GRI-98/0150: Long-Term Durability of the Clock Spring® System. Report: A monitoring program developed to confirm that the Clock Spring® system provides a permanent repair for certain pipeline defects, 1998.
4. GRI-98/0032: Field Validation of Composite Repair of Gas Transmission Pipelines. Report: This is an assessment of long-term performance of Clock Spring® fiberglass composite reinforcements on gas transmission pipelines, 1998.

5. GRI-97/0304: Recommended Procedures for Clock Spring® Field Monitoring. Report: Since 1987 many gas companies participated in installation of Clock Spring® for repair of gas pipes, 1997.
6. GRI-92/0507: Long Term Reliability of Gas Pipeline Repairs by Reinforced Composites. Report: It showed (in Section 5.2 Adhesive Test Data p108) that for Clock Spring® the thinnest adhesive layers provided the best adhesive performance in tensile tests, 1992.
7. ASME PCC-2 Article 4.1, Non-metallic Composite Repair System for Pipelines and Pipework: High Risk Applications, 2006.
8. ISO TS 24,817, Petroleum, petrochemical and natural gas industries—Composite repairs for pipework—Qualification and design, installation, testing and inspection, 2006.
9. GRI 97/0413 Evaluation of a Composite System for the Repair of Mechanical Damage−Stress Engineering Services, 1997.
10. NACE 07-144−Guidelines for Repairing Damaged Pipelines using Composite Materials−C Alexander, Nashville TN, March 2007.

The following websites have a wealth of reports:

1. Gas Technology Institute (GTI) 1948 to present (formerly IGT) www.gastechnology.org
2. NYSEARCH (NE Gas Association) 1990 to present www.nysearch.org
3. OTD−GTI (Operations Technology Development Company) http://www.gastechnology.org/webroot/app/xn/xd.aspx?it=enweb&xd=OTD/otdhome.xml
4. Pipeline Research Council International 1952 to present (old AGA Pipeline Research Council) www.prci.org
5. PHMSA R&D Matrix 2005 to present http://primis.phmsa.dot.gov/matrix/

References

GRI-98/0032, 1998. Field Validation of Composite Repair of Gas Transmission Pipelines. Final Report-Gas Technology Institute, DesPlaines, IL.

Laughlin, S., March 2011. Long term durability of Clock Spring® repairs recent removals and examinations. Pipeline and Gas Journal 238 (3) (Edition).

Lesmana, D.S., January / February 2013. Long term durability of composite sleeve repair and its application as a permanent pipeline repair in Indonesia. Petromin Pipeliner Magazines, 39 (1).

Lesmana, D.S., September 2011. Stopped in it's track − crack arrestor installation in Indonesia. World Pipeline Magazine (Edition). http://www.energyglobal.com/magazines/issue.aspx?seo=world-pipelines&month=9&year=2011.

Porter, P.C., 2000. Composite Pipeline Repairs—Clock Spring® Is Different. Clock Spring® Company L.P.

Patrick, A.J., 2004. Composites − Case Studies of Pipeline Repair Applications. Clock Spring® Company L.P.

This page intentionally left blank

Fiber wrapped steel pipes for high-pressure pipelines

7

L. Deaton
Neptune Research, Inc., Lake Park, FL, USA

7.1 Introduction

This chapter is divided into six sections. The first section, High-pressure piping systems, provides an analytical means to identify what systems are to be considered high-pressure systems. Barlow's equation is employed along with the concept of safety factor to generate examples of high-pressure systems for various pipe diameters. In the second section, Repair system options, various resins, fabrics, and wrapping methods available to the repair design engineer in developing a repair solution are discussed. Existing off-the-shelf solutions are discussed, as well as prepreg and field-wetted systems. Next, in Load sharing in Fiber Reinforced Polymer (FRP) wrapped pipes, we discuss the amount of reinforcement available to the design engineer if a system is wrapped in the pressurized (loaded) as compared to the depressurized (unloaded) condition. Graphic demonstration is provided that illustrates how the amount of load an FRP carries is proportional to the ratio of the FRP modulus and the steel modulus. After a brief discussion on pipe system flaws, load sharing in a flawed pipe is discussed in the section titled Load sharing of a wrapped, flawed pipe. The chapter concludes by discussing cyclic loading issues and how they affect the repair of a high-pressure piping system. Example equations are provided to demonstrate how a repair laminate solution is generated.

7.2 High-pressure piping systems

A high-pressure piping system is not a well-defined group, such as classifications of steels or chemicals. One company could call a 250-psi line a high-pressure line, while another company might consider the same 250 psi to be a low-pressure line. Because of this ambiguity and based on interactions with various industries, it is the author's opinion that a high-pressure line typically operates in the vicinity of 1400−2200 psi.

A better way to categorize a line would be by using the hoop stress and a desired factor of safety. Hoop stress can be found from Barlow's law, specifically, $\sigma_h = PD/2t$. Typical ANSI grade B pipe (Welded and Seamless Wrought Steel Pipe, American National Standards Institute ASME/ANSI B 36.10) is rated to an ultimate tensile strength of $S_{UT} = 60{,}000$ psi and a yield strength of $S_y = 35{,}000$ psi. A factor of safety of 2.0 will provide a reasonable margin to failure while still allowing for axial, torsion, and bending loads. Therefore, a "rough" guide for identifying if a system is a high-pressure system would be as shown in Eqn (7.1).

Rehabilitation of Pipelines Using Fiber-reinforced Polymer (FRP) Composites. http://dx.doi.org/10.1016/B978-0-85709-684-5.00007-2

Table 7.1 Maximum allowable operating pressures for ANSI Grade B schedule 40 (standard) pipe

Nominal pipe diameter (in)	Yield strength S_y (psi)	T_w (in)	f_s	D_i (in)	P (psi)
6	35,000	0.280	2	6.07	1614
8	35,000	0.322	2	7.98	1412
10	35,000	0.370	2	10.02	1292
12	35,000	0.410	2	11.94	1202

$$P = \frac{2S_y T_w}{f_s D_i} \tag{7.1}$$

where

P = system pressure
S_y = yield strength of steel
T_w = pipe wall thickness
f_s = factor of safety against yield
D_i = inside diameter of pipe

Table 7.1 lists maximum allowable operating pressures for ANSI Grade B schedule 40 (standard) pipe of 6, 8, 10, and 12 in.

Alternatively, Eqn (7.1) can be rearranged to solve for f_s for a given section of pipe, as shown in Eqn (7.2).

$$f_s = \frac{2S_y T_w}{P D_i} \tag{7.2}$$

If the factor of safety for a system is approximately 2 or less, then it should be considered a high-pressure system.

There are some unique concerns associated with high-pressure systems. While not common in newer systems, many older systems might have been constructed with lower strength steels, and therefore the pipe wall thickness is higher than typical schedule 40 pipe. Thicker pipe walls are generally heavier and have greater bending and torsion loads. On the other hand, some high-strength steels have reduced toughness and corrosion resistance, so there are a variety of characteristics that must be considered when designing a high-pressure system.

7.3 Repair system options

Hoop, axial, shear, bending, and torsion stresses should all be considered in the design of a repair system. For those systems whose loads are primarily hoop stress, uniaxial fabric is a good option for the repair. If the axial, bending, and torsional loads are

nontrivial, then the designer should consider using a biaxial fabric. The effective fabric strength will have to be determined in order to utilize the wrap angle that will offer the best reinforcement for a given application.

The choice of binding resin should also be clearly identified by the repair design engineer. There are two primary options available: water-activated polyurethane and two-part epoxies. Polyurethanes are generally easier to work with and have a significant advantage when wrapping pipe under water. Epoxies, especially novalac-based epoxies, are highly resistant to a wide range of industrial chemicals and offer greater strength. Epoxies also tend to bind better directly to steel and may not require the use of a primer layer. Epoxies generally have a higher temperature rating than the polyurethanes.

With the advantages of higher strength, greater useful temperature range, and higher chemical resistance falling to epoxies, the ease of use generally is allocated to polyurethanes. Because the installer can initiate the activation of polyurethane, these types of wraps can be preimpregnated at the factory to ensure that an optimal fiber-to-resin ratio is maintained. Rolls of polyurethane-soaked fabrics are supplied to the installer in moisture-proof bags, which are then opened at the worksite and exposed to moisture to begin the chemical reaction.

Epoxy repairs, because of their greater strength, are typically called for in repairing high-pressure systems. The epoxy must be activated by mixing the part A and part B components. Once activated, the epoxy is then applied to the fabric at the worksite in a process called field wetting, which can be performed by hand or with a portable resin application machine. There are also precured repair systems available that utilize various prewound laminates or plates that are secured in place with epoxy. These systems typically require the use of some type of tension-retaining mechanism to maintain preload in the precured laminates until the epoxy sufficiently cures.

There are two basic wrapping techniques: straight circumferential wrapping and spiral wound wrapping. If a repair is of sufficiently small size, circumferential wrapping has the benefit of ease of installation; however, many repairs are applied over extended distances of pipe and spiral wound wrapping is a more viable option. Depending on local geometry and pipe connections, various automated wrapping machines are available to aid in the wrapping of pipes over long distances.

Proper surface preparation is crucial to ensuring effective load transfer between the pipe and the reinforcement. The presence of local gaps and voids between the pipe and the repair effectively removes the reinforcement for that area. This is because the metal can strain (or yield) within the void. If the gap or void is excessive, then the pipe may fail before the FRP ever begins to carry load. To guard against this risk, the pipe surface should be prepared using a wire brush, sand blasting, or similar tool to remove loose surface corrosion or foreign material until the pipe is NACE 2 level or near-white finish. This will allow the resin to properly bond with the pipe. Epoxy fillers are also used to fill voids that are too excessive.

The repair design engineer must also consider the expected lifespan of the repair. The American Society of Mechanical Engineer's Post Construction Committee 2 (ASME's PCC-2) *Repair of Pressure Equipment and Piping* qualification testing specifies 1000 h validation testing, but even this is relatively short compared to some

desired lifetimes of several years. Some university studies have performed 10,000 h, or approximately 1 year, long-term creep tests (Walwrath, 2012), which suggests 55−65% residual strength under constant load, but there is a fair amount of initial data scatter. Dr. Walwrath concludes that: "It appears that if samples can survive initial loading and some initial creep time, then most of the initial strength can be retained." Room temperature creep rupture strengths, based on a power law model, were extrapolated to retain about 50% of initial tensile strength after 50 years. Elevated temperature tests resulted in extrapolated 50-year creep rupture strength of about 43% of initial tensile strength.

Specimens tested over longer times (the maximum time was 14,429 h or 1.6 years) did not fail in creep rupture. These tests were stopped and specimens were loaded to failure. In general, residual strengths were equivalent to or even somewhat greater than initial tensile results. Professor Walwrath theorizes that there may be a possible strengthening mechanism taking place due to matrix creep resulting in better load distribution among fibers. However, to further investigate these phenomena will require additional testing and at this point the data are far too immature to employ these findings in engineering design.

7.4 Load sharing in FRP wrapped pipes

Understanding how load is shared in a pipeline composite reinforcement will better assist the repair design engineer in meeting the needs of the pipeline owner. The most important thing to remember is that unless an FRP is applied with significant preload, the reinforcement will not take any of the loads below the conditions on which it was installed. This is illustrated graphically in Figure 7.1.

Although bonded with the pipe, on a microscale, the FRP remains a separate component and does not actually carry any load until the substrate either strains via elastic deformation or strains via plastic deformation (yielding) to allow the composite to begin to carry load, also by straining. The modulus of steel is approximately 29×10^6 psi and is significantly greater than the modulus of most composites used in pipe repair. For this example, let us assume the modulus of the composite is approximately 8×10^6 psi. These moduli are represented in Figure 7.1 by the slopes of the lines and are derived from the definition of Young's Modulus as $E = \sigma/\varepsilon$; however, it is not exactly proper to use the term "stress," as the cross-sectional area of the pipe will increase when the FRP repair is applied.

Examination of the steel pipe in Figure 7.1 shows that the pipe has a constant stiffness until reaching the yield point. The pipe can handle load beyond yield, but load cannot be increased without the risk of failure. If an FRP is applied while under load, then the steel is already under elastic strain and the FRP reinforcement is carrying no load until the system pressure exceeds the pressure at which the repair was applied. The combined modulus of steel and FRP governs the system stiffness until the yield strain of steel is attained, at which point the modulus of the FRP governs the system stiffness until the ultimate strain of the FRP is attained. This is illustrated in Figure 7.1 where the "Steel with FRP Applied While Loaded" line branches off from the "Steel

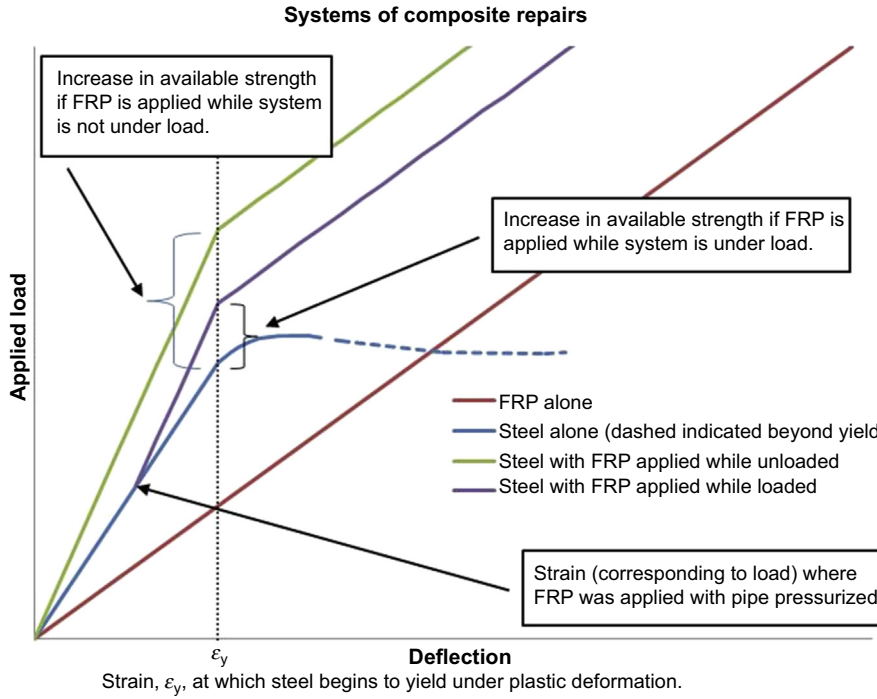

Figure 7.1 Load sharing in FRP reinforced pipes.

Alone" line. The right bracket illustrates the amount of available strength from the FRP when the yield point of steel is reached.

Now compare this to the line "Steel with FRP Applied While Unloaded". The slope is steeper from the beginning, indicating that the FRP is carrying load from the start. As in the case of "FRP Applied While Loaded," once the yield strain of steel is attained, the modulus of the FRP again governs the system. However, the left bracket now indicates the additional load the system was able to carry.

In this example, the respective load capacity was arbitrarily selected based on the yield strain of the steel pipe substrate. In practice, it is extremely difficult to predict in advance exactly where the yielding of steel will begin. This is because the nature of the pipe defect can rarely be known exactly, and approximations and assumptions are routinely made in designing the repair system. Let us discuss several of these defect types.

7.5 Pipe system flaws and defects

The simplest defect is an external flaw, generally occurring as a result of corrosion external to the pipe. In repairing these types of flaws, the repair assumes that the cause of the corrosion has been arrested, and there may be remaining steel substrate which the FRP can be bonded to. The repair typically consists of restoring the lost circular

geometry of the pipe using an epoxy filler and then wrapping the repair for reinforcement. In performing the required repair laminate thickness, the design engineer can assume the remaining wall thickness is available for loading.

Internal wall loss is slightly more difficult. It may be a result of either a corrosive action or a flow erosion process. Because the source of the material loss is inaccessible, the design engineer should not allow for any remaining wall thickness in the repair design calculations for loading unless the conditions causing the erosion have been mitigated. Therefore, a reinforcement to address internal wall loss will generally be thicker than a repair reinforcing an external loss.

In situations where there is a complete penetration of the pipe wall, the calculations are even more complex. Not only must the design engineer neglect pipe wall thickness, but since the interior pressure is acting directly on the FRP, the ability of the laminate to withstand fracture must also be considered. These repairs are more difficult than cases where the pipe wall integrity remains intact (albeit with a reduced thickness), because now the working fluid can act as a wedge to pry the repair laminate away from the pipe surface.

7.6 Load sharing of a wrapped, flawed pipe

Now that we have briefly described the effects of wall loss on the repair design, let us reconsider the wisdom of applying the repair to a pipe while under pressure. We have already discussed the reduced load-sharing capability of a pipe repaired in this manner, but with thinner walls, even in a localized area, another problem begins to emerge.

We recall that for every applied load, there is a corresponding strain. If a laminate is applied to a pipe with a locally reduced thickness, then this local area experiences a proportionally larger strain. When the pipe is depressurized, the strain relaxes and the system returns to its unloaded dimensions, unless yielded. If an FRP is applied and the loaded strain is sufficient, then there is a real risk that the laminate will debond from the pipe during the unloading process. If this debonding were to propagate, it is possible that the entire repair might separate from the substrate. In high-pressure systems, the risk of debonding is even greater since the local strains are greater due to the larger loads experienced by the pipe.

Proper life cycle inspections are advised to examine for laminate debonding. Extensive discussion of nondestructive testing (NDT) methods is beyond the scope of this text, but the main methods are briefly described. The easiest but least reliable method of inspection is a visual inspection looking for blisters, cracking, or localized swelling. Tap testing of a laminate can give clues to the nature of the FRP by listening to the tone of the repair when gently tapped with a coin or small hammer. A crisp, sharp response is usually affiliated with a repair that is in good condition, whereas a dull thud or muted response indicates some type of damping exists. This would be an indication of a possible void or delamination. Another method of NDT is radiographic testing, but the ability to accurately discern damage to the FRP requires great skill, as many FRP reinforcements are radiographically transparent.

Because high-pressure systems are under increased load compared to low-pressure systems, the design engineer usually cannot neglect the axial, bending, and torsional loads in calculating the available pipe strength. Geometric changes to the pipe system are also more of a concern in high-pressure systems. Bends, tees, and reducers all provide for stress concentration factors that must be accounted for. Some of the factors that are necessary to reasonably calculate the stress concentration are temperature, size, and load orientation. Shigley and Mishkey (1989) have done an excellent job of describing the effect of geometric changes on stress concentrators.

In every repair, the piping system should be carefully examined to determine the associated bending stresses and torques. By applying beam theory, pipeline systems can also be modeled as a fixed−fixed, infinite, continuous, simply supported, or even a cantilevered beam, depending on the exact geometry and connections to associated equipment. The bending stress is calculated by first examining the section modulus of the system. The reader will recall the section modulus, $S = I/c$, and therefore the bending stress is found by $\sigma_b = M/S$.

The strain must be taken into account as well, since laminates do not fail in a ductile manner as do steels and most metals. The bending strain is found by $\varepsilon = \sigma/E$, and by substitution, it can easily be shown that the strain in a beam is given by $\varepsilon = Mc/EI$. The two most common guides in designing composite pipeline repairs, specifically The American Society of Mechanical Engineer's Post Construction Committee 2 (ASME's PCC-2) *Repair of Pressure Equipment and Piping* and the International Standards Organization (ISO) 24,817, *Petroleum, Petrochemical, and Natural Gas Industries—Composite Repairs for Pipework and Vessels—Qualification and Design, Installation, Testing, and Inspection*, place limits on strain that are well below the short-term strain limit as calculated directly by Hooke's law. This is a conceptual change for most mechanical engineers who are trained in the classical stress design theory. Also note that composites are anisotropic and will therefore have different values for allowed stress and strains in the hoop and axial directions. The repair design engineer should check both allowed stress and allowed strains in axial and hoop directions against appropriate standards when developing a repair solution.

7.7 Cyclic loading

When examining the specific details of a high-pressure piping repair, the design engineer should consider the effect of cyclic loading on the repair. There is a general scarcity of published research available on the subject of fatigue failure of FRP reinforcement of pipes. General concepts are discussed in the airline and wind turbine industries, and comparisons can be made to composites in general, including the pipeline repair industry. There are three possible means of failure for FRP repairs when subject to cyclic loading: cyclic debonding of the adhesive, interlaminar failure, and adherent failure (Goeij et al., 1999). While Goeji, Van Tooren, and Beukers' article is specifically referencing adhesively bonded joints, their findings are consistent with findings observed in field applications of piping repairs.

There are data in the literature (Reifsnider, 1991) to suggest that composite repairs follow similar behavior as steels with respect to following the typical Wohler *S*−*N* curve, as shown in Figure 7.2.

To generate the S−N curves, material samples are placed under a cyclic load until failure. The process is repeated for multiple stress ranges to generate the curve. The results are then plotted graphically. Although reinforced polymers have shown that they are generally less susceptible to fatigue failure than metals, fatigue failure can still occur (Firehole Composites, 2010).

Failure is typically initiated as a crack in the polymer matrix and rarely occurs in the fiber matrix. The number of load cycles required to initiate the development of a crack is called the *initiation time*. The time to failure after a crack is initiated is usually much less than the initiation time, such that when a crack does develop, the FRP is in close proximity to failure and only a few more cycles may be all that is required to begin crack propagation.

The Wohler curve is traditionally divided into three sections: the comparatively flat, initial low-cycle fatigue section, the sloping high-cycle fatigue section, and the final endurance limit section. It is generally desirable to operate in either the low-cycle fatigue or the endurance limit sections, as the composite behavior is fairly predictable. Operation in the sloped, endurance limit section should be avoided. Although the Wohler curve is plotted as a single line, there is considerable room for data scatter based on material manufacturing flaws, installation craftsmanship issues, and load measurement uncertainty. The International Standards Organization, ISO 24,817, introduces a cyclic loading severity term, R_c, as the ratio of the minimum to maximum pressure to which the system is exposed. ISO 24,817 allows for the calculation of a derating factor, $f_{c,}$ based on R_c and the number of cycles the repair is anticipated to experience during the repair lifetime. For low-cycle applications, defined in ASME's PCC-2 as $N < 7000$ cycles, f_c is taken as unity and need not be included in repair calculations. For endurance limit calculations, the design engineer is advised to consult with the repair product vendor to understand how the testing was performed and under what conditions of temperature and pressure to ensure that appropriate conditions exist in the field compared to laboratory testing.

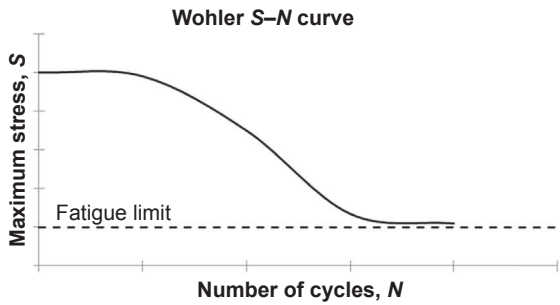

Figure 7.2 Wohler fatigue limit.

7.8 Sample problem 1

Consider the pipe with an external defect resulting in a reduced wall thickness, as shown in Figure 7.3. The existing flaw has reduced the system operating pressure from an initial value P_{design} to P_{damaged}. It is desired to restore the system to its original capacity.

The amount of capacity to add is $\Delta P = P_{\text{design}} - P_{\text{damaged}}$. The reader will recall that stress is the result of force acting over an area, as shown in Eqn (7.3).

$$\sigma = \frac{\text{Force}}{\text{Area}} \tag{7.3}$$

Examining Figure 7.3, it is seen that the applied force F per unit length of the pipe is the product of the pressure and the internal radius, or $F = Pr$. The area per unit length resisting this force is the remaining thickness of the pipe wall, T_{w}, and the required repair laminate thickness, t_{repair}. However, we should not use any of the available strength in the pipe wall to restore the system back to design pressure, as it may already be close to yielding and therefore having capacity to just resist the pressure P_{damaged}. Therefore, Eqn (7.3) is now modified to become Eqn (7.4).

$$\sigma_{\text{composite}} = \frac{\text{Force}}{\text{Area}} = \frac{\Delta P r}{t_{\text{repair}}} \tag{7.4}$$

Rearranging terms in Eqn (7.4) to get an expression for the required repair laminate thickness is shown in Eqn (7.5).

$$t_{\text{repair}} = \frac{\Delta P r}{\sigma_{\text{composite}}} \tag{7.5}$$

In order to complete the design, we must come up with an expression for $\sigma_{\text{composite}}$ that can be substituted into Eqn (7.5). If we assume that the steel in the area of the flaw is limited to yield strength S_{y}, then the strain in the steel is shown in Eqn (7.6).

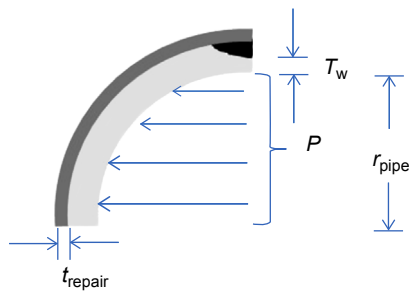

Figure 7.3 Pipe with external defect.

$$\varepsilon_s = \frac{S_y}{E_s} \tag{7.6}$$

Additionally, we can assume that the strain in the laminate is the same as the strain in the steel, or $\varepsilon_c = \varepsilon_s$. Therefore, $\sigma_c = \varepsilon_c E_c = \varepsilon_s E_c$. Substitution of Eqn (7.6) into this expression now results in Eqn (7.7).

$$\sigma_c = \frac{S_y E_c}{E_s} \tag{7.7}$$

By substituting Eqn (7.7) into Eqn (7.5), we now arrive at an expression that can be used to determine the required laminate thickness for a desired increase in system pressure.

$$t_{repair} = \frac{rE_s}{S_y E_c}\Delta P \tag{7.8}$$

7.9 Sample problem 2

Suppose flaw exists in a pipe that has reduced the wall thickness to T_w. It is desired to restore the system to a design pressure P. In this case, however, the wall loss might be so severe that it is unreasonable to assume that the steel does not yield. Again we construct a free body diagram of the quarter pipe to balance the internal pressure forces with the restraining force of the remaining pipe wall and the repair laminate. Such a case is shown in Figure 7.4.

We can see in Figure 7.4 that $Pr = S_y T_w + \varepsilon_c E_c\, t_{repair}$. Solving for t_{repair} and replacing the radius, r, with D/2 yields Eqn (7.9).

$$t_{repair} = \frac{1}{\varepsilon_c E_c}\left(\frac{PD}{2} - S_y T_w\right) \tag{7.9}$$

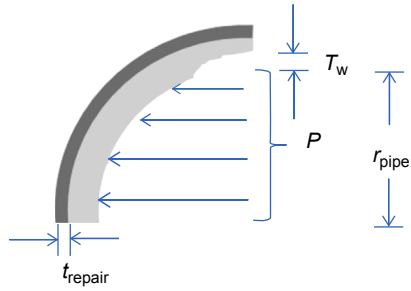

Figure 7.4 Pipe with internal defect.

Generally, Eqn (7.9) is a more useful expression than Eqn (7.8) in designing pipe repairs. Note that the repair thickness is defined in terms of composite strain, ε_c, and not in terms of stress, σ_c. This allows the design engineer to specify a maximum strain in the repair solution. Also, the final system pressure is specified instead of a desired ΔP increase. The reader will also note that Figure 7.4 is drawn with an interior wall loss. From a design perspective, if interior wall loss is occurring, then it is generally safer to assume that the remaining wall thickness will eventually be reduced to zero, that is, $T_w = 0$, as interior corrosion is difficult to arrest.

Finally, the reader should note that neither Eqn (7.8) nor (7.9) includes derating coefficients for factors such as temperature, service life, cyclic loading, or other factors such as pipe geometry. These factors are now applied in Eqn (7.10) to generate an expression for the final design repair thickness.

$$t_{design} = (f_{temperature}\, f_{service}\, f_{cyclic}\, f_{other}) t_{repair} \tag{7.10}$$

The derating coefficients can have a pronounced effect on the required number of layers to attain the desired repair performance over the specified life of the repair. The design engineer should closely examine the derating factor testing from a materials supplier to understand how the factors were arrived at.

7.10 Future trends

The trend in nearly every component is to make things smaller, lighter, stronger, less expensive, and to deliver them at a faster rate with a greater performance envelope. Composite repair to high-pressure piping systems is not immune to this trend. Chemical compatibility, corrosion resistance, and ease of application are all requirements that will need to be considered.

Today's composites are very good in terms of their strength, flexibility, and resistance to chemical attack. They are primarily composed of glass, carbon, or aramid threads woven on a loom similar to other textiles. Attempts to employ more environmentally friendly repairs have met with mixed success, with the natural fibers, primarily hemp derivatives, not meeting the performance characteristics of the mineral fibers.

The largest issues encountered in the composite pipeline repair industry are those associated with resin limitations, both in high-temperature and low-temperature (cryogenic) applications. Resin strength, elongation, and thermal expansion will vary depending on if the resin is post cured or nonpost cured. Post curing involves heating the resin to an elevated temperature for a specified period of time to allow the polymeric matrix to fully bind and lock in place. Post curing is routinely performed on composite parts for the aviation, sporting goods, electronics, and automotive industries as the specified parts are comparatively small and can fit into autoclave ovens. This involves curing composites under high pressure and temperature. Large autoclaves are used in the aviation industry, where wing and fuselage parts can be large, but the weights to strength requirements are sufficient to warrant the additional effort.

In the pipeline industry, it is difficult to autoclave a field-installed repair, and only a limited number of systems are available to post-curing at high temperatures; however, the associated cost is high compared to simply adding a few more layers. Developing an economical means to post cure a wrap remains an area of active research for the community.

Finally, as composite repairs become more familiar to the pipeline repair industry, there is a high probability that the entire industry will become more standardized. Similar to how the steel industry developed a common means of specifying steel strengths, such as American National Steel Institute (ANSI) and American Petroleum Institute (API) have established standards for pipe, there will be more standards instituted into the nonmetallic repair design by the pipeline industry to ensure that the repairs meet specified performance standards.

This will make the repairs more reliable and therefore will also contribute toward greater acceptance of FRP repairs on pipes. It will also raise the barrier to entry for small firms, and those firms that exist today by providing marginal quality repairs may find that they will have difficulty meeting industry standards.

Some examples of performance standardization are to specify the conditions under which material testing is performed. Tensile tests can vary significantly based on the rate the load is applied. We have discussed how composite materials perform differently if they are post cured or nonpost cured, and the author has personally observed some firms advertising post cured material properties to design a repair for a field application where it is known that post curing is not available. It is a matter of certainty that the repair will fail, and every unsuccessful repair harms the industry.

Until such time that repair performance is standardized, the pipeline owner or maintenance manager should seek out reputable firms with a knowledgeable engineering staff to perform testing and design based on reputable test results. The best way to do this is to ask questions from your repair provider and to join a professional group that is developing standards.

7.11 Sources of further information

Anyone desiring to learn more about the repair of pipes and pressure vessels should begin with the American Society of Mechanical Engineers Post Construction Committee 2 (PCC-2) *Repair of Pressure Equipment and Piping*, paying special interest to Part 4, "Non Metallic and Bonded Repairs." The equations and formulas in PCC-2 are derived from a more in-depth analysis published by the International Standards Organization (ISO) document 24,817, *Petroleum, Petrochemical, and Natural Gas Industries—Composite Repairs for Pipework and Vessels—Qualification and Design, Installation, Testing*, *and Inspection*. ASME also offers a series on composite materials that covers nearly every aspect of composite materials and can be downloaded from the ASME website. The Pipeline Research Council International (PRCI) *Pipeline Repair Manual*, catalog #L52047, also provides a good discussion on the repair of fluid transport systems.

For academic applications, *Engineering Mechanics of Composite Materials*, by Isaac M. Daniel and Ori Ishai, is a good textbook that discusses the behavior of composite materials from micromechanical and macromechanical perspectives.

The American Society of Testing and Materials (ASTM) offers a full range of test methods and processes for validating composite materials. In addition to tensile test and lap shear tests, it is wise to validate the chemical compatibility of the composite repair systems with a pipe's specific contents. Compatibility testing should be performed in compliance with ASTM D 543, *Chemical Resistance of Plastics to Chemical Reagents*, or similar approved standardized tests. For elevated temperature applications, the pipeline owner should request Differential Scanning Calorimetry results that are performed under ASTM D6604, *Standard Practices for Glass Transition Temperatures of Hydrocarbon Resins by Differential Scanning Calorimetry*, to ensure that the operating temperature is below the glass transition temperature (T_g) of the composite resin.

References

American Society for Testing and Materials, www.astm.org.

Creep and Rupture Tests for Fiber Reinforced Composite Material, David E. Walwrath, 2012, Dept of Mechanical Engineering, University of Wyoming, walwrath@uwyo.edu.

Fatigue Life Prediction in Composite Materials, Firehole Composites, 2010.

Goeij, Van Tooren, Beukers, March 1999. Composite joints under cyclic loading. Materials & Design 20, pp. 213−221.

Petroleum, Petrochemical, and Natural Gas Industries—Composite Repairs for Pipework and Vessels—Qualification and Design, Installation, Testing, and Inspection, International Standards Organization (ISO) 24817.

Pipeline Research Council International, www.prci.org.

Repair of Pressure Equipment and Piping, American Society of Mechanical Engineer's Post Construction Committee 2 (ASME's PCC-2).

Fatigue of Composite Materials, 1991. Scribd. Reifsnider, K.L., Virginia Polytechnic Institute and State University, Blacksburg, VA, USA.

Shigley, Mishkey, 1989. Mechanical Engineering Design. McGraw-Hill, Inc.

Welded and Seamless Wrought Steel Pipe, American National Standards Institute ASME/ANSI B 36.10.

This page intentionally left blank

Finite element analysis (FEA) of fiber-reinforced polymer (FRP) rehabilitation of cracked steel and application to pipe repair

8

C.C. Lam
University of Macau, Macau, China

8.1 Introduction

The use of fiber-reinforced polymer (FRP) for new construction and strengthening of older structures has increased steadily. FRPs offer numerous advantages over steel, including excellent corrosion resistance, good fatigue resistance, and low coefficient of thermal expansion, as well as being lightweight. An additional advantage of FRP is in the endless ways in which polymers and fibers can be combined in a material to suit the specific needs of a structure (Meier, 1992). There are three commonly used fibers for producing FRP for civil engineering applications: glass, aramid, and carbon/graphite. These are strong ceramic materials that depict both a stiff and a brittle behavior. The cost of glass fiber is relatively lower than the other two fibers. However, its poor durability in alkaline cementitious environments has caused concern. Aramid fiber is an aromatic organic compound made of carbon, hydrogen, oxygen, and nitrogen. Its advantages are low density, high tensile strength, and high impact resistance. Its drawbacks include its low compressive properties and degradation in sunlight. Carbon fiber is produced from one of the three precursors: polyacylonitrile (PAN), rayon, and mesophase/isotropic pitches. These fibers, or their allotropic form graphite, have the most desired properties from the civil engineering applications viewpoint (Kaw, 1997). Mechanical properties of some commonly used FRPs are shown in Table 8.1 (ISIS Canada 2001). Application of FRP composites to strengthen reinforced concrete (RC) structures has become very popular during the last two decades. Major applications of FRP on strengthening RC structures include: (1) flexural strengthening of RC beams and slabs; (2) shear strengthening of RC beams; (3) strengthening of axially and eccentrically loaded RC columns; and (4) seismic retrofit of RC columns. A state-of-the-art summary of the application of FRP strengthening of RC structures can be found in several references (Meier et al., 1993; ACI 440R-96, 1996; Karbhari and Seible, 2000; Deniaud and Cheng, 2000; Teng et al., 2004).

Besides the application of FRP on RC structures, there are other researches which were focused on the application of FRP on repairing steel members. Roberts (1995) carried out experimental work to examine the behavior of crack growth retardation in steel plates reinforced with carbon fiber composite patching. Fatigue tests of

Rehabilitation of Pipelines Using Fiber-reinforced Polymer (FRP) Composites. http://dx.doi.org/10.1016/B978-0-85709-684-5.00008-4

Table 8.1 Properties of typical commercial FRP systems

FRP system	Areal weight (g/m^2)	Density (g/cm^3)	Thickness (mm)	Tensile strength (MPa)	Modulus in tension (GPa)	Elongation at failure (%)
Replark (Mitsubishi)						
Type 30	300	1.8	0.167	3400	230	1.5
Type HM	200	2.1	0.143	1900	640	0.3
Mbrace (Master Builders)						
CF130	300	1.82	0.165	3480	227	1.5
Tyfo Fibrwrap (Composite Retrofit International)						
SHE51	930	0.72	1.3	552	27.6	2.0
Sika						
SikaWrap Hex 103C	618	1.8	1.0	960	73.1	1.3
CarboDur S	2240	1.6	1.2–1.4	2800	165	1.7

ASTM A-516 Gr 70 pressure steel vessel were carried out. The thickness of the steel plate (t_s) was 15.9 mm, and the width and length of the specimens were 120 and 144 mm, respectively. An initial machine notch (length = 52 mm) was introduced into the specimens. Fatigue loading was applied to introduce a precrack (length = 8 mm). Therefore, the initial crack length was about 60 mm. Then, the unpatched specimen was loaded with a cyclic tensile loading range ($\Delta P = 4.76$ kN) and a stress ratio equal to 0.05. The test was terminated when the final crack length reached about 98 mm and the corresponding fatigue cycle number (N) was 5,345,000. Another specimen was repaired by carbon fiber-reinforced polymer (CFRP) patching on both sides. The length of the CFRP plate was 140 mm, and the width was 60 mm with the edge of the plate located at the tip of the machine notch (the CFRP plate covered the precrack only). Initially, the same fatigue loading which was used for loading the unpatched specimen was applied to the patched specimen. However, the crack did not propagate during this applied loading range. The cyclic loading range was increased to $\Delta P = 5.22$ kN under the same stress ratio of 0.05. Under this cyclic loading range, the fatigue life of the patched specimen was about 28,500,000. The increase in fatigue life was about five times. This testing showed that the patch slowed down the growth rate of the propagating crack and in some cases, arrested the crack altogether. Repairs of cracked steel elements using CFRP material patching were examined by Kennedy and Cheng (1998). Steel plates (dimension = 750 × 400 × 6.5 mm) with a central crack (80 mm) were tested under uniaxial tensile loading (far end stress = 100 MPa). At the crack location, some of the specimens were reinforced with CFRP (four or six layers) on one side. Other test parameters included the patch length, patch width, type of tapered end, and patch pattern. In their study, the strain distribution in a cracked steel plate with and without CFRP patching was examined. It was shown that the strain at the cracked tip could be reduced by applying CFRP patching. Higher stiffness patches reduced the crack tip stresses while

lower stiffness patches reduced the stress concentrations in the steel at the patch edge. Based on these experimental and numerical studies, minimum bond lengths for load transfer and for load redistribution were proposed.

The fatigue behavior of a riveted steel bridge repaired by bonding CFRP plates was studied by Bassetti et al. (2000a,b) and Colombi et al. (2003a,b,c). Fatigue tests on central notch steel specimens with a 30-mm initial crack length were carried out. The dimensions of the steel plate specimens were 1000 × 300 × 10 mm. The notched steel plates were reinforced on both sides with CFRP plates (500 × 50 × 1.2 mm (or 1.4 mm)). Prestressing of the CFRP plate was introduced in some of the specimens. The CFRP plates were placed 10 mm from the crack tip symmetrically on both sides. The applied stress range ($\Delta\sigma$) was 80 MPa with $R = 0.4$. Compared to the fatigue life of unpatched specimens, test results showed that the increase in fatigue life for the patched specimens varied from 3.5 to 20 times. In addition, fatigue tests on a cross-girder of the riveted steel bridge reinforced by CFRP plates were also performed in order to show the applicability of the technique to bridge reinforcement. It was shown that the application of prestress of CFRP plates prior to bonding introduces a compressive stress which prevents further cracking by promoting a crack closure effect. Jones and Civjan (2003) carried out experimental and finite element studies to examine the fatigue behavior of cracked steel plates repaired with CFRP patching. Two different configurations of cracks were tested: the center crack and the symmetric edge notched crack. The initial crack lengths for the center crack specimens ($2a_i$) and symmetric edge notched crack specimens (a_i) were 11.4 and 5.7 mm, respectively. Different types of CFRP materials (CFRP plate and CFRP sheet) were used in the studies. It was shown that the maximum increase in fatigue life was less than two times. However, in most of the examined cases, the increase in fatigue life was less than 50%. It was reported that the epoxy performance was critical to the overall behavior and all specimen failures were initiated by CFRP debonding. Fatigue tests of steel beam specimens repaired by CFRP patching were carried out by Tavakkolizadeh and Saadatmanesh (2003). Steel beams (S127 × 4.5) with an edge notch in the tensile flange were tested under cyclic loading at various stress levels. The length of the steel beams was 1.22 m, and they were tested under a two-point loading (loads were 200 mm apart symmetrically located with respect to midspan). CFRP patching was applied on the tensile flange of the steel beam. The width and length of the CFRP plate were 76 mm and 300 mm, respectively, and the thickness was 1.27 mm. The modulus of elasticity was 144 GPa. The fatigue life of the steel beams without CFRP patching was evaluated at various values of stress range (207, 241, 276, 310, and 345 MPa). For the steel beams with CFRP patching, one more stress range (379 MPa) was included in the study. It was observed that the fatigue life of specimens with CFRP patching was increased by 2.5−3.4 times. This improvement was equivalent to upgrading the detail from the AASHTO category D to category C (AASHTO, 2000).

As shown in several research results that the fatigue life of metallic structures can be extended by bonding FRP patching, it is considered that similar techniques can also be applied in fatigue repair of piping systems. The fatigue life of a cracked piping system depends very much on the applied stress range as well as on the stress intensity factor (SIF) at the crack tip. Therefore, investigation of the SIF of a cracked

piping system is necessary for the prediction of its fatigue life. Yukio (2002) reviewed the solutions of calculating the SIF, and limit load prediction of pipe with a circumferential through-wall crack subjected to axial and bending loads and a closed-form expression is derived for the limit load under combined tension and bending loading. On the other hand, the SIF of cracked circular tube can be obtained by finite element method (FEM) (Kou and Burdekin, 2008). As it is known that the application of bonded FRP composite can help to reduce the crack opening displacement (COD), as a result, the SIF at crack tip can be reduced which can help to extend the fatigue life of a metallic structure. In the following sections, a brief introduction about some finite element analysis (FEA) of cracked plate with FRP patching is presented. Then, the effect of several parameters, such as the FRP patching stiffness, patch width and length, and the reduction of SIF of cracked steel plate is discussed. After that, the FEA of cracked circular tube structure with bond FRP patching is presented and the results are discussed.

8.2 Finite element analysis of cracked steel plate

8.2.1 Background

In the design of metal structures, such as steel structures, ductile fracture failure, which consists of exceeding the tensile strength of the material on the net section, or local or global instability of members or frames, is considered most often. However, when dealing with structures or mechanical equipment subjected to cyclic or impact loading, other modes of failure can take place at stress levels that can be substantially lower than the ultimate or yield strength of the material. These modes of failure either take the form of slow propagation of a crack under cyclic loading in a process called fatigue or take the form of a sudden propagation of a crack when a critical stress is exceeded in a process called brittle fracture. Fracture is the result of cracks forming in a structural component either instantaneously as the stress reaches a critical value or gradually under the action of repeated loading. In the presence of a crack, the behavior and safety of a structure or structural component can be compromised since cracks can lead to sudden fracture. The behavior of cracks in a structure is strongly dependent on the state of stress at the crack tip and the ability of the material to resist

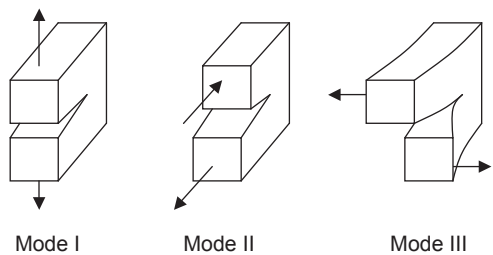

Figure 8.1 Three modes of stress pattern that can be applied to a crack.

propagation. Assuming a crack having a border defined by a simple curve or straight line, and crack extension in the crack plane, Irwin (1957) showed that the stress field in the region dominated by the singularity of stress can be regarded as the sum of three invariant stress patterns taken in proportions which depend upon loads, dimensions, and shape factors. The three stress patterns are due to (Figure 8.1): the opening mode (Mode I), the forward shear mode (Mode II), and the parallel or antiplane shear mode (Mode III). An illustration of the stress field in the vicinity of a crack tip is shown in Figure 8.2. Based on the assumption that the material is linear elastic, the stress field (σ_{xx}, σ_{yy}, and τ_{xy}) at the tip of a crack for a Mode I fracture can be described by the following equations:

$$\sigma_{xx} = \frac{K_I}{\sqrt{2\pi r}}\cos\frac{\theta}{2}\left(1 - \sin\frac{\theta}{2}\sin\frac{3\theta}{2}\right) \tag{8.1}$$

$$\sigma_{yy} = \frac{K_I}{\sqrt{2\pi r}}\cos\frac{\theta}{2}\left(1 + \sin\frac{\theta}{2}\sin\frac{3\theta}{2}\right) \tag{8.2}$$

$$\tau_{xy} = \frac{K_I}{\sqrt{2\pi r}}\sin\frac{\theta}{2}\cos\frac{\theta}{2}\cos\frac{3\theta}{2} \tag{8.3}$$

where K_I is known as the SIF for a Mode I fracture. In general K_I is obtained from the following equation:

$$K_I = \beta\sigma\sqrt{\pi a} \tag{8.4}$$

where the geometry factor, β, accounts for factors such as the applied stress distribution, the shape and location of the crack within the component, and the size and shape of the plate or component in which the crack is located, and a is the crack length.

When composite patching is provided to the cracked surface of a steel member, the composite patching provides deformation constraint to the cracked mouth. Rose (1982) carried out an analytical study estimating the reduction of the crack extension force when a cracked plate is repaired by reinforcing patches bonded on its faces. Rose pointed out that there are two main effects of the bonded reinforcing

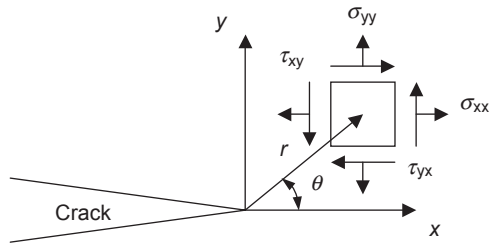

Figure 8.2 The stress field in the vicinity of a crack tip.

patches on the cracked surface: (1) to reduce the stress in the uncracked plate at the prospective location of the crack and (2) to restrain the opening of the crack. Chue et al. (1994) applied a 3-D finite element model to study the behavior of plates with an inclined central crack under biaxial loading repaired by patching. In the development of the 3-D finite element model, one of the challenges was to model the adhesive layer and the composite layer. Due to the very small thickness of the layers, very small elements were needed to model the adhesive and the composite layers (Figure 8.3(a)). As a result, the computational time for the analysis was significantly increased. In order to overcome the 3-D finite element modeling problem of adhesive layer, Sun et al. (1996) presented a simple analysis method using the Mindlin plate theory in order to reduce the computational time. The researchers modeled the cracked plate and the fiber-reinforced polymer (FRP) patching using the Mindlin plate elements, and the adhesive layer was modeled with effective spring elements connecting the patch and the cracked plate (Figure 8.3(b)). As the adhesive layer was modeled by spring elements, a larger element size could be used for modeling the steel plate and the FRP patching so that the number of degrees of freedom could be reduced significantly. However, one of the problems with using effective spring elements to model the adhesive layer is that a suitable spring stiffness should be assigned to the effective spring elements in different orientations.

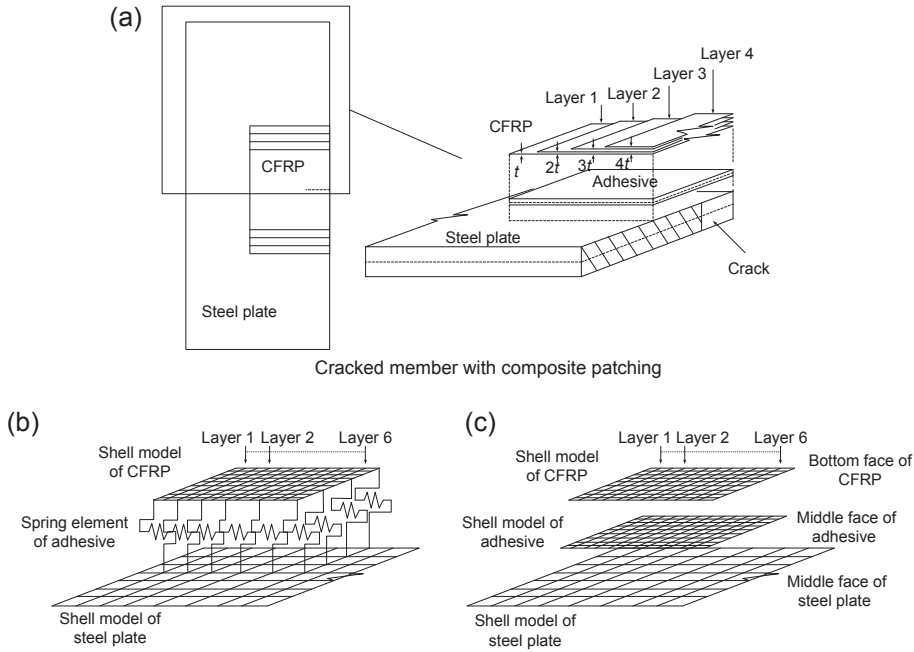

Figure 8.3 Illustration of modeling of cracked member with composite patching.

8.2.2 Three layers FE modeling technique

Naboulsi and Mall (1996) proposed a finite element model in which all the material properties of the three materials (the cracked plate, adhesive layer, and composite patching) are included. The FE model proposed by Naboulsi and Mall is similar to the model developed by Sun et al.; however, instead of modeling the adhesive layer by effective spring elements, Naboulsi and Mall modeled the three materials by using Mindlin plate elements (this is also known as the three layers technique, as shown in Figure 8.3(c)). Then, suitable constraint conditions were applied to limit the displacement of the nodes in the cracked plate, the adhesive layer, and the FRP patching layer. The numerical results obtained using Mindlin plate elements were compared with those using 3-D elements. It was shown that the three layers technique results in a better prediction of SIF of the cracked plate than that obtained from the plate model with springs when compared with the 3-D finite element analysis results. Naboulsi and Mall (1996) concluded that the three layers technique provided an economic 2-D finite element model with a minimal difference to the 3-D model.

Although it was shown that the 2-D three layers technique gave good predictions of SIF of the cracked plate with bonded FRP patching, the 2-D plate model could not capture the differential crack growth rate of the unpatched side and the patched side of a cracked plate with a single-side patching. Therefore, the three layers model was further modified and the results of SIF of cracked steel plate with FRP patching are presented in the following sections.

8.2.3 Comparison of the SIF based on the modified three layers model and the three layers model

The finite element models of cracked steel plate with single-side FRP patching were set up based on the experimental studies by Kennedy and Cheng (1998) of the strain/stress distribution of cracked steel plate with single-side CFRP patching. In the finite element analysis, the effect of varying parameters such as the patch length, patch width, and stiffness of patching to the SIF were investigated. A total of 10 tests were reported by Kennedy and Cheng (1998) in their test program. Of the 10 specimens tested, five were bonded by CFRP patching on one side with a rectangular taper end, four were bonded by CFRP patching on one side with a mixed taper end, and one served as the control specimen which was not bonded by any CFRP patching. All plate specimens were CAN/CSA-G40.21 300 W steel and with outside dimensions of 400 $\times$ 750 mm and thickness of 6.4 mm. The gripping mechanism used in the test setup consisted of a 31.8-mm-thick end plate gripped by the MTS testing machine and spliced to the specimen by two 12.7-mm-thick plates at each end, as shown in Figure 8.4. A uniform stress distribution was assumed to be developed across the width of the plate at a distance away from the bolted ends. A through-thickness crack of 80 mm long was saw-cut in the center of each plate. The saw-cut radiated from an 8-mm-diameter hole drilled in the center of the plate. One plate was tested without CFRP patching for reference and the rest of the cracked plate specimens were patched on one side with carbon fiber sheets of various testing details. While the total patch

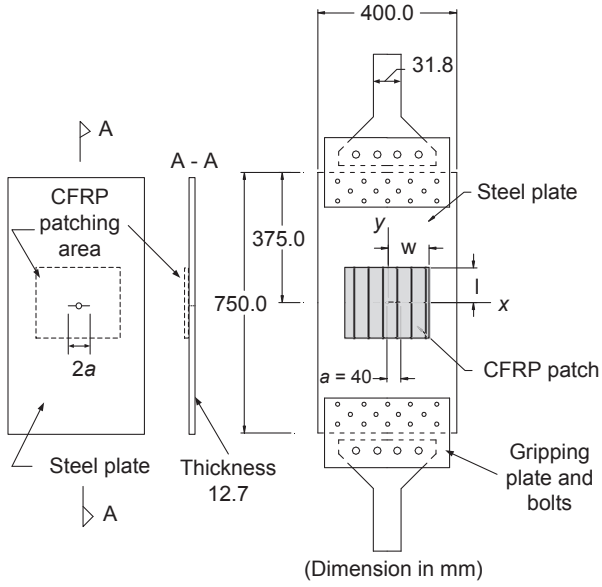

Figure 8.4 Typical test setup and a gauged specimen tested by Kennedy and Cheng (1998).

width was $2w$, the total patch length was 2l, and the total crack length was $2a$, reference to patch dimensions is denoted by the "half-parameters"—namely, w, l, and a, as shown in Figure 8.4. The x and y-axes represent the horizontal and vertical centerlines of the plate, respectively, as illustrated in the figure.

The carbon fiber sheet supplied by Mitsubishi Chemical Co. (1999) was applied to the steel plates using a hand lay-up procedure. The corresponding two-part epoxy was used as the matrix material of the CFRP and also as the adhesive between the steel plate and the CFRP. The average thickness of the CFRP was 0.23 mm/layer with an elastic modulus equal to 128,093 MPa. Six layers of carbon fiber sheet were applied to three of the specimens, providing a patch to an adherend stiffness ratio, $E_{frp}t_{frp}/E_st_s$, of 0.16, where E_{frp} is the modulus of elasticity of the patch material, t_{frp} is the thickness of the patch material, E_s is the elastic modulus of the steel material, and t_s is the thickness of the steel material. To obtain results for a different adherend stiffness ratio ($E_{frp}t_{frp}/E_st_s = 0.107$), two specimens were patched with only four layers of fiber. Two different bond lengths ($l = 30$ and 100 mm) and three different patch widths ($w = 80$, 120 and 160 mm) were studied. Three of the test patches had a 5 mm/layer (2.6°) taper on both edges, perpendicular to the applied load. The remaining two specimens had a 3 mm/layer (4.4°) taper on one of the edges and a 20 mm/layer (0.7°) taper on the other, as shown in Table 8.2. The test specimens are designated with a four-character label, *Rw*ln, where R indicates a rectangular patch, w indicates the patch width (1 = 160 mm, 2 = 120 mm, and 3 = 80 mm), l indicates the patch length (1 = 100 mm and 2 = 30 mm), and n is either 4 or 6, depending on the number of layers of composite applied. For example, R116 represents a specimen

Table 8.2 Summary of test specimen variables (Kennedy & Cheng, 1998)

Specimen	Width *w* (mm)	Length *l* (mm)	Layer *n*	Taper (mm)		Shape of patching
				Top	Bottom	
Unpatched	–	–	–	–	–	–
R116	160	100	6	5	5	Rectangular
M216	120	100	6	5	5	Mixed
M214	120	100	4	5	5	Mixed
M316	80	100	6	5	5	Mixed
M314	80	100	4	5	5	Mixed
R226	120	30	6	3	20	Rectangular
R224	120	30	4	5	5	Rectangular
R326	80	30	6	5	5	Rectangular
R324	80	30	4	3	20	Rectangular

with six layers of CFRP patching and patch width and length equal to 160 and 100 mm, respectively. All the tension tests were conducted in the MTS 1000 machine. Each specimen was loaded at a stroke-controlled rate of 1 mm/min. A data acquisition system was used to collect the strain readings from the gauges mounted on the specimens.

The three layers technique developed by Naboulsi and Mall (1996) was used to model the test specimens which were tested by Kennedy and Cheng (1998). In the three layers finite element model, the cracked steel plate, the adhesive layer, and the CFRP patching are modeled using the shell elements based on the Mindlin plate assumption. Static analysis is carried out to obtain the strain results and the SIF around the crack tip is obtained using the contour integral method. Since Mindlin plate elements are used to model the cracked steel plate, it is assumed that the SIF varies linearly through the thickness of the plate. With this assumption, the SIF of the unpatched side and patched side can be obtained. The equations for evaluating the SIF of the unpatched side and patched side are shown in the following section. In order to examine this assumption, a modified three layers model with the cracked steel plate modeled using 3-D brick elements and the adhesive layer as well as the CFRP patching using shell elements based on the Mindlin plate assumption are proposed. There are two advantages for using the modified three layers model. Firstly, since only the cracked plate is modeled by 3-D brick elements and the adhesive layer and CFRP patching are modeled by shell elements, the computational and modeling time is reduced significantly compared to a traditional 3-D model with the cracked plate, adhesive layer, and CFRP patching all modeled by 3-D elements. Secondly, as the

cracked steel plate is modeled using the 3-D brick elements, the SIF around the crack tip through the thickness of the plate can be directly obtained from the analysis results.

The three layers technique was used to model the test specimens using the finite element program ABAQUS Version 6.4-1 (Hibbitt et al., 2004). Eight node shell elements (S8R, eight nodes general purpose shell element in ABAQUS) were used in the modeling, and the model represents one quarter of a patched plate with an internal through-thickness crack. A typical finite element model of the steel plate with the adhesive layer and the CFRP patching is shown in Figure 8.5. Due to the singularity properties of stress and strain at the crack tip, collapsed node elements were used at the crack tip to simulate the singularity properties of stress and strain around the crack tip numerically. As shown in Figure 8.5, three of the nodes of the original eight nodes element are collapsed at the crack tip and two midnodes are moved to the quarter point of the sides. With such arrangement of the nodes, singularity properties of strain exist within the elements (Barsoum, 1976). Therefore, the singularity properties of stress and strain can be captured by the collapsed node elements around the crack tip. In general, the shell element is assigned to represent the midplane of the corresponding plate. In this study, since a tapered end condition is used in the CFRP patching of the test specimens, the reference face of the patching is set at the bottom face of the patching in the finite element model by including a parameter "offset = −0.5" in the command statement "*Shell section" in the input file of ABAQUS. Hence, different thicknesses can be assigned to different layers of the CFRP patching. The reference faces for the adhesive layer and steel plate layer are set at the midplane of the plate in the through thickness direction. Illustrations of the shell elements for modeling the CFRP patching, the adhesive layer, and the steel plate are shown in Figure 8.6. Constraints are used to enforce compatibility between the plate−adhesive and the adhesive−CFRP patching

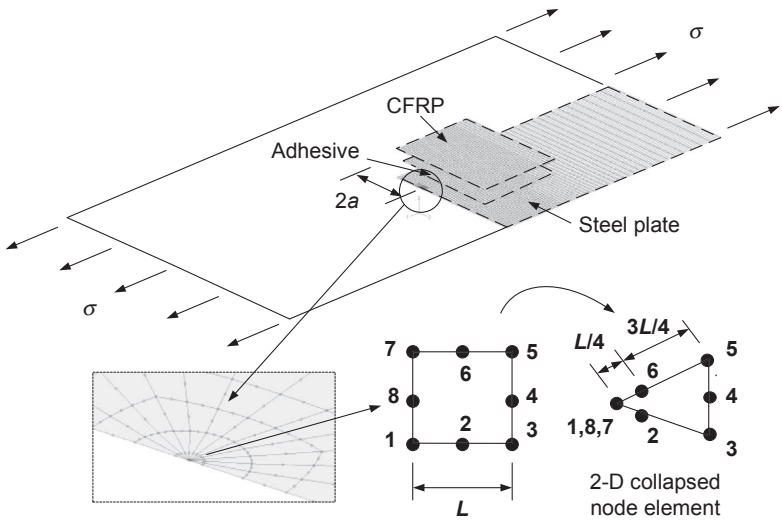

Figure 8.5 Three layers finite element model.

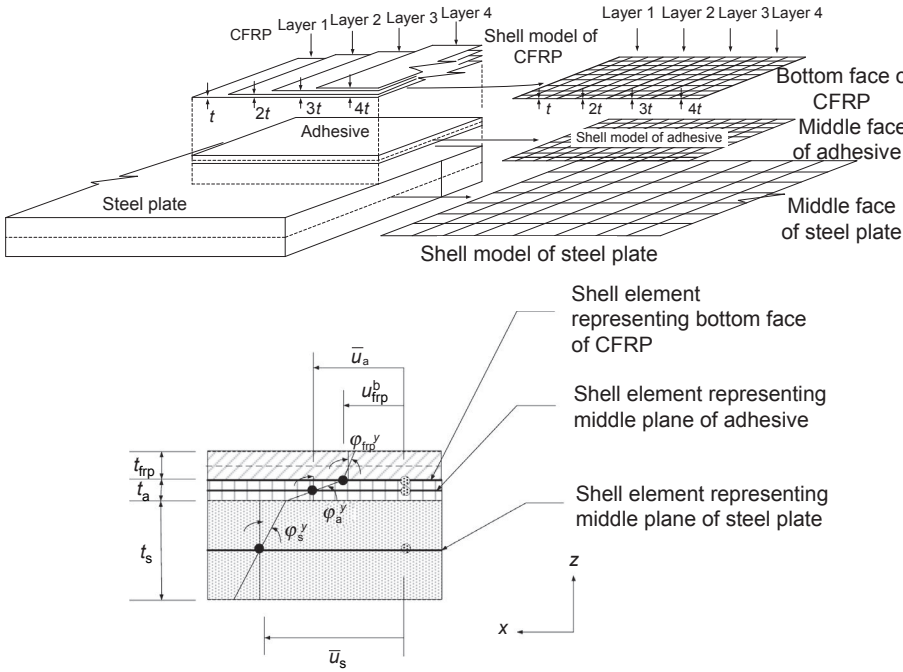

Figure 8.6 Illustration of the three layers finite element model and the displacement relationship along the *x*-direction.

interface based on Mindlin assumptions. The Mindlin plate theory (Timoshenko and Woinowsky-Kriege, 1959) assumes a linear displacement field in the plate thickness and allows for the transverse shear deformation of the plate. In the three layers technique proposed by Naboulsi and Mall (1996), the cracked plate layer, the adhesive layer, and the CFRP patching layer are assumed to have a linear displacement field across the thickness which satisfies the following relations:

$$u_{\text{frp}} = \overline{u}_{\text{frp}} + \varphi^y_{\text{frp}} z_{\text{frp}} \quad u_a = \overline{u}_a + \varphi^y_a z_a \quad u_s = \overline{u}_s + \varphi^y_s z_s \tag{8.5 a,b,c}$$

$$v_{\text{frp}} = \overline{v}_{\text{frp}} + \varphi^x_{\text{frp}} z_{\text{frp}} \quad v_a = \overline{v}_a + \varphi^x_a z_a \quad v_s = \overline{v}_s + \varphi^x_s z_s \tag{8.6 a,b,c}$$

$$w_{\text{frp}} = \overline{w}_{\text{frp}} \qquad w_a = \overline{w}_a \qquad w_s = \overline{w}_s \tag{8.7 a,b,c}$$

where $\overline{u}$, $\overline{v}$, and $\overline{w}$ are the midplane displacements along the *x*, *y*, and *z* directions (*x* and *y* are in the plane of the plate and *z* is in the thickness direction), respectively, and φ^x, φ^y are the rotations of the cross section along the *x* and *y* axes. The subscript symbols frp, *a*, and *s* are used to denote the composite patching, the adhesive, and the steel plate, respectively. The symbols representing the longitudinal displacements in the *x*-direction and the rotations are also shown in Figure 8.6. According to Naboulsi and Mall (1996), at the plate−adhesive interface where the *z* coordinates for the cracked

plate and the adhesive are equal and at the adhesive−composite patching interface where the z coordinates for the adhesive and the composite patching are equal, the displacement field's equations reduce to:

$$u_{\text{frp}} = u_a \quad v_{\text{frp}} = v_a \quad w_{\text{frp}} = w_a \tag{8.8 a,b,c}$$

$$u_a = u_s \quad v_a = v_s \quad w_a = w_s \tag{8.9 a,b,c}$$

Therefore, for the plate−adhesive interface, the relationships between the midplane displacements are:

$$\overline{u}_s - \overline{u}_a - \varphi_a^y \frac{t_a}{2} - \varphi_s^y \frac{t_s}{2} = 0 \quad \text{and} \quad \overline{v}_s - \overline{v}_a - \varphi_a^x \frac{t_a}{2} - \varphi_s^x \frac{t_s}{2} = 0 \tag{8.10 a,b}$$

For the composite−adhesive interface, the relationships between the midplane displacements are:

$$\overline{u}_a - \overline{u}_{\text{frp}} - \varphi_{\text{frp}}^y \frac{t_{\text{frp}}}{2} - \varphi_a^y \frac{t_a}{2} = 0 \quad \text{and} \quad \overline{v}_a - \overline{v}_{\text{frp}} - \varphi_{\text{frp}}^x \frac{t_{\text{frp}}}{2} - \varphi_a^x \frac{t_a}{2} = 0 \tag{8.11 a,b}$$

However, it has been mentioned that the reference face for the composite is at the bottom face location. The relationships between the displacements of the midplane and the bottom face of the composite are:

$$u_{\text{frp}}^b = \overline{u}_{\text{frp}} + \varphi_{\text{frp}}^y \frac{t_{\text{frp}}}{2} \quad \text{and} \quad v_{\text{frp}}^b = \overline{v}_{\text{frp}} + \varphi_{\text{frp}}^x \frac{t_{\text{frp}}}{2} \tag{8.12 a,b}$$

where u_{frp}^b and v_{frp}^b are the displacement of the bottom face of the composite patching.

Therefore, for the composite−adhesive interface, the displacement relationships become:

$$\overline{u}_a - u_{\text{frp}}^b - \varphi_a^y \frac{t_a}{2} = 0 \quad \text{and} \quad \overline{v}_a - v_{\text{frp}}^b - \varphi_a^x \frac{t_a}{2} = 0 \tag{8.13 a,b}$$

Symmetric boundary conditions are applied to the edges. According to the test setup, the steel plate was connected to two splice members at both ends by bolting and the splice members were connected to the MTS machine. Since the thickness of each splice member is two times the thickness of the tested steel plates, rotational and out of plane displacements were assumed to be restrained at the loading edge of the steel plate in the finite element models. Suitable axial displacement was applied to the loading edge so that a far end mean axial stress in the steel plate of 100 MPa was obtained.

The material properties which are shown in Table 8.3 (Kennedy and Cheng, 1998) are used in the finite element analysis. The thicknesses of the steel plate (t_s), the adhesive layer (t_a), and the CFRP patching (t_{frp}) are 6.35, 0.06, and 0.23 mm/ply, respectively. Static analysis is carried out to obtain the strain distributions, and the SIF is obtained

Table 8.3 Material properties of steel plate, adhesive, and CFRP plate for finite element modeling (Kennedy & Cheng, 1998)

Steel plate	Elastic modulus	E_s	200,000 MPa
	Poisson's ratio	ν_s	0.3
Adhesive	Elastic modulus	E_a	3000 MPa
	Poisson's ratio	ν_a	0.34
CFRP composite	Longitudinal elastic modulus	E_{frp1}	128,093 MPa
	Transverse elastic modulus	E_{frp2}	6900 MPa
	Poisson's ratio	ν_{frp}	0.17
	Shear modulus	G_{frp}	4480 MPa

using the contour integral function in ABAQUS. This SIF represents the SIF value of the midplane of the cracked steel plate. The SIFs of the unpatched side and patched side are calculated assuming that the SIF varies linearly across the thickness of the plate, as mentioned above. In addition, the SIF is assumed to be linearly proportional to the deformation of the steel plate near the crack tip. The longitudinal displacement of the steel plate and the rotation of the nearest node to the crack tip are obtained from the finite element analysis. Since this longitudinal displacement represents the displacement of the midplane of the plate, the longitudinal displacement of the patched side (u_p) and unpatched side (u_f) of the plate is evaluated using the following relations:

$$u_p = u_m - \frac{t_s \varphi_m}{2} \quad \text{and} \quad u_f = u_m + \frac{t_s \varphi_m}{2} \tag{8.14 a,b}$$

where u_m and φ_m are the longitudinal displacement and rotation of the nearest node to the crack tip of the reference plane, as shown in Figure 8.7, and t_s is the thickness of the plate. It is assumed that the SIF varies linearly across the thickness and is proportional to the longitudinal displacement. Therefore, with the SIF of the midplane of the cracked plate (K_m), the SIFs of the patched face (K_p) and unpatched face (K_f) are:

$$K_p = K_m\left(\frac{u_p}{u_m}\right) = K_m\left(1 - \frac{t_s \varphi_m}{2u_m}\right) \text{ and } K_f = K_m\left(\frac{u_f}{u_m}\right) = K_m\left(1 + \frac{t_s \varphi_m}{2u_m}\right) \tag{8.15 a,b}$$

In the three layers finite element model discussed above, a linear relationship relating the SIF to the longitudinal displacement near the crack tip was assumed in the prediction of the SIF of the unpatched and the patched side of the cracked plate. In order to examine this assumption, a modified three layers finite element model is proposed. The modified model uses 3-D brick elements to model the cracked plate and shell elements to model both the CFRP patching and the adhesive layer. Since

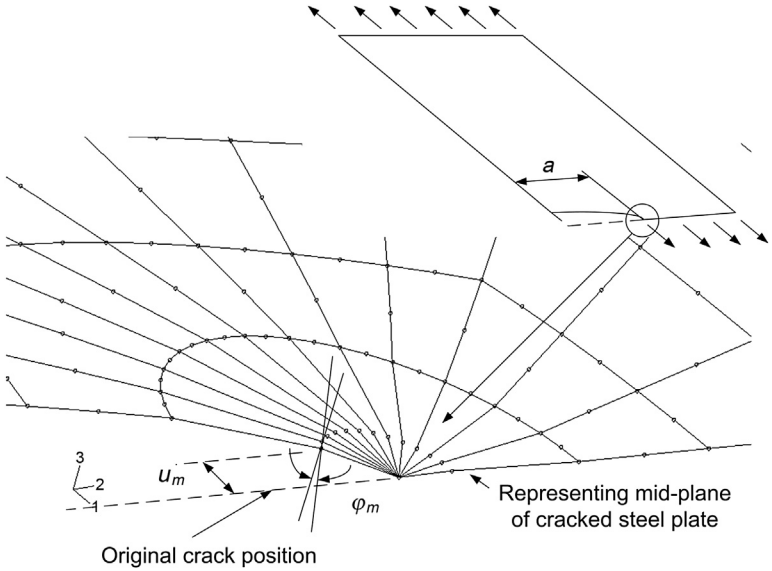

Figure 8.7 Longitudinal displacement and rotation of the nearest node to the crack tip of the three layers model.

the cracked plate is modeled by the 3-D brick elements, the SIF at the crack tip through the thickness direction can be obtained numerically. A typical 3-D brick element (C3D20, 20 nodes brick element in ABAQUS) model is shown in Figure 8.8. As shown in the figure, the 3-D brick elements with collapsed nodes are assigned at the crack tip location. The SIFs at the crack tip through the thickness direction of the plate are obtained using the contour integral function in the ABAQUS program. The boundary conditions and material properties used in the three layers model are also applied to the modified three layers model. Similar to the three layers model, the reference faces for the adhesive layer are set at the midplane of the plate in the through-thickness direction, and the reference face for the composite is at the bottom face location. Therefore, the displacement constraints used in the three layers model are also applied to the modified three layers model to enforce the compatibility along the adhesive−CFRP patching interface. Since the 3-D brick elements are used to model the steel plate, the displacements of the nodes on the patched side of the steel plate are made compatible with the displacement of the nodes of the adhesive layer as follows:

$$u_s^T - \overline{u}_a - \varphi_a^y \frac{t_a}{2} = 0 \quad \text{and} \quad v_s^T - \overline{v}_a - \varphi_a^x \frac{t_a}{2} = 0 \tag{8.16 a,b}$$

where u_s^T and v_s^T are the displacements of the patched side of the steel plate and the description of u_s^T is shown schematically in Figure 8.9.

The CODs of the patched side and the unpatched side of the three layers model predicted by Eqn 8.14(a) and (b) are shown to be close to the results of the modified three

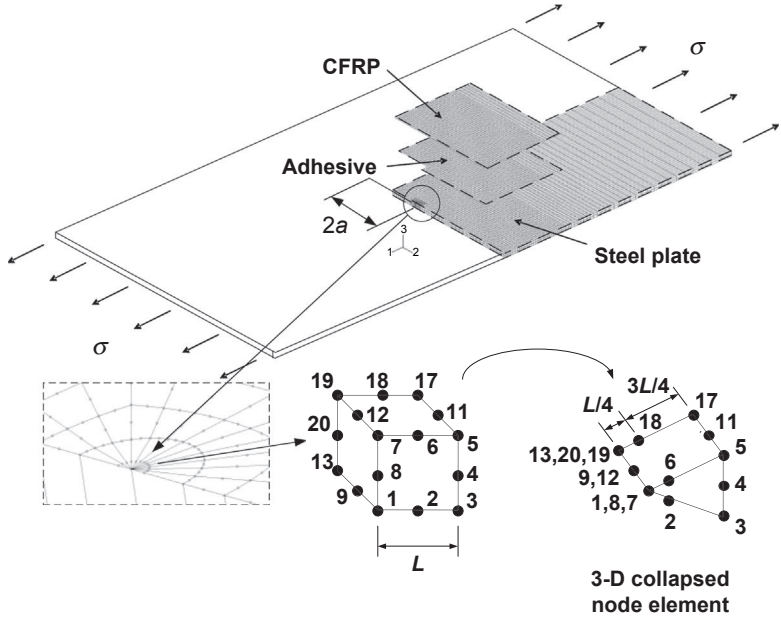

Figure 8.8 The modified three layers model (3-D brick and shell model).

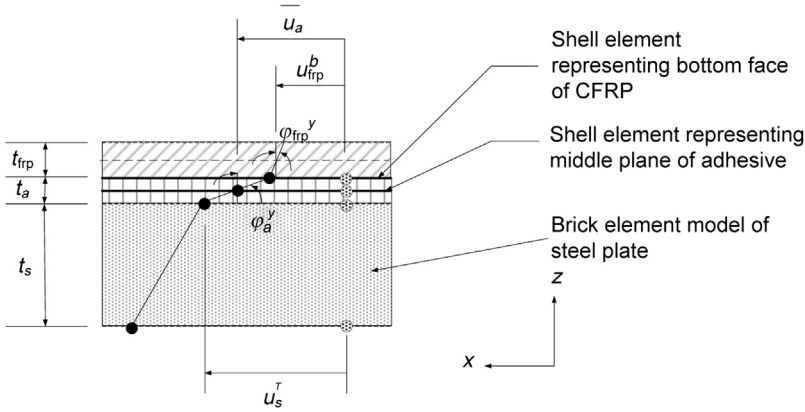

Figure 8.9 Displacement relationship of the modified three layers model along the *x*-direction.

layers model (Figure 8.10). The predictions of the SIF of the three layers model according to Eqn 8.15(a) and (b) are compared to the results from the modified three layers model as well. The SIFs at the crack tip across the thickness of the steel plate of the FE model of R116 (shown as R116FE in the figure) of the three layers model and the modified three layers model together with the SIF of the plain steel model are shown in Figure 8.11. For the plain steel model, the brick model gives almost the same value of SIF as that of the three layers model on the unpatched surface,

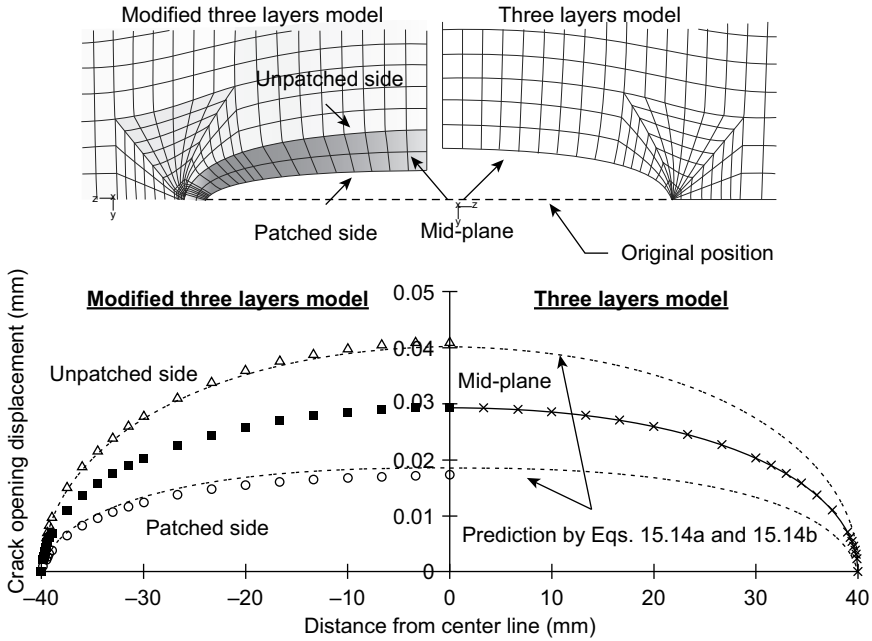

Figure 8.10 Deformed shape and crack displacements of the two types of finite element model of specimen R116.

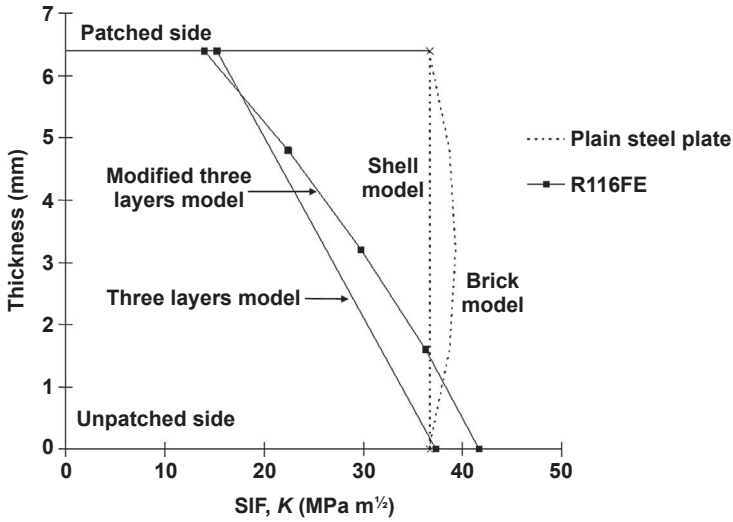

Figure 8.11 Comparison of the SIF across the plate thickness of the modified three layers model and the three layers model.

but a slightly higher value of SIF is observed for the region across the thickness of the plate. This higher value of SIF is expected due to the presence of a plane strain condition in that region. Figure 8.11 also shows that the SIF reduces significantly on the patched side but increases slightly on the unpatched side when comparing the SIF of the plain steel model to that of both models with single-side CFRP patching. In addition, the modified three layers model gives a slightly smaller value of SIF when compared to that of the three layers model on the patched side, but a higher value of SIF is observed on the unpatched side for the modified three layers model. In general, the three layers model underestimates the SIF across the thickness of the plate when compared to those of the modified three layers model.

The results of the SIF obtained from the three layers model and the modified three layers model and the $SIF_{3\text{-}D}/SIF_{3\text{-}L}$ ratios are shown in Table 8.4. With the finite element results of the modified three layers model as a reference, it is shown in the table that the three layers model overestimates the SIF on the patched side of the plate and underestimates the SIF on the unpatched side by about 10% on average. It is shown from the results of the modified three layers model (Figure 8.11) that the SIF varies nonlinearly through the thickness of the crack tip, and the predictions of SIF based on the three layers model on the patched side and the unpatched side cannot properly reflect the SIF variation through the thickness. Therefore, even though the SIF obtained from the three layers model gives a slightly conservative prediction on the patched side, it is suggested that the modified three layers model should be adopted when evaluating the through thickness SIF of cracked steel plate with single-sided patching.

The effect of patching parameters on the SIF is shown in Table 8.5. The SIF ratios as shown in the table represent the ratio of the SIF based on the modified three layers model ($SIF_{3\text{-}D}$) to the SIF based on the plain steel model (SIF_{steel}). The SIF ratios of the patched side vary from 0.37 to 0.50, whereas the ratios for the unpatched side vary from 1.11 to 1.18. Hence, it is shown that the CFRP patching can reduce the SIF of the patched side of the cracked plate substantially. The effect of patch length on the SIF is obtained, for example, by comparing the SIF results of models R116FE, R216FE, and R316FE. It is shown that when the patch width decreases from 160 to 80 mm, the ratio of SIF only increases from 0.38 to 0.42 on the patched side and decreases from 1.14 to 1.12 on the unpatched side, respectively. Therefore, the SIF on the patched side slightly decreases with decreasing patch width. Similar behavior is observed for models with four layers of CFRP patching. For the effect of patch length, it is shown that by increasing the patch length from 30 mm (R226FE) to 100 mm (R216FE), the ratio of the SIF on the patched side increases from 0.37 to 0.40 but decreases from 1.18 to 1.13 on the unpatched side, respectively. Although more reduction of the SIF on the patched side can be achieved by increasing the patch width and/or reducing the patch length, the SIF on the unpatched side will also be increased. In addition, for the models studied, it is shown that the patch width and patch length have only a marginal effect on the SIF. However, the effect of the number of layers of CFRP patching on the reduction of the SIF is more pronounced. Table 8.5 shows that the average SIF ratio is 0.39 (representing a 61% decrease) for specimens with six layers of CFRP patching and 0.47 (representing a 53% decrease) for specimens with four

Table 8.4 Ratio of SIF value of the modified three layers model to the plain steel model

Specimens	Width *w* (mm)	Length *l* (mm)	Layer *n*	Taper (mm)	Modified three layers model SIF (K) MPa $\sqrt{m}$		$SIF_{3\text{-}D}/SIF_{steel}$	
					Patch	Unpatch	Patch	Unpatch
Plain steel	–	–	–	–	36.59	36.59	1.00	1.00
R116FE	160	100	6	5	13.99	41.65	0.38	1.14
R216FE	120	100	6	5	14.58	41.24	0.40	1.13
R316FE	80	100	6	5	15.50	41.01	0.42	1.12
R226FE	120	30	6	3	13.48	43.01	0.37	1.18
R326FE	80	30	6	5	14.05	42.47	0.38	1.16
				Average	**14.32**	**41.88**	**0.39**	**1.15**
R214FE	120	100	4	5	17.32	40.76	0.47	1.11
R314FE	80	100	4	5	18.12	40.57	0.50	1.11
R224FE	120	30	4	5	16.34	42.12	0.45	1.15
R324FE	80	30	4	3	16.85	41.71	0.46	1.14
				Average	**17.16**	**41.29**	**0.47**	**1.13**

Table 8.5 SIF results of FE models with tapered and nontapered end of CFRP patching

Specimens	Width *w* (mm)	Length *l* (mm)	Layer *n*	Nontaper end SIF (K) MPa √m		Taper end SIF (K) MPa √m		Nontaper/taper	
				Patch	Unpatch	Patch	Unpatch	Patch	Unpatch
R116FE	160	100	6	14.60	42.99	13.99	41.65	1.04	1.03
R216FE	120	100	6	15.32	42.86	14.58	41.24	1.05	1.04
R316FE	80	100	6	16.23	42.52	15.50	41.01	1.05	1.04
R226FE	120	30	6	14.08	44.24	13.48	43.01	1.04	1.03
R326FE	80	30	6	14.72	43.59	14.05	42.47	1.05	1.03
							Average	**1.05**	**1.03**
R214FE	120	100	4	18.03	42.20	17.32	40.76	1.04	1.04
R314FE	80	100	4	18.87	42.04	18.12	40.57	1.04	1.04
R224FE	120	30	4	16.97	43.42	16.34	42.12	1.04	1.03
R324FE	80	30	4	17.53	42.96	16.85	41.71	1.04	1.03
							Average	**1.04**	**1.04**

layers of CFRP patching. In addition, the SIF on the unpatched side of the cracked plate is on average about 14% higher than that of the plain steel model. A summary of the ratio of SIF is shown in Figure 8.12. In general, when comparing the SIF of the plain steel model to the model with CFRP patching, the reduction of the SIF on the patched side for models with six layers of CFRP patching is about 20% more than that for models with four layers of CFRP patching.

8.3 Finite element analysis of SIF of cracked plate with single-side FRP patching

8.3.1 FE model with updated crack tip shape

The effect of several parameters, such as the number of layers of FRP patching, patch length and width, and the reduction of SIF of cracked steel plate with single-side CFRP patching was presented in the previous section. It is shown that the reduction of SIF is more significant on the patched side than on the unpatched side. Fatigue crack growth depends very much on the magnitude of SIF at the crack tip. Therefore, for cracked steel plate with single-side CFRP patching, the crack growth rate on the patched side will not be the same as that on the unpatched side. Lee and Lee (2004) proposed a numerical procedure in which the finite element model of cracked plate with single-side FRP patching is updated according to the predicted SIF. This numerical procedure is demonstrated in the following section, and a detailed discussion regarding the crack tip update procedure and the corresponding SIF at crack tip through the thickness is presented.

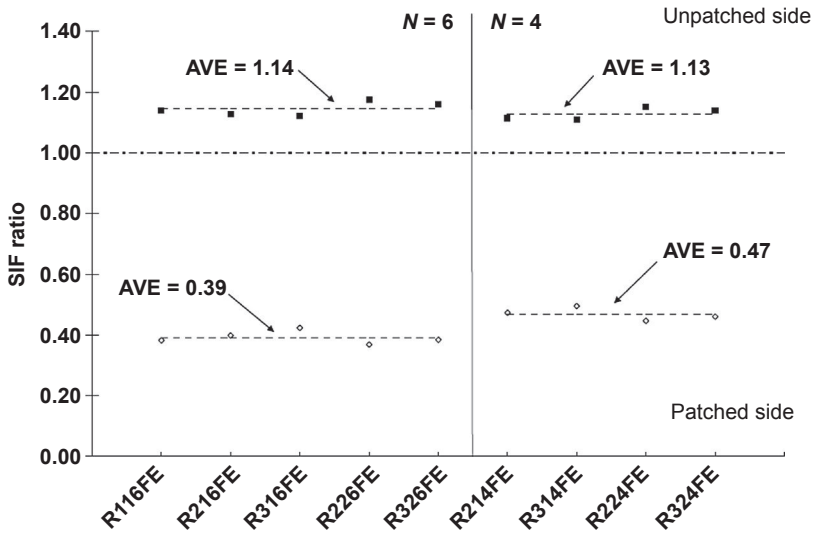

Figure 8.12 Summary of the SIF ratio of specimens with CFRP patching.

Finite element analyses of cracked steel plates with single-side FRP patching were carried out to study the effect of single-side FRP patching on the change of stress intensive factor across crack tip at different stages of crack propagation. Finite element models were set up using the commercial finite element program ABAQUS (Hibbitt et al., 2004). The modified three layers model which was discussed in Section 8.2.2 is used to model the tested steel specimens with single-side FRP patching. Eight node shell elements (S8R, eight nodes general purpose shell element in ABAQUS) were used to model the adhesive and the FRP plates and 20-node brick elements (C3D20, 20 nodes brick element in ABAQUS) were used to model the steel plates. In this study, two different crack patterns—edge crack and central crack—were considered and analyzed. Detail dimension of the cracked plate and the patched FRP is shown in Figure 8.13(a) and (b), and the material properties are shown in Table 8.6. For the current finite element analysis, the FRP patching of the finite element model was modeled by assigning the material properties of Sika Carbodur (Sika, 2003) for the CFRP. The thicknesses of the steel plate and CFRP were 9.5 mm and 3.6 mm, respectively, in order to achieve an adherend stiffness ratio (ETR) equal to 0.33. The adhesive and the CFRP patching were modeled using shell elements. Composite shell elements were used to model the CFRP plates and the adhesive between the CFRP plates. As illustrated in Figure 8.14, there are three layers of CFRP plate, each 1.2 mm thick and two layers of adhesive of 0.5 mm thick. These five layers of materials were modeled by using the composite shell element. The material properties of each layer of the materials were assigned to the shell element by introducing the key word "composite" in the input file of ABAQUS (Hibbitt et al., 2004). In order to obtain the SIF through the thickness of the plate, 3-D brick elements were used to model the cracked steel plate. At the location of crack tip, collapsed elements with middle nodes located at the quarter point were used in order to obtain the stress intensity factor at the

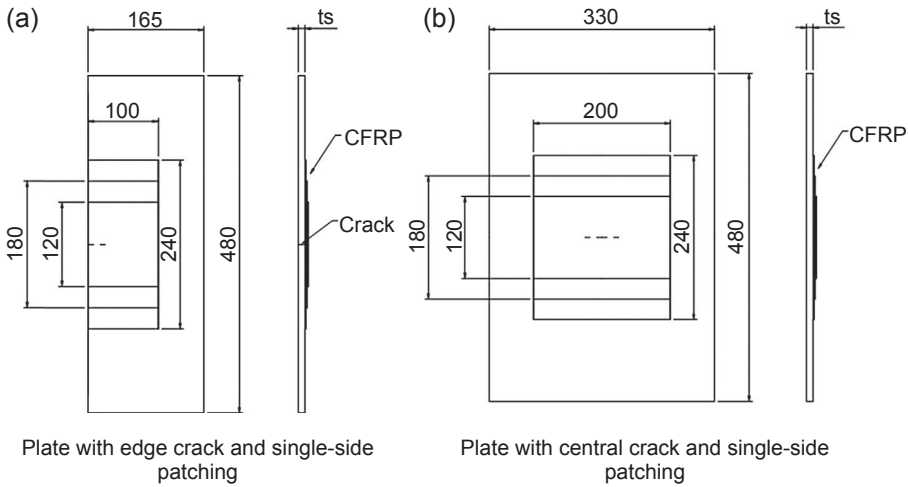

Figure 8.13 Dimension of the cracked plate and the patched FRP.

Table 8.6 Material properties for the finite element analysis

Steel plate	E_s	200,000 MPa
	ν_s	0.3
CFRP plate	E_{frp1}	175,000 MPa
	E_{frp2}	9000 MPa
	ν_{frp}	0.28
	G_{frp}	4500 MPa
Adhesive	E_a	4500 MPa
	ν_a	0.34
	G_a	1680 MPa

Note: E_{frp1} is the elastic modulus along the loading direction and E_{frp2} is the elastic modulus along the transverse direction.

crack tip by means of contour integration methods. Suitable constraints were used to enforce the compatibility along the plate−adhesive and the adhesive−FRP interface. The conditions of constraints which were discussed in previous sections were applied to the current finite element models as well.

Due to the various values of SIF across the thickness of the plate, different crack propagation lengths at crack tip across the thickness of the plate are expected. The numerical procedures proposed by Lee and Lee (2004) for evaluating different crack propagation lengths at crack tip across the thickness of the plate and the corresponding SIF are adopted in the current finite element analysis. According to the Paris law (Paris and Erdogan, 1960) the number of cycles for a crack to grow from the initial crack

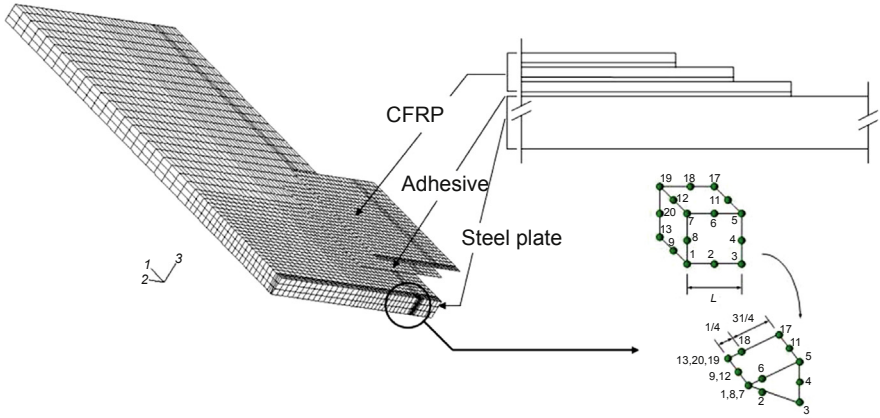

Figure 8.14 Finite element model of cracked steel plate with CFRP patching.

length (a_i) to the final crack length (a_f) can be predicted by the following equation (Eqn (8.17)):

$$N = \int_{a_i}^{a_f} \frac{1}{C(\Delta K)^m} \mathrm{d}a \tag{8.17}$$

where N is the number of cycles required for the initial crack (a_i) to grow to the size of the final crack length (a_f). Since ΔK varies with the crack growth in practical situations, the Euler algorithm is often used and the corresponding number of cycles (N) in the $j + 1$ term is shown in the following equation (Lee and Lee, 2004):

$$N^{(j+1)} = N^{(j)} + \Delta N^{(j)} = N^{(j)} + \frac{\Delta a^{(j)}}{C\left[\Delta K(a^{(j)})\right]^m} \quad j = 0, 1, 2, \ldots, n \tag{8.18}$$

where n is the number of intervals.

In the finite element analysis, a model with uniform initial crack length ($a_i = 25.4$ mm) was used as a starting analysis. FRP patching was applied at one side of the cracked steel plate. As was discussed in the previous section, since the SIF varies across the crack front in the case of single-sided repairs, different crack growth rates of the patched side and unpatched side should be considered. In this study, local increments across the crack front are considered, as shown in Figure 8.15. The Paris law can be used at any point along the crack front as follows:

$$\frac{\mathrm{d}a_i}{\mathrm{d}N} = C(\Delta K_i)^m \tag{8.19}$$

where $\mathrm{d}a_i$ and ΔK_i are the local crack growth increment and SIF range at an arbitrary point i along the crack front, respectively. Similarly, the following equation can be derived from Eqn (8.19) at j term: with $\Delta N = \frac{\Delta a_i^{(j)}}{C(\Delta K_i^{(j)})^m} = \frac{\Delta a_{\max}^{(j)}}{C(\Delta K_{\max}^{(j)})^m}$

$$\Delta a_i^{(j)} = \left(\frac{\Delta K_i^{(j)}}{\Delta K_{\max}^{(j)}}\right)^m \Delta a_{\max}^{(j)} \quad i = 1, 2, \ldots. \tag{8.20}$$

where $\Delta a_{\max}^{(j)}$ is the maximum crack growth increment at the point where the maximum SIF range, and $\Delta K_{\max}^{(j)}$, across the crack front occurs. Equation (8.20) can be used to calculate the local increment of crack growth at each point along the crack front. As the advanced crack tip shape is dependent on the SIF range, a very fine crack growth value is assigned during the analysis. A maximum crack growth value $\left(\Delta a_{\max}^{(j)}\right)$ of the unpatched side equal to 1.5875 mm (1/16 in) was used in the analysis. This crack growth value is about 6.25% of the length of the initial crack length. After the first successive analysis of the SIF across the uniform initial crack front, the crack growth values through the thickness of the plate were calculated by Eqn (8.20) with the

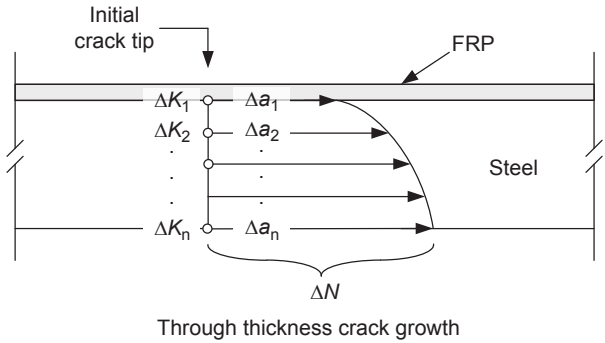

Figure 8.15 Illustration of the local increments along the crack front.

material constants (m) equal to 3 (Barsom and Rolfe, 1999). Then, another finite element model was set up by using the updated nonuniform crack length, and the corresponding SIF across the crack tip was analyzed. This procedure was repeated until the crack length of the unpatched side reached 63.5 mm. The finite element models which represent four different crack lengths are shown in Figure 8.16. The SIF of the crack front according to two far end stress levels ($\sigma_{\min} = 14$ MPa and $\sigma_{\max} = 283$ MPa) were used and the corresponding stress range ($\Delta\sigma$) was 269 MPa. After the first successive analysis of the SIF along the uniform initial crack front, the crack growth values through the thickness of the plate were calculated using Eqn (8.20) with the material constant m equal to 3 (Barsom and Rolfe, 1999), in which the SIF range (ΔK) was defined as the difference between $K_{\max}$ and $K_{\min}$. Then, another finite element model was set up by using the updated nonuniform crack front and the corresponding SIF along the crack. With a maximum crack growth value $\left(\Delta a_{\max}^{(j)}\right)$ of the unpatched side equal to 1.5875 mm, 24 finite element models for each case were formed according to the results of the SIF to achieve a final crack length of 63.5 mm, which is defined as a_f for edge crack models, and 127 mm, which is defined as $2a_f$ for central crack models.

8.3.2 Evaluation of geometrical correction factor for cracked steel plate with single-side FRP patching

The crack growth propagation and the normalized SIF ($\Delta K/\Delta\sigma$) through the thickness of the crack of every two steps are shown in Figure 8.17 for the edge crack models with ETR value equal to 0.33. As discussed previously, a uniform crack length ($a_i = 25.4$ mm) was used as a starting analysis. With this assigned uniform crack length, the variation of the SIF is slightly nonlinear through the thickness of the crack (Figure 8.17). As a result, the crack grows at a different rate on the patched side and on the unpatched side. Crack propagation was then calculated through the thickness of the plate according to Eqn (8.20) and the original uniform crack shape changed to a nonuniform crack shape. The change of SIF was then predicted according to the nonuniform crack shape. With the nonuniform propagation of the crack tip, the

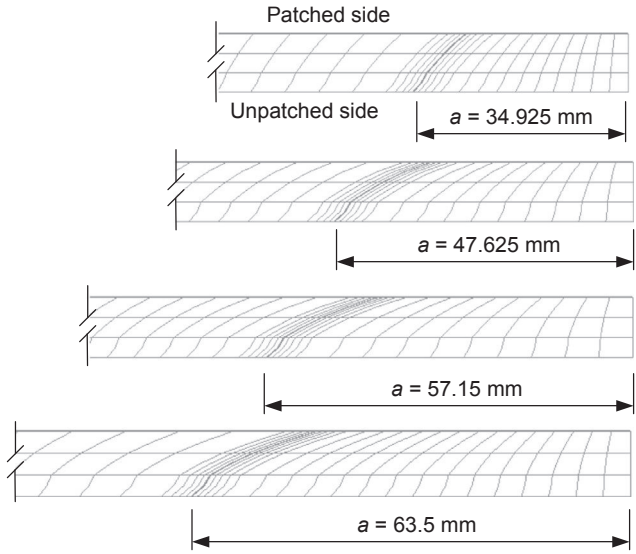

Figure 8.16 Finite element models with four different crack lengths.

through-thickness values of $\Delta K/\Delta\sigma$ became more uniform as the crack length increased. It is shown that the $\Delta K/\Delta\sigma$ of the unpatched side is about 2.7 times larger than that on the patched side when the crack length is short ($a_i = 25.4$ mm). As the crack length increased, a significant drop in the ratio of $\Delta K/\Delta\sigma$ of patched and unpatched side was observed. When the crack length of unpatched side reached 63.5 mm (2.5 times a_i), the difference in $\Delta K/\Delta\sigma$ between the patched and unpatched

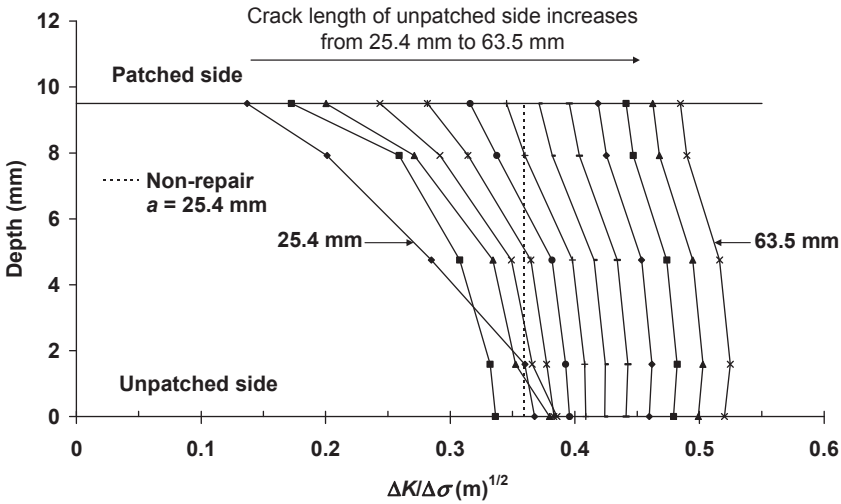

Figure 8.17 Through thickness normalized SIF ($\Delta K/\Delta\sigma$) versus crack length of edge cracked FE model with single-side CFRP patching.

side was less than 10%. As the crack length increases, $\Delta K/\Delta\sigma$ of the unpatched side is close to the value of $\Delta K/\Delta\sigma$ of the patched side. A general expression of $\Delta K/\Delta\sigma$ versus the ratio of crack length to the width of the steel plate (a/b) of nonrepaired model is shown in Eqn (8.21):

$$\Delta K/\Delta\sigma = f(a/b)\sqrt{\pi a} \tag{8.21}$$

where $f(a/b)$ is a correction factor for the geometry of the specimen. For plate with edge crack subjected to uniform far end stress, $f(a/b)$ is calculated according to Eqn (8.22) (Gross and Srawley, 1964):

$$f(a/b) = 1.12 - 0.231\left(\frac{a}{b}\right) + 10.55\left(\frac{a}{b}\right)^2 - 21.72\left(\frac{a}{b}\right)^3 + 30.39\left(\frac{a}{b}\right)^4 \tag{8.22}$$

where a is the edge crack length and b is the width of plate. With $a = 25.4$ mm and $b = 165$ mm, the corresponding $\Delta K/\Delta\sigma$ was calculated for the nonrepaired model according to Eqns (8.21) and (8.22), and the values are shown in Figure 8.18 as well for comparison. Comparing the values of $\Delta K/\Delta\sigma$ of plates with single-side CFRP patching and the nonrepaired plates, the reduction in $\Delta K/\Delta\sigma$ on the patched side was around 62%. On the other hand, almost no reduction in the value of $\Delta K/\Delta\sigma$ was observed on the unpatched side for those plates.

The ratio of $\Delta K/\Delta\sigma$ along through thickness direction at the crack tip of steel plate with central crack and single-side CFRP patching is shown in Figure 8.18. Similar to the case of plates with an edge crack and with single-side patching, it is shown from the figure that for plates with a central crack, a significant reduction of the normalized SIF

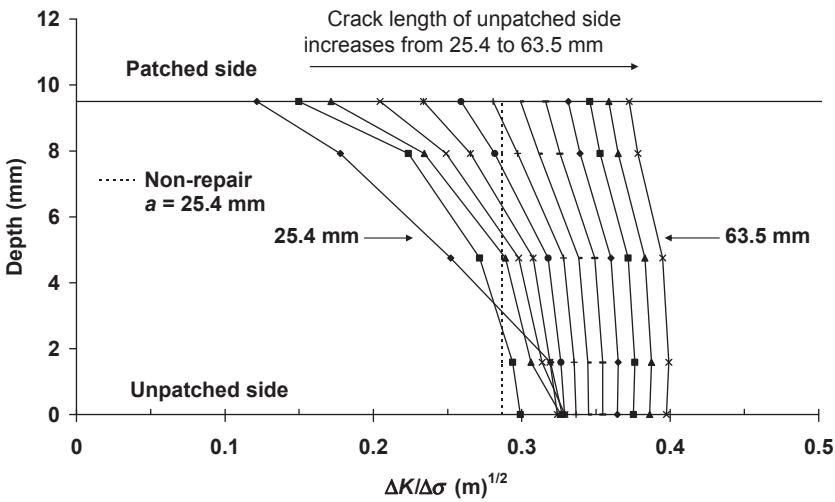

Figure 8.18 Through thickness normalized SIF ($\Delta K/\Delta\sigma$) versus crack length of central cracked FE model with single-side CFRP patching.

($\Delta K/\Delta\sigma$) is observed on the patched side for plates with initial crack length a_i equal to 25.4 mm. The value of $\Delta K/\Delta\sigma$ of nonrepaired plates with initial crack length ($2a_i$) equal to 50.8 mm and steel plate width ($2b$) equal to 330 mm was calculated according to Eqn (8.21) with the correction factor $f(a/b)$ obtained according to Eqn (8.23) (Tada et al., 1985), as follows:

$$f(a/b) = \left(1 - 0.025\left(\frac{a}{b}\right)^2 + 0.06\left(\frac{a}{b}\right)^4\right)\sqrt{\sec\left(\frac{\pi a}{2b}\right)} \tag{8.23}$$

where a is half of the crack length and b is half of the width of cracked plate. Compared to the nonrepaired plates, the reduction of $\Delta K/\Delta\sigma$ on the patched side is around 58%. However, the values of $\Delta K/\Delta\sigma$ on the unpatched side were observed to be a little larger than those of the nonrepaired plates. As the crack becomes longer, the value of $\Delta K/\Delta\sigma$ of the patched side increases and approaches the value of the unpatched side. When a/b is equal to 0.38 (crack length corresponding to final crack length), the reduction of $\Delta K/\Delta\sigma$ is about 27% on the patched side and 16% on the unpatched side.

The normalized SIF range ($\Delta K/\Delta\sigma$) can be obtained according to Eqn (8.21) where $f(a/b)$ is the correction factor which accounts for the geometry of the specimen. From the finite element results, the SIF, K, is obtained for plates with different crack patterns and patching conditions. Therefore, with Eqn (8.21), the corresponding value of $f(a/b)$ could be obtained according to Eqn (8.24), which is based on the finite element results:

$$f(a/b) = \frac{\Delta K}{\Delta\sigma\sqrt{\pi a}} \tag{8.24}$$

The results of $f(a/b)$ for the unpatched side of plates with an edge crack and single-side patching are shown in Figure 8.19 along with the results of the nonrepaired

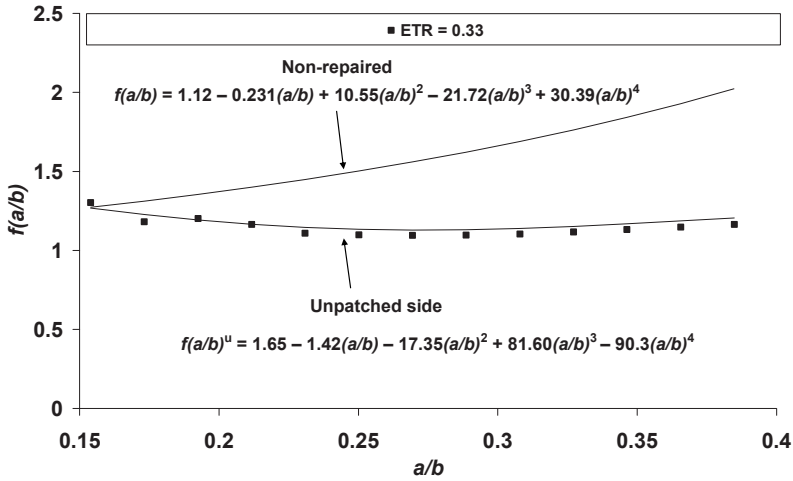

Figure 8.19 Value of $f(a/b)$ versus crack length-to-plate width ratio (a/b) of edge cracked model with single-side CFRP patching.

model. As shown in Figure 8.19, for plates with an edge crack and single-side patching, the values of $f(a/b)$ of unpatched side are almost the same as that of the nonrepaired plates when the crack length is short. However, as the crack length increased, the values of $f(a/b)$ of the plates with single-side patching were reduced significantly. For plate with a central crack, the results of $f(a/b)$ of plates with single-side patching are shown in Figure 8.20. It is shown from the figure that the values of $f(a/b)$ are a bit larger than that of the nonrepaired plates when the crack length is short. As the crack length increases, the values of $f(a/b)$ are reduced. However, the reduction is not as much as that found in the plates with an edge crack. Based on regression analysis of the data, a single equation which takes the form similar to the equation for nonrepaired model was developed for determining the value of $f(a/b)^u$ for plates with single-side patching. The correction functions are:

1. For plates with an edge crack and single-side patching:

$$f(a/b)^u = 1.65 - 1.42\left(\frac{a}{b}\right) - 17.35\left(\frac{a}{b}\right)^2 + 81.60\left(\frac{a}{b}\right)^3 - 90.3\left(\frac{a}{b}\right)^4 \tag{8.25}$$

2. For plates with a central crack and single-side patching:

$$f(a/b)^u = 1.96 - 8.82\left(\frac{a}{b}\right) + 26.55\left(\frac{a}{b}\right)^2 - 33.55\left(\frac{a}{b}\right)^3 + 15.06\left(\frac{a}{b}\right)^4 \tag{8.26}$$

Based on the finite element results of the SIF, equations of the correction factor which considered the crack pattern and patching pattern were predicted for models with different forms of crack pattern and patching pattern. With the correction factor

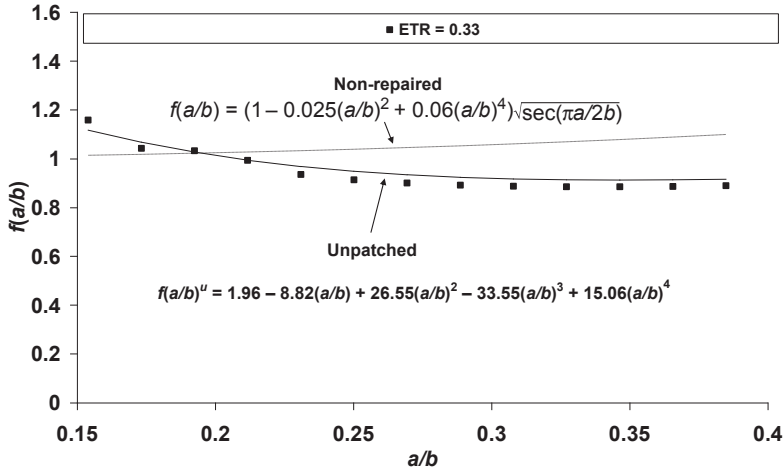

Figure 8.20 Value of $f(a/b)$ versus crack length-to-plate width ratio (a/b) of central cracked model with single-side CFRP patching.

of different forms of crack pattern and patching pattern, the fatigue life of each model could be predicted.

8.4 Finite element analysis of cracked steel circular pipe repaired with FRP patching

8.4.1 Introduction of steel circular pipe with crack

Circular hollow member is one of the most common structural members which can be used as the major component such as the oil or gas circular pipe system, underground infrastructure (such as the piping system for the transportation of water and wastewater), or the structural members of a truss. The circular member is usually connected by welding. Due to the demanding loads, continual use, and the environment effect, cracking is one of the major problems for the circular member. Traditionally, repair of the cracked pipe system can be done by replacing the entire cracked pipe, by rewelding the cracked section, or by repairing with a welded steel patch (Figure 8.21). However, in most instances, fatigue cracks reappear in the weld fill areas when the traditional weld repair method is employed. The application of composite materials is considered as one of the possible alternative repair methods for repairing heavy steel equipment such as the boom members of draglines, circular pipe, and other forms of circular members of steel structures. A number of researches in the past decade showed that the application of composite materials on repairing cracked steel pipe is effective. Duell et al. (2008) carried out experimental and numerical studies on the application of carbon composite overwrap pipeline with machined flaws. Carbon composite was wrapped around the flawed area of the pipeline and the repaired pipeline was tested by pressurizing the test specimen with an air actuated, hydraulic power unit. It was found that the repaired pipeline failed with an internal pressure which is 50% more than that for an unrepaired pipeline. Alexander and Ochoa (2010) studied the application of a composite reinforcing method to repair the offshore risers by developing integrated analytical and experimental methods.

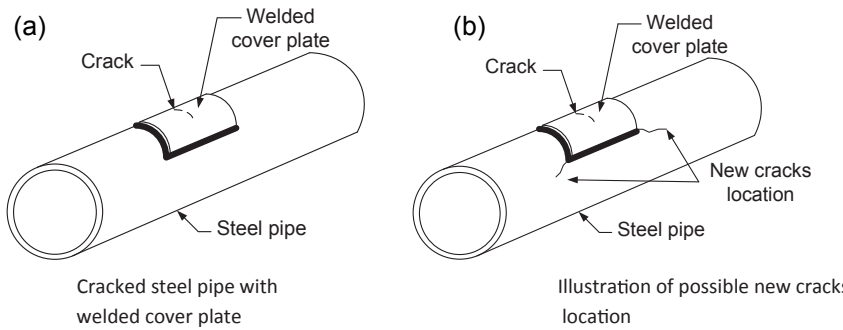

Figure 8.21 Illustration of cracked steel pipe with welded cover plate.

Full-scale pipe members with bonded carbon/epoxy shells were tested under (1) pressure only loading, (2) tension with constant pressure loading, and (3) bending with both pressure and tension held constant loading. Test results showed that the maximum strain can be reduced below the design level with the presence of the composite reinforcement. Kim and Harries (2011) carried out a study on the fatigue behavior of damaged steel beams repaired with CFRP strips. Four notched steel beams were repaired by bonding CFRP strips and tested under cyclic loading with different stress ranges. It was shown that the fatigue life of the repaired beam was significantly influenced by the stress range. However, there is no direct comparison of the fatigue life of nonrepaired beam and repaired beam. Moreover, the reduction of SIF of crack tip was not studied in their research. In general, the application of composite materials for repairing defected pipe can be in two major forms: (1) flexible wet lay-up form and (2) procured layered form. Due to the difference in geometry of the plate type and the tube type members, the effect of single-side patching on the reduction of SIF may be different. In the following section, the finite element model and analysis of cracked circular pipe with FRP patching are presented and the efficiency of the repair is discussed.

8.4.2 FE model of cracked pipe with FRP patching

For the finite element model, the thickness of the steel tube was taken as 9.5 mm and the outside diameter of the steel tube was taken as 400 mm. The total length of the steel tube was taken as 4000 mm with a circumferential through-wall crack located at the midspan. The initial half circumferential through-wall crack length was 25.4 mm, and the final crack length was 63.5 mm. The initial half crack length, the final half crack length, and the dimensions of patching were taken as the same as those used in previous finite element models of cracked steel plates with CFRP patching. The cross-section dimension and an illustration of the circumferential through-wall crack are shown in Figure 8.22. Due to symmetry, only a quadrant of the steel tube was modeled. The modified three layers model technique, which was used in Section 8.2.2 for modeling the cracked steel plate with CFRP patching, was adopted for modeling the cracked steel circular tube with CFRP patching. As in the previous model, the cracked steel tube was modeled by 3-D brick elements (C3D20, 20 node brick element in ABAQUS), and the adhesive and CFRP patching were modeled using shell elements (S8R, eight node general purpose shell element in ABAQUS). At the location of the crack tip, 3-D collapsed node elements were used and the SIF around the crack tip was obtained using the contour integral method. A typical finite element model of the cracked steel tube is shown in Figure 8.22. Symmetrical boundary conditions were assigned at the symmetrical plane along the longitudinal and circumferential direction and a uniform axial stress of 100 MPa was assigned at the far end of the steel tube.

In the previous finite element parametric study of cracked steel plate with CFRP patching, the material properties of the 1.2-mm-thick CFRP plate (Sika, 2003) were assigned for the CFRP patching. In order to compare results of the plate model and the tube model, the same material properties of the CFRP plate were assigned for

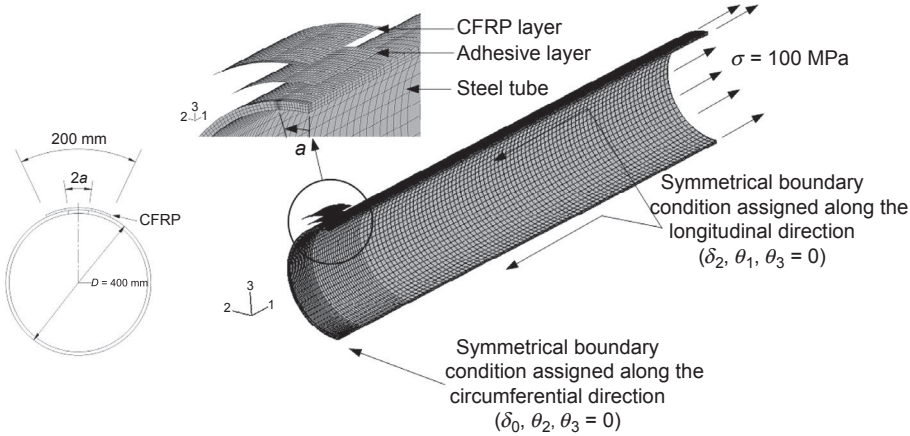

Figure 8.22 Illustration of the finite element model of circumferential through-wall cracked steel pipe.

the cracked steel tube model with CFRP patching. The material properties of steel, CFRP plate and the corresponding adhesive are listed in Table 8.7. The number of layers assigned for the CFRP plate was three. Therefore, the total thickness of CFRP plate was 3.6 mm, and the corresponding adherend stiffness ratio of steel to CFRP (ETR) was 0.33. The corresponding thickness of the adhesive was 0.5 mm.

The finite element results of the SIF of cracked steel circular tube structure without FRP patching were compared to the prediction proposed by Lacire et al. (1999). According to Lacire et al. (1999), the SIF for a circumferential through-wall crack in a

Table 8.7 Material properties of steel, adhesive, and CFRP of tube model

Steel tube	Elastic modulus	E_s	200,000 MPa
	Poisson's ratio	ν_s	0.3
CFRP plate composite	Longitudinal elastic modulus	E_{frp1}	175,000 MPa
	Transverse elastic modulus	E_{frp2}	9000 MPa
	Poisson's ratio	ν_{frp}	0.28
	Shear modulus	G_{frp}	4500 MPa
Adhesive for CFRP plate	Elastic modulus	E_a	4500 MPa
	Poisson's ration	ν_a	0.34
	Shear modulus	G_a	1680 MPa

pipe under axial load and bending moment can be expressed by the following equations:

$$K_I = (F_t\sigma_t + F_b\sigma_b)\sqrt{\pi R_m \theta} \tag{8.27}$$

where K_I is the SIF; F_t and F_b are the corresponding geometrical factors which represent the normalized SIF; R_m is the mean radius of the pipe; θ is half of the circumferential angle of crack (Figure 8.22); and σ_t and σ_b are the applied tensile and bending stresses calculated by:

$$\sigma_t = \frac{P}{2\pi R_m t} \quad \text{and} \quad \sigma_b = \frac{M}{\pi R_m^2 t} \tag{8.28 a,b}$$

where P is the applied axial force; M is the applied bending moment; and t is the wall thickness of the tube. The geometrical factors for axial load (F_t) and bending moment (F_b) are calculated by the following equations:

Geometrical factor for axial load:

$$F_t = \left[A_t + B_t\left(\frac{\theta}{\pi}\right) + C_t\left(\frac{\theta}{\pi}\right)^2 + D_t\left(\frac{\theta}{\pi}\right)^3 + E_t\left(\frac{\theta}{\pi}\right)^4\right] \tag{8.29}$$

where

$$\begin{aligned}
A_t &= 1\\
B_t &= -1.040 - 3.1831\xi - 4.83\xi^2 - 2.369\xi^3\\
C_t &= 16.71 + 23.10\xi + 50.82\xi^2 + 18.02\xi^3\\
D_t &= -25.85 - 12.05\xi - 87.24\xi^2 - 30.39\xi^3\\
E_t &= 24.70 - 54.18\xi + 18.09\xi^2 + 6.745\xi^3\\
\xi &= \log\left(\tfrac{t}{R_m}\right)
\end{aligned}$$

Geometrical factor for bending moment:

$$F_b = \left(1 + \frac{t}{2R_m}\right)\left[A_b + B_b\left(\frac{\theta}{\pi}\right) + C_b\left(\frac{\theta}{\pi}\right)^2 + D_b\left(\frac{\theta}{\pi}\right)^3 + E_b\left(\frac{\theta}{\pi}\right)^4\right] \tag{8.30}$$

where

$$\begin{aligned}
A_b &= 0.65133 - 0.5774\xi - 0.3427\xi^2 - 0.0681\xi^3\\
B_b &= 1.879 + 4.795\xi + 2.343\xi^2 - 0.6197\xi^3\\
C_b &= -9.779 - 38.14\xi - 6.611\xi^2 + 3.972\xi^3\\
D_b &= 34.36 + 129.9\xi + 50.55\xi^2 + 3.374\xi^3\\
E_b &= -30.82 - 147.6\xi - 78.38\xi^2 - 15.54\xi^3\\
\xi &= \log\left(\tfrac{t}{R_m}\right)
\end{aligned}$$

The applicable range of the above equations is $1.5 < R_m/t < 80.5$ and $0 < \theta/\pi < 0.611$.

8.4.3 Reduction of SIF of cracked steel circular pipe with FRP patching

For the finite element model, since only axial stress was assigned, based on Eqn (8.27), the normalized SIF is predicted by the following equation:

$$\frac{K_I}{\sigma_t} = F_t\sqrt{\pi R_m \theta} \tag{8.31}$$

By assigning four different circumferential half crack lengths, a, equal to 25.4, 38.1, 50.8, and 63.5 mm, finite element models of a cracked steel circular tube with and without CFRP patching were formed and analyzed. As the mean radius of the tube is 195.25 mm, the corresponding R_m/t value is 20.55 and the θ/π values for the four circumferential crack lengths ($a = 25.4$, 38.1, 50.8, and 63.5 mm) are 0.042, 0.064, 0.085, and 0.106, respectively. These are within the applicable range of the equations proposed by Lacire et al. (1999). The finite element results of the normalized SIF and the results obtained by Lacire et al. (1999) are shown in Figure 8.23. As shown in the figure, the finite element results are generally in good agreement with the prediction of Lacire et al. (1999). Since 3-D brick elements were used for modeling the cracked circular tube, variation of the SIF across the thickness along the crack tip was obtained in the finite element analysis while the equations proposed by Lacire et al. (1999) did not reflect this variation.

Comparisons of the normalized SIF of a cracked tube of different crack lengths with and without CFRP plate patching are shown in Figure 8.23. For the tubes with CFRP

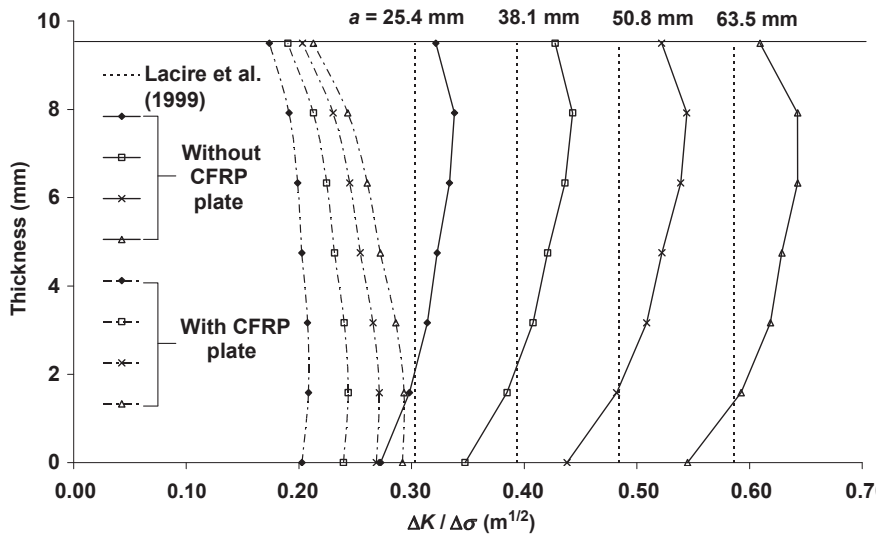

Figure 8.23 Comparison of FE results of normalized SIF of cracked steel circular tube with and without CFRP plate patching for various circumferential half crack lengths.

plate patching, it is shown that the normalized SIF values of the patched side of the tube with different crack lengths are all smaller than the SIF values of the tubes without CFRP patching when the crack length was equal to 25.4 mm. A plot of the normalized SIF versus crack length is shown in Figure 8.24. It is shown that for the tube without CFRP patching, the SIF increases significantly when the crack length increases. On the other hand, for the tube with CFRP patching, the increase of SIF is not as significant as the models without CFRP patching, especially for the patched side.

The COD of two cracked circular tubes (one without patching and one with CFRP plate patching) with a half crack length of 63.5 mm is shown in Figure 8.25 (magnitude of displacement was magnified by 1000 times). Due to the presence of the crack only on one side of the tube, the section stiffness became nonsymmetric about the out-of-plane axis (2-axis in the figure). This change of section stiffness causes the crack opening to displace not only along the longitudinal direction (the 1-axis), but also in the transverse direction (the 3-axis), as shown in Figure 8.25(a). With the presence of the CFRP patching on the cracked region, part of the reduced stiffness of the tube was recovered and the COD was observed only along the longitudinal direction (the 1-axis), as shown in Figure 8.25(b). Numerical values of the longitudinal CODs of tubes with and without CFRP plate patching (crack length equal to 25.4 and 63.5 mm) are shown in Figure 8.26. As shown in the figure, even for the cracked tube with a crack length of 63.5 mm, the maximum longitudinal COD of tubes with CFRP plate patching is less than that of the cracked tube without CFRP patching and the crack length of 25.4 mm. Therefore, a significant reduction of the COD could be obtained by applying CFRP patching on the crack region of circular tube structure.

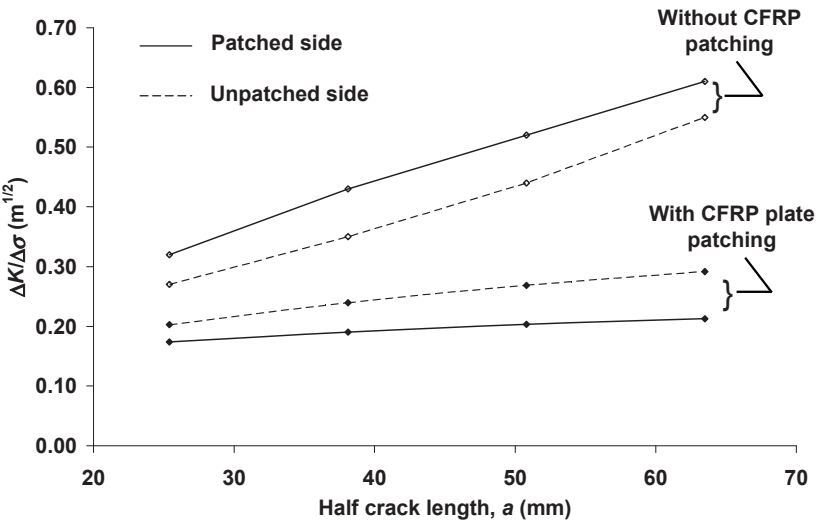

Figure 8.24 The normalized SIFs of cracked steel circular tube with and without CFRP plate patching versus half crack lengths.

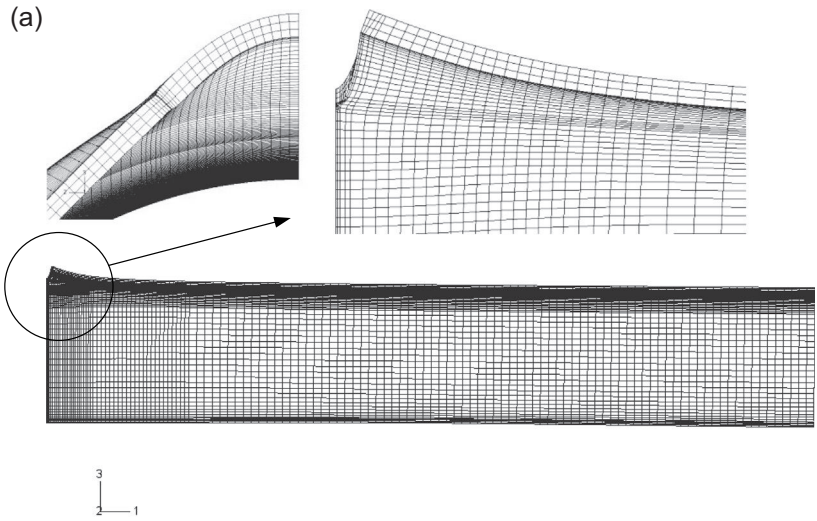

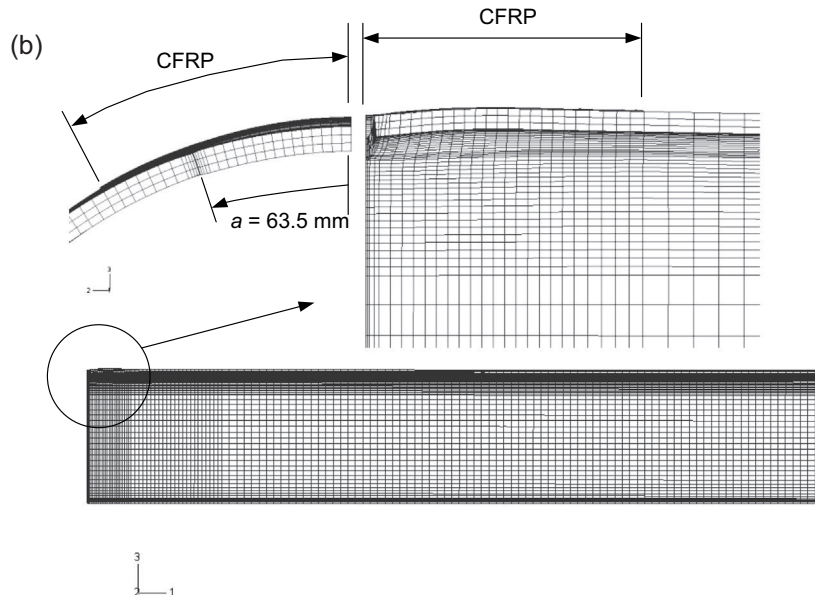

Figure 8.25 Comparison of crack opening displacement of cracked steel circular tube with and without CFRP plate patching.

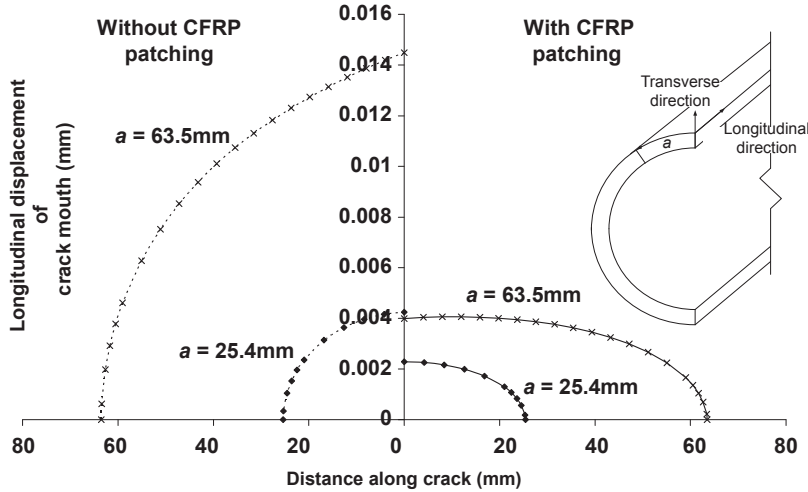

Figure 8.26 Longitudinal crack opening displacement of models with and without CFRP plate patching (half crack lengths of 25.4 and 63.5 mm).

8.4.4 Implications on field repair

In the previous sections, some of the researches about using FRP patching on strengthening and rehabilitating cracked steel members were discussed. The application of the FRP patching can provide additional constraint to reduce the crack opening, as well as to share part of the loading through the noncracked part. As a result, the SIF at the crack tip can be reduced. The reduction of the SIF at the crack tip for the member with FRP patching can be obtained numerically by means of FEM. Detail modeling procedures and the effects of different parameters on the reduction of the SIF are presented and discussed as well. As the fatigue life of a cracked member depends very much on the value of the SIF at crack tip, a significant reduction of the SIF at crack tip implied that the fatigue life of the cracked member can be extended. In the following section, the application of FRP patching for field repair is briefly discussed.

Application of FRP patching can be used in several field repairs, such as corrosion repair of steel pipe, strengthening the welded region of steel pipe, and repair of cracked steel pipe. Some piping systems that are exposed to harsh environments may experience serious corrosion problems. As a result, the wall thickness of the pipe may be reduced significantly. For this case, FRP patching can be applied to the corroded pipe to recover or even strengthen the stiffness of the pipe. Uniaxial fiber can be applied along the longitudinal direction for strengthening the axial stiffness of the pipe. Meanwhile, the uniaxial fiber can be applied in the hoop direction at the end of the longitudinal FRP patching in order to provide enough constraints for anchoring the FRP patching. Seica and Packer (2007) carried out experimental studies to investigate FRP materials for the rehabilitation of tubular steel members for underwater applications. Two different types of FRP materials were used in their studies. They

concluded that in general, the ultimate bending strength, flexural stiffness, and rotation capacity of tubular steel members with FRP wrapping can be increased. In their studies, it is shown that the ultimate strength of the tubular steel members with FRP wrapping and cured in air was increased by 16% and 27% relative to the bare steel member. The corresponding flexural stiffness was increased by 7% and 18%.

Traditionally, a cracked steel member can be repaired by gouging and welding at the location of crack or by welding a cover plate over the cracked region to bypass the loading. However, additional weight will be added to the structure by the welding of cover plate and fatigue crack will appear again at the location of the reweld as well. Application of FRP patching is an alternative method for fatigue crack repair of steel structures. An illustration of the FRP patching for fatigue crack repair of steel pipe is shown in Figure 8.27. Before the FRP is applied to the steel pipe, surface grinding or sandblasting should be done in order to remove all rust or paint on the surface to be repaired. Then, adhesion primer or conditioner should be applied to the steel surface for improving the long-term durability. The composite fiber is applied using a hand lay-up procedure after applying a two-part epoxy compound to the steel. This sequence is repeated until the desired patch thickness is reached. The FRP patching should be cured for a sufficient time before loading is applied to the repaired member. It is recommended that the patch width should be at least two times the crack length and additional protection of the FRP patching should be provided for protecting the patching from harsh environments. Lee et al. (2002) presented a repair method of repairing underground buried pipes with resin transfer molding. The repair method is summarized into five major steps: (1) removing deposits and protrusions in the pipe, (2) pulling the reinforcement by connecting it to a rope, (3) closing two covers at both ends of reinforcement, (4) injecting the resin to the composite, and (5) resin wetting and curing. Compression tests of the reinforcement made by their proposed method were carried out, and it was found that the compressive load capability of the reinforced pipe increased by 15%.

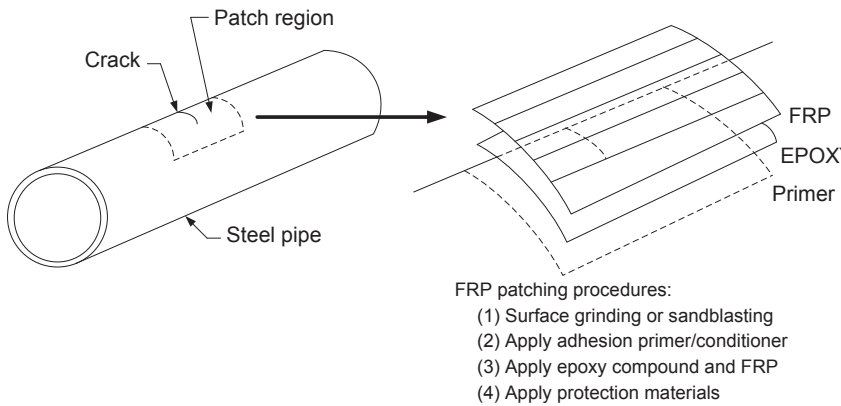

Figure 8.27 Illustration of the FRP patching for fatigue crack repair of steel pipe.

8.5 Summary and conclusions

Composite fiber patching techniques are being considered as alternatives to traditional methods of strengthening and fatigue crack repair in steel structures due to the growing use of FRP composite materials to different engineering structures. The behavior of cracks in a structure is strongly dependent on the state of stress at the crack tip and the ability of the material to resist propagation. One of the important parameters that relates to fatigue crack growth is the SIF at the crack tip. It is believed that the presence of the FRP patching at the crack tip can reduce the stress in the uncracked plate at the prospective location of the crack and can restrain the opening of the crack as well. As a result, the SIF at the crack tip can be reduced and the fatigue life of the member can be extended. One of the methods for predicting the SIF of a cracked member is by means of FEM. In this chapter, finite element models were developed to study the reduction of the SIF of cracked steel plates with single-side CFRP patching. Two types of finite element models—the three layers finite element model (Naboulsi and Mall, 1996) which used shell elements to model the cracked steel plates, the adhesive, and the CFRP patching and a modified three layers finite element model proposed in this study which used shell elements to model the adhesive and the CFRP patching and brick elements to model the cracked steel plates—were studied, and the results of the SIFs obtained from these two finite element models were compared. It should be noted that a linear relationship of SIF through the plate thickness was assumed in the three layers model, whereas the SIF through the thickness of the plate of the modified three layers model could be obtained numerically since 3-D brick elements were used to model the cracked steel plate. The SIF results obtained from the three layers model and the modified three layers model showed that the three layers model overestimated the SIF on the patched side and underestimated the SIF on the unpatched side. Based on the results of the modified three layers finite element model, it is shown that the SIF was reduced significantly on the patched side and the SIF values varied through the thickness of the cracked steel plate with single-side CFRP patching. The modified three layers finite element models were adopted to analyze the effect of single-side CFRP patching of cracked steel plates on the variation of the SIF across the thickness of the crack tip at different stages of crack propagation. The numerical procedure of crack propagation from Lee and Lee (2004) was applied in updating the crack tip shape and the corresponding SIF. Based on the finite element results of the SIF, equations of the correction factor which considered the crack pattern and patching pattern were predicted for models with different forms of crack pattern and patching pattern.

A finite element study of the reduction of SIF of cracked steel circular tube repaired by CFRP patching is also presented in this chapter. The cracked steel circular tube was modeled using 3-D brick elements and the adhesive and CFRP patching were modeled by using shell elements. In order to verify the finite element results of the cracked steel circular tube without CFRP patching, the SIFs of models with half circumferential crack lengths of 25.4, 38.1, 50.8, and 63.5 mm were compared with the predictions proposed by Lacire et al. (1999). It was shown that the finite element results compared

well with the prediction of Lacire et al. (1999) for the unrepaired circular tube. For the tubes with CFRP patching, it was shown that the normalized SIF values of the patched side of the tube with different crack lengths were all smaller than the SIF values of the tubes without CFRP patching when the crack length was equal to 25.4 mm. As the SIF is reduced significantly for the member with CFRP patching, it is believed that the corresponding fatigue life can be extended.

References

ACI 440R-96, 1996. State-of-the Art Report on Fiber Reinforced Plastic (FRP) Reinforcement for Concrete Structures. American Concrete Institute (ACI) Committee 440, Farmington Hills, MI.

Alexander, C., Ochoa, O.O., 2010. Extending onshore pipeline repair to offshore steel risers with carbon-fiber reinforced composites. Composite Structures 92, 499−507.

American Association of State Highway and Transportation Officials (AASHTO), 2000. Standard Specifications for Highway Bridges, sixteenth ed., Washington, DC.

Barson, J.M., Rolfe, S.T., 1999. Fracture and fatigue control in structures. ASTM Manual Series: MNL 41, 213.

Barsoum, R.S., 1976. On the use of isoparametric finite elements in linear fracture mechanics. International Journal for Numerical Methods in Engineering 10, 25−37.

Bassetti, A., Colombi, P., Nussbaumer, A., 2000a. Finite element analysis of steel members repaired by prestressed composite patch. In: IGF 2000, XV Congresso Nazionale Del Gruppo Italiano Frattura, Bari.

Bassetti, A., Nussbaumer, A., Colombi, P., 2000b. Repair of riveted bridge members damaged by fatigue using CFRP materials. In: Advanced FRP Materials for Civil Structures, Bologna, Italy, 19th October 2000, pp. 33−42.

Chue, C.H., Chang, L.C., Tsai, J.S., 1994. Bonded repair of a plate with inclined central crack under biaxial loading. Composite Structure 28 (1), 39−45.

Colombi, P., Bassetti, A., Nussbaumer, A., 2003a. Crack growth induced delamination on steel members reinforced by prestressed composite patch. Fatigue and Fracture of Engineering Materials and Structures 26, 429−437.

Colombi, P., Bassetti, A., Nussbaumer, A., 2003b. Delamination effects on cracked steel members reinforced by prestressed composite patch. Theoretical and Applied Fracture Mechanics 39, 61−71.

Colombi, P., Bassetti, A., Nussbaumer, A., 2003c. Analysis of cracked steel members reinforced by pre-stress composite patch. Fatigue and Fracture Engineering of Materials and Structures 26, 59−66.

Canada, I.S.I.S., 2001. Reinforcing Concrete Structures with Fiber Reinforced Polymers, Manual No. 3. ISIS Canada Corporation, Winnipeg, Canada.

Deniaud, C., Cheng, J.J.R., 2000. Behaviour of Reinforced Concrete Beams Strengthened in Shear. Structural Engineering Report No. 234. University of Alberta, Department of Civil & Environmental Engineering.

Duell, J.M., Wilson, J.M., Kessler, M.R., 2008. Analysis of a carbon composite overwrap pipeline repair system. International Journal of Pressure Vessels and Piping 85, 782−788.

Gross, B., Srawley, J.E., 1964. Stress Intensity Factors for a Single Notch Tension Specimen by Boundary Collocation of a Stress Function. NASA TN D-2395.

Hibbitt, Karlsson, Sorenson, Inc., 2004. ABAQUS Version 6.4-1, ABAQUS/Standard User's Manual Volumes I and II. Pawtucket, RI.

Irwin, G.R., 1957. Analysis of stresses and strains near the end of a crack transverse plate. Journal of Apply Mechanics 24, 361.

Jones, S.C., Civjan, S.A., 2003. Application of fiber reinforced polymer overlays to extend steel fatigue life. Journal of Composites for Construction 7 (4), 331−338.

Karbhari, V.M., Seible, F., 2000. Fiber reinforced composites—advanced materials for the renewal of civil infrastructure. Applied Composite Materials 7, 95−124.

Kaw, A.K., 1997. Mechanics of Composite Materials. CRC Press.

Kennedy, G.D., Cheng, J.J.R., 1998. Repair of Cracked Steel Elements Using Composite Fiber Patching. Structural Engineering Report No. 221. University of Alberta, Department of Civil & Environmental Engineering.

Kim, Y.J., Harries, K.A., 2011. Fatigue behaviour of damaged steel beams repaired with CFRP strips. Engineering Structures 33, 1491−1502.

Kou, K.P., Burdekin, F.M., 2008. Stress intensity factors for a wide range of long-deep semi-elliptical surface cracks, partly through-wall cracks and fully through-wall cracks in tubular members. Engineering Fracture Mechanics 73 (12), 1693−1710.

Lacire, M.H., Chapuliot, S., Marie, S., 1999. Stress intensity factors of through wall cracks in plates and tubes with circumferential cracks. ASME PVP 388, 13−21.

Lee, D.G., Chin, W.S., Kwon, J.W., Yoo, A.K., 2002. Repair of underground buried pipes with resin transfer molding. Composite Structures 57, 67−77.

Lee, W.-Y., Lee, J.-J., 2004. Successive 3D FE analysis technique for characterization of fatigue crack growth behavior in composite-repaired aluminum plate. Composite Structures 66, 513−520.

Meier, U., 1992. Carbon fiber-reinforced polymers: modern materials in bridge engineering. Structural Engineering International 1 (12), 7−12.

Meier, U., Deuring, M., Meier, H., Schwegler, G., 1993. CFRP Bonded Sheets, Fiber-reinforce-plastic (FRP) Reinforcement for Concrete Structures: Properties and Applications. Elsevier Science, Amsterdam, The Netherlands.

Mitsubishi Chemical Co, 1999. Carbon Fiber Prepreg Sheet (Replark™). Available from http://www.m-kagaku.co.jp/english/aboutmcc/division/prod/carbonfiber/r-products.htm.

Naboulsi, S., Mall, S., 1996. Modeling of a cracked metallic structure with bonded composite patch using the three layer technique. Composite Structures 35, 295−308.

Paris, P.C., Erdogan, F., 1960. A critical analysis of crack propagation laws'. Journal of Basic Engineering 85, 528−534.

Roberts P.D., 1995. Crack Growth Retardation by Carbon Fiber Composite Patching: An Application to Steel Pressure Vessel Repair (Master of Science thesis). University of Alberta, Department of Mechanical Engineering.

Rose, L.R.F., 1982. A cracked plate repaired by bonded reinforcements. International Journal of Fracture 18 (2), 135−144.

Seica, M.V., Packer, J.A., 2007. FRP materials for the rehabilitation of tubular steel structures, for underwater applications. Composite Structures 80, 440−450.

Sika Carbodu Technical Data Sheet, 2003. Sika Canada Inc. Available from http://www.sika.ca/con-tds-sikacarbodur-ca.pdf.

Sun, C.T., Klug, J., Arendt, C., 1996. Analysis of cracked aluminum plates repaired by bonded composite patches. AIAA Journal 34 (2), 369−374.

Tada, H., Paris, P.C., Irwin, G.R., 1985. The Stress Analysis of Cracks Handbook, second ed. Paris Productions, Inc., St. Louis.

Tavakkolizadeh, M., Saadatmanesh, H., 2003. Fatigue strength of steel girders strengthened with carbon fiber reinforced polymer patch. Journal of Structural Engineering 129 (2), 186−196.

Teng, J.G., Lam, L., Chen, J.F., 2004. Shear strengthening of RC beams with FRP composites. Processing of Structural Engineering Materials 6, 173−184.

Timoshenko, S., Woinowsky-Kriege, S., 1959. Theory of Plates and Shells. McGraw-Hill Publishing Co.

Yukio, T., 2002. Evaluation of leak-before-break assessment methodology for pipes with a circumferential through-wall crack. Part I: stress intensity factor and limit load solutions. International Journal of Pressure Vessels and Piping 79 (6), 385−392.

This page intentionally left blank

Finite element analysis (FEA) modelling of fiber-reinforced polymer (FRP) repair in offshore risers

9

P.H. Chan[1], *K.Y. Tshai*[1], *M. Johnson*[2], *S. Li*[2]
[1]University of Nottingham, Semenyih, Malaysia; [2]University of Nottingham, Nottingham, UK

9.1 Introduction

Risers in offshore operations are subjected to corrosion during their service life cycle. The use of relatively inexpensive, high strength to weight ratio fiber-reinforced polymer composite (FRPC) as a load bearing pipe repair sleeve is an emerging technology that is becoming common for offshore applications. Risers experience complex loading profiles and experimental investigations often incur substantial time, complicated instrumentation, and setup costs. Using finite element analysis (FEA) code, the characteristics of FRPC repair on risers subjected to different types of operational and environmental loadings can be studied to support the design of a repair in accordance with various governing riser design standards. A high precision finite element model is capable of capturing the stress−strain behavior of the composite repair system (CRS).

This chapter will first outline the conventional offshore riser repair techniques and their limitations which, in turn, provide the motivation for adoption of composite repair. A brief discussion about the application of FRPC in pipeline repair, its limitations, current practices, and material types will be given. A subsequent section provides information on the industrial design and safety standards used in designing and assessing the performance of offshore risers, corroded pipelines, and pipelines repaired with FRPC. The typical loading conditions of an offshore riser are also discussed so that the requirements of CRS can be understood.

Detailed description of the modelling of risers repaired with FRPC is presented, where assumptions and significant input properties are explained. Results and discussion on FEA of the CRS subjected to typical load cases sustained by an operating riser are given. The effects of varying design parameters in the CRS are presented.

The chapter concludes with the positive viability of using FEA to model the CRS. Future trends on the application of FRPC in repairing offshore risers such as optimization, automation, and possible studies are summarized.

Rehabilitation of Pipelines Using Fiber-reinforced Polymer (FRP) Composites. http://dx.doi.org/10.1016/B978-0-85709-684-5.00009-6

9.2 Background

9.2.1 Conventional offshore riser repairs and their limitations

Risers are critical components in offshore operations as they are the only links between the seabed and the surface, whether for drilling or production. A riser is a long, slender, vertical cylindrical pipe placed at or near the sea surface and extending to the ocean floor (Chakrabarti and Frampton, 1982). Risers are subjected to various types of loading, including fatigue that can cause mechanical damage. Being submerged under water, risers are also exposed to a salt water environment which can induce external corrosion on the surface, hence degrading their performance. Depending on the function of the riser, it can also be subjected to attack from corrosive substances inside the pipe.

In order to maintain safe operations as well as prolonging the lifespan of risers, repair techniques applicable to offshore risers have been available. An obsolete repair technique involves bringing the corroded section of the riser to the surface where conventional onshore repair techniques or replacement of parts can be done (Webb, 1981). This method is the least favorable as production needs to be halted, causing major inventory losses. An alternative repair technique employs a cofferdam to be temporarily installed around the riser to provide a dry and safe area for carrying out normal weld-repair. However, this method is limited to shallow depths where damage on the pipe is near to the water surface (Tiratsoo, 2003). Small damage such as pinhole leaks can be mended by a steel clamp that is welded to the riser and becomes a permanent part of the riser system. For risers that are dangerously weakened, a sleeve can be bolted or welded around the riser. The annular gap is then filled with a grout material such as epoxy that serves to transfer the hoop load to the sleeve (Palmer and King, 2008).

The repair techniques mentioned above necessitate the mobilization of heavy steel clamps and application of hyperbaric welding. Such procedures are not only expensive but also pose numerous safety issues such as underwater explosion, electric shock, and accumulation of nitrogen diffused into the bloodstream of the welder.

9.2.2 Direction of the industry: CRS

In recent years, oil reserves have been discovered at great depths. A report by the US Minerals Management Service (the federal agency responsible for offshore leases and oil activities) stated that 12 deepwater discoveries were made in the Gulf of Mexico alone in 2003, three of which were at a depth greater than 2500 m (Ochoa and Salama, 2005). At such depth, it is apparent that there is a need for economical and simplified maintenance methods of the offshore facilities, including riser repair. To address these matters, in situ riser repair using composite materials has emerged as an attractive option to the industry as it is capable of ensuring the safety of the underwater installer and minimizing the cost in terms of time and production loss. Such materials offer appealing attributes such as high specific strength and specific stiffness (hence they

are lightweight), good corrosion resistance, superior thermal insulation, no need for welding, simple installation, lower cost and the elimination of having to shut down the pipeline (Ochoa and Salama, 2005; Patrick, 2004). Attempts to extend onshore pipeline repair techniques to offshore steel risers were carried out by Alexander and Ochoa (2010). In their work, a full-scale test of internal pressure (P_{in}), tensile load (F_t), and bending load (M_b) was conducted on a 219 mm diameter, 10.3-mm-thick grade X46 steel pipe with a 50% loss in thickness being machined onto the pipe surface. The main repair entailed attaching a pair of precured carbon half cylinders, which provided an effective solution.

9.2.3 Limitations of the application of composite repair for offshore risers

For the past 10 years, the use of composite materials in repairing onshore pipelines has been investigated extensively and improved and is now generally accepted as one of the principal repair techniques (Alexander, 2006; Patrick, 2004). However, the application of this technology in repairing offshore risers has not been validated technically. There are two main barriers that hinder the establishment of this technology: the lack of data regarding long-term damage mechanisms for material life prediction and in-service integrity monitoring (Ochoa and Salama, 2005). Due to the nature of the composite material, where a wide variety of reinforcement and matrix combinations are available along with the existence of different manufacturing parameters such as lay-up pattern and tension, fiber volume fraction, cure pressure and temperature profiles, uncertainties are present regarding the application of a composite repair.

Although composite materials are used widely in the aerospace and automotive industries, there are still no standardized tests for accelerated "aging" under given constraints or appropriate life prediction of the materials. Another consideration in repairing offshore risers using composite material is the interface between the composite and the steel riser. For successful load transfer from the steel riser to the composite reinforcement, adequate bonding must be established at the interface. There have been multiple studies on the bond strength between steel and FRPC, particularly in patch repair, but there is still a lack of measured data considering its application in pipes and risers (i.e., sleeve repair). There are no definite studies on the fatigue bond strength between steel and FRPC subjected to combined loadings.

9.3 Composite riser repair and relevant standards

Composite repairs have been utilized in onshore transmission pipelines for the past decade. These repairs are used on pipe sections that have been weakened due to corrosion and mechanical damage. A survey conducted by the US Department of Transportation showed that the overall costs can be reduced by 24% using composite repair instead of welded pipe sleeves. Compared to replacement of the whole defective pipe section, the cost has been reduced by approximately 73% (RSPA, 2000).

9.3.1 Types of composite repair

The two main categories of composite repairs are wet lay-up systems (in situ composites) and precured sleeve systems. Wet lay-up systems involve the use of on-site wetted or preimpregnated (i.e., prepreg) laminates where final curing of the composites takes place at the repair site. Precured sleeve systems use premanufactured and quality controlled laminate repair sleeves (i.e., precured half cylinder) which are sized for the specific pipe diameter (Rehberg et al., 2010; Patrick, 2010). Wet lay-up systems have the advantage of flexibility where they can be applied to pipes with varying non-straight geometries and diameters. Precured sleeves can only be fabricated for a designated pipe diameter of straight geometry.

9.3.2 Types of materials

The difference in materials used in CRS is in their fiber reinforcement. The two main types of fiber reinforcement used in the CRS are carbon fiber and glass fiber. The first widely used CRS for onshore pipelines was designed by Clock Spring, Inc. in the 1980s. This repair system utilizes E-glass/Polyester laminate with a methacrylate adhesive that bonds the precured composite layers (Fawley, 1994). AquaWrap® introduced a wet lay-up CRS consisting of a water-activated prepreg that is installed over the damaged area (Alexander, 2005). There are various other products developed by AquaWrap® that utilize both glass fiber and carbon fiber, finished in the form of woven and stitched fabrics (Air Logistics, 2006). Diomandwrap® is a premier carbon wrap system developed by Citadel Technologies, Inc. The wrap used in this repair system is a bidirectional carbon fiber woven fabric which can provide reinforcement in the hoop and axial directions (Citadel Technologies, 2011).

In general, carbon fiber is superior in terms of strength and stiffness over glass fiber, while glass fiber has a cheaper raw material cost. Use of carbon fiber is more expensive but can be justified by its high stiffness, in particular. High stiffness of the repair ensures that the CRS supports a high proportion of the load applied to the damaged pipe. However, a drawback of carbon fiber in direct contact with a steel surface is the initiation of galvanic corrosion, especially in the presence of an electrolyte such as seawater, which accelerates the process. Thus any direct contact should be avoided in CRS (Tavakkolizadeh and Saadatmanesh, 2001). In order for glass fiber composites to take a similar share of the load to that of carbon fiber composites, a significantly thicker repair section is required which has the implication on weight and installation of the repair. Alternatively, prestressing the glass fiber in tension increases the load distribution on the repair material. This would raise the demand on the installation of the repair.

9.3.3 Standards and guidelines

For any pipeline repair system to be applicable in the industry, it must fulfil the requirements set by the relevant governing bodies. This includes the American Society of Mechanical Engineers (ASME), American Petroleum Institute (API), International Organization for Standardization (ISO), and Det Norske Veritas (DNV).

9.3.3.1 Standards for pipeline design

ASME B31.4 (2006) Pipeline Transportation for Hydrocarbon Liquid and Other Liquids and ASME B31.8 (2003) Gas Transmission and Distribution Piping System are standards related to the design of pipelines which provide information on the stress and strain limits of industrial oil and gas pipelines. Although not specifically intended for offshore risers, these standards provide a good foundation for pipeline design that in turn defines the requirements on the repair using FRPC materials.

9.3.3.2 Standards for riser design

Offshore risers design is more complicated than onshore pipelines due to additional stresses, fatigue and harsh environments. The API RP 2RD (1998) Design of Risers for Floating Production Systems and Tension-Leg Platforms (TLPs), API RP 1111 (1999) Design, Construction, Operation and Maintenance of Offshore Hydrocarbon Pipelines (Limit State Design), DNV-OS-F201 (2010) Dynamic Risers and ABS (2008) Guide for Building and Classing Subsea Riser Systems provide a better insight into the design of risers.

9.3.3.3 Standards for pipeline and riser repair

For the design of a CRS, the thickness of the repair (i.e., layers of laminate needed) is dependent on the additional strength that a corroded or mechanically damaged riser requires. ASME B31G (1991) Method for Determining the Remaining Strength of Corroded Pipelines and DNV-RP-F101 (2010) Corroded Pipelines are standards that provide guidelines to assess the condition of corroded pipelines. Once the corroded pipelines are proven to be nonfunctional or approaching failure, the ASME PCC-2 (2008) Repair of Pressure Equipment and Piping, Article 4.1, Non-Metallic Composite Repair Systems for Pipelines and Pipework: High Risk Application, the ISO/TS 24817 (2006) Composite Repairs for Pipework and the DNV-RP-F113 (2007) Pipeline Subsea Repair can be employed to determine the required properties and parameters of the composite repair.

9.4 Loading conditions of a riser

Owing to the nature of a riser being submerged in deep water in an approximately vertical position, its loading conditions are more complicated than onshore pipelines. In the design of a riser, the different loads can be categorized into functional loads, environmental loads, installation loads and accidental loads.

9.4.1 Functional loads

Functional loads are the loads that the riser has to sustain during its operation. One of the major functional loads of a riser is internal pressure, which arises from the fluid content being transported by the riser itself. Two internal pressure conditions must

be considered in riser design: the burst pressure, P_b, and the design pressure, P_d. The burst pressure, also known as the test pressure, is the pressure at which total failure of the pipe occurs and the internal fluid is no longer contained. The design pressure, also known as the maximum allowable operating pressure, is the maximum pressure at which a riser system may be operated in accordance with the provisions of the design code. Besides the internal pressure, a near constant tension is applied to the riser to avoid buckling and excessive bending stress due to platform motion, wave and current forces, and vortex induced vibration (VIV) (Stanton, 2006). The magnitude of this tension depends on the weight of the riser, buoyancy modules attached to the riser and the scale of wave and current forces.

9.4.2 Environmental loads

Environmental loads are caused by wind, waves and current forces, and VIVs (Stanton, 2006). These forces can induce platform motions which displace the risers relative to where they are connected to the platform, causing excessive bending stresses. The majority of these loads are naturally occurring and hence, are time dependent. Loads such as wave and current forces are cyclic in nature and thus can cause fatigue to the risers.

9.4.3 Installation loads

Installation loads are those imposed on the riser during deployment. Such loads are dependent on the installation procedures and the method in which the riser is tied in to the main production unit on the platform. Nevertheless, installation loads are not of major concern in the study of riser repair systems as they occur prior to any defects sustained by the riser.

9.4.4 Accidental loads

Accidental loads are those that occur inadvertently due to abnormal operating conditions, technical failure and human error. Accidental loads are those that are unpredictable and situational dependent, such as soil-sliding, earthquakes, and impacts from foreign objects. It is normally not necessary to combine these loads with other functional and environmental loads unless site-specific conditions indicate such requirement.

9.5 Design of an FRPC repair for riser

9.5.1 Design requirements of the CRS

Design Requirements:

1. The composite material wrapped on the riser must be able to sustain stresses induced by various loadings to which a riser is susceptible. These stresses must not exceed the designated

limits, while the deformation strain must be kept below a threshold value where it will affect the load carrying capacity of the repaired riser.

2. The interfacial bond between the steel riser and the composite materials must be well-established such that the composite will not delaminate from the steel surface. If the steel-composite interface bond is not strong enough, adequate stress transfer from the steel riser to the composite material will not take place.

9.5.2 Residual strength of a corroded riser

Before conducting a repair on a corroded pipe, analysis must be done to determine whether a repair is sufficient to restore the strength of the riser. This can be evaluated using the codes provided in ASME B31G (1991). The standard used here is compliant for onshore pipelines where the equations are only functions of the corrosion dimensions and internal pressure. Nevertheless, it provides a basis for determining the required thickness of the composite laminate.

1. Folias factor, M:

$$M = 0.032\frac{L^2}{D_o t_p} + 3.3 \qquad \text{if} \qquad L^2/D_o t_p \geq 50 \tag{9.1}$$

$$M = \sqrt{1 + \frac{2.51(L/2)^2}{D_o t_p} - \frac{0.054(L/2)^4}{\left(D_o t_p\right)^2}} \qquad \text{if} \qquad L^2/D_o t_p \leq 50 \tag{9.2}$$

2. Flow stress, σ_{flow}:

$$\sigma_{\text{flow}} = \text{SMYS} + 68.95\ \text{MPa} \tag{9.3}$$

3. Burst failure pressure of corroded pipe, $P_{b,\,\text{corroded}}$:

$$P_{b,\text{corroded}} = \frac{\sigma_{\text{flow}} \cdot 2t_p}{D_o}\left[\frac{1 - \frac{2}{3}\cdot\frac{d}{t_p}}{1 - \frac{2}{3}\cdot\frac{d}{t_p}\cdot\frac{1}{M}}\right], \quad \sqrt{0.8\left(\frac{L}{D_o}\right)^2\left(\frac{D_o}{t_p}\right)} \leq 4.0 \tag{9.4}$$

$$P_{b,\text{corroded}} = \frac{\sigma_{\text{flow}} \cdot 2t_p}{D_o}\left[\frac{1 - \frac{d}{t_p}}{1 - \frac{d}{t_p}\cdot\frac{1}{M}}\right], \quad \sqrt{0.8\left(\frac{L}{D_o}\right)^2\left(\frac{D_o}{t_p}\right)} \geq 4.0 \tag{9.5}$$

where M is the Folias factor; L and d are the longitudinal extent and depth of the corroded defect; D_o, t_p and σ_{flow} are the outer diameter, nominal wall thickness, and flow stress of the pipe, respectively; while SMYS is the specific minimum yield strength.

9.5.3 Minimum repair thickness of the composite laminate

The composite repair laminate must be thick enough to sustain the load transferred from defective pipelines. Otherwise, transverse cracking of the matrix due to high stresses can cause the laminate repair to fail. The minimum required laminate thickness can be determined through ASME PCC-2 (2008).

The minimum required laminate thickness, $t_{\min}$ of a repaired pipe subjected to P_{in} is determined by

$$t_{\min} = \frac{D_o}{2\text{SMYS}} \cdot \left(\frac{E_p}{E_c}\right) \cdot (P_d - P_s) \tag{9.6}$$

where E_p is the tensile modulus for pipe material, E_c is the tensile modulus for the composite laminate in the circumferential direction of the pipe and P_s is the maximum allowable pressure for the pipe with defect as determined from ASME B31G (1991).

When the pipe is subjected to combined P_{in}, F_t, and M_b, the minimum required laminate thickness is calculated via the following equation:

$$t_{\min} = \frac{D}{2\text{SMYS}} \cdot \left(\frac{E_p}{E_a}\right) \cdot \left(\frac{2F}{\pi D^2} - P_s\right) \tag{9.7}$$

where E_a is the tensile modulus for the composite in the axial direction of the pipe and F is the sum of axial loads due to P_{in}, F_t and M_b in units of Newtons.

The design pressure, P_d, of the pipe is determined from API RP 1111 (1999):

$$P_d \leq 0.80 P_t \tag{9.8}$$

$$P_t \leq f_d f_e f_t P_b \tag{9.9}$$

$$P_b = 0.45(\text{SMYS} + U)\ln\frac{D_o}{D_i}, \quad D_o/t_p \geq 15 \tag{9.10}$$

where P_t is the hydrostatic test pressure (internal minus external pressure), f_d is the P_{in} design factor (0.75 for risers), f_e is the weld joint factor (only materials with factor 1.0 are acceptable) and f_t is the temperature derating factor as specified in ASME B31.8 (2003) (1.0 for temperatures less than 121 °C). P_b is the burst pressure of pipe with no defect, U is the specified minimum ultimate tensile strength and D_i is the internal pipe diameter. With this minimum thickness of the repair laminate, the burst strength of the corroded pipe will be at least equal to that of a pipe without corrosion.

9.5.4 Axial length of the laminate repair

In order to prevent delamination of the composite material from repaired pipe and to ensure sufficient axial load transfer from the pipe to the composite, the adhesion surface area between reinforcement material and the pipe must be large enough.

The length to which the laminate repair should extend over each side of the corroded region is determined by

$$L_{\text{over}} = 2.5\sqrt{D_o t_p/2} \tag{9.11}$$

where L_{over} is the overlap length of the composite laminate.

The total axial length of the repair is given by

$$L = 2L_{\text{over}} + L_{\text{defect}} + 2L_{\text{taper}} \tag{9.12}$$

where L_{defect} is the axial length of the defect and L_{taper} is the taper length. It can be seen that the required total axial length of the repair is computed solely based on the dimensions of the pipe and its corroded region, and the material properties of both the pipe and the composite have not been taken into account.

9.6 Finite element modelling

As discussed in the previous section, risers are designed to sustain various types of static and cyclic loadings. Considering the substantial length and geometry of typical risers, the construction of a test facility for FRPC riser repair would require significant investment. Numerical approaches, on the other hand, provide an efficient, cost-effective means to study the effects of different load cases on the CRS of a riser. Amongst the many numerical approaches available, FEA is a popular technique used to provide a fast and accurate prediction of the deformation behavior, that is, stress and strain of structural objects subjected to various forms of loadings, including static, cyclic and nonlinearity in material properties, geometries and contact conditions. The remaining parts of this chapter provide a detailed illustration of the application of finite element modelling for analyzing the FRPC repair of an offshore riser within a general-purpose finite element package ABAQUS® Standard, with case studies covering combined effects of static and cyclic loads. This will be followed by a parametric study on the effects of the FRPC wrap thickness, fiber types and fiber orientation/angle.

9.6.1 Common assumptions in the modelling of CRS

In FEA, if the ratio of wall thickness to radius is equal to or less than 10%, the component can be considered a thin walled structure. For both the riser and the composite repair sleeve,

$$\frac{\text{wall thickness}, t}{\text{radius}, R} \leq 0.1$$

Hence, both parts are modelled as thin wall cylinders and meshed with general purpose, reduced integration shell elements, S4R. These elements are suitable for large strain analysis involving inelastic deformation of materials with a nonzero effective *Poisson's* ratio. Transverse shear deformation is also included. The components are not subjected to hourglass effects or transverse shear locking. The use of fewer integration points with S4R elements benefits the analysis process with reduced computing and storage requirements.

In a CRS, the composite laminate is bonded to the steel riser surface such that effective load transfer from the weakened riser to the composite can take place. Within the FEA model, perfect bonding is assumed between the contact surface interfaces of the riser and the composite laminate. This is an idealization of the FRPC repair in offshore risers. However, variation in material types, installation techniques and parameters tend to result in localized microvoids between surface interfaces of the repair (i.e., between the riser-FRPC and between FRPC laminates) where less than perfect bonding is often observed.

In reality, a riser system consists of multiple segments of finite length pipe members joined together to form a long slender pipe that extends from the platform above water to the seabed. Within the FEA model, the riser is assumed to be an infinitely long pipe with only a segment of the pipe being simulated. The values of different loadings are assumed to be independent along the length of the riser but only the most critical scenarios will be considered. The actual presence and effects of joints are not considered in the present study.

9.6.2 Materials

9.6.2.1 Riser materials

Pipe materials used for steel risers are typically selected from a range of welded or seamless carbon steel pipes that are standardized by the American Petroleum Institute pipe specification, API 5L. An example is the API 5L X60 grade steel pipe, which is the material used in the Petrobras project involving the design and installation of an steel catenary risers (SCR) in the Marlim Field floating production system (Serta et al., 1996). The stress−strain relationship can be defined using the Ramberg−Osgood model, Eqn (9.13). The model response, shown in Figure 9.1, was found capable of representing the relationship accurately (Walker and Williams, 1995).

$$E_p\varepsilon = \sigma + \alpha\left(\frac{|\sigma|}{\sigma^0}\right)^{n-1} \tag{9.13}$$

where E_p is the Young's modulus of the steel pipe, ε and σ are the nominal strain and stress, respectively, α is the Ramberg−Osgood's model yield offset constant, n is the hardening exponent and σ^0 is the yield stress. The parameters shown in Table 9.1 were extracted from tests run by Ruggieri and Dotta in their study of numerical modelling of crack growth in high-pressure pipeline steels (Ruggieri and Fernando, 2011).

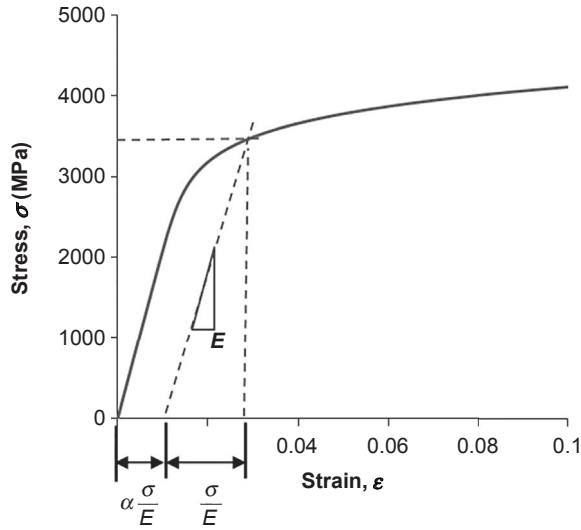

Figure 9.1 Stress–strain curve of API 5L X60 steel represented by the Ramberg–Osgood model.

9.6.2.2 FRPC materials

Carbon fiber and E-glass fiber coupled with an epoxy matrix are the most common FRPC materials used in structural applications. The specific composites used in this study are AS4 (3501-6) carbon/epoxy prepreg and 21 × K43 Gevetex (LY556/HT917/DY063) E-glass/epoxy. The material properties of these composite systems were resolved from the First World-Wide Failure Exercise (WWFE) (Soden et al., 1998a). The WWFE is a joint effort among researchers from different institutes and organizations with the aim of closing the knowledge gap between theoreticians and design practitioners in the field of predicting failure responses of FRPC laminates and thus providing more robust and accurate failure criterion (Hinton et al., 2004). The mechanical properties of the selected materials are determined from extensive experiments, where different specimens are fabricated and tested, depending upon the property sought (Soden et al., 1998b). The main properties required as input data for definition of the FRPC laminate repair within the FEA model are summarized in Table 9.2.

Table 9.1 Mechanical properties of API 5L X60 steel pipe

Parameter	Value
Young's modulus, E (GPa)	210
Poisson's ratio, v	0.3
Yield stress, σ° (MPa)	483
Ramberg–Osgood's Model yield offset, α	1
Hardening exponent in Ramberg–Osgood's model, n	12

Table 9.2 Mechanical properties of the two types of laminates used in the study of the composite repair of corroded riser (Soden et al., 1998b)

Fibre type	AS4	E-glass 21 × K43 Gevetex
Matrix	3501-6 epoxy	LY556/HT907/DY063 epoxy
Specification	Prepeg	Filament winding
Manufacturer	Hercules	DLR
Fibre volume fraction, v_f	0.6	0.62
Longitudinal modulus, E_1 (GPa)	126	53.48
Transverse modulus, E_2 (GPa)	11	17.7
In-plane shear modulus, G_{12} (GPa)	6.6	5.83
Major Poisson's ratio, v_{12}	0.28	0.278
Through thickness Poisson's ratio, v_{23}	0.4	0.4

9.6.3 FRPC laminate lay-up

The FRPC laminate lay-up is modelled based on the consideration that automation of the composite repair in offshore risers is inevitable in the near future. The FRPC laminate is thus assumed to be a unidirectional tape wound around the riser, which in turn provides feasibility of being implemented by an automated wrapping module. Using such a repair technique, fiber reinforcement aligned in the axial direction is not practically achievable. An axially orientated (AO) laminate is only possible through the application of precured half shells that are bonded to the riser section to form a cylinder. This type of repair is only applicable to a designated riser diameter (see Section 9.3.1). The laminate is modelled in such a way that the fibers are aligned in the hoop direction, that is, hoop orientated (HO), with case studies on varying the helical angle of the wrap. However, the AO laminate is also included for comparison purposes.

9.6.3.1 Boundary conditions

The correct boundary conditions must be assigned to the model to ensure that the behavior of the riser and composite repair can be captured when different loads are applied. In addition, accurate boundary conditions will also prevent fictitious stress concentration in the model. Symmetric boundary conditions are often applied to minimize the size of the FEA model, hence simulation time. Owning to the symmetrical geometry of the corroded riser pipe being studied, the pipe can be effectively simplified and modelled as a quarter symmetry structure, as shown in Figure 9.2. The approach is similar to the study conducted by Li and Reid (1992) on the symmetry condition for

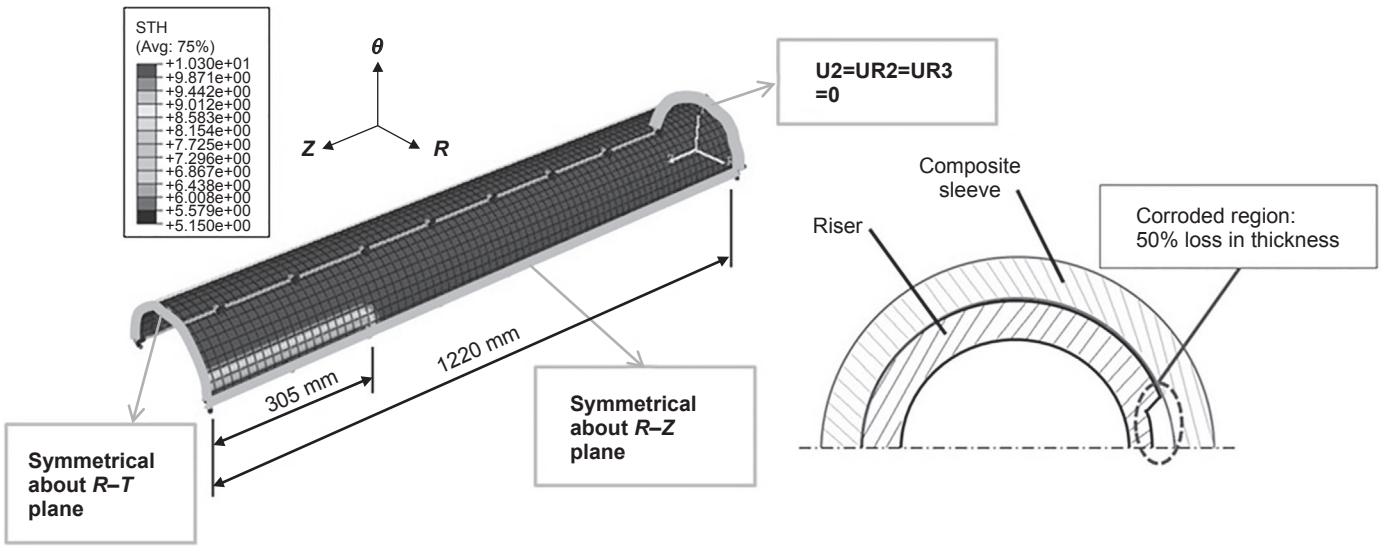

Figure 9.2 Boundary conditions and section view of the model.

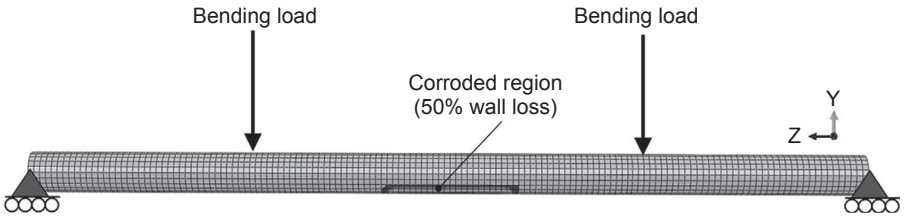

Figure 9.3 Four point bending setup and boundary conditions of the full pipe model.

laminated fiber-reinforced composite structures. If on-axis (i.e., axial or hoop orientated) composite laminates are used, both the corroded riser and composite wrap can be modelled as a quarter cylinder with reflective symmetry boundary conditions.

When off-axis composite laminates are included, the reflective symmetry conditions are not applicable and a full cylinder must be modelled, as shown in Figure 9.3. A four-point bending setup is used so that the entire extent of the repaired region is sustaining the maximum bending moment.

9.6.4 Interaction properties

9.6.4.1 Interaction properties for perfect bonding

In ABAQUS®, the basic model that governs the contact between two surfaces is the standard coulomb friction model. The model assumes that no relative motion occurs between two contacting surfaces if the equivalent frictional stress, τ_{eq}, is less than or equal to the critical stress, τ_{crit}:

$$\tau_{eq} \leq \tau_{crit} \tag{9.14}$$

where τ_{crit} is proportional to the contact pressure:

$$\tau_{crit} = \mu P_{cont} \tag{9.15}$$

while μ is the friction coefficient and P_{cont} represents the contact pressure. In the FEA model, perfect bonding between the steel riser and composite laminate surfaces, herein known as the steel–composite interface, was characterized through a "rough" tangential friction formulation within ABAQUS®. With this friction formulation, the friction coefficient, μ, has a value of infinity which prevents the separation of the two surfaces once they come into contact.

9.6.4.2 Interaction properties for steel–composite disbonding and interlaminar delamination

The static and fatigue disbonding at the steel–composite interface and interlaminar delamination of the composite are simulated. Fracture mechanics is used to describe the delamination and disbonding behaviors, where the strengths of the interlaminar and steel–composite bonds are characterized by their relative energy release rates. Since

the corroded riser with a CRS is subjected to combined loadings in the hoop, longitudinal and transverse directions, mixed mode behavior is assumed. The Benzeggagh and Kenane (BK) fracture criterion is used to determine the critical equivalent strain energy release rate, G_{equivC}. The relationship between the mode I (tensile), II (in-plane shear) and III (out-of-plane shear) energy release rates and G_{equivC} is given in Eqn (9.16):

$$G_{\text{equivC}} = G_{\text{IC}} + (G_{\text{IIC}} - G_{\text{IC}})\left(\frac{G_{\text{II}} + G_{\text{III}}}{G_{\text{I}} + G_{\text{II}} + G_{\text{III}}}\right)^{\eta} \tag{9.16}$$

When the system is subjected to the combined loadings, the G_{IC}, G_{IIC}, G_{IIIC}, and G_{I}, G_{II}, G_{III} are the critical energy release rates and energy release rates in mode I, II and III, respectively. The values of G_{IC}, G_{IIC}, and G_{IIIC} for the interlaminar level of composite material were taken from Liao and Sun (1996), where the values were determined experimentally by implementing a new analytical series solution for AS4 (3501-6 C/E). In the case of steel−composite interface, the values were obtained from Andre and Linghoff (2009), in which the G_{IC}, G_{IIC}, and G_{IIIC} were determined experimentally via double-cantilever beam and end-notch flexure tests. The corresponding values are listed in Table 9.3.

The virtual crack closure technique criterion is selected as it is suitable for modelling disbonding at the steel−composite interface and delamination in the laminated composite where the failure criteria is highly dependent on the mixed-mode ratio. This criterion is used in the static loading case for combined loadings of P_{in}, F_t and M_b in order to determine the limiting bending load that causes catastrophic failure of the corroded riser repaired with FRPC. The crack tip node debonds when the fracture criterion, $f_{\text{criterion}}$, reaches the value 1.0:

$$f_{\text{criterion}} = \frac{G_{\text{equiv}}}{G_{\text{equivC}}} \tag{9.17}$$

where G_{equiv} is the equivalent strain energy release rate and G_{equivC} is determined from Eqn (9.16).

Table 9.3 Fracture and fatigue properties

		Steel−composite interface	Composite laminate interface
Critical strain energy release rate, G_c (N/m)	Mode I	1070	94.44
	Mode II	3644	661.11
	Mode III	3644	850
Fatigue constants	c_1	0.5	0.21164
	c_2	−0.1	−6.25
	c_3	7.03226×10^{-12}	0.33
	c_4	4.6	5.55

The cyclic transverse bending load acting on the riser is analyzed via a low cycle fatigue analysis. The onset and progressive damage of the corroded riser repaired with FRPC was studied and characterized through the Paris Law. The fatigue crack growth initiation criterion, f, and crack evolution are represented by Eqn (9.18) and Eqn (9.19), respectively:

$$f = \frac{N}{c_1(G_{\max} - G_{\min})^{c_2}} \geq 1.0 \tag{9.18}$$

$$\frac{da}{dN} = c_3(G_{\max} - G_{\min})^{c_4} \tag{9.19}$$

where N is the number of cycles, $G_{\max}$ and $G_{\min}$ are the energy release rates when the model is loaded up to maximum and minimum loads, respectively, and c_1, c_2, c_3, and c_4 are the material constants. The material constants were adapted from NASA's reports on fatigue characterization of a graphite epoxy composite and development of benchmark examples for fatigue growth predictions prepared by O'Brien et al. (2010) and Krueger (2011). Madelpech et al.'s (2009) study on the fatigue behavior of a disbond in metallic structures repaired with bonded composite patch provided the material constants of fatigue crack growth at the steel−composite interface. The fatigue criterion constants are shown in Table 9.3.

9.7 Typical load cases

Based on the loading conditions of a riser as discussed in Section 9.4, a set of typical load cases are derived and studied with the aid of FEA. The effects due to functional and environmental loads are considered and are represented in terms of internal pressure, effective tension and effective bending moment. This is aligned with the load acceptance criteria obtained from Section 9.4, analysis methodology of the DNV-OS-F201 (2010), where the main loading effects considered are the differential pressure, bending moment and effective tension. In order to investigate the deterioration of a corroded riser and performance improvement of the FRPC repaired riser, these case studies are manifested in three different conditions:

1. bare riser without corrosion damage (BR),
2. riser with corroded region characterized as material loss in the wall thickness (RC) and
3. corroded riser repaired with composite laminate.

For the three conditions of riser pipe described above, isolated static load, combined static loads and cyclic load cases were simulated.

9.7.1 Design conditions

To aid with the design of the CRS, a study on the repaired riser pipe subjected to complex loadings is required. Theoretical equations impose the use of a deteriorating factor

to account for aspects that will reduce the performance of a riser. However, due to the variation of cases considered in this study of CRS, it is more convenient to apply the limit state analysis which is interpreted on an elastic−plastic basis to determine the stresses corresponding to the design loads (DLs). Based on Section 9.5, Design Criteria for Riser Pipes of DNV-OS-F201 (2010), the serviceability limit state (SLS) requires that the riser must be able to remain in service and operate properly, corresponding to criteria governing the normal operation of the riser. The technique used here is known as the double-elastic slope method and is founded on a single unified design basis developed by Alexander (2007) in his thesis on the development of CRS for reinforcing offshore risers. This design technique is derived from several oil and gas industry design codes and standards and is similar to the criterion of collapse load in section 6-153 of the ASME Boiler and Pressure Vessel Code (1998), Section VIII, Division 2. The double-elastic slope method allows the computation of the plastic analysis collapse load (PACL), that is, the load at which the material reaches failure after a certain amount of plastic deformation occurs. It is important to consider some level of plasticity as it is needed for load transfer from the steel riser to the composite.

The first step of this method is to simulate an FEA model of a noncorroded pipe. The load is then plotted as the ordinate while the strain is plotted as the abscissa in a linear graph. Subsequently, a double-elastic curve (DEC) that has a gradient half of the linear elastic region of the load−strain curve is plotted through the origin. The PACL corresponds to the intersection of the DEC and stress−strain curves. Finally, the DL is determined by dividing the PACL with a margin value, which in this case is 2. The maximum permissible strain limit is defined as the strain value at the intersection of the DEC and DL curves.

9.7.2 Individual static load

9.7.2.1 Internal pressure, P_{in}

A static loading of constant P_{in} is applied to the internal surface of the riser. This load represents the net value of the P_{in} caused by the fluids which the riser transports. Based on a list of SCR available at different TLP, namely Auger (1994), Mars (1997), Ram-Powell (1997) and Marlim Semi (1995), the operating pressure of SCR ranges from 14 to 43 MPa (Howells, 1995). The DL for P_{in} as computed from the double elastic slope method is 22 MPa while the maximum permissible hoop strain, $\varepsilon_{h\text{-max}}$, determined at the design conditions is 0.1875%, as shown in Figure 9.4. The curve for the RC in Figure 9.4 clearly shows that corrosion on the external surface of a riser significantly deteriorates its load carrying capacity. At design conditions ($P_{\text{in}} = 22$ MPa), the maximum permissible strain is exceeded, for example, at 0.275%, which means that the riser is not fit for application.

9.7.2.2 Tensile load, F_t

The tension mimics the load applied on the riser to avoid buckling and excessive bending. In the design of risers, it must be ensured that the risers are capable of sustaining the tensile stress caused by the tensioning systems without distorting their

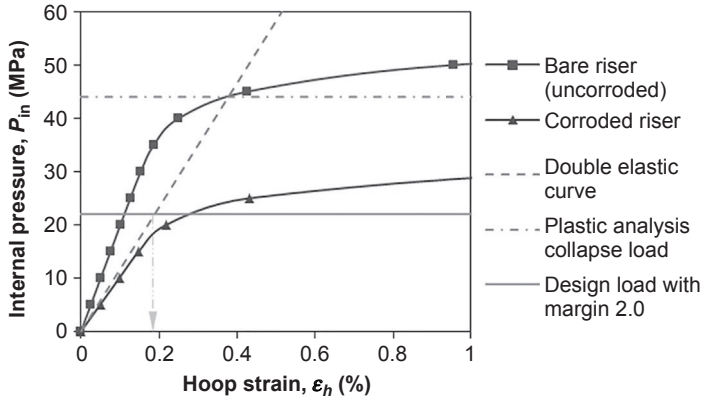

Figure 9.4 P_{in} versus ε_h for bare riser and corroded riser.

performance. The first SCR installed from a moored floating platform in a water depth of 910 m utilized a design top tension of 1780 kN. This SCR was installed as part of a program conducted by Petrobras to evaluate the use of SCRs connected to moored platforms, as well as to produce design guidelines based on numerical and scale modelling (Machado Filho et al., 2001). The DL for F_t as calculated from the double-elastic slope method has a similar value of 1785 kN while the maximum permissible axial strains, $\varepsilon_{a\text{-max}}$, at design conditions is 0.225% (Figure 9.5). The performance of the RC is poorer than that of the BR. However, the reduction in load carrying capacity is not as much when compared to hoop pressure.

9.7.2.3 *Bending moment,* M_b

A typical riser pipe is frequently subjected to bending moment, M_b, arising due to the combination of wind, wave and current forces. It can be varied significantly

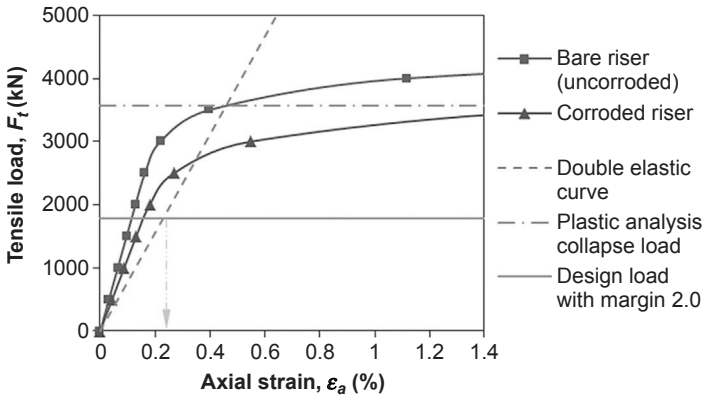

Figure 9.5 F_t versus ε_a for bare riser and corroded riser.

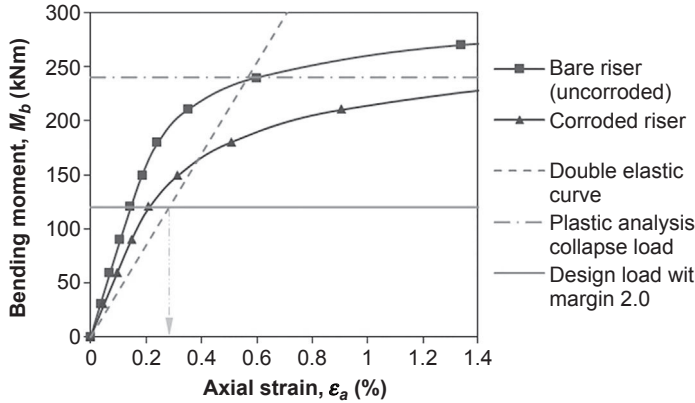

Figure 9.6 M_b versus ε_a for bare riser and corroded riser.

depending on geographical location of the platform, water depth and wind speed. Although tension is applied to the risers to minimize the lateral movements, bending stress acting on the risers is still inevitable. As shown in Figure 9.6, the DL for M_b is determined as 120 kNm while the maximum permissible axial strains, $\varepsilon_{b\text{-max}}$, at design conditions is 0.265%. The strength performance of the RC is lower as anticipated. Similar to the case of pure F_t, the corroded region does not impose a detrimental effect to the strength carrying capacity of the riser as the maximum strain limit was not exceeded at the design condition. The values of the DL and maximum permissible strain for each individual static loading case is summarized in Table 9.4.

9.7.3 Combined static loads

The P_{in} and F_t were set constant at design conditions, which are 22 MPa and 1785 kN, respectively. The response for the riser is then obtained by applying a range of M_b on the riser. Under combined P_{in}, F_t, and M_b loads, the axial strain is found to be the dominant mode of failure, arising due to the positive axial tensile stress contributed by both

Table 9.4 Static design loads and maximum permissible strain

	Design load (DL)	Maximum permissible strain
Internal pressure	$P_{\text{in}} = 22$ MPa	Hoop $\varepsilon_{\text{h-max}} = 0.1875\%$
Tension	$F_{\text{t}} = 1785$ kN	Axial $\varepsilon_{\text{a-max}} = 0.225\%$
Bending moment	$M_{\text{b}} = 120$ kNm	Axial $\varepsilon_{\text{b-max}} = 0.265\%$

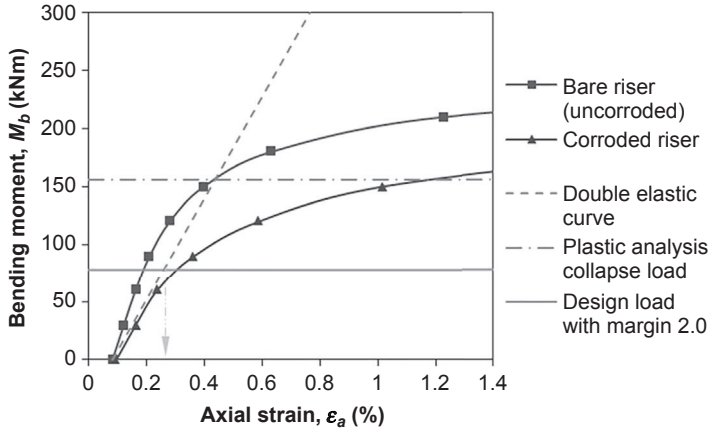

Figure 9.7 M_b versus ε_a for bare riser and corroded riser subjected to combined P_{in}, F_t, and M_b.

the tension and bending. Hence, it is used as the main component for determining the performance of the repair. By comparing Figure 9.7 with Figure 9.6, it is obvious that the maximum permissible strain is reached at a much lower M_b when subjected to combined loadings. At zero M_b, the strain value does not correspond to zero due to the existence of combined hoop and tensile loads. The DL is determined to be 78 kNm (M_b), that is, 30% less than M_b being applied alone, while the maximum permissible strain, axial $\varepsilon_{b\text{-max}}$, at design conditions is 0.265%. When the RC was subjected to pure M_b, the maximum permissible strain was not exceeded at the design condition (see Figure 9.6). However, Figure 9.7 shows that combined loading causes the RC to reach failure at a lower load. The maximum permissible strain was exceeded at the design condition, for example, at 0.3%, which emphasizes the need for repair.

9.7.4 Cyclic loading

Cyclic loading is imposed on the riser and the CRS in an effort to study the interlaminar strength within the composite as well as the bonding strength at the steel-composite interface. Direct low cycle fatigue analysis was carried out to mimic the real life subsea conditions of an operating riser. Data on the cyclic bending load were based on the work of Khan et al. (2011) in a nonlinear dynamic analysis of marine risers under random loads in the Indian Offshore. In their study, it was found that the maximum bending stress (along the length of the riser) due to random wave and current forces is 263.73 MPa. This value is interpreted as the maximum amplitude of the cyclic bending while the computed average of the random wave, having a period of 14.4 s, was taken as input data in the FEA model. The stress amplitude for bending is set to vary between zero and maximum values while the amplitude for internal pressure and tensile load is set constant at the DL throughout the time step.

An initial "defect" is modelled at both the edge of the steel—composite interface and interlayer of the composite laminate, as shown in Figure 9.8. The dimensions of the

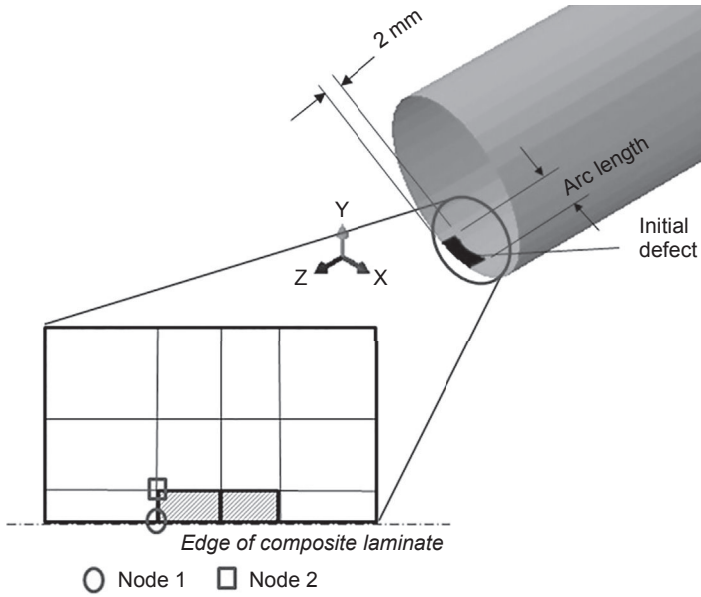

Figure 9.8 Defect region and locations of Node 1 and Node 2 on laminate.

defect are 2 × 2 mm along the axial and arc length, respectively, similar to that quoted from Considine et al.'s (2010) work in the study of inherent defect size in composite materials.

9.7.4.1 *Interlaminar and steel–composite bond strength under static loading*

As shown in Figure 9.9 and Figure 9.10, mode I separation has a negligible effect. The dominant separation is in mode II, with a slight contribution from mode III, indicating

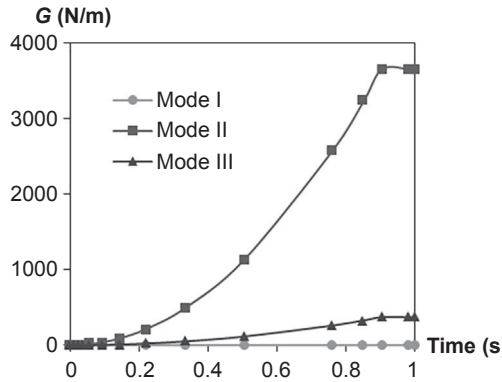

Figure 9.9 Strain energy release rate for AO laminate.

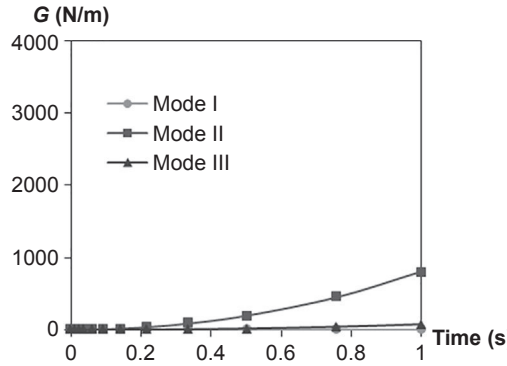

Figure 9.10 Strain energy release rate for HO laminate.

that disbonding at the steel–composite interface and delamination within the composite under combined P_{in}, F_t and M_b are highly due to in-plane and out-of-plane shear stresses. Nevertheless, these two failure mechanisms are unlikely to occur at design conditions. As depicted in Figure 9.11, $f_{criterion}$ is higher at the node located at the side edge of the laminate (Node 1 in Figure 9.8) as this represents the initial defect region. The disbonding did not propagate to the inner node (Node 2 in Figure 9.8) as the G_{equiv} did not reach the G_{equivC}. Further increases in the bending load cause failure outside the composite repaired region where maximum permissible strain is exceeded (Figure 9.12).

9.7.4.2 *Interlaminar and steel–composite bond strength under cyclic loading*

Results show that the CRS is more susceptible to failure at the steel–composite interface. The disbonding was observed to propagate rapidly, as shown by the curves in Figure 9.13 and Figure 9.14. The AO laminate was able to sustain higher stress in the axial direction before disbonding takes place (Figure 9.13) and vice versa for

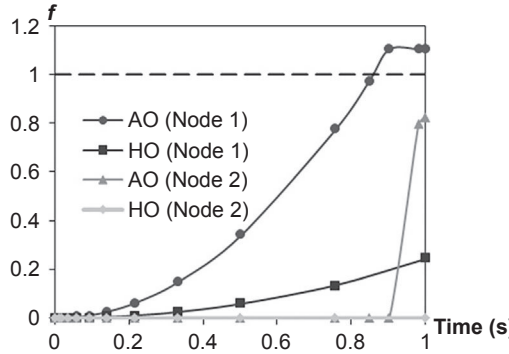

Figure 9.11 $f_{criterion}$ for AO and HO laminate at Node 1 and Node 2.

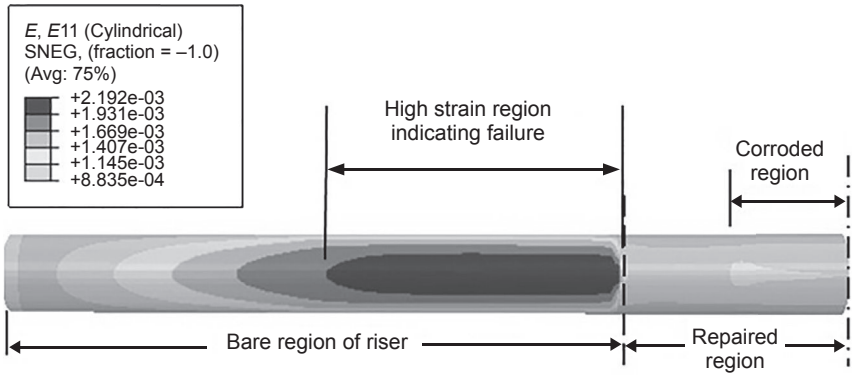

Figure 9.12 Contour plot of axial strain.

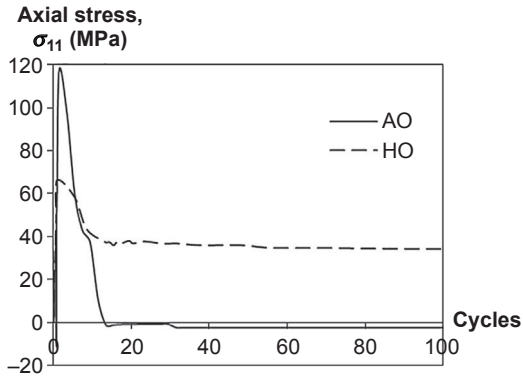

Figure 9.13 Axial stress versus number of cycles for AO and HO laminates.

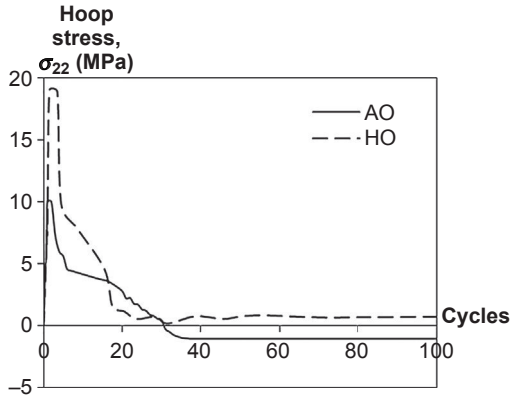

Figure 9.14 Hoop stress versus number of cycles for AO and HO laminates.

the HO laminate (Figure 9.14). Once disbonding occurs, the stress levels on the laminate drop to much lower values, indicating that load transfer from the corroded riser to the laminate repair is no longer effective. The high rate of disbonding propagation may be attributed to the coarse meshing. A finer mesh can provide a better propagation rate but is compromised by a longer simulation time.

9.8 Parametric study

A parametric study is important for the optimization of the CRS. Those conducted here are aimed directly at the FRPC material where thickness, fiber type, and wrap orientation are considered and are based on the cases of individual static loading as well as the combined static loadings of internal pressure, tension and bending moment.

9.8.1 Wrapping angle/orientation of FRPC

When an offshore riser is subjected to combined loadings, it is bound to experience different levels of principal stresses, that is, axial, hoop and radial stresses. However, the out-of-plane radial stress is negligible in the current case due to the usage of the thin shell formulation. A variation in the design of wrapping angle/orientation of the FRPC is prudent in providing an effective reinforcement to resist potential failure in these principal directions.

The wrapping of laminate is assumed to traverse along the length of the repair section in a helical manner such that an angle, θ, relative to the axis of the riser exists. As the repair consists of several layers of laminates, the wrapping process will have to go back and forth along the length of the repair section. In real life, there are bound to be "end effects" in the helical winding of composite tape where accurate angle orientation is not fully achievable. However, as the repair extends sufficiently far beyond the corroded region of the riser, the end effects are negligible and are not included in the FEA model. Varying the laminate wrapping angle from 30° to 90° (hoop direction) in steps of 15°, producing $[\pm\theta]_n$ of laminate, allows the effect of orientation to be observed.

From Figure 9.15, it is apparent that an HO laminate is ideal for reinforcing the hoop strength of a corroded riser when it is purely subjected to P_{in}. Vice versa, the $[\pm 30°]_s$ laminate, which has fibers aligned closest to the axis of the riser, provides highest strengthening when the riser is subjected to pure F_t and M_b, respectively (Figure 9.16, Figure 9.17). When subjected to combined P_{in}, F_t, and M_b, the performance of the repaired riser deteriorates (i.e., increasing strain values) as the wrapping angle of the FRPC laminate relative to the longitudinal axis increases (Figure 9.18). Hence, there is a need for reinforcement in both hoop and axial direction and application of $[\pm 45°]$ wrapping angle can provide both.

The curve for a corroded riser repaired with $[\pm 30°]$ laminate in Figure 9.18 shows an anomaly as the M_b increases to a high value. This is attributed to the fact that a further increase in load causes the formation of a plastic hinge where local deformation takes place at the points of loading and the load is not transferred to the repaired region.

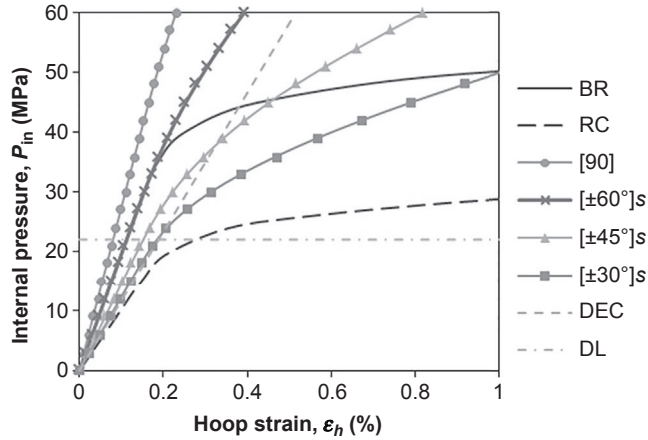

Figure 9.15 P_{in} versus ε_h for riser repaired laminate of varying wrapping angle.

9.8.2 FRPC thickness

By determining the optimal range of thickness required in the repair, the number of wraps can be determined. This can prevent material wastage and hence reduce the cost of the repair. Figure 9.19 shows the strain values of corroded risers repaired with varying thickness subjected to a bending moment of 78 kNm (DL). The graph is split into two halves by the line representing the maximum permissible strain, $\varepsilon_{a\text{-max}}$. The upper half is the undesirable condition where $\varepsilon_{a\text{-max}}$ is exceeded and the lower half represents the opposite condition. The strain values of the repaired risers decrease as the repair thickness increases. Using Eqn (9.7) of ASME PCC-2, the minimum laminate thickness calculated based on maximum reinforcement where the fibers are

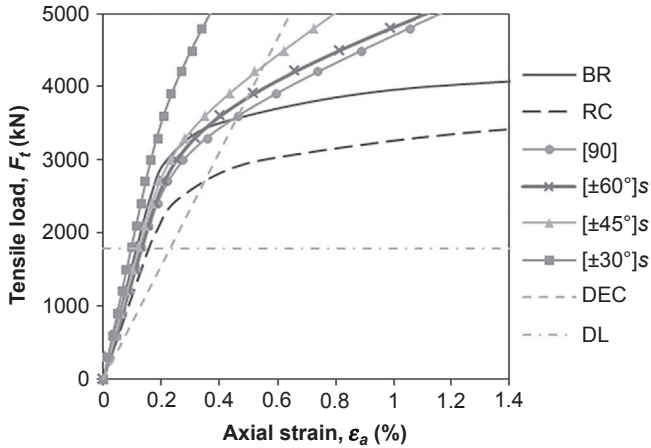

Figure 9.16 F_t versus ε_a for riser repaired laminate of varying wrapping angle.

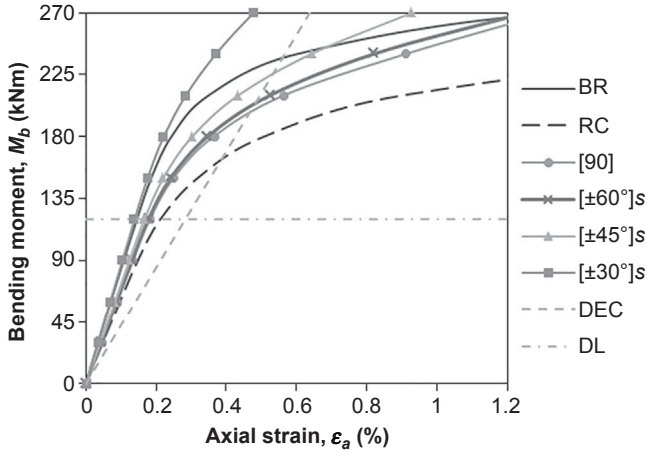

Figure 9.17 M_b versus ε_a for riser repaired laminate of varying wrapping angle.

aligned in the axial direction of the pipe (i.e., 0°) is approximately 3 mm. This thickness is insufficient for application of angle plies $[\pm 45]_s$ and $[\pm 60]_s$. By using the correct wrapping angle, the repair thickness can be reduced, hence saving material usage.

9.8.2.1 FRPC types

There are two typical types of fiber reinforcement used in repair of onshore pipelines: carbon fiber and glass fiber. The selected materials are discussed in Section 9.6.2.2. The model discussed here uses a repair laminate with a ±30° wrap angle with varying material.

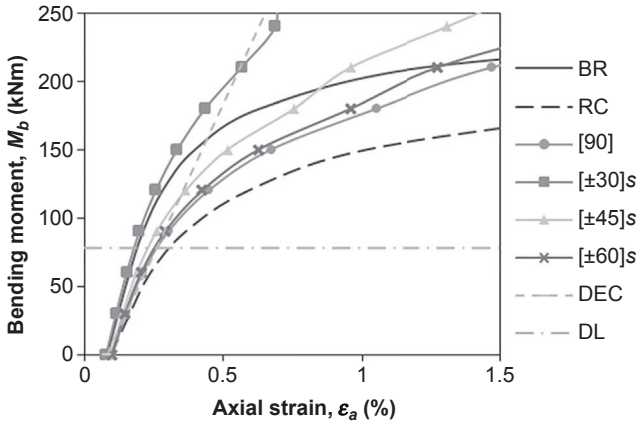

Figure 9.18 M_b versus ε_a for riser repaired laminate of varying wrapping angle subjected to combined loading.

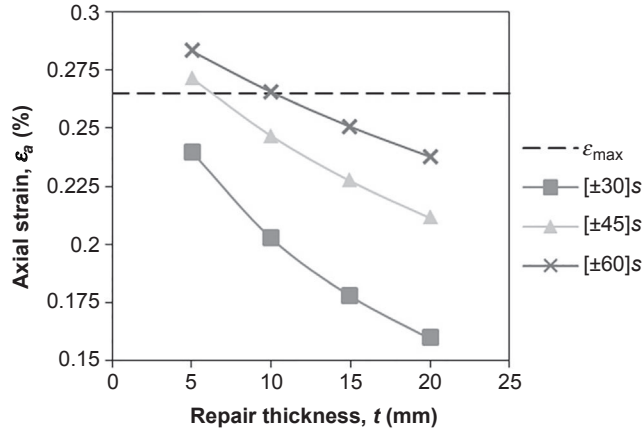

Figure 9.19 ε_a versus t for riser repaired laminate of varying thickness.

From Figure 9.20, it is clear that carbon fiber reinforcement has better strengthening than glass fiber. By applying carbon fiber instead of glass fiber for the reinforcement of corroded risers, less material is used for the same amount of strengthening. It is advantageous as it can reduce the weight of the repair as well as the installation lead time. As direct contact between carbon and steel initiates galvanic corrosion, measures to eliminate this problem have to be taken into consideration. The few alternatives include the use of a nonconductive layer of fabric between carbon and steel and the use of an isolating epoxy film.

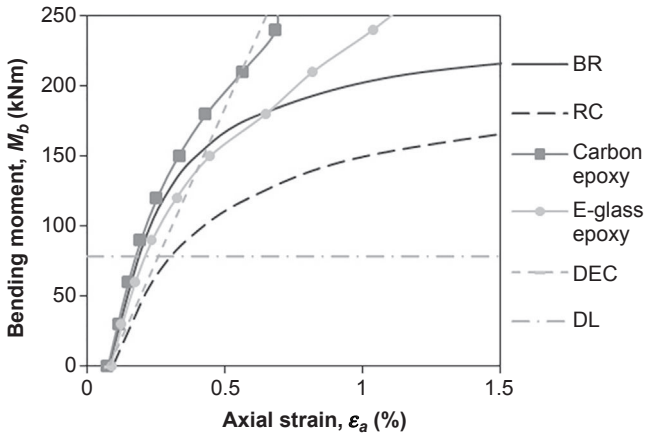

Figure 9.20 M_b versus ε_a for riser repaired with ±30° wrap angle, carbon epoxy and E-glass epoxy laminates.

9.9 Further studies on wrap tension

The pretension refers to the amount of tension applied on the FRPC during the winding onto the corroded riser. Although works on the pretension of FRPC in pipeline rehabilitation are scarce, the effect of pretension on patch repairs of steel and concrete columns has been investigated in multiple studies. In a study of concrete column strengthening by lateral pretensioning of FRPC, it was found that pretensioned FRPC materials can increase the load bearing capacity up to 35% compared with no pretensioning (Mortazavi et al., 2003). In addition, pretensioning of FRPC can result in a compressive stress in the steel structure to compensate for the tensile stress induced by live loads (Nozaka and Ueda, 2008). It is believed that pretension in FRPC in the application of repair for offshore risers will induce similar effects. Stress models derived for wound structures and filament winding shall be studied so that they can be implemented into the FEA code.

9.10 Conclusions

The need for composite repair in offshore subsea pipe risers is in high demand. However, research in this field of study remains scarce, with limited work being done on static loading without taking into consideration cyclic, thermal or fatigue loadings. Guidelines and standards related to riser design and pipeline repair as well as materials characterization can be used as a foundation for the design of CRS applicable to offshore risers.

FEA has proven to be a useful tool for the design and analysis of the CRS. With properly characterized input data of the material properties, FEA models were able to capture the stress−strain behavior of the FRPC, simulate the effects of coupled loadings and optimise the parameters and performance of the CRS.

9.10.1 Future trends

Application of FRPC in the repair of offshore risers has proven to be a viable option. FEA can be used as an optimization tool to expand the study on the CRS to mimic the real life conditions of a subsea riser. Different aspects covering the FEA model of the composite repair on offshore risers provide a broad scope of research to be conducted. Factors such as the response of FRPC under impact and fatigue loading have to be investigated in order to increase the confidence of its application in riser repair. The cyclic nature of wind, wave and current forces can deteriorate the lifespan of the CRS significantly. In addition, different parametric studies related to the cure profile, wrap tension and variation in initial defect and subsea environmental conditions including a salt water environment, temperature and pressure differential at varying water depth are practical elements to be considered. These parameters can alter the material properties of the FRPC and affect its long term performance.

Although the ability of CRS to strengthen corroded risers has been proven, the current application of CRS involving either wet lay-up of composite laminates or installation of fully cured composite shells can be cumbersome when brought to the site of

repair in offshore subsea conditions. The inaccessible environment of deep water suggests the need for automation of the repair system. A method of applying the composite material may be simplified by using prepreg tapes that can be readily wound wrapped around the corroded section of the riser. This allows the repair to be done in considerably compact surroundings. Research by different parties with regards to automated pipe crawling robots that travel along the outside surface of a pipe is being conducted. The development of such a robot can be further improved by attaching modules for riser surface preparation, winding and curing of FRPC and controls of different parameters such as winding pattern, pretension and the FRPC thickness. Along with the FEA that provides useful design information, the use of FRPC for offshore risers extended to greater water depths can then be made feasible.

9.10.2 Sources of further information and advice

This section provides further information on research, industrial projects, publications and current development of the use of FRPC in repairing offshore risers.

Stress Engineering, Inc. is one of the major companies that has run multiple full-scale tests to validate the performance of numerous onshore pipeline composite repair products that are available in the market. Full reports documenting the validation of composite repair products are available (Alexander, 2005; Worth, 2005; Francini and Kiefner, 2006). Various publications on the development of the CRS for offshore riser application are also available under Chris Alexander of Stress Engineering, Inc. A program cosponsored by the Pipeline Research Council International, Inc. (PRCI) involves the full-scale testing of corroded risers with a CRS placed in a seawater test facility for 10,000 h subjected to combined pressure, tension and bending loads (Alexander, 2012).

Literature on different studies of corroded pipelines repaired with FRPC demonstrates the experimental and FEA modelling works being conducted. It should be noted that most work done is associated with static loading of pure internal pressure (Batisse and Bailleul, 2007; Duell et al., 2008; Esmaeel et al., 2012) and combined static loadings (Alexander and Ochoa, 2010; Shouman and Taheri, 2011). Testing and FEA modelling on cyclic loadings are still limited, with the majority of the studies focussing on cyclic pressure (Alexander, 2005; Lukács et al., 2010, 2011). Studies on loading and surrounding conditions that simulate actual subsea environments are still scarce.

Additional information such as material and bonding properties between steel and composite can be obtained by reviewing literature related to composite patch repair on a steel structure. A comprehensive amount of studies have been conducted and can be used as a basis to model the bonding between the composite repair material and steel riser.

References

ABS, 2008. Guide for Building and Classing Subsea Riser Systems. American Bureau of Shipping, New York.

Air Logistics, 2006. Field-Applied Composite Systems: AquaWrap™. Product Information Brochure.

Alexander, C., 2005. Evaluation of the Aquarap® System in Repairing Mechanically-Damaged Pipes. Report Prepared for Air Logistics, Inc., PN114315CRA, Azusa, California.

Alexander, C., 2006. Assessing the use of composite materials in repairing and reinforcing offshore riser pipes. In: Presentation to Minerals Management Service (MMS) Regional Operations Technology Assessment Committee (ROTAC) Meeting.

Alexander, C., 2007. Development of Composite Repair System for Reinforcing Offshore Riser (Ph.D. thesis), Texas A&M University.

Alexander, C., Ochoa, O.O., 2010. Extending onshore pipeline repair to offshore steel risers with carbon-fiber reinforced composites. Composite Structures 92, 499−507. http://dx.doi.org/10.1016/j.compstruct.2009.08.034.

Alexander, C., April−May 2012. Design of an optimized composite repair system for offshore risers using integrated analysis and testing techniques. In: Offshore Technology Conference. http://dx.doi.org/10.4043/23164-MS.

Andre, A., Linghoff, D., 2009. Damage modelling of adhesive joint in composite reinforced metallic beams. In: NSCC, September.

API Recommended Practice 2RD, 1998. Design of Risers for Floating Production Systems (FPSs) and Tension-Leg Platforms (TLPs). American Petroleum Institute, Washington, DC.

API Recommended Practice 1111, 1999. Design, Construction, Operation and Maintenance of Offshore Hydrocarbon Pipelines (Limit State Design). American Petroleum Institute, Washington, DC.

ASME B31.4, 2006. Pipeline Transportation Systems for Liquid Hydrocarbons and Other Liquids. The American Society of Mechanical Engineers, USA.

ASME B31.8, 2003. Gas Transmission and Distribution Piping System. The American Society of Mechanical Engineers, USA.

ASME B31G, 1991. Manual for Determining the Remaining Strength of Corroded Pipelines. The American Society of Mechanical Engineers, USA.

ASME PCC-2, 2008. Repair of Pressure Equipment and Piping. The American Society of Mechanical Engineers, USA.

ASME Boiler and Pressure Vessel Code, 1998. Section VIII, Division 2: Mandatory Experimental Stress Analysis. The American Society of Mechanical Engineers, USA.

Batisse, R., Bailleul, M., 2007. Sensitivity Analysis of Clock Spring Repair to Hydrogen Gas-Effect on Burst Pressure. Report for Naturally, D0020-WP4-P-0. , January.

Chakrabarti, S.K., Frampton, R.E., 1982. Review of riser analysis. Applied Ocean Research 4 (2), 73−90. http://dx.doi.org/10.1016/S0141-1187(82)80002-3.

Citadel Technologies, 2011. Diamondwrap®: Structural Carbon/Epoxy Rehab System for the Prevention and Repair of Corroded Piping System. Product Information Brochure.

Considine, J.M., Vahey, D.W., Rowlands, R.E., Turner, K.T., 2010. Inherent defect size: calculation and use for composite materials. In: 16th US National Congress of Theoretical and Applied Mechanics, June.

DNV-Offshore Standard-F201, 2010. Dynamic Risers. Det Norske Veritas, Norway.

DNV-Recommended Practice-F101, 2010. Corroded Pipelines. Det Norske Veritas, Norway.

Duell, J.M., Wilson, J.M., Kessler, M.R., 2008. Analysis of a carbon composite overwrap pipeline repair system. International Journal of Pressure Vessels and Piping 85, 782−788. http://dx.doi.org/10.1016/j.ijpvp.2008.08.001.

Esmaeel, R.A., Khan, M.A., Taheri, F., 2012. Assessment of the environmental effects on the performance of FRP repaired steel pipes subjected to internal pressure. Journal of Pressure Vessel Technology 134 (4), 1−7. http://dx.doi.org/10.1115/1.4005944, 041702.

Fawley, N.C., 1994. Development of Fibreglass Composite Systems for Natural Gas Pipeline Service. Report Prepared for Gas Research Institute, GRI-95/0072, March.

Francini, R.B., Kiefner, J.F., 2006. Evaluation of the Aquawrap® composite Repair System. Report Prepared for Air Logistics Corporation, Report No. 06−41, April.

Hinton, M.J., Kaddour, A.S., Soden, P.D., 2004. The World-Wide Failure Exercise: its origin, concept and content. In: Failure Criterion in Fibre Reinforced Polymer Composites: The World-wide Failure Exercise. Elsevier, Oxford, pp. 2−26.

Howells, H., 1995. Advances in steel catenary riser design. In: Presented at DEEPTEC 95, Aberdeen.

ISO/TS 24817, 2006. Petroleum, Petrochemical and Natural Gas Industries − Composite Repairs for Pipework − Qualification and Design, Installation, Testing and Inspection. International Organization for Standardization, Switzerland.

Khan, R.A., Kaur, A., Singh, S.P., Ahmad, S., 2011. Nonlinear dynamic analysis of marine risers under random loads for deepwater fields in Indian offshore. Procedia Engineering 14, 1334−1342. http://dx.doi.org/10.1016/j.proeng.2011.07.168.

Krueger, R., 2011. Development and Application of Benchmark Examples for Mode II Static Delamination Propagation and Fatigue Growth Predictions. Report Prepared for NASA, NASA/CR-2011−217305, Hampton, Virginia.

Li, S., Reid, S.R., 1992. On the symmetry conditions for laminated fibre-reinforced composite structures. International Journal of Solids Structures 29 (23), 2867−2880. http://dx.doi.org/10.1016/0020-7683(92)90145-J.

Liao, W.C., Sun, C.T., 1996. The determination of mode III fracture toughness in thick composite laminates. Composite Science and Technology 56, 489−499. http://dx.doi.org/10.1016/0266-3538(96)00009-7.

Lukács, J., Nagy, G., Török, I., Égert, J., Pere, B., 2010. Experimental and numerical investigations of external reinforced damaged pipelines. Procedia Engineering 2, 1191−1200. http://dx.doi.org/10.1016/j.proeng.2010.03.129.

Lukács, J., Nagy, G., Török, I., 2011. The role of the external and internal reinforcing on the structural integrity of damaged steel pipelines. Procedia Engineering 10, 2514−2519. http://dx.doi.org/10.1016/j.proeng.2011.04.414.

Machado Filho, R.Z., Mourelle, M.M., Franciss, R., Lima, C.S., Eisemberg, R., Ferreira, A., 2001. The monitoring system for a steel catenary riser suspended from a floating platform in deepwater. In: Proceedings of 20th Offshore Mechanical & Arctic Engineering Conference (OMAE).

Madelpech, P., Juaneda, S., Pradels, M., 2009. Bonded composite patch to repair metallic structures: fatigue behaviour of a disbond. In: Proceeding of 17th International Conference on Composite Materials, July.

Mortazavi, A., Pilakoutas, K., Son, K.S., 2003. RC column strengthening by lateral pretensioning of FRP. Construction and Building Materials 17 (6−7), 491−497. http://dx.doi.org/10.1016/S0950-0618(03)00046-1.

Nozaka, K., Ueda, K., 2008. Effect of pre-tensioning on peeling failure bonded CFRP strips. In: Proceedings of the Fourth International Conference on FRP Composites in Civil Engineering (CICE), July.

O'Brien, T.K., Johnston, W.M., Toland, G.J., 2010. Mode II Interlaminar Fracture Toughness and Fatigue Characterization of Graphite Epoxy Composite Material. Report Prepared for NASA, NASA/TM-2010−216838, Hampton, Virginia.

Ochoa, O.O., Salama, M.M., 2005. Offshore composites: transition barriers to an enabling technology. Composite Science and Technology 65 (15−16), 2588−2696. http://dx.doi.org/10.1016/j.compscitech.2005.05.019.

Palmer, A.C., King, R.A., 2008. Subsea Pipeline Engineering, second ed. Pennwell.
Patrick, A.J., 2004. Composites − Case Studies of Pipeline Repair Applications. Pigging Product and Services Association.
Patrick, A.J., 2010. The use and application of composite repairs. PetroMin Pipeliner.
Rehberg, T., Schad, M., Green, M., 2010. Non-metallic Composite Repair Systems for Pipes and Pipelines. Pipe Technology 3R International. Special Edition.
RSPA Department of Transportation 98-4733, 2000. Pipeline Safety: Gas and Hazardous Liquid Pipeline Repair.
Ruggieri, C., Fernando, D., 2011. Numerical modeling of ductile crack extension in high pressure pipelines with longitudinal flaws. Engineering Structures 33 (5), 1423−1438. http://dx.doi.org/10.1016/j.engstruct.2011.01.001.
Serta, O.B., Mourelle, M.M., Grealish, F.W., Harbert, S.J., Souza, L.F.A., 1996. Steel catenary riser for the marlim field FPS P-XVIII. In: Proceedings of 28th Offshore Technology Conference, May. http://dx.doi.org/10.4043/8069-MS.
Shouman, A., Taheri, F., 2011. Compressive strain limits of composite repaired pipelines under combined loading states. Composite Structures 93 (6), 1538−1548. http://dx.doi.org/10.1016/j.compstruct.2010.12.001.
Soden, P.D., Hinton, M.J., Kaddour, A.S., 1998a. Lamina properties, lay-up configurations and loading conditions for a range of fibre-reinforced composite laminates. Composite Science and Technology 58 (7), 1011−1022. http://dx.doi.org/10.1016/S0266-3538(98)00078-5.
Soden, P.D., Hinton, M.J., Kaddour, A.S., 1998b. Biaxial test results for strength and deformation of a range of e-glass and carbon fibre reinforced composite laminates: failure exercise benchmark data. Composite Science and Technology 62 (12−13), 1489−1514. http://dx.doi.org/10.1016/S0266-3538(02)00093-3.
Stanton, P., 2006. Overview of Deepwater Drilling and Production Risers. Technip.
Tavakkolizadeh, M., Saadatmanesh, H., 2001. Galvanic corrosion of carbon and steel in aggressive environments. Journal of Composites for Construction 5 (3), 200−210.
Tiratsoo, J. (Ed.), 2003. Pipeline Pigging and Integrity Technology, third ed. Clarion Technical Publishers.
Walker, A.C., Williams, K.A.J., 1995. Strain based design of pipelines. In: Proceedings of the ASME 14th International Conference on Ocean, Offshore and Arctic Engineering, Copenhagen, Denmark, 5, 345−350.
Webb, G.D., 1981. Inspection and repair of oil and gas production in deep water. Ocean Management 7, 313−326. http://dx.doi.org/10.1016/0302-184X(81)90018-4.
Worth, F., 2005. Analysis of Aquawrap® for Use in Repairing Damaged Pipelines. Report for Air Logistics Corporation, 1−19.

Abbreviations

AO	Axially orientated
API	American Petroleum Institute
ASME	American Society of Mechanical Engineers
BR	Bare riser without corrosion damage
CRS	Composite repair system
DCB	Double-cantilever beam
DEC	Double-elastic curve
DL	Design load
DNV	Det Norske Veritas

ENF	End-notched flexure
FEA	Finite element analysis
FPS	Floating production system
FRPC	Fiber-reinforced polymer composite
HO	Hoop orientated
ISO	International Organization for Standardization
MAOP	Maximum allowable operating pressure
PACL	Plastic analysis collapse load
RC	Riser with corrosion damage
SCR	Steel catenary riser
SLS	Serviceability limit state
SMYS	Specific minimum yield strength
TLP	Tension-leg platforms
VCCT	Virtual crack closure technique
VIV	Vortex induced vibration
WWFE	World-Wide Failure Exercise

Nomenclature

c_1, c_2, c_3, c_4	Material constants for fatigue criterion
d	Depth of the corrosion defect
D_o	Outer diameter of the pipe
E_a	Tensile modulus of the composite laminate in axial direction of the pipe
E_c	Tensile modulus of the composite laminate in circumferential direction of the pipe
E_1	Elastic modulus of FRPC in the direction parallel to fibers
E_2	Elastic modulus of FRPC in the direction perpendicular to fibers
E_p	Tensile modulus of the pipe material
f	Fatigue crack growth initiation criterion
$f_{\text{criterion}}$	Fracture criterion
f_d	Internal pressure design factor
f_e	Weld joint factor
f_t	Temperature derating factor specified in ASME B31.8
F_t	Tensile load
F	Sum of axial loads due to internal pressure, tensile load and bending moment
G	Shear modulus
G_{equiv}	Equivalent strain energy release rate
G_{equivC}	Critical equivalent strain energy release rate
G_{IC}	Critical energy release rate in mode I
G_{IIC}	Critical energy release rate in mode II
G_{IIIC}	Critical energy release rate in mode III
L	Longitudinal extent of corroded area
L_{defect}	Axial length of the defect
L_{over}	Overlap length of the repair
L_{taper}	Taper length of the repair
M	Folias factor
M_b	Bending moment

n	Ramberg−Osgood's model hardening exponent
N	Number of cycles
P_b	Burst pressure of the pipe with no defect
$P_{b,\text{corroded}}$	Burst pressure of the corroded pipe
P_{cont}	Contact pressure
P_d	Design pressure
P_{in}	Internal pressure
P_t	Hydrostatic test pressure (internal minus external pressure)
t_{min}	Minimum required laminate thickness
t_p	Nominal thickness of the pipe
V	Poisson's ratio
v_f	Fiber volume fraction of FRPC
a	Ramberg−Osgood's model yield offset constant
ε	Nominal strain
$\varepsilon_{a\text{-max}}$	Maximum permissible axial strain under tensile load
$\varepsilon_{b\text{-max}}$	Maximum permissible axial strain under bending moment
$\varepsilon_{h\text{-max}}$	Maximum permissible hoop strain under internal pressure
σ	Nominal stress
σ_{flow}	Flow stress of the pipe
σ^0	Yield stress of the pipe
τ_{eq}	Equivalent frictional stress
τ_{crit}	Critical frictional stress
μ	Friction coefficient
θ	Helical angle relative to the axis of the riser

Design of fibre-reinforced polymer overwraps for pipe pressure

10

N. Saeed[1,2], *H.R. Ronagh*[1]
[1]The University of Queensland, Brisbane, QLD, Australia; [2]Cooperative Research Centre for Advanced Composite Structures, Port Melbourne, VIC, Australia

10.1 Introduction

Steel pipelines have become the main network of oil and gas transmission over the last 50 years. In Europe alone, the total length of the gas transmission system has increased from about 30,000 km to over 120,000 km between 1975 and 2004 (EGIG, 2005). Carrying corrosive substances plus being located in harsh environments (for near-sea and some subsea pipelines) has resulted in a sharper than expected reduction in the life expectancy of these pipes due to internal/external corrosion or erosion. Apart from replacement, which is a long-term and costly solution, the only short-term alternative to continue using a partly damaged pipe is to reduce its operating pressure. This is not cheap either due to lowered productivity. Developing pipe rehabilitation techniques have made it possible to save kilometres of pipelines at low cost. More efficient methods are becoming available gradually and the design and technology behind the solution is taking shape, resulting in more cost-effective and reliable methods.

Ideally, a repaired pipeline should revert to its original design pressure capacity and be able to sustain pressure fluctuations during the extended life time after repair. A proper repair method should not only reinstate the original pressure capacity but also meet general criteria, such as ease of installation and economic viability, in addition to addressing technical criteria such as being impact resistance and nongalvanic (Alexander et al., 2008).

Conventionally, most steel pipelines were repaired by removing the corroded section and replacing it with a new pipe or by reinforcing the defected section with an external steel sleeve (Mohitpour et al., 2003). Recently, fibre-reinforced polymer (FRP) composite overwrap repair systems have been introduced and overwhelmingly accepted as an alternative repair system for pipelines.

Repair with FRP materials presents several advantages over conventional methods. Firstly, the repair is quicker to be performed as the application is easy and straightforward. Secondly, the pipeline can continue to operate while the repair is being carried out. Thirdly, the risk of fire and explosion due to welding or cutting is completely eliminated (Duell et al., 2008). Last but not the least, and contrary to the common belief, FRP repair is more economical than other repair methods conventionally used. In one comparative study (Koch et al., 2001), it was found that FRP repair was in fact 24%

Rehabilitation of Pipelines Using Fiber-reinforced Polymer (FRP) Composites. http://dx.doi.org/10.1016/B978-0-85709-684-5.00010-2

cheaper than the welded steel sleeve repair and 73% cheaper than replacing the defected pipe section. FRP overwrap repair can retard the growth of external corrosion by isolating the external defect from corrosive environments, so it can be considered as a lifetime repair.

Design of this newer system has been integrated into the American Society of Mechanical Engineers (ASME) ASME B31.4 (ASME, 2009) and ASME B31.8 (ASME, 2010) pipeline codes and in CSA Z662 (CSA, 2007). The method involves reinforcing of the corroded part of a pipeline by wrapping FRP around its perimeter for a certain length that exceeds that of corrosion. The main parameter to design for is the required pressure capacity. This chapter discusses methods of designing overwrap repair for a corroded steel pipe at a given pressure.

10.2 State of the art

The behaviour of pipes repaired with composite overwraps has been studied by many researchers in order to understand the effects of different parameters such as material properties and loading conditions.

The Gas Research Institute (GRI) conducted the first study on the full-scale testing of the Clock-Spring® repair system. After performing a series of tests on the Armor-Plate®, Alexandra and Wilson (1999) proposed guidelines for the use of composite materials in pipeline repairing systems and came up with the stress modelling of pipelines strengthened with FRP under different loading conditions. Another investigation was performed using Glass FRP (GFRP), Aramid FRP (AFRP) and Carbon FRP (CFRP) by Toutanji and Dempsey (2001). The results revealed that CFRP performs better in comparison with AFRP and GFRP when it comes to increasing the burst strength of pipes.

In 2002, an experimental test was conducted on the FRP-reinforced pipes by Meniconi et al. (2002). These tests were verified with finite element analysis (FEA) and showed that overwraps only take part in carrying the loads after steel yielding. Kessler et al. (2004) did some investigations on an FRP with the trade name Diamond-Wrap®. They did two tests on the repaired pipes; the first was to study the effectiveness of rapier on pipes with different depths of axisymmetric defects. It showed an almost 140% increase in the burst strength. The cyclic fatigue pressure testing was the second test performed in this study; the results revealed a considerable increase in the service life of the repaired pipes.

Perrut et al. (2006) investigated the repair of dented pipes and performed a low cycle fatigue followed by bursting tests. It was shown that the overwrap system is adequate as a permanent repair for the dented pipes. It was also indicated that using two layers of glass/epoxy did not affect the strain output of the damaged area favourably compared to using one layer only.

Freire et al. (2007) carried out an extensive experimental study to investigate the effectiveness of FRP overwrap repair on externally and internally damaged pipelines. They concluded that the use of composite overwrap could restore the bursting pressure resistance of both types of repaired pipes to the level of undamaged pipes.

Alexander (2007) and Alexander and Ochoa (2010) performed experiments in conjunction with FEA and based on the obtained results presented an innovative design to extend the existing composite repair techniques to offshore pipes. Their research led to an easily deployable CFRP repair system based on the limit analysis method and strain-based design techniques.

Based on the experimental and numerical results of Duell et al. (2008), the length of defect in the hoop direction does not have a considerable influence on the failure pressure. The full-scale evaluation was performed on pipe samples with externally machined defects.

Shouman and Taheri (2009, 2011) did an experimental and numerical study to investigate the behaviour of repair in externally defected pipes under combined loading. They considered internal pressure, axial force and moment and proved that increasing the thickness of the wrap would not improve the strength of the pipe in the axial direction. Furthermore they found that the length of composite repair affects the bending response of the repaired pipe.

In 2006, the first revision of two international codes, one by the International Organization for Standardization (ISO), ISO/TS-24817 (ISO, 2006) and the other the ASME PCC-2 (ASME, 2006), were published to assist engineers in designing a reliable composite overwrap repair. The former is recognised as a general code that covers pipes with different materials from steel to FRP while the latter is specifically focused on steel pipes.

In order to use composites for the repair of damaged pipelines, it is crucially important that they be designed based on a valid code to ensure that sufficient reinforcement has been provided. ASME PCC-2 and ISO/TS 24817 provide required parameters to design a repair system with sufficient stiffness, strength and thickness. The design revolves around the determination of a minimum thickness for the FRP wrap that reinstates the design pressure in the pipe in the presence of other probable loads.

10.3 Design of composite overwraps for pressure

Both of the aforementioned codes design the repair of pipes in the hoop and axial directions so that the original design pressure can be reinstated then select the stronger of the two as the design repair.

In the axial direction, both codes design for an equivalent imaginary force that is supposed to induce similar overall stress in the system as all other loads and moments combined. ISO presents this equivalent force as

$$F_{\text{eq}} = \frac{\pi}{4} pD^2 + \sqrt{F_{\text{ax}}^2 + 4F_{\text{sh}}^2} + \frac{4}{D}\sqrt{M_{\text{ax}}^2 + M_{\text{to}}^2} \tag{10.1}$$

in which p is the internal design pressure; D is the external diameter of pipe; F_{sh} is the applied shear load; M_{to} is the applied torsional moment; F_{ax} is the applied axial load and M_{ax} is the applied moment about the cross-sectional axis of the pipe. Unlike ISO, ASME does not propose any particular equation to calculate the equivalent axial force

but rather leaves it to the designer to calculate based on his judgement. ASME only indicates that the axial tensile load generated by a bending moment is $4M/D$.

When it comes to the hoop direction, ISO proposes Eqn (10.2) in order to calculate an equivalent pressure:

$$p_{\text{eq}} = p\left[1 + \frac{16}{(\pi D^2 p)^2}\left(F_{\text{sh}} + \frac{2}{D}M_{\text{to}}\right)^2\right] \tag{10.2}$$

ASME's hoop design equation is only based on internal pressure. ASME ignores the contribution of other loads such as the shear force and the torsional moment in generating hoop stresses. As is seen, ISO is a rather more advanced code when it comes to the calculation of effective axial force and effective pressure.

In addition to these equations, there is a pressure called 'live pressure' (denoted by P_{live}) that is used in both codes for the design of overwrap repair. Live pressure is basically the operating pressure at the time of application of repair which is naturally lower than or equal to the maximum allowable working pressure of the defected pipe.

With regard to designing composite overwrap repairs against the equivalent design pressure and the equivalent axial load, a range of composites are recognised by the code. These are typically those with aramid (AFRP), carbon (CFRP), glass (GFRP) or polyester or similar reinforcement material in a polyester, vinyl ester, epoxy or polyurethane matrix. The output of design is the thickness of repair laminate t_{design}, which will be expressed as the number of wraps n_{w} for installation purposes. Equation (10.3) gives the number of wraps based on the thickness of an individual wrap t_{layer}:

$$n_{\text{W}} = \frac{t_{\text{design}}}{t_{\text{layer}}} \tag{10.3}$$

Both design codes have taken the same approach towards considering the treatment of corrosion based on the extent of damage. The codes identify two potential defect Types: A and B, as per below:

- **Type A:** The defect is within the steel but is not leaking and is not expected to become a through-wall defect during the extended life of the repaired pipe. The defect can be internal or external. In Type A, the depth of defect is the only design parameter which in both codes is considered to be fully circumferential with a constant remaining pipe wall thickness.
- **Type B:** The defect is through-wall and the leaking steel requires both structural strengthening and sealing of the through-wall defect. For active internal corrosion, if the remaining wall thickness is expected to become smaller than 1 mm at the end of the pipe's service life, the repair design should be performed assuming a through-wall defect. Unlike Type A, the shape of the defect has a significant effect on the repair design in Type B. The considered defect shapes for Type B are circumferential, circular, near-circular and none circular shapes with an aspect ratio smaller than five.

Due to the similarities between the two major codes, design based on ISO 24817 is presented in detail followed by an elaboration of the major differences that exist between ISO and ASME.

10.4 Design based on ISO 24817

According to ISO 24817, each repair shall be allocated to a particular class following completion of a risk assessment. Repair classes are defined in Table 10.1. Class 1 repair covers design pressures up to 1 MPa (10 bar) and design temperatures up to 40 °C and is appropriate for the majority of the utility service systems. This class is intended for systems that are not safety-sensitive. Class 2 repair covers design pressures up to 2 MPa (20 bar) and design temperatures up to 100 °C excluding hydrocarbons. This class is appropriate for systems that possess specific safety-related functions. Class 3 repairs cover all fluid types and pressures up to the qualified upper pressure limit. This class is appropriate for systems transporting produced fluids. Applications in which the service conditions are more onerous or not included in the above are designated as Class 3. This classification will be used in defining the composite allowable strain and the pipe's derating service factor, which are required for certain design methods that will be discussed in the following sections. Depending on the class of repair and the target repair lifetime, allowable strains in the composites can be chosen from Table 10.2. The ratio of E_a/E_c identifies different FRP composites where E_c and E_a are the composite repair circumferential and axial elastic modules, respectively.

For defect Type A:

For this defect type, based on the available information and the project specifications, the designer is allowed to select different levels of design complexity based on his own judgement.

Table 10.1 Repair classes (ISO, 2006)

Repair class	Typical service	Design pressure	Design temperature
Class 1	Low specification duties, e.g. static head, drains, cooling medium, sea (service) water, diesel and other utility hydrocarbons	<1 MPa	<40 °C
Class 2	Fire, water/Deluge systems	<2 MPa	<100 °C
Class 3	Produced water and hydrocarbons, flammable fluids, gas systems Class 3 also covers operating conditions more onerous than described	Qualified upper limit	Qualified upper limit

Table 10.2 Allowable strain for composite laminates as a function of repair lifetime (ISO, 2006)

Modulus	Allowable strain Class 1%			Allowable strain Class 2%			Allowable strain Class 3%		
Repair lifetime (years)	2	10	20	2	10	20	2	10	20
For $E_a > 0.5E_c$									
ε_c	0.40	0.32	0.25	0.35	0.30	0.25	0.30	0.27	0.25
ε_a	0.40	0.32	0.25	0.35	0.30	0.25	0.30	0.27	0.25
For $E_a > 0.5E_c$									
ε_c	0.40	0.32	0.25	0.35	0.30	0.25	0.30	0.27	0.25
ε_a	0.25	0.16	0.10	0.10	0.10	0.10	0.10	0.10	0.10

- Method 1: Applicable to low level corrosion as judged by the designer and where long-term performance data are not available.
- Method 2: Applicable to cases where either due to high corrosion or lack of evidence to the contrary, the steel pipe cannot be relied upon and where long-term performance data are not available.
- Method 3: Elaborate design based on long-term performance testing data.

For defect Type B:

For this defect type, the designer has to design the repair based on one of the methods mentioned for defect Type A in addition to designing it as a through-wall defect. The results are to be compared and the stronger chosen.

10.4.1 Type A: method 1

This method is often chosen when there is adequate evidence that suggests the remaining thickness of the pipe is still significant. In this case, contribution of the remaining thickness of the pipe is considerable. The desired outcome of the design as mentioned previously is the minimum thickness of the composite wrap that reinstates its capacity to the original noncorroded capacity. Design parameters required are the equivalent axial force, the equivalent internal pressure, the live pressure, the tensile modulus of steel and composite and the allowable stress of steel.

Here, it is assumed that the steel pipe is capable of handling the axial stresses reasonably well and the repair composite is only helping in the hoop direction. As a result, the composite has to be adequately strong in the hoop direction only. The minimum required thickness is then calculable using Eqn (10.4):

$$\varepsilon_c = \frac{P_{eq}D}{2E_c t_{min}} - s\frac{t_s}{E_c t_{min}} - \frac{P_{live}D}{2(E_c t_{min} + E_s t_s)} \tag{10.4}$$

where P_{live} is the internal pressure in the pipe at the time of repair application. Having ε_c from Table 10.2, the minimum thickness can be easily calculated from Eqn (10.4). ISO indicates that the repair thickness should not exceed D/6.

There is a bit of controversy around the incorporation of P_{live} in this equation. The authors believe that P_{live} does not affect the repair laminate thickness. Because the composite is only applied after P_{live} has pressurised the steel to an initial strain, the composite would not contribute in carrying the original pressure and as such P_{live} should not affect the strain in the composite. This is elaborated further in Chapter 12.

10.4.2 Type A: method 2

This method is used for nonleaking pipes if the designer decides to ignore the remaining strength of the corroded pipe in the load carrying capacity due to high level corrosion or lack of adequate information on the extent and geometry of corrosion and the mechanical properties of the existing pipe. This method calculates the repair thickness based on the composite allowable strain only. Two thicknesses are to be found: one based on stresses in the hoop direction and one based on stresses in the axial direction, as given in Eqns (10.5) and (10.6), respectively. The greater of the two represents the minimum thickness of the required repair composite. The composite must have load carrying capacity in the longitudinal as well as the circumferential direction due to the fact that the composite is the only material relied upon to carry the loads being axial and/or circumferential.

$$t_{min} = \frac{1}{\varepsilon_c}\left(\frac{p_{eq}D}{2E_c} - \frac{F_{eq}}{\pi D}\frac{\nu}{E_c}\right) \tag{10.5}$$

$$t_{min} = \frac{1}{\varepsilon_a}\left(\frac{F_{eq}}{\pi D E_a} - \frac{p_{eq}D\nu}{2E_c}\right) \tag{10.6}$$

In Eqns (10.5) and (10.6), ε_c and ε_a are the composite repair allowable circumferential and axial strains, and ν denotes Poisson's ratio of the composite repair laminate in the circumferential direction. ε_c and ε_a should be determined based on Table 10.2.

10.4.3 Type A: method 3

The designer is allowed to choose this method provided that he has access to long-term performance data. ISO has proposed three different methods for carrying out performance-based testing. These methods are described in Annex E of ISO/TS 24817 as

- Survival testing, in which the repair system is subjected to a period of sustained loading for 1000 h;
- Regression testing, based on a series of tests on the repair system over different time periods and extrapolation to design life; and

Table 10.3 Service factor f_{perf}, for performance data of repair systems (ISO, 2006)

Service factor	Class 1			Class 2			Class 3		
Repair lifetime (years)	2	10	20	2	10	20	2	10	20
1000 h data	0.83	0.65	0.5	0.67	0.58	0.5	0.6	0.55	0.5
Design life data	1	0.83	0.67	0.83	0.75	0.67	0.75	0.71	0.67

- Regression testing of representative coupons followed by confirmation of long-term coupon test results with survival testing.

Once the data are obtained, similar to the first two methods, two possibilities would arise: (1) design assuming that part of the steel is intact or (2) design ignoring the steel. Equation (10.7) contains the formula for calculating t_{min} for case (1) and Eqn (10.8) the formula for case (2).

$$t_{min} = \left(\frac{p_{eq}D}{2} - st_s\right)\left(\frac{1}{s_{lt}f_{perf}}\right) \tag{10.7}$$

$$t_{min} = \left(\frac{p_{eq}D}{2} - \frac{\nu F_{eq}}{\pi D}\right)\left(\frac{1}{s_{lt}f_{perf}}\right) \tag{10.8}$$

As is seen, these are essentially similar to Eqns (10.4) and (10.5), with the only difference that the incorporation of P_{live} in the design is interestingly (and correctly, as will be discussed in Chapter 12) ignored, and $E_c\varepsilon_c$ is replaced with s_{lt}, which is the lower confidence limit of the long-term sustained stress. The resultant t_{min} is then increased by the inverse of f_{perf}, which is the service derating factor determined from Table 10.3. When it comes to the axial direction, the code does not see any need to consider the deratings and the lower confidence limits and allows the use of Eqn (10.6) without any modification for the service derating and the lower confidence limit of stress.

10.4.4 Type B: through-wall defects

By definition, a defect within the pipe is through-wall if the remaining pipe wall thickness at any point is 1 mm or less or if it is expected to be so at the end of the (after repair) extended design life of the pipe. Design of repair then varies based on the defect shape. ISO 24817 has considered three different shapes of defects, which are circular or near circular, axial slots, and circumferential slots. The design for a through-wall defect is experimentally based and requires performance test data. The equations are long and not to be repeated here. As an introduction only, ISO equations for circular or near-circular defects are presented below.

10.4.4.1 Through-wall circular or near-circular defect

In order to design repair of pipes defected by through-wall circular or near-circular shaped defects, ISO presents Eqn (10.9):

$$p = f_{T2} f_{leak} \sqrt{\left\{ \frac{0.001 \gamma_{LCL}}{\frac{(1-\nu^2)}{E_{ac}} \left\{ \frac{3}{512 t_{min}^3} d^4 + \frac{1}{\pi} d \right\} + \frac{3}{64 G t_{min}} d^2} \right\}} \tag{10.9}$$

where E_{ac} is the combined tensile modulus equal to $\sqrt{E_a E_c}$; G is the shear modulus of the repair laminate; p is the design internal pressure; ν is the Poisson's ratio of the repair laminate; d is the diameter of defect; t_{min} is the thickness of repair laminate; γ_{LCL} is the 95% lower confidence limit of energy release rate; f_{T2} is the temperature derating factor for through-wall defects and f_{leak} is the service derating factor given in Eqn (10.10).

Equation (10.9) is only valid for defects with $d \leq \sqrt{6Dt}$, where D is the pipe external diameter and t is the pipe wall thickness. The value of f_{leak} is determined either from Eqn (10.10), where $t_{life\text{-}time}$ is the design life, or in the presence of long-term performance data from Eqn (10.11), where f_D is the degradation factor defined in Annex G of ISO/TS 24817.

$$\begin{cases} f_{leak} = 0.83 \times 10^{-0.02088(t_{life-time}-1)} & \text{Class 1} \\ f_{leak} = 0.75 \times 10^{-0.01856(t_{life-time}-1)} & \text{Class 2} \\ f_{leak} = 0.666 \times 10^{-0.01584(t_{life-time}-1)} & \text{Class 3} \end{cases} \tag{10.10}$$

$$\begin{cases} f_{leak} = 0.83 f_D & \text{Class 1} \\ f_{leak} = 0.75 f_D & \text{Class 2} \\ f_{leak} = 0.666 f_D & \text{Class 3} \end{cases} \tag{10.11}$$

10.5 Design based on ASME PCC-2

The ASME PCC-2 approach is similar to ISO 24815 with only minor differences that are discussed below:

- ASME PCC-2 doesn't define any repair class but has two different articles about nonmetallic composite repairs. Article 4.1 talks about high-risk applications and Article 4.2 talks about low-risk applications.
- For the case in which the pipe contribution in carrying the load is considered, ASME PCC-2 suggests an equation similar to that of ISO 24817 (Eqn (10.4)) with two differences: the substitution of the term 'pipe allowable stress' by 'Specific Minimum Yield Stress', which

Table 10.4 Allowable (long-term) strain for repair laminate (ASME, 2011)

Load type	Symbol	Rarely occurring (%)	Continuously sustained (%)
$E_a > 0.5E_c$	ε_c	0.40	0.25
$E_c > 0.5E_a$			
Circumferential	ε_c	0.40	0.25
Axial	ε_a	0.25	0.10

Table 10.5 Service factor for repair laminate (ASME, 2011)

Test	Service factor (f)
1000 h data	0.50
Design life data	0.67

is the minimum yield stress of a pipe grade, and the assumption that the steel pipe yields, behaving as an elastic-perfectly plastic material without any hardening after yield.

- In ASME-PCC2, the allowable strain for repair laminate is slightly different from the ISO standard. ASME values are as given in Table 10.4.
- In the design of through-wall defects, the following differences are apparent. Firstly, the service factor, f_{perf}, is set to 0.333 or as per Table 10.5 if the performance data are available. This factor has also been used instead of f_{leak}, so ASME does not define a different derating factor for through-wall defects.
- In all through-wall equations of ASME, the ISO's ν^2 term is defined as $\frac{\nu_{ca}^2 Ea}{E_c}$, where ν_{ca} is the Poisson's ratio for the composite laminate in the circumferential direction.
- ASME PCC-2 does not offer any solutions for the circumferential through-wall defect.

10.6 Composite overwrap repair, application methods

Many composite overwrap repair systems have been introduced to the pipeline industry, their differences being in fibres, adhesive, resin and method of application. Carbon fibre, glass fibre and aramid fibre (Kevlar reinforcement) are the usual fibres used in these composite systems to provide for the required strength and stiffness. In general, two types of composite repair, namely layered system and wet lay-up system, are currently used for pipeline repair (Figure 10.1).

For layered systems, FRP composite is manufactured and cured in the factory and transferred to the field as a rigid product. Then it is bonded to the defected pipe by means of an adhesive. Repair using this system is limited to straight pipes only.

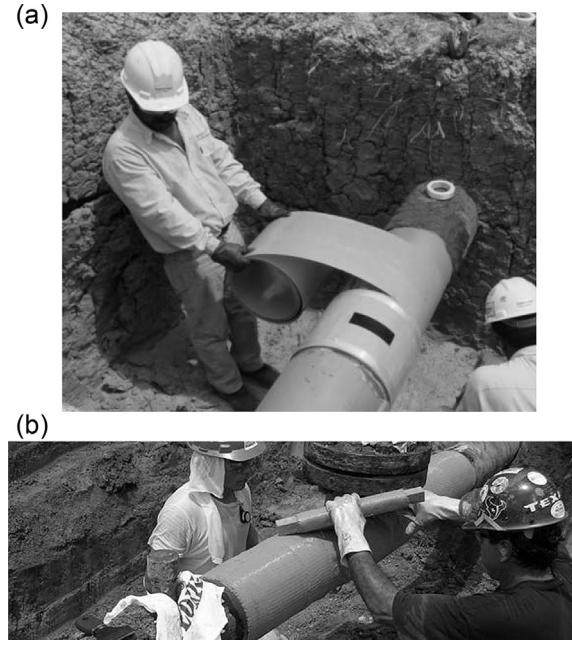

Figure 10.1 Two different types of composite systems: (a) layered system-ClockSpring® (Clock Spring® Company, 2007) and (b) wet lay-up system-Armor Plate® (Citadel Technologies, 2007, Armor Plate, 2011).

Unlike the layered systems, the wet lay-up systems are shaped into a composite onsite and due to their ease of application are more widely used. They typically come in two different types. The first type involves some type of fabric or sheet made of usual fibres (including carbon fibres, glass fibres and aramid fibres), impregnated by in situ application of resin to the materials. The second variations of the wet lay-up systems are cloths preimpregnated in the factory which are activated by heat, water or other catalysts in the field. These kinds of systems are normally protected in sealed bags and cold environments because once the bag is opened, the chemical reaction between the material and moisture in the environment temperature begins and the product will start curing.

To promote adhesion between the pipe and repair, the pipe is cleaned using sandblasting or other tools. This will remove rust, paint, oil, marine growth and other foreign matter that may cause initiation of debonding. During the cleaning process the surface of steel gets roughed and the roughness depends on the method of cleaning. Roughness can provide a sufficient mechanical bonding between steel and repair. The ISO publishes a number of standards relating to surface preparation of steel. ISO 8504-1 provides guidance on preparation of steel substrates before coating and the methods that are available for cleaning steel surfaces are explained. ISO 8501-1, ISO 8502-12 and ISO 8503-1 provide methods of assessing surface cleanliness and roughness. After cleaning of the pipe surface, in order to restore the pipe to its original

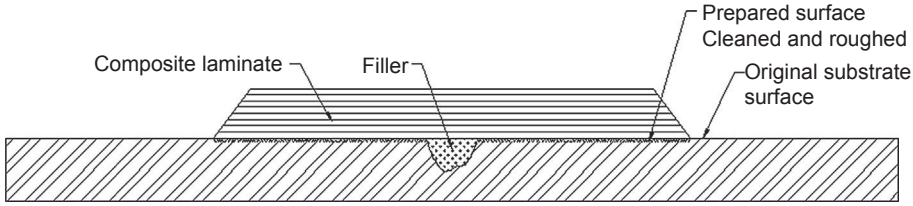

Figure 10.2 Typical section of composite repair.

geometry (from the outer side), all of the defected areas (corroded or mechanically damaged) are filled with a filler (usually a two-part, high-compressive-strength epoxy putty), which would also help with the transfer of the load from the pipe to the wrap (Green, 2010).

After preparing of the pipe surface and applying the putty, the composite laminate is applied circumferentially along the cleaned area from one side to another side. The number of required layers is determined by designer based on a proper design method. All of the design methods are explained in previous sections. The typical section of a pipe repaired by overwrap system is shown in Figure 10.2.

Acknowledgement

The authors gratefully acknowledge the support of the Cooperative Research Centre for Advanced Composite Structures (CRC-ACS) Ltd.

References

Alexander, C., Cercone, L., Lockwood, J., 2008. Development of a carbon-fibre composite repair system for offshore risers. In: The 27th International Conference on Offshore Mechanics and Arctic Engineering, OMAE2008. The American Society of Mechanical Engineering, Estoril, Portugal.

Alexander, C., Ochoa, O.O., 2010. Extending onshore pipeline repair to offshore steel risers with carbon-fiber reinforced composites. Composite Structures 92, 499−507.

Alexander, C.R., 2007. Development of a Composite Repair System for Reinforcing Offshore Risers. Doctor of Philosophy, Texas A&M University.

Alexander, C.R., Wilson, F.D., 1999. Analysis, testing and proposed guidelines for repairing pipelines with composite materials. In: Pressure Vessel and Piping Conference. Boston, MA.

Armor Plate, I. 2011. http://armorplateinc.com/. (online accessed 12.07.11).

ASME, 2006. Repair of Pressure Equipment and Piping.

ASME, 2009. B31.4: Pipeline Transportation Systems for Liquid Hydrocarbons and Other Liquids.

ASME, 2010. B31.1: Power Piping.

ASME, 2011. Pcc-2: Repair of Pressure Equipment and Piping.

Citadel Technologies, 2007. http://www.cittech.com.

Clock Spring Company. 2007. http://www.clockspring.com/. (online accessed 10.07.11).
CSA, 2007. Z662−07: Oil and Gas Pipeline Systems.
Duell, J.M., Wilson, J.M., Kessler, M.R., 2008. Analysis of a carbon composite overwrap pipeline repair system. International Journal of Pressure and Piping 85, 782−788.
EGIG, 2005. 6th Report of European Gas Pipeline Incident Data Group, December, 2005, 6th EGIG Report 1970−2004, Gas pipeline Incidents, 2−31.
Freire, J.L.F., Vieira, R.D., Castro, J.T.P., Benjamin, A.C., 2007. Part 5: rupture tests of pipeline containing complex-shaped metal loss defects. Experimental Techniques 31, 57−62.
Green, M., 2010. Composites Offer Effective Offshore Pipe Repair Alternative. Offshore: PennWell Corporation.
ISO, 2006. ISO/TS 24817: Petroleum, Petrochemical and Natural Gas Industries—Composite Repairs for Pipework—Qualification and Design, Installation, Testing and Inspection. ISO.
Kessler, M.R., Walker, R.H., Kadakia, D., Wilson, J.M., Duell, J.M., Goertzen, W.K., 2004. Evaluation of carbon/epoxy composites for structural pipeline repair. In: The Fifth International Pipeline Conference, IPC2044. American Society of Mechanical Engineers, Calgary, Alberta, Canada, pp. 1427−1432.
Koch, G.H., Brongers, M.P.H., Thompson, N.G., Virmani, Y.P., Payer, J.H., 2001. Corrosion Cost and Preventive Strategies in the United States. Federal Highway Administration, Office of Infrastructure Research and Development.
Meniconi, Luiz C.M., Freire, José L.F., Vieira, Ronaldo D., Diniz, J.L.C., 2002. Stress analysis of pipelines with composite repairs. In: The Fourth International Pipeline Conference, Calgary, Alberta, Canada.
Mohitpour, M., Golshan, H., Murray, A., 2003. Pipeline Design & Construction: A Practical Approach, second ed. American Society of Mechanical Engineers, New York, NY.
Perrut, V.A., Meniconi, L.C.M., Filho, B.G.D.S., 2006. Evaluation of composite sleeves for reinforcement of dented pipeline. In: The Sixth International Pipeline Conference, IPC2006, September 25−29, 2005. The American Society of Mechanical Engineering, Calgary, Alberta, Canada.
Shouman, A., Taheri, F., 2009. An investigation into the behaviour of composite repaired pipelines under combined internal pressure and bending. In: 28th International Conference on Ocean, Offshore and Arctic Engineering. American Society of Mechanical Engineers, Hawaii.
Shouman, A., Taheri, F., 2011. Compressive strain limits of composite repaired pipelines under combined loading states. Composite Structures 93, 1538−1548.
Toutanji, H., Dempsey, S., 2001. Stress modeling of pipelines strengthened with advanced composites materials. Thin-Walled Structures 39, 153−165.

This page intentionally left blank

Effect of live pressure on overwrap design

11

A.S. Virk[1], H.R. Ronagh[2], N. Saeed[2,3]
[1]Griffith University, Gold Coast, QLD, Australia; [2]The University of Queensland, Brisbane, QLD, Australia; [3]Cooperative Research Centre for Advanced Composite Structures, Port Melbourne, VIC, Australia

11.1 Introduction

Pipelines are used to transport oil and natural gas and during the course of service the pipelines are subjected to harsh operating conditions which include high pressure, corrosive environments and accidental damage. Transportation of oil or gas over time can lead to internal and/or external metal loss in a pipeline, due to erosion and/or corrosion. The reduction in the wall thickness of a pipeline sanctions a reduction in the operating capacity. In order to re-establish the designed operating capacity of an eroded, corroded or damaged pipeline, repairs have to be carried out. Conventionally, most steel pipelines are repaired by removing the corroded part and replacing it with a new pipe or by reinforcing the defected part with an external steel sleeve (Mohitpour et al., 2003; Freire et al., 2007; Pipelines International, 2009).

Recently, fibre-reinforced polymer (FRP) matrix composite overwrap repair systems have been introduced and accepted as an alternative repair system. They have been integrated into the American Society of Mechanical Engineers (ASME) ASME B31.4 (ASME, 2009) and B31.8 (ASME, 2010) pipeline codes and also Canadian Standards Association (CSA) CSA Z662 (CSA, 2007). This method involves reinforcing the corroded part of a pipeline by wrapping FRP around the pipe. Repair with FRP materials presents several advantages over conventional methods. Firstly, the repair is quicker to be performed as the application is easy and straightforward, and the repair can be performed on an operational pipeline. The risk of fire and explosion is completely eliminated (Duell et al., 2008) as the repair is performed at considerably lower temperatures than welding. FRP repair is also more economical than other repair methods conventionally used. In one comparative study, it was found that the FRP repair was 24% cheaper than the welded steel sleeve repair and 73% cheaper than replacing the defected pipe section (Koch et al., 2001).

FRP overwrap repair systems can be considered as a lifetime repair for the cases where they can retard the growth of external corrosion by isolating the external defect from the corrosive environment. During the past decade it has been proven that FRP is a viable repair system and can be performed adequately under different environmental conditions in industrial projects (Duell et al., 2008). The behaviour of pipes repaired with composite overwraps has been studied by many researchers in order to understand the effects of different parameters (Alexander et al., 2008; Alexander and

Rehabilitation of Pipelines Using Fiber-reinforced Polymer (FRP) Composites. http://dx.doi.org/10.1016/B978-0-85709-684-5.00011-4

Ochoa, 2010; Kessler et al., 2004; Meniconi et al., 2002) and different loading conditions (Shouman and Taheri, 2011; Alexander and Ochoa, 2010).

ASME PCC-2 and ISO 24,817 pipes/pipelines composite repair codes were developed in order to provide the rules for designing a reliable and robust repair. Equation (11.1) has been proposed by ASME PCC-2 and ISO 24,817 for the design of composite repair when the defected pipe contributes to the load carrying capacity:

$$\varepsilon_c = \frac{PD}{2E_c t_{\min}} - s\frac{t_s}{E_c t_{\min}} - \frac{P_{\text{live}} D}{2(E_c t_{\min} + E_s t_s)} \tag{11.1}$$

In Eqn (11.1), P_{live} is the internal pressure in the pipe at the time of the repair application, E_c and E_s are the composite and the steel module of elasticity, t_s is the remaining pipe wall thickness, $t_{\min}$ is the minimum required thickness of the composite layer, D is the pipe diameter, P is the design pressure and finally ε_c is the composite allowable strain. The only difference between the two codes is the definition of s—ASME PCC-2 identifies it as the specific minimum yield stress while ISO 24,817 recognizes it as the pipe allowable stress.

Equation (11.1) indicates that the thickness of composite repair depends on P_{live}. In order to assess the validity of this equation, two different approaches are followed in this chapter: analytical and finite element analysis (FEA) modelling.

11.2 Incorporation of live pressure in the design: analytical model

As shown in Eqn (11.1), both design codes have included P_{live} in their design equations for defect Type A, Method 1, although interestingly (and correctly as will be seen here) have not considered it for defect Type A, Method 3. The inclusion means that the amount of internal pressure at the time of the repair application has a significant effect on the design of the repair composite laminate. To the contrary, the authors believe that P_{live} does not affect the repair laminate thickness. Because the composite is only applied after P_{live} has pressurized the steel to an initial strain, the composite would not contribute in carrying the original pressure and as such P_{live} should not affect the strain in the composite. The applied composite repair will only be strained when the internal pressure differs from P_{live} pressure. Using the following analytical approach, this can be proven.

Assuming that the pipe to be repaired is thin-walled (diameter to thickness ratio is more than 20, which is the case considered in the codes) and the repair is applied on the defected pipe at the internal pressure P_{live}, the strain in the damaged pipe, ε_0, due to the internal pressure, P_{live}, before applying the repair can be found from Eqn (11.2):

$$\varepsilon_0 = \frac{P_{\text{live}} D}{2E_s t_s} \tag{11.2}$$

After applying the repair, the average elastic modulus of the pipe and composite assembly, E_{av}, is calculated using Eqn (11.3):

$$E_{av} = \frac{E_c t_{min} + E_s t_s}{(t_{min} + t_s)} \tag{11.3}$$

The strain in the repaired pipe at the internal pressure $P_{yield,}$ which causes yielding of the steel pipe, is then calculated from simple equilibrium, as given in Eqn (11.4):

$$\varepsilon_{elastic} = \frac{1}{E_{av}} \frac{(P_{yield} - P_{live})D}{2(t_{min} + t_s)} + \varepsilon_0 = \frac{(P_{yield} - P_{live})D}{2(E_c t_{min} + E_s t_s)} + \frac{P_{live} D}{2E_s t_s} \tag{11.4}$$

The yield strain of the pipe is also given by

$$\varepsilon_{elastic} = \frac{s}{E_s} \tag{11.5}$$

Equating Eqns (11.4) and (11.5) and solving for P_{yield} gives

$$P_{yield} = \frac{2s(E_c t_{min} + E_s t_s)}{DE_s} - P_{live} \frac{E_c t_{min}}{E_s t_s} \tag{11.6}$$

For the simplicity of calculations, the behavior of the pipe steel is assumed to be elastic-perfectly plastic. Therefore as the pressure rises above P_{yield}, the steel pipe carries no further load and any further load is only carried by the composite. Hence, the strain in the composite due to the pressure beyond P_{yield} is given by

$$\varepsilon_{plastic} = \frac{(P - P_{yield})D}{2E_c t_{min}} \tag{11.7}$$

Finally, the total hoop strain in the pipe, which is calculated by summing all the strains, becomes

$$\varepsilon_s = \varepsilon_{elastic} + \varepsilon_{plastic} = \frac{s}{E_s} + \frac{(P - P_{yield})D}{2E_c t_{min}} \tag{11.8}$$

The strain in the composite repair laminate is then calculable using Eqn (11.9)

$$\begin{aligned} \varepsilon_c &= \varepsilon_{elastic} + \varepsilon_{plastic} - \varepsilon_0 \\ &= \frac{(P_{yield} - P_{live})D}{2(E_c t_{min} + E_s t_s)} + \frac{P_{live} D}{2E_s t_s} + \frac{(P - P_{yield})D}{2E_c t_{min}} - \frac{P_{live} D}{2E_s t_s} \end{aligned} \tag{11.9}$$

Substituting for P_{yield} from Eqn (11.9) and simplifying gives

$$\varepsilon_c = \frac{PD}{2E_c t_{\min}} - s\frac{t_s}{E_c t_{\min}} \tag{11.10}$$

Equation (11.10) suggests that the strain in the composite repair laminate is independent of the live pressure acting on the pipe at the time of repair application.

11.3 Finite element parametric study

To further evaluate the validity of including P_{live} in Eqn (11.1), a parametric study was carried out using FEA. A range of repair scenarios were assumed and the repair thickness was calculated according to ASME PCC-2 and ISO 24,817 (Eqns (11.1) and (11.10)). The corresponding hoop strain in the pipe and the repair laminate for each design scenario were estimated using FEA at the design pressure, then compared to the allowable composite strain. The geometrical and mechanical properties of the pipe to be repaired are given in Table 11.1. The design pressure for the pipe was calculated to be 27.25 MPa according to ASME B31.4, considering a design factor of 0.72 (ASME, 2009).

The repair laminate was assumed to be reinforced with a bidirectional carbon fibre woven fabric with equal number of tows by weight in the weft and warp direction. The matrix was assumed to be epoxy. The laminate properties used for the FEA simulation were calculated using rule-of-mixtures (Daniel and Ishai, 1995), assuming a fibre volume fraction of 40%. The laminate elastic properties are given in Table 11.2. To calculate the repair thickness, the composite allowable strain (ε_c) was limited to 0.3%, selected as a number in between the two extremes (0.25% and 0.40%) proposed by ASME PCC-2 and also equal to the allowable strain for a class 2 repair with a 10 year lifetime.

Different design scenarios that were considered in this study are presented in Table 11.3. The erosion/defect was assumed to be circumferential with a constant circumferential depth and the wall thinning was considered in the range of 30−80% in increments of 10%. The maximum allowable internal pressure for the corroded pipe was calculated based on ASME B31.4 considering the remaining wall thickness of the pipe. In the study, the live pressure varied from 0 to 100% of the maximum allowable live pressure in steps of 25%. The minimum laminate thickness for each repair situation was calculated using Eqn (11.1) (based on ISO 24,817 and ASME PCC-2) and Eqn (11.10), as given in Table 11.3.

Table 11.1 Pipe material and pipe size

Pipe material: *API 5L X65*		**Pipe size: 150 ND**	
Modulus (GPa)	200	OD (mm)	168.3
Yield (MPa)	448	Wall (mm)	7.11

Table 11.2 Laminate mechanical properties

Modulus in thickness direction (MPa), E_{TT}	7560
Modulus in hoop direction (MPa), E_{HH}	50,600
Modulus in axial direction (MPa), E_{AA}	50,600
Poisson's ratio, ν_{TH}	0.05
Poisson's ratio, ν_{TA}	0.05
Poisson's ratio, ν_{HA}	0.04
Shear modulus (MPa), G_{TH}	3170
Shear modulus (MPa), G_{TA}	2200
Shear modulus (MPa), G_{HA}	3170
Allowable repair laminate circumferential strain, ε_c	0.3%

The pipe was modelled assuming an elastic, perfectly plastic behaviour with a yield stress of 448 MPa. The material orientation for the anisotropic repair laminate is shown in Figure 11.1. The repair laminate through thickness modulus, E_{TT}, and the axial modulus, E_{AA}, were orientated along the directions '1' and '2', respectively, as shown in Figure 11.1(b).

The pipe and the repair laminate were modelled using 2D axisymmetric elements because the defect was assumed to be circumferential with a constant depth (Abaqus CAX4R, which is a 4-node bilinear axisymmetric quadrilateral, reduced integration and hourglass control element). The finite element (FE) mesh consisted of 800 and 2400 elements for the pipe and the repair laminate, as shown in Figure 11.1(a). The repair laminate thickness for each model is given in Table 11.3.

The axisymmetric pipe and composite repair laminate were constrained using symmetrical boundary conditions along the wall thickness in the *Y*-axis near the lower end of the assembly, as shown in Figure 11.2. The pressure load was applied to the internal surface of the tube. The pressure load for all models started from P_{live} and gradually ramped up to the design pressures.

The interface between the pipe and the repair laminate for models with zero P_{live} were modelled using tie constraints, that is the bond between the pipe and the repair laminate was assumed to be perfect. In the other models, the interface between the pipe and the repair laminate was modelled using standard surface-to-surface contact between the pipe outer surface and the repair inner surface. The tangential (sliding) behaviour of the contact surface was modelled as rough surface, that is once the contact surface nodes came into contact, the sliding ceased. The normal behaviour of the contact surface was modelled using penalty method and no separation was allowed once the surfaces came into contact. The above specified interaction properties led to a perfect bond between the contact surfaces once they came into contact. For the models where the repair was applied at nonzero live pressure, a small gap was modelled between the pipe and the repair laminate, as shown in Figure 11.3. The

Table 11.3 Different design scenarios

Defect depth %	Maximum allowable internal pressure in damaged pipe	t_{min} (mm)										
		ASME PCC-2			ISO 24,817							
		P_{live} (percentage of the maximum allowable internal pressure)										
		0	25	50	75	100	0	25	50	75	100	Equation (11.10)
80	5.45	10.9	10.4	9.9	9.5	9.0	12.1	11.6	11.1	10.6	10.1	10.9
70	8.18	8.8	8.3	7.7	7.2	6.8	10.6	10.0	9.4	8.8	8.3	8.8
60	10.90	6.7	6.2	5.7	5.3	4.9	9.1	8.4	7.8	7.3	6.8	6.7
50	13.63	4.6	4.2	3.8	3.5	3.2	7.6	6.9	6.4	5.9	5.4	4.6
40	16.35	2.5	2.3	2.0	1.8	1.7	6.0	5.5	5.0	4.6	4.2	2.5
30	19.08	0.4	0.4	0.3	0.3	0.3	4.5	4.1	3.7	3.4	3.1	0.4

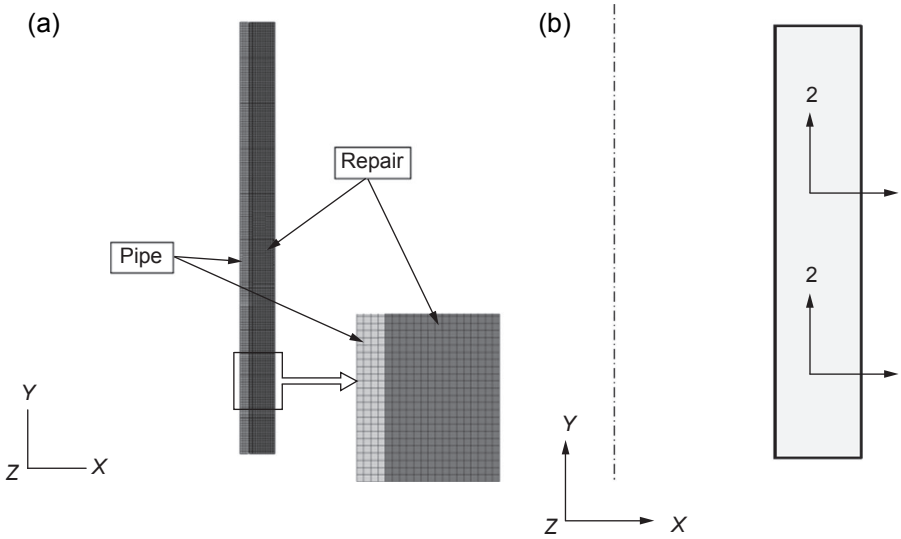

Figure 11.1 (a) FEA mesh and (b) material orientation for repair laminate.

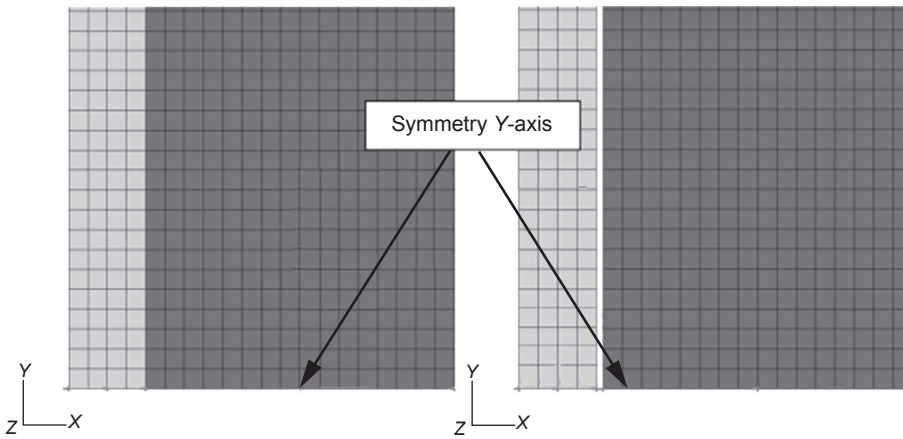

Figure 11.2 Boundary condition definition for the FEA model.

gap was equal to the expansion of the pipe under P_{live} load. Consequently, when the live pressure was applied, the pipe outer diameter and the repair inner diameter came into contact, as shown in Figure 11.3, and a perfect bond was simulated.

The strain in the composite repair laminate predicted by FEA at the design pressure for the repair designed according to ASME, ISO (Eqns (11.1) and (11.10) are shown in Figure 11.4). Ideally the strain in the repair laminate at the design pressure should not exceed the allowable composite strain, but the maximum strain in the repair laminate designed according to Eqn (11.1) (ASME/ISO) exceeds the allowable composite strain for various repair situations (Figure 11.4).

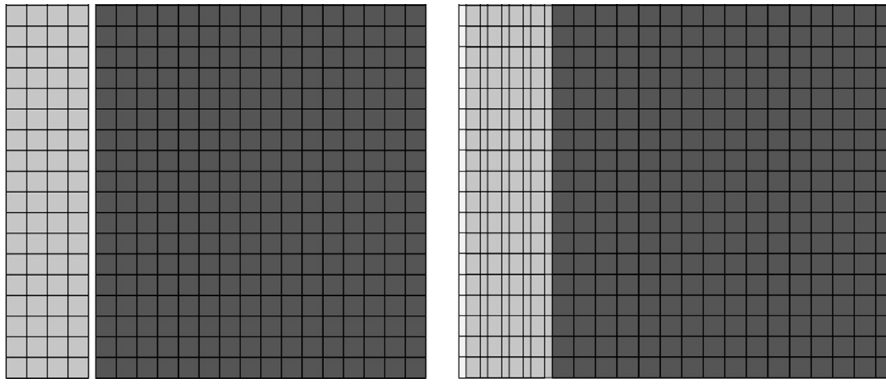

Figure 11.3 FEA model ($P_{live} > 0$) showing the gap between pipe and repair laminate.

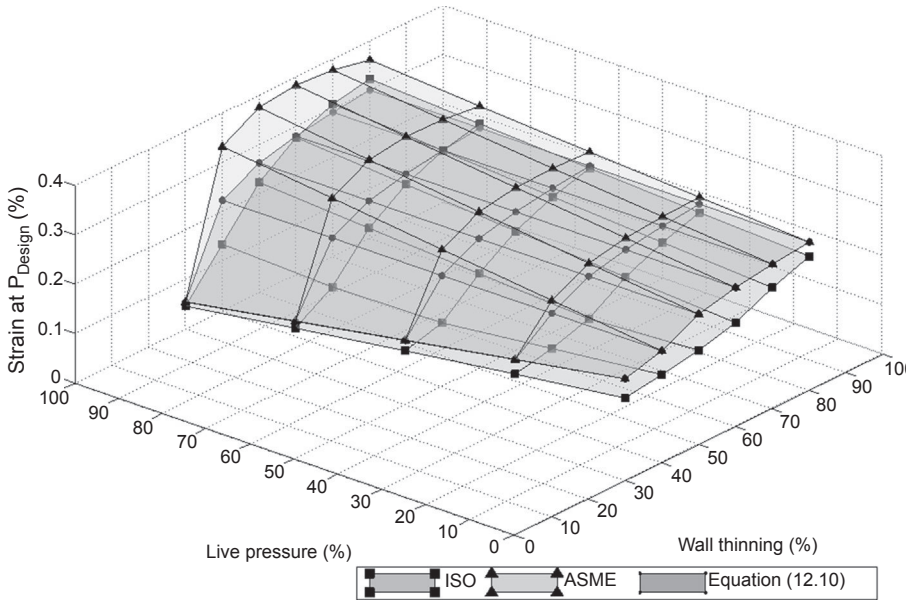

Figure 11.4 Comparing strain in the composite at design pressure.

At zero live pressure, the repair thicknesses calculated using ASME and Eqn (11.10) are similar, which bring about similar strains in the composite repair. The corresponding strain varies from 0.21 to 0.3% for wall thinning of 30−80%, respectively. The repair thickness calculated using ISO was larger than that calculated using ASME and Eqn (11.10) because the ISO standard uses allowable stress in Eqn (11.1) and the allowable stress is lower than the yield stress of the pipe material. The strain in the ISO repair laminate at the design pressure was 0.17−0.27% for wall thinning of 30−80%, respectively, which is lower than ASME and Eqn (11.10) laminate strain.

As the live pressure increases, the repair thickness designed according to ASME decreases for a given wall thinning because in Eqn (11.1) subtraction of strain due to

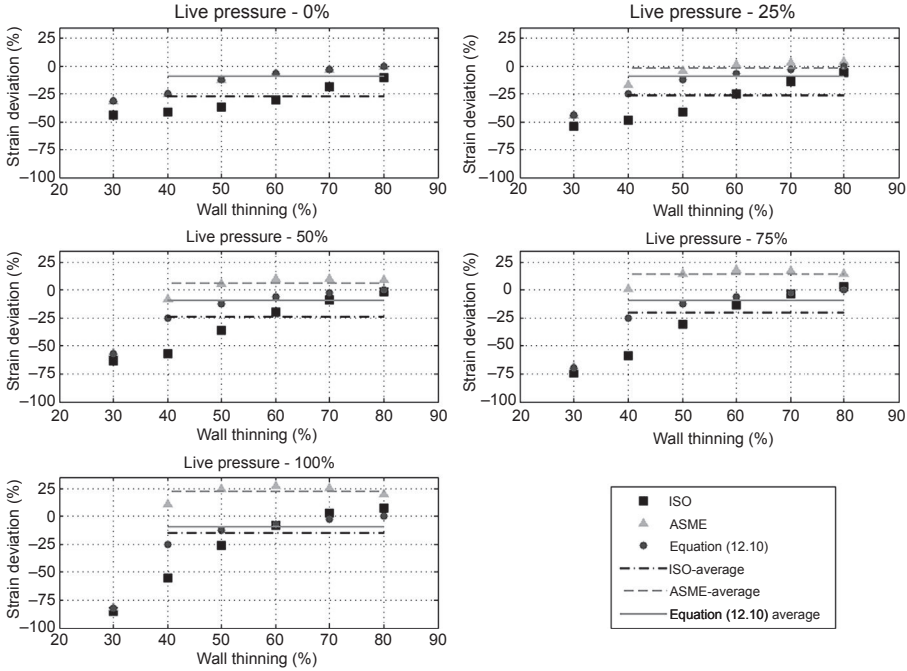

Figure 11.5 Strain deviation in the composite repair at design pressure.

P_{live} gives a thinner repair (Table 11.3). The repair thickness generated using Eqn (11.10) stays the same as it is independent of the live pressure. Comparing the strain in the repair laminates (Figure 11.4), it is clear that the strain in the ASME laminate is more than the strain given by Eqn (11.10) for nonzero live pressure. The strain in the ASME laminate increases linearly with the rise in the live pressure and exceeds the allowable strain, suggesting that the repair wall thickness is inadequate to limit the strain in the repair laminate. The strain in the Eqn (11.10) laminate is not affected by the live pressure and remains unchanged, signifying that the strain in the composite repair is independent of the live pressure.

For the majority of design situations the ISO laminate repair thickness is larger than the Eqn (11.10) laminate thickness because in Eqn (11.1) 's' is allowable stress, which is less than the yield stress of the pipe material. But at higher live pressures and larger wall thinning, P_{live} becomes a dominating factor and the repair thickness predicted by the ISO standard is smaller than that given by Eqn (11.10) (Table 11.3). The strain in the ISO laminate predicted by FEA was considerably less than that given by Eqn (11.10) for the majority of the design situations, but at maximum live pressure and higher wall thinning (the most critical repairs), the strain in the ISO laminate exceeds the allowable composite strain.

At the maximum live pressure, the strain in the composite repair designed according to ASME and ISO (Eqn (11.1)) varies from 0.05 to 0.36% and 0.05 to 0.32%, respectively, for wall thinning of 30−80%. The strain in the repair designed using Eqn (11.10) varies from 0.05 to 0.3% for wall thinning of 30−80%, respectively.

The pipe design pressure is calculated using a design factor of 0.72 according to ASME B31.4. This design factor causes the repaired pipe to yield only if the wall thinning of the eroded pipe is more than 28% (1−0.72 = 0.28). As 30% wall thinning is close enough to 28%, the yielding of the pipe is easily influenced by the assumptions made to calculate the repair thickness, that is the pipe is thin-walled, the stress is uniformly distributed through the wall thickness and only hoop stress is considered. Whereas FEA takes into account the radial stress in the pipe, Poisson's ratio effect (contraction in the axial direction due to hoop stress) and the constraints applied by the repair to the contraction of the pipe in the axial direction (because of the bond between the repair and pipe, stiffness of the repair resists the pipe's axial contraction). These factors alter the assumed uniform stress gradient through the pipe and increase the pressure required to yield the repaired pipe. The significant loading (straining) of the composite repair laminate only takes place after the pipe yields. This is because the elastic modulus of the pipe (200 GPa) is higher than the composite modulus (≈50 GPa), and thus the majority of the load is carried by the pipe, until the pipe yields. Therefore the strain in the composite laminate for 30% pipe wall thinning is not used to derive any conclusions.

The deviation of the composite laminate strain (predicted by FEA) from the designed allowable strain in the composite is shown in Figure 11.5 (zero signifies no deviation). The strain in the repair laminate designed according to the ASME standard is 10% (average, ignoring 30% wall thinning) lower than the allowable composite strain at zero live pressure. But as the live pressure increases, the strain in the composite increases and exceeds the allowable composite strain by 22% (average, ignoring 30% wall thinning). The repair laminate designed according to the ISO standard gives an average deviation of −27% to −16% in the composite strain for zero live pressure to maximum live pressure, respectively. As the live pressure increases, the strain in the composite decreases for smaller wall thinning, but for larger wall thinning, the strain in the composite increases and exceeds the allowable composite strain.

The strain in the laminate design according to Eqn (11.10) gives an average deviation of −10% for all of the design cases, hence the strain in the composite repair is not influenced by the live pressure in the tube.

A similar study was carried out by the authors using glass fibre-reinforced epoxy composites as the repair material, and a similar trend in the composite strain values was observed for the repair designed using ASME, ISO and Eqn (11.10). The results are presented in Saeed et al. (2012).

11.4 Conclusions

The repair laminate thickness calculated using ASME standard (Eqn (11.1)) underestimates the required repair thickness when the internal pressure is not zero during the repair installation; as such, the hoop strains in the laminate exceed the allowable laminate strain.

The repair laminate thickness calculated according to ISO standard is conservative for most design cases but gives inadequate repair thickness for situations in which the live pressure and wall thinning are larger.

The live pressure does not influence the hoop strain in the repair laminate at the design pressure. A correct estimate for the composite repair thickness is calculated by ignoring the live pressure and using the yield stress as pipe allowable stress in the repair equation.

Acknowledgements

This work was undertaken as part of a CRC−ACS research program, established and supported under the Australian Government's Cooperative Research Centres Program.

References

Alexander, C., Cercone, L., Lockwood, J., 2008. Development of a carbon-fibre composite repair system for offshore risers. In: The 27th International Conference on Offshore Mechanics and Arctic Engineering, OMAE2008. The American Society of Mechanical Engineering, Estoril, Portugal.

Alexander, C., Ochoa, O.O., 2010. Extending onshore pipeline repair to offshore steel risers with carbon-fiber reinforced composites. Composite Structures 92, 499−507.

ASME, 2009. B31.4: Pipeline Transportation Systems for Liquid Hydrocarbons and Other Liquids.

ASME, 2010. B31.1: Power Piping.

CSA, 2007. Z662−07: Oil and Gas Pipeline Systems.

Daniel, I.M., Ishai, O., 1995. Engineering mechanics of composite materials: book review. Applied Mechanics Reviews 48, B113.

Duell, J.M., Wilson, J.M., Kessler, M.R., 2008. Analysis of a carbon composite overwrap pipeline repair system. International Journal of Pressure and Piping 85, 782−788.

Freire, J.L.F., Vieira, R.D., Diniz, J.L.C., Meniconi, L.C., 2007. Part 7: effectiveness of composite repairs applied to damaged pipeline. Experimental Techniques 31, 59−66.

Kessler, M.R., Walker, R.H., Kadakia, D., Wilson, J.M., Duell, J.M., Goertzen, W.K., 2004. Evaluation of carbon/epoxy composites for structural pipeline repair. In: The Fifth International Pipeline Conference, IPC2044. American Society of Mechanical Engineers, Calgary, Alberta, Canada, pp. 1427−1432.

Koch, G.H., Brongers, M.P.H., Thompson, N.G., Virmani, Y.P., Payer, J.H., 2001. Corrosion Cost and Preventive Strategies in the United States. Federal Highway Administration, Office of Infrastructure Research and Development.

Meniconi, L.C.M., Freire, J.L.F., Vieira, R.D., Diniz, J.L.C., 2002. Stress analysis of pipelines with composite repairs. In: The Fourth International Pipeline Conference. Calgary, Alberta, Canada.

Mohitpour, M., Golshan, H., Murray, A., 2003. Pipeline Design & Construction: A Practical Approach, second ed. American Society of Mechanical Engineers, New York, USA.

Pipelines International, 2009. Evaluating Different Rehabilitation Approaches [Online]. Available: http://pipelinesinternational.com/news/evaluating_different_rehabilitation_approaches/009345/ (accessed July 2011).

Saeed, N., Ronagh, H., Virk, A., Ashraf, M., 2012. Investigating the effects of pipe live pressure on the design of composite overwrap repairs. In: The Australasian Structural Engineering Conference (ASEC 2012). Perth.

Shouman, A., Taheri, F., 2011. Compressive strain limits of composite repaired pipelines under combined loading states. Composite Structures 93, 1538−1548.

Clamp and overwrap repairs of oilfield pipelines

12

L.P. Djukic[1,2], *W.S. Sum*[3], *K.H. Leong*[3], *A.G. Gibson*[4]
[1]Advanced Composite Structures Australia Pty Ltd, Port Melbourne, VIC, Australia; [2]Cooperative Research Centre for Advanced Composite Structures Ltd, Port Melbourne, VIC, Australia; [3]PETRONAS Research, Kajang, Selangor, Malaysia; [4]Newcastle University, Newcastle-upon-Tyne, UK

12.1 Introduction

A long-standing challenge with the use of metallic oil and gas (O&G) infrastructure is the management of corrosion damage. The forms of damage during the service life of pipelines can include gouging, denting and corrosion. This infrastructure is used in dry conditions (e.g. sections of risers above water and piping on platforms), wet conditions (e.g. risers at the splash zones) or fully submerged underwater conditions (e.g. subsea risers or pipelines).

Several factors influence the selection of a pipeline repair method. Generally, new technologies are not readily accepted by O&G operators because, in the absence of established service track records, the risk of hydrocarbon loss in the event of failure is deemed to be unacceptably high. Moreover, the severity of the pipeline damage, location, operating and environmental conditions, fluid composition, cost and urgency for repair all contribute to the ultimate selection of a repair method.

Repairs of oilfield pipelines can be broadly categorized into two forms. The first involves cutting and replacing the damaged section, which generally involves welding and other hot work operations. The second involves the application of some external fixtures or attaching a fresh piece of material over the damaged area, which could also involve hot work. Depending on the requirements of the repair, the latter category can be further broken down into two subcategories, each requiring an added external structure. The first is a repair where the pipeline strength is reinstated, either completely or partially with an appropriate pressure derating. The second is a leak containment repair, where the reinstatement of the pipeline strength is not the main consideration. Combined functionality repairs can be designed and used as required.

When selecting the repair method, one of the main considerations is minimization of the shutdown time. Performing repairs 'live' without a shutdown presents the highest economic benefit (McGeorge et al., 2009). It is understood that generally wall thinning defects can be repaired live, while through-wall leaking defects require shutdown, although a hot-tap bypass could minimize interruption to operation. Hence, it is necessary to develop methods that could rapidly repair or avert leaking defects thus minimizing any downtime. Normally, when corrosion monitoring

Rehabilitation of Pipelines Using Fiber-reinforced Polymer (FRP) Composites. http://dx.doi.org/10.1016/B978-0-85709-684-5.00012-6

systems are effectively implemented, potential leaks are avoided by the timely installation of an external repair to the corroded region.

A well accepted method of repair involving an external fixture is the utilization of mechanical clamps (also known as sleeves) to encase the damaged region. These can be applied for both leak containment and strengthening (Coley and Caraballo, 2011). The clamps are typically metallic and consist of two-piece flanged shells with oversized annuli that fit over the pipe, with perimeter elastomeric seals for fluid containment. The clamps are fixed together via a series of bolts on the flanges. For underwater applications, they are normally fitted with aluminium anode blocks for cathodic protection.

A variation of this technology, often referred to as a grouted sleeve, consists of in-fill grouting of the annulus between sleeve and pipe (Sum and Leong, 2014; Shamsuddoha et al., 2013a,b; Leong et al., 2009). Grouted sleeves can be considered for both leak-proofing and pipeline strengthening (D'Mello and Boswell, 1999). The in-fill grout, of which cementatious and polymeric versions have been used, serves as a load transfer medium from the damaged section of the pipe to the sleeve. This provides not only hoop reinforcement but also axial strengthening to corroding or leaking pipes and can be particularly useful in arresting external corrosion of pipes, while restoring the pipe to its original rated pressure.

Repair clamps cover a range of API[1] pipe sizes between 1.5 and 48 in, depending on the supplier. They are rated for different standard pressures (e.g. 1000, 1500 psi) but can be designed for higher pressures. Weight can be an issue for larger sizes and higher pressures, hence limiting the scope of application due to increasing complexity of installation of the clamp. Operators typically stock up on clamps for standard pipe sizes for unplanned repairs. However, humidity can affect the stored clamps, causing corrosion even before installation.

While metallic repair clamps have been demonstrated to be effective, there are several drawbacks associated with their use. Firstly, highly corrosive service environments make these metallic repairs susceptible to degradation over time. Secondly, metallic repairs are typically heavy, thus requiring special infrastructure for installation, and sometimes additional pipe supports are necessary after installation.

The use of composite repairs is an alternative to metals. Compared to metal repairs, composites present several key advantages. Firstly, there are weight savings coming from the use of lower density composites and these can permit simplified installation procedures. Secondly, the smaller relative density difference between the water and composite material leads to reduced submerged installation weight for water applications. Lastly, greater corrosion resistance of the repair allows enhanced durability and hence obviates the need for corrosion protection.

The use of composites in the repair of pipelines is not new, with composite overwrap repairs having been used effectively previously (Alexander and Ochoa, 2010; Shamsuddoha et al., 2012; Djukic et al., 2014a; Leong et al., 2011; Gibson et al., 2011). The overwrap method involves wrapping the damaged pipe with concentric

[1] American Petroleum Institute.

layers of fibre-reinforced polymer. Two common methods are prepreg composite and precured composite bonded into position, examples of which include ProAssure™ Wrap Extreme and Clock Spring™, respectively. There are also commercial systems that involve a wet lay-up method; however, a major drawback of these is the difficulty to ensure consistent quality of the installed repair since they are reliant on the skills of the bonder.

Composite overwrap repairs can provide both strengthening and leak reinforcements to the pipe. Specially formulated resins are required for underwater applications where there are limitations with adhesion and curing. These repairs can be applied in situ without hot work, to partially or completely restore the pressure capacity of a corroded or ruptured pipe, with the added corrosion protection benefit. Composite overwraps are primarily suited to onshore or offshore shallow water applications, due to the reliance on personnel to manually apply the composite onto the defect area. In addition, the overwraps require stringent surface preparation to ensure optimum adhesion and effectiveness of the repair, which is not always practical under field conditions.

Composite clamp repairs have been the subject of research in the past few years (Sum and Leong, 2014; Shamsuddoha et al., 2013a,b). The most recent advancement in repair clamps is the composite repair clamp, ProAssure™ Clamp. This is a fibre-reinforced polymer matrix composite repair solution equivalent to a metal mechanical clamp. This repair method presents the aforementioned advantages associated with composites over metallic clamps, with the repair taking a form known to operators.

This chapter details current industry codes for composite repair and case studies of both of the composite repair methods mentioned above through the use of two recently developed and field-tested repair systems, ProAssure™ Clamp and ProAssure™ Wrap Extreme.

12.2 Industry repair codes

The use of composite materials for repairing oilfield pipelines and pipings has been of continued interest in the O&G industry for many years (McGeorge et al., 2009; Shamsuddoha et al., 2012; Djukic et al., 2014a; Ochoa and Salama, 2005; Frassine, 1997; Goertzen and Kessler, 2007; Duella et al., 2008). The main composite pipeline repair codes currently used in the O&G industry are ISO/TS 24817 (2006) and ASME PCC-2 (2011). The codes cover two main types of pipe defects for testing, namely wall thinning defect (Type A) and through-wall leak (Type B). Together, the two codes cover overwrap and clamp repair of pipelines. However, coverage of the latter is markedly limited with no specific reference to clamps made of composites. The use of these codes should be combined with other good practices for repair and composites, and guidance can be sought in documents such as those produced by DNVGL[2] (Recommended PracticeV, 2012; StandardV–C501−Co, 2013).

[2] Previously, Det Norske Veritas, or DNV.

Codes such as ISO 14692-2 (2002), while not directly applicable to repair, cover the conditions under which glass-reinforced plastics pipings are expected to perform in oilfield environments and hence provide guidelines for setting parameters to which composite repairs should conform. In addition, ISO 14692-2 provides valuable insight into the physical limitations of composite, be it pipelines or repairs.

12.3 Composite repair clamps

12.3.1 Overview

A recent development in repair clamps for pipelines is the ProAssure™ Clamp. The concept of the composite repair clamp is shown in Figure 12.1. It comprises two half cylindrical shell sections (referred to herein as half-clamp) with flanges, which are brought together over a pipe and fastened using bolts to effect the repair. Seals made from an elastomer, or an alternative sealing material, are located within grooves machined into the composite at both ends of the clamp and along the flanges, forming a pressure tight annulus between the pipe and the clamp. In the event of a leaking defect, this annulus is pressurized by the fluid being transported by the pipeline. The only contact between the repair system and the pipe is from the seals. The annulus between the clamp and pipeline can also be filled with grout for strengthening of pipelines with wall thinning defects. Variant designs could include a double sealing system, as well as other seal configurations and clamping mechanisms.

12.3.2 Materials and construction

The ProAssure™ Clamp is constructed from a 1200 g/m^2 E−glass biaxial non-crimp fabric reinforcement and vinyl ester resin. The use of glass allows the cost of the clamp to be kept low, compared to carbon, for example. In addition, glass is preferred over carbon, which poses galvanic corrosion concern in certain applications if left unaddressed (Tavakkolizadeh and Saadatmanesh, 2001). Vinyl ester resin is selected due to its well-known performance in marine conditions and good chemical resistance to a wide range of chemicals, including sour crude, up to 100 °C. It has a measured glass

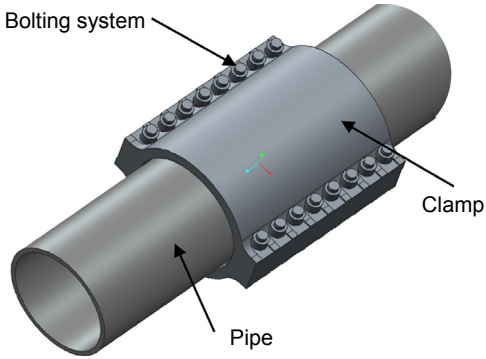

Figure 12.1 Concept of the composite clamp system.

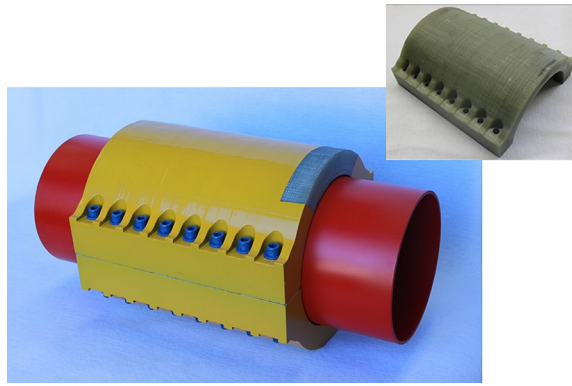

Figure 12.2 A representative picture of a ProAssure™ Clamp. Inset shows an unassembled half-shell.
Djukic, L.P., Sum, W.S., Leong, K.H., Hillier, W.D., Eccleshall, T.W., Leong, A.Y.L., 2015. Development of a fibre-reinforced polymer composite clamp for metallic pipeline repairs. Materials and Design, 70, 68−80.

transition temperature (T_g) of 110 °C, hence allowing the clamp to withstand up to a maximum service temperature of 80 °C. This is consistent with the requirements of ISO/TS 24817 (2006) and ASME PCC-2 (2011), covering composite repairs, which state that the maximum service temperature should be 30 °C less than the T_g of the material in the case of a through-wall defect in the pipe.

Plies are laid up to be parallel to the upper and lower surfaces of the flanges and parallel to the inner mould line, in a 0/90 configuration with respect to the pipe axis. The flanges are thickened, per the design requirements, through the use of additional glass ply insertions. These additional plies span the width of the flange and are located between plies that span the entire cross section of the clamp. This allows sufficient resistance to localized compressive loads applied when tightening bolts.

The clamp is manufactured via Vacuum Bag Resin Infusion, a process that is similar to Vacuum Assisted Resin Transfer Moulding, at room temperature. Machining and drilling are required to form the necessary grooves that house the seals and the holes for the fasteners, respectively. Alternative manufacturing approaches may be used, such as wet lay-up and resin transfer moulding. A typical ProAssure™ Clamp is shown in Figure 12.2.

12.3.3 Leak containment

For a clamp designed to a maximum allowable working pressure (MAWP) of 7 MPa,[3] and for a repair of an 8 in nominal diameter pipeline, it has a 35-mm shell thickness (S), 56-mm flange thickness (F) and an inner mould line of diameter (D_i) of 223 mm, leaving a clearance gap between the clamp inner mould line and pipe (i.e. an annulus) of

[3] A pressure of 7 MPa is selected because it represents a commonly encountered value used for standard repair clamps in the industry; the clamps could theoretically be designed to higher MAWPs as required.

approximately 2 mm. Seals used to afford pressure containment are located in grooves of 20 mm width (C_w) and 6.0 mm depth (D). These dimensions are shown in Figure 12.3. The design methodology for sizing the composite clamp consists of pressure vessel and bolt tension calculations, followed by finite element (FE) verification that accounts for deformation in the clamp shells. The aims are to keep the strains in the composite clamp low, allowing large margins on the composite strength, and to minimize the deformation (for sealing), so the maximum strain limit is set at not more than 0.25% for the composite laminate (Djukic et al., 2015).

The seals in the clamp comprise either a standard hardness rubber (SHR) or a high hardness rubber (HHR), both of which are prepared via water-jet cutting from larger sheets. The seal is applied in a 'picture frame' configuration; each half-clamp has an associated fully enclosed semicircular annulus, thus preventing fluid (leaking from a

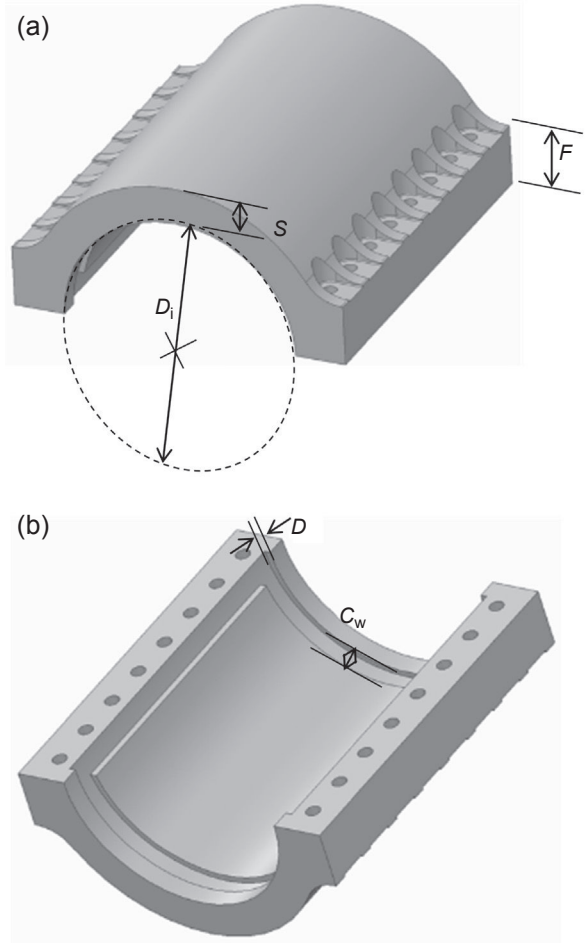

Figure 12.3 Clamp features and sizing: (a) external and (b) internal.

Table 12.1 ProAssure™ Clamp: pressure containment properties

Test type	Seal type	Hold temperatures (°C)	Hold time	Passed 10.5 MPa requirement (Y/N)	Failure pressure at highest hold temperature (MPa)
Short-term	SHR	RT, 65, 80	60 s	Y	19.2
Short-term	HHR	RT, 80	60 s	Y	22.6
Long-term	SHR	65	1000 h	Y	No failure

N.B. Bolts were tightened to a torque of 135 Nm during installation, and pressurization was done at a rate of approximately 1 MPa/min. The pipe is drilled (and tapped) with a single quarter in BSP through hole to simulate leaking.

damaged pipe) from moving between the annulus created by each half-clamp. In other words, when the clamps are loaded, only one half-clamp is pressurized by the fluid loading from a leaking pipe, while the other half is not due to the isolated pressurized faces of the clamp.[4] The clamp is locked in position using M12 socket head capscrews of 150 mm length, manufactured in accordance with DIN192, equivalent to ASTM A574 (2013), alongside M12 2H black nuts manufactured in accordance with ASTM A194 (2013) and M12 Samson washers with a hardness of 38−48 Rockwell.

The pressure containment capability of the clamp, comprising both short- and long-term (survival) performance, at room temperature (of approximately 20 °C), 65 °C and 80 °C is summarized in Table 12.1 (Djukic et al., 2014b, 2015). The intermediate temperature of 65 °C is used in accordance with the requirements of ISO 14692-2 (2002), which is a standard for glass fibre-reinforced polymer pipes used in the O&G industry.

The clamp survived the 10.5 MPa design pressure at RT, 65 °C and 80 °C. The clamp also comfortably holds a pressure of 10.5 MPa at 65 °C (maintained in a water bath) for 1000 h.[5] For the short-term tests, a single through-thickness hole is used to simulate leaking. For the long-term test, on the other hand, a thinned down area with a through-thickness hole drilled in the centre is used to simulate leaking following extended corrosion in the pipe (see Figure 12.4). The dimensions of the thinned down area (with a maximum thickness loss of 70%) and the hole (of nominal size 5 mm) are based on ISO/TS 24817 (2006), while the procedures for the long-term test are as per ASTM D1599 (1999), which is selected as the nearest guidance since it is recommended in ISO 14692 for stress rupture tests of composite pipes. Figure 12.5 shows the water bath used to maintain the temperature of the tested pipe.

[4] Polymer shims may be used to prevent the clamp from deflecting excessively away from the pipe on the pressurized face.

[5] This test condition was held for the 1000-h duration specified in ASME PCC-2 (2011) and witnessed by a third party certification body, Lloyd's Register.

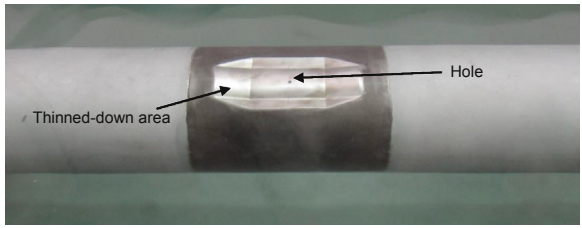

Figure 12.4 Thinned down area and hole on the test pipe.

Although both SHR and HHR are more than adequate to hold the design pressure, nonetheless, the hardness of the seal has a direct influence on the ultimate failure mode and pressure of the clamp. Pressure containment of the clamp failed by extrusion of a softer seal (see Figure 12.6), while a harder seal is able to delay extrusion to beyond failure of the composite shell, via interlaminar shear fracture in the flange (see Figure 12.7).

Under long-term test conditions of 1000 h at 65 °C, the clamp can hold a constant pressure of 10.5 MPa without sustaining any significant damage. Using strain gauges, strains in the composite were monitored at several key locations on the external surface of the clamp. There were no significant changes in all strain values throughout the test, and the measured strain values remained below 0.072%, well below the design limit of 0.25%.

ISO 14692-2 offers some guidance for predicting the composite lifetime using recommended conservative regression gradients. These gradients are based on the experience and amount of relevant material data. This information may be coupled with long-term test results to estimate the lifetime of the clamp in field applications.

12.3.4 Pressure containment

A variant of the above-mentioned leak containment clamp is the pressure containment clamp, which has grout injected into the annulus between pipe and clamp. The grout plays an important role in transferring the load from any defect in the corroded pipe to the clamp. By doing so, the original rated pressure of the pipe can be reinstated.

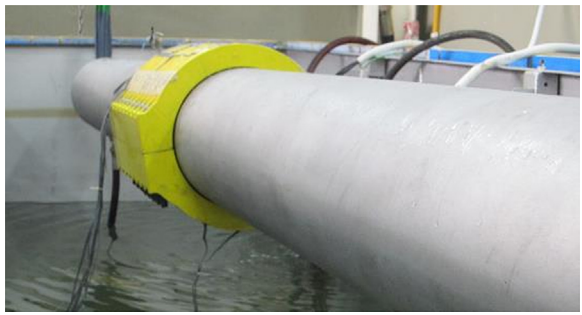

Figure 12.5 Apparatus for long-term survival test.

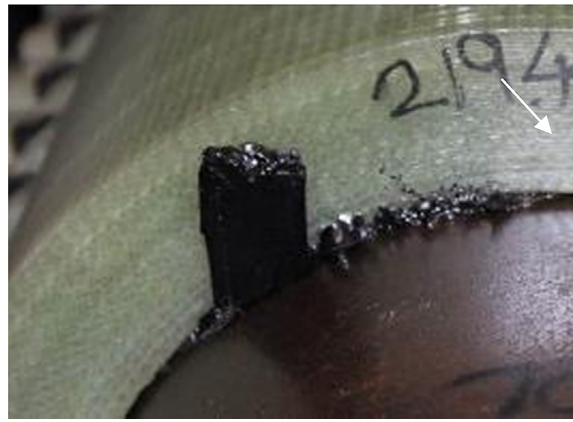

Figure 12.6 Seal extrusion that brought about loss of pressure containment to the clamp with a softer seal.
Djukic, L.P., Sum, W.S., Leong, K.H., Hillier, W.D., Eccleshall, T.W., Leong, A.Y.L., 2015. Development of a fibre reinforced polymer composite clamp for metallic pipeline repairs. Materials and Design, 70, 68−80.

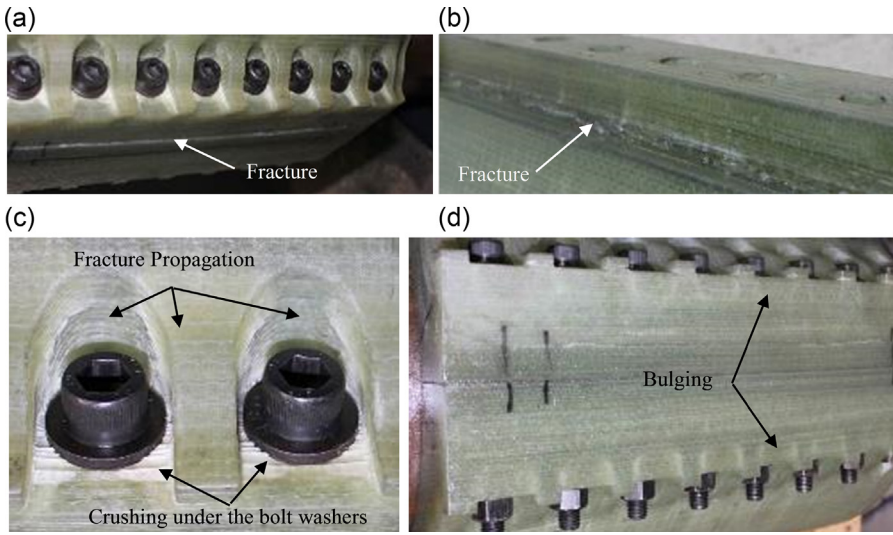

Figure 12.7 Failure modes for clamp with a harder seal: (a) shear fracture in flange from outside; (b) shear fracture in flange from inside; (c) fracture propagation and crushing around bolt rebates; (d) bulging in flanges.
Djukic, L.P., Sum, W.S., Leong, K.H., Hillier, W.D., Eccleshall, T.W., Leong, A.Y.L., 2015. Development of a fibre-reinforced polymer composite clamp for metallic pipeline repairs. Materials and Design, 70, 68−80.

One of the most critical conditions in such a repair is the presence of voids or gaps in the grout surrounding the pipe defect (Sum and Leong, 2014). Large local strains form on the pipe at these locations and can initiate yielding. This is an important consideration for installers of grouted sleeves, who should emphasize proper filling of the pipe defect area. It has been shown that even cracks or voids in other locations of the grout have an insignificant effect on the integrity of the repair compared to a small gap at the pipe defect. Figure 12.8 shows the different configurations of gaps analysed through finite element analysis and a chart of the corresponding maximum strain values of the pipe for each configuration.

Other recommendations for design of these repairs (Sum and Leong, 2014) include specifying a thin layer of grout to efficiently transfer the load from defect to sleeve and a sufficiently stiff composite sleeve to provide the required support to reduce strains in the corroded section of the pipe.

12.4 Composite overwrap repairs

12.4.1 Overview

A recent development in overwrap repair for pipelines is the ProAssure™ Wrap Extreme.[6] While it is generally similar to other composite overwrap systems, it differs from many of its commercial counterparts in that it is designed to be applicable, curable and functional in dry, wet and fully submerged environments. At the same time, it also has superior long-term properties, as well as maximum service temperature limits, as characterized by its glass transition temperature (T_g) values. It is supplied as a prepreg to minimize reliance on the skills of bonders, thus ensuring better consistency in quality of the installed repairs. Helical wrapping, with 50% overlap per revolution, is recommended for pressure containment repairs using ProAssure™ Wrap Extreme, while for leak containment circumferential wrapping is preferred whenever possible. In the following sections, overwrap repairs are generally discussed, giving particular reference to ProAssure™ Wrap Extreme only where specific properties and characteristics are listed and/or described.[7]

Good adhesion between the composite repair and the corroded substrate is key for effective load transfer between the pipe and the composite overwrap and to prevent the ingress of water into the repair−substrate interface. To ensure this is achieved, the surface of the pipeline first needs to be properly prepared, and this is often done using grit blasting. A primer designed to be used in conjunction with the overwrap system is then applied, followed by wrapping the composite prepreg onto the damaged area of the pipe. The composite is cured by temperature supplied either by its surrounding (i.e. air or water), by heat supplied by the fluid being transported by the pipeline or through external heating such as that provided with blankets.

[6] ProAssure™ Wrap Extreme was formerly marketed as PipeAssure™.

[7] The qualification of ProAssure™ Wrap Extreme to ISO/TS 24817 has been witnessed and signed off by Det Norske Veritas (DNV).

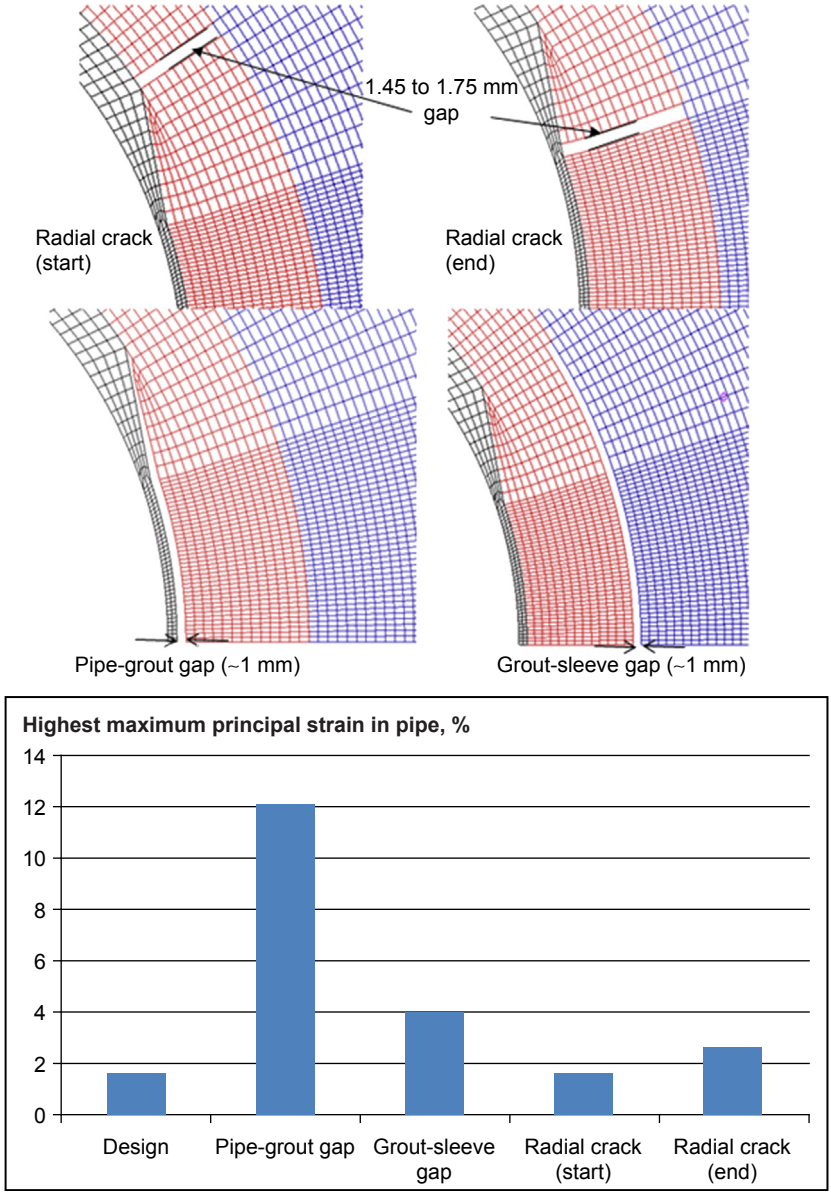

Figure 12.8 Different repair conditions of the grouted sleeve and the corresponding predicted highest maximum principal strain in the pipe.
Sum, W.S., Leong, K.H., 2014. Numerical study of annular flaws/defects affecting the integrity of grouted composite sleeve repairs on pipelines. Journal of Reinforced Plastics and Composites 33 (6), 556–565.

12.4.2 Materials

ProAssure™ Wrap Extreme is an epoxy-based system that allows universal applicability across the range of environmental conditions seen in repair of O&G infrastructure, for both out-of-water (OOW) (i.e. dry and wet conditions) and in-water (IW) (i.e. fully submerged conditions) applications. The prepreg is typically supplied in 300 mm width rolls with an areal weight of 1730 g/m^2 and contains E-glass fabric reinforcement impregnated with a specially formulated resin. The reinforcement layer consists of a chopped strand mat backed woven roving, composed of 350 g/m^2 glass in the warp (longitudinal or 0°) and 280 g/m^2 glass in the weft (transverse or 90°). Each ply, in its cured state, has a laminate thickness of approximately 0.85 mm.

Two separate primers, one for use OOW and the other IW, have been developed for the ProAssure™ Wrap Extreme system. The OOW primer is recommended to be applied at a thickness of 1150 g/m^2, while the IW primer at an approximate thickness of 3600 g/m^2. The in-plane mechanical properties of ProAssure™ Wrap Extreme are summarized in Table 12.2.

Two chemical types generally used for pipeline repair are epoxy and polyurethane (PU) resins. PUs have the advantage of curing at ambient temperatures via water activation, but the downside is that they are also easily hydrolysed in water and they have relatively low T_g values. In contrast, epoxy resins are more moisture stable and can be formulated to provide high T_g and environmental stability using aromatic amino compounds (Klein, 1991; Varma and Gupta, 2000). However, most thermosetting systems can only be applied on dry surfaces and are adversely affected by surface moisture and contaminants. Hence, ProAssure™ Wrap Extreme is a modified proprietary formulation that enhances adhesion in water environments.

12.4.3 Cure and surface preparation considerations

Unlike the case of a composite clamp which is manufactured under shop-floor conditions that allow close control of the curing process, overwrap repairs are applied and cured in the field. Hence, it is not always practical to replicate laboratory cure conditions and the surface preparation of the substrate that have been used to determine the properties and performance of the overwrap repair system. To this end, a good understanding of the cure behaviour of the overwrap composite material and the composite−substrate interface properties is essential to ensure that repairs are properly applied and the acceptable performance is achieved in the field.

Since T_g is dependent on the cure temperature, for the purpose of selecting an overwrap composite material to match service temperature requirement it is reasonable to assume that cure temperature of the composite is equal to the operating temperature of the pipeline. Apart from the pipeline itself, the fluid being transported in it is also a very significant heat sink, to which the repair will acclimatize (Liu et al., 2014). If an elevated cure temperature were required, a large amount of external heat would be required to adequately raise the repair temperature above the fluid temperature,

and in some cases this external temperature application could be expected to go beyond the temperature at which the composite will begin to undergo thermal degradation. Furthermore, it is even more difficult to transfer heat to achieve the required temperature in the composite at the interface with pipe, which is considered a more critical region, due to its close proximity to the pipe.

Djukic et al. (2014a) have studied the effects of cure temperature and time on shear properties and T_g, of ProAssure™ Wrap Extreme. A summary of the results is given in Table 12.3. The shear strength data based on single lap shear joint (SLJ) tests show that the strength of the unconditioned composite−steel joints is in excess of the required strength of 5 MPa, per ISO/TS 24817 (2006) Annex B, at 40 °C, 55 °C and 80 °C, for both the OOW and IW conditions. Under hot/wet conditions ISO/TS 24817 requires a minimum failure strength of 5 MPa, and this failure strength should be at least 30% of that of the unconditioned equivalents. It is noteworthy that hot/wet conditioning was performed for a period of greater than 2000 h in all cases (Djukic et al., 2014a), which is more than double the minimum time frame (1000 h) required to achieve a long-term conditioning result as per ISO/TS 24817. The extended conditioning period was observed in order for the specimens to reach a weight close, or equivalent, to equilibrium. It can be seen from Table 12.3 that, as with in the unconditioned case, the hot/wet OOW and IW lap shear strengths at 40 °C, 55 °C and 80 °C also surpass the code requirements.

ISO/TS 24817 states that the T_g of the composite matrix must exceed the operating temperature of the pipeline by greater than 20 °C for Type A defects or 30 °C for Type B defects. Hence, from Table 12.3, it is clear that under OOW conditions, the composite is suitable for service temperatures of 40 °C, 55 °C and 80 °C for wall thinning defect requirements, as soon as the composite has been cured, but not for through-wall defects. The T_g climbs during hot/wet conditioning, possibly due to postcuring of the composite at the elevated hot/wet conditioning temperature, whereby the through-wall defect requirements are met following conditioning. Hence, for OOW cured laminates, a postcure is recommended prior to service of through-wall defect repairs.

Based on a 55 °C IW cure, it can be seen from Table 12.3 that the T_g of the composite is approximately 23 °C higher than that of the equivalent OOW cure case, hence meeting both wall thinning and through-wall defect requirements immediately upon curing. This shows that ProAssure™ Wrap Extreme has an added advantage when used IW.

Table 12.4 clearly illustrates how different surface treatments can have a direct effect on the interfacial shear strength between the (composite repair) laminate and the metal substrate to which it is bonded. The three mechanical surface treatments studied by Islam (Islam, 2014) represent some of the more common metal surface field cleaning techniques used in the O&G industry. Between them, grit blasting is preferred for maximum SLJ strength, although the needle gun technique and even wire brushing appear to still be acceptable since they produce SLJ strength values greater than the minimum value of 5 MPa required by ISO/TS 24817. It can be seen that this observation holds true for both OOW and IW environments.

Table 12.2 In-plane mechanical properties of ProAssure™ Wrap Extreme at RT and 55 °C

	Unconditioned				Conditioned[b]			
	RT		55 °C[b]		RT		55 °C[c]	
Property[a]	Avg	SD	Avg	SD	Avg	SD	Avg	SD
Out-of-water								
E, LT (GPa)	17.5	0.6	16.7	0.2	–	–	17.0	0.3
σ_u, LT (MPa)	235	18	232	7.7	–	–	132	6.7
ε_u, LT (%)	1.35	0.08	1.39	0.04	–	–	0.77	0.05
E, TT (GPa)	15.9	0.291	15.4	0.440	–	–	15.4	0.4
σ_u, TT (MPa)	217	7.8	208	11.4	–	–	110	6.4
ε_u, TT (%)	1.37	0.04	1.36	0.09	–	–	0.72	0.04
ν_{LT}	0.183	0.009	0.162	0.011	–	–	0.184	0.022
G (GPa)	3.284	0.413	2.354	0.312	–	–	2.510	0.38
τ_p (MPa)	80.3	7.5	50.0	6.9	–	–	47.5	4.4
γ_p (%)	2.42	0.3	2.13	0.2	–	–	1.91	0.20

In-water[c]								
E, LT (GPa)	16.9	0.4	16.9	0.4	–	–	16.6	0.6
σ_u, LT (MPa)	208	23.1	208	23.1	–	–	119	9.1
ε_u, LT (%)	1.23	0.13	1.23	0.13	–	–	0.71	0.04
E, TT (GPa)	15.0	0.4	15.0	0.4	–	–	14.7	0.5
σ_u, TT (MPa)	182	25.2	182	25.2	–	–	100	9.6
ε_u, TT (%)	1.22	0.18	1.22	0.18	–	–	0.68	0.07
ν_{LT}	0.192	0.011	0.192	0.011	–	–	0.196	0.016
G (GPa)	2.86	0.25	2.86	0.25	–	–	2.75	0.6
τ_p (MPa)	65.1	7.4	65.1	7.4	–	–	47.2	5.0
γ_p (%)	2.26	0.16	2.26	0.16	–	–	1.77	0.33

[a]Cured at 55 °C for 48 h.
[b]Test specimens were hot/wet conditioned in fresh water at the intended test temperature until near weight/weight equilibrium was achieved, according to ASTM D5229.
[c]Based on substitute ocean water prepared according to ASTM D1141.

Table 12.3 T_g **values and single lap shear joint properties of ProAssure™ Wrap Extreme at RT and 55 °C**

	Unconditioned				Conditioned[b]			
	RT		ET[c]		RT		ET[c]	
Property[a]	Avg	SD	Avg	SD	Avg	SD	Avg	SD
Out-of-water								
T_g 40 °C (°C)	70.3	2.1	–	–	94.8	3.4	–	–
T_g 55 °C (°C)	76.5	1.2	–	–	113.8	1.6	–	–
T_g 80 °C (°C)	101.6	2.0	–	–	140.4	2.7	–	–
τ_{SLJ} 40 °C (MPa)	14.4	1.8	14.8	1.7	–	–	11.7	2.5
τ_{SLJ} 55 °C (MPa)	15.7	1.7	13.3	1.8	–	–	8.0	1.1
τ_{SLJ} 80 °C (MPa)	9.2	1.0	8.2	1.0	–	–	6.9	0.6

In-water[d]								
T_g 40 °C (°C)	–	–	–	–	–	–	–	–
T_g 55 °C (°C)	99.9	0.6	–	–	–	–	–	–
T_g 80 °C (°C)	–	–	–	–	–	–	–	–
τ_{SLJ} 40 °C (MPa)	13.9	0.5	12.5	0.5	–	–	10.8	1.3
τ_{SLJ} 55 °C (MPa)	11.5	1.5	11.0	1.5	–	–	9.7	1.1
τ_{SLJ} 80 °C (MPa)	5.9	0.6	5.6		–	–	6.8	1.1

N.B. SLJs were manufactured using 5-mm-thick ASTM A36 steel. Pipe specimens were manufactured from API 5L X42 pipe with an outer diameter of 168.3 mm and a wall thickness of 6.4 mm, over strength to 61 ksi yield, thereby representing a pipeline closer to X61. The steel substrates were prepared to a surface roughness of 50−60 μm by grit blasting using Garnet 16/40 grit, verified by means of Testex tape measurements according to ASTM D4417.

[a]Curing conditions used, respectively: 40 °C for 96 h, 55 °C for 48 h and 80 °C for 24 h.

[b]Test specimens were hot/wet conditioned in fresh water at the intended test temperature until near weight/weight equilibrium was achieved, according to ASTM D5229.

[c]Elevated temperature tests at equivalent cure temperatures.

[d]Based on substitute ocean water prepared according to ASTM D1141.

Table 12.4 Effects of surface treatment versus lap shear strength for OOW and IW conditions

Surface treatment	SLJ strength (MPa)	
	Out-of-water	In-water
Grit blasted[a]	10.8 ± 0.9	9.0 ± 1.0
Wire brushed	6.6 ± 0.6	5.3 ± 0.4
Needle gunned	7.1 ± 0.4	8.2 ± 0.5

N.B. Composite used is ProAssure™ Wrap Extreme, while substrate is an equivalent X65 carbon steel. The composite was co-cured onto the substrate by curing at 55 °C for 48 h.
[a]Based on 30−60 grit size.

12.4.4 Pressure containment

The repair laminate thickness for wall thinning due to corrosion, i.e. Type A defect, is designed using short-term pipe spool survival test calculations according to ISO/TS 24817 (2006) Annex C. Figure 12.9 shows the specimen configurations based on guidelines in the standard used by Djukic et al. (2014a) to assess the pressure containment performance of ProAssure™ Wrap Extreme, and the results achieved are given in Table 12.5.

Helical winding, with 50% overlap per revolution, is used for the repairs. The average angle of the ply in the longitudinal (0°) direction is approximated to be ±15° to the circumferential direction of the pipe. The angles vary slightly between plies depending on the proximity to the centre of the pipe and the thickness of the wrap. Variation in ply angle is to be expected, especially in field repairs, and the comprehensive test program carried out by Djukic and coworkers demonstrates that there is ample conservatism in the design guidelines recommended in ISO/TS 24817.

The pressure values given in Table 12.5 show that irrespective of whether the repairs are applied OOW or IW, or if they are cured at 40 °C, 55 °C or 80 °C, the design pressure of 32.6 MPa is surpassed. During pressure testing, the pipe spool exhibited yielding in the region immediately adjacent to the overwrap repair (see Figure 12.10) when pressurized to approximately 38 MPa, at which point pressurization is terminated.

The ultimate failure for the case of OOW cure at 55 °C occurred at approximately 42 MPa, and the fracture can be seen from Figure 12.11(b) to occur outside of the repaired region. Therefore, Type A composite repairs are capable of sustaining pressures beyond that of the virgin pipe strength in the region containing the defect, hence demonstrating the effectiveness of overwrap repairs for restoring the original pressure rating of corroded, or otherwise damaged, pipelines. When compared with an unrepaired pipe with an 80% wall loss Type A defect, which fails at an average pressure of 12.6 MPa, the overwrap composite is able to restore pressure containment by more than threefolds.

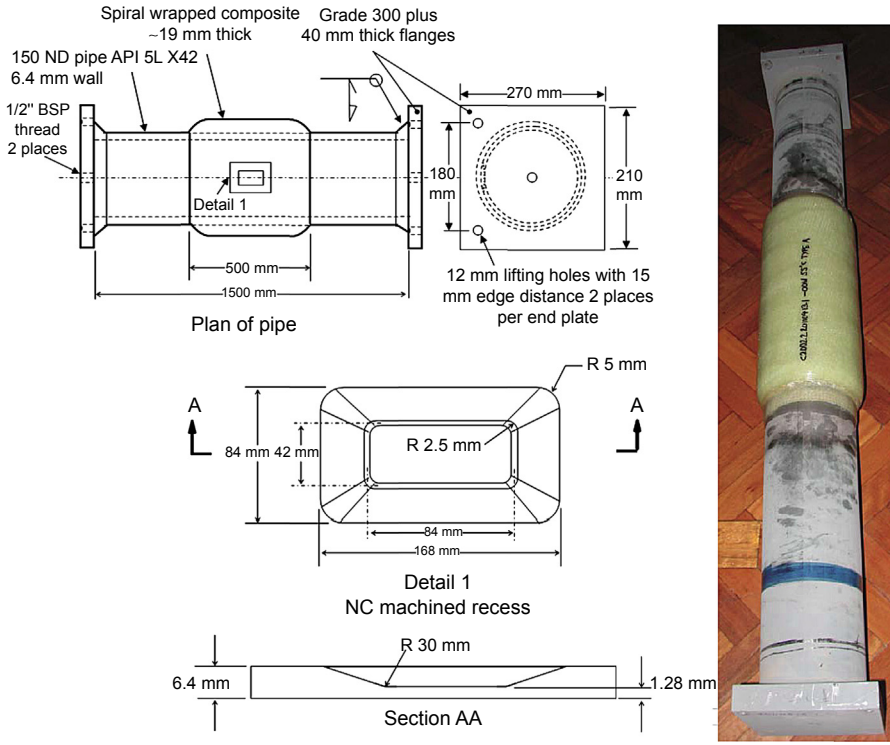

Figure 12.9 Details of a representative Type A repair test.
Djukic, L.P., Leong, A.Y.L., Falzon, P.J., Leong, K.H. 2014. Qualification of a composite system for pipeline repairs under dry, wet, and water-submerged conditions. Journal of Reinforced Plastics and Composites 33 (6), 566−578.

12.4.5 Leak containment

A series of Type B pressure tests carried out by Djukic et al. (2014a) on test spools containing different Type B (hole) defect sizes and repaired using ProAssure™ Wrap Extreme is summarized in Table 12.6. They used circumferential wrapping and a constant laminate thickness as well as a lay-up sequence for their test program. Figure 12.12 shows the specimen configurations for a 10 mm hole based on guidelines given in ISO/TS 24817 (2006). The failure pressure values, as given in Table 12.6, are defined by the onset of weepage during the pressure tests, as illustrated in Figure 12.13.

For the hole diameters considered—10, 15 and 25 mm for OOW cured conditions and 15, 20 and 25 mm for the IW cured conditions—leak containment capacity, as expected, generally decreases with through-wall defect size. For the OOW cured case, the sustainable pressure dropped from 24 to 10.9 MPa (average) and 9.2 MPa (average) when the hole size is correspondingly increased from 10 to 15 mm and 25 mm. Similarly, for the IW cured case, the sustainable pressure values averaged 13.7, 10.4 and 6.6 MPa for the 10, 20 and 25 mm hole size, respectively. It will be noted that OOW repairs are superior to their IW counterparts.

Table 12.5 Type A pressure containment capacity as a function of cure temperature for the OOW and IW conditions

Test spool	Cure temperature[a] (°C)	Maximum applied pressure[b] (MPa)	Pass/fail
No repair			
1	N/A	11.8	N/A
2	N/A	12.9	N/A
3	N/A	13.0	N/A
Out-of-water			
1	40	37.5	Pass
2	55	37.8	Pass
3	55	38.0	Pass
4	55	38.1	Pass
5	55	38.0	Pass
6	80	38.0	Pass
In-water			
1	40	37.5	Pass
2	55	37.1	Pass
3	55	36.9	Pass
4	55	37.8	Pass
5	55	37.9	Pass
6	55	37.6	Pass
7	80	36.6	Pass

[a]Curing conditions used, respectively: 40 °C for 96 h, 55 °C for 48 h and 80 °C for 24 h.
[b]The repairs are designed to withstand the undamaged pipe rating of 32.6 MPa. Pressurization is terminated approximately 5 MPa above this value.

It appears that the effect of a 5 J impact on the repair over a 25 mm hole is insignificant, where in the OOW cured case failure occurred at a stress of 10.2 MPa (c.f. 6.8 to 13.5 MPa when unimpacted), while in the IW cured case the value is 9.7 MPa (c.f. 4.5 to 7.8 MPa when unimpacted).

A hole leak or through-wall, i.e. Type B defect, repair is designed based upon the laminate/substrate interface toughness parameter (energy release rate) value that is determined as described in ISO/TS 24817 (2006). If failure occurs via delamination (D), whereby water is found to weep from the sides of the repair, the result is considered admissible for calculation. If the failure occurred through other means, such as weeping through the laminate thickness of the repair via microcracks (M) or yielding of the pipe (Y), then the result is considered inadmissible.

The method for determining the repair laminate/substrate interface toughness parameter (energy release rate) for pipes with through-wall defects is briefly described

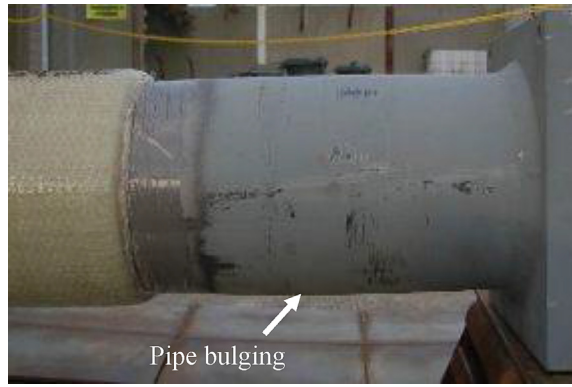

Figure 12.10 Bulging in the pipe is observed when over pressurized, while the Type A repair remains intact, thus confirming the effectiveness of the repair to restore pressure containment to a severely 'corroded' pipe.
Djukic, L.P., Leong, A.Y.L., Falzon, P.J., Leong, K.H., 2014. Qualification of a composite system for pipeline repairs under dry, wet, and water-submerged conditions. Journal of Reinforced Plastics and Composites 33 (6), 566−578.

in the following paragraphs. Using the experimentally determined failure pressure values, the repair laminate/substrate interface toughness parameter is calculated using the formulae presented in Eqns (12.1) and (12.2):

$$p_i = A(d_i)\sqrt{\gamma_i} \tag{12.1}$$

where

$$A(d_i) = \sqrt{\left\{\frac{0.001}{\frac{(1-\nu^2)}{E_{ac}}\left\{\frac{3}{512t_i^3}d_i^4 + \frac{1}{\pi}d_i\right\} + \frac{3}{64Gt_i}d_i^2}\right\}} \tag{12.2}$$

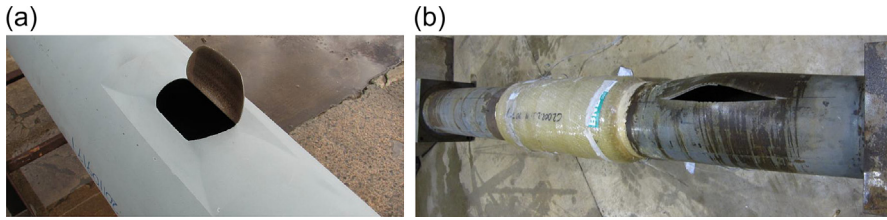

Figure 12.11 (a) Failure of an unrepaired Type A pipe and (b) failure of a repaired Type A pipe showing rupture outside of the repaired region.
Djukic, L.P., Leong, A.Y.L., Falzon, P.J., Leong, K.H., 2014. Qualification of a composite system for pipeline repairs under dry, wet, and water-submerged conditions. Journal of Reinforced Plastics and Composites 33 (6), 566−578.

Table 12.6 Type A pressure containment capacity as a function of through-wall defect size for the OOW and IW conditions (Djukic et al., 2014a)

Test no.	Hole diameter (mm)	Weep pressure (MPa)	Failure mode	Admissible for calculation (Y/N)
Out-of-water				
1	10	–	Y	N
2	10	24.0	D	Y
3	10	–	Y	N
4	15	8.4	D	Y
5	15	12.5	D	Y
6	15	11.7	D	Y
7	25	7.2	D	Y
8	25	6.8	D	Y
9	25	13.5	D	Y
10 (Impacted)	25	10.2	D	Y
In-water				
1	15	13.6	D	Y
2	15	12.8	D	Y
3	15	14.8	D	Y
4	20	8.5	D	Y
5	20	11.0	D	Y
6	20	11.6	D	Y
7	25	4.5	D	Y
8	25	7.8	D	Y
9	25	7.5	D	Y
10 (Impacted)	25	9.7	D	Y

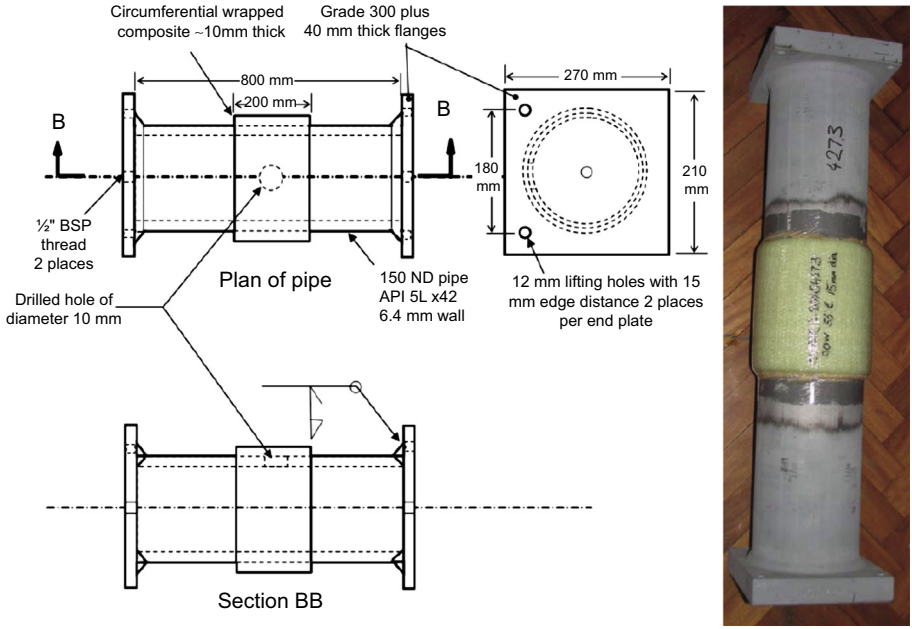

Figure 12.12 Details of a representative Type B repair test.
Djukic, L.P., Leong, A.Y.L., Falzon, P.J., Leong, K.H., 2014. Qualification of a composite system for pipeline repairs under dry, wet, and water-submerged conditions. Journal of Reinforced Plastics and Composites 33 (6), 566—578.

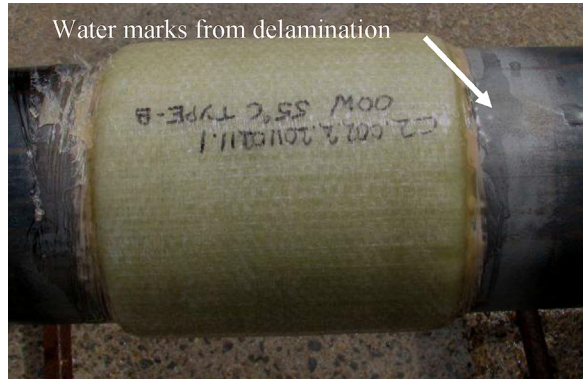

Figure 12.13 Type B repair failure is characterized by weepage.
Djukic, L.P., Leong, A.Y.L., Falzon, P.J., Leong, K.H., 2014. Qualification of a composite system for pipeline repairs under dry, wet, and water-submerged conditions. Journal of Reinforced Plastics and Composites 33 (6), 566—578.

and where

n is the number of observed data points,
p_i is the pressure, expressed in MPa, at failure of observation i,
$A(d_i)$ is the function of defect size and repair laminate properties of observation i,
G is the shear modulus of the repair laminate, in MPa,
v is Poisson's ratio of the repair laminate,
d_i is the diameter of the defect, in mm,
t_i is the thickness of the repair laminate, in mm,
E_{ac} is the combined tensile modulus of the repair laminate, $\sqrt{E_a E_c}$, in MPa. Note that in this case, E_a is taken as E_{TT} and E_c is taken as E_{LT}.

The mean energy release rate in J/m^2 (γ_{mean}) is then calculated according to Eqn (12.3) using the individual results of all tests, while the 95% lower confidence limit (γ_{LCL}) is computed using Eqn (12.4). σ is the variance of measurement of pressure, calculated using Eqn (12.5). t_v is the statistical Student's t-value and is based on a two-sided 0.025 level of significance, that is, 95% lower confidence limit.

$$\gamma_{mean} = \left(\frac{\sum_{i=1}^{n} A(d_i) p_i}{\sum_{i=1}^{n} A(d_i)^2} \right)^2 \tag{12.3}$$

$$\gamma_{LCL} = \left(\frac{\sum_{i=1}^{n} A(d_i) p_i}{\sum_{i=1}^{n} A(d_i)^2} - t_v \sigma \sqrt{\frac{1}{\sum_{i=1}^{n} A(d_i)^2}} \right)^2 \tag{12.4}$$

$$\sigma = \sqrt{\frac{\sum_{i=1}^{n} \left(p_i - A(d_i) \sqrt{\gamma_{mean}} \right)^2}{n-2}} \tag{12.5}$$

Further details of above calculations and equations are given in ISO/TS 24817 Annex D.

In the case of the ProAssure™ Wrap Extreme system, by using the values given in Table 12.6 for OOW repairs, Djukic et al. (2014a) reported representative values of 120.1 and 57.7 J/m^2 for γ_{mean} and γ_{LCL}, respectively. For IW repairs, they reported a representative γ_{mean} value of 107.7 J/m^2 and a representative γ_{LCL} value of 78.7 J/m^2. These values can be used to work out through-wall repairs with similar geometries. It is noteworthy that, due to statistical reasons, the OOW γ_{mean} value is 11.5% higher than that of the IW; however, the OOW γ_{mean} value is actually 26.6% lower than the IW.

12.5 Conclusions

Composite repairs are emerging as a viable and increasingly preferred alternative to metallic repairs in the O&G industry. Depending on the form of damage in the pipeline, classified per ISO/TS 24817 (2006) as wall thinning (Type A) or leaking defect (Type B), generally an appropriate composite repair solution can be selected. The use of composite instead of metal presents key advantages in reduced weight, smaller relative density when used in water leading to ease of installation and greater corrosion resistance. Composite repairs also present the opportunity to move away from hot work operations typical of metallic repairs, thereby enhancing safety and reducing interruption to operations.

In this chapter, clamp and overwrap composite repairs for oilfield pipelines are discussed with particular reference to work carried out on two products, namely ProAssure™ Wrap Extreme and ProAssure™ Clamp. These two composite solutions have been shown to allow both pressure and leak containment repairs to be carried out on high-pressure pipelines, in dry (e.g. pipings on an oil platform and in a manufacturing plant), wet (e.g. risers at the splash zone) and fully water-submerged (e.g. subsea pipelines) environments through a temperature range of approximately room temperature to 80 °C. However, the temperature is not limited to this range, because depending on the need, there is a scope to widen this temperature range through appropriate composite material selection.

Figures 12.14–12.17 show applications of the ProAssure™ products. It can be seen that overwrap repairs can be successfully applied on the platform, in the splash zone as well as in the sea. Obviously the complexity increases as repairs move from dry to wet and subsea environments. This is not only restricted to application of the composite laminate but also to related activities such as removal of existing coatings and surface preparation, as well as additional requirements such as the need for scaffolding, absailers and/or a service barge. A similar scenario applies to the clamp repair solution, which is generally advantageous over the overwrap repair method in cases of deeper

Figure 12.14 Overwrap repairs are also advantageous for repairing piping, especially where there is restricted and limited access.

Figure 12.15 Repair installation at the splash zone of an offshore platform; ex-factory rubbery-based coatings are prone to degradation over time in service and could be repaired with a system like ProAssure™ Wrap Extreme.

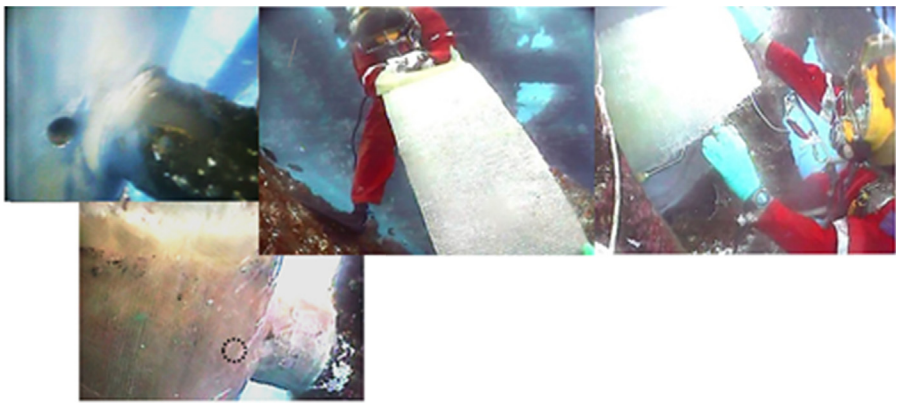

Figure 12.16 Subsea repairs, in this case to rectify a through-wall defect, could be carried out with a system like ProAssure™ Wrap Extreme.

Figure 12.17 Installing a composite repair clamp onto a pipe with a through-wall defect.

water and when the repair time window is relatively short. The surface preparation requirement for clamps is generally less stringent than for overwraps. They are more suited for isolated defects and when space restrictions are not an issue.

While the benefits of composite repairs are well known, current recommended quality control procedures and inspection techniques still leave much to be desired. Most composite repair contractors propose hardness measurement as well as visual inspection; however, more reliable and less skill-dependent techniques are required. Enhanced efforts to develop field quality control and inspection techniques will, among other factors, determine the level of growth in the use of composite repairs in the industry.

The industry has also called for more effort to be directed at establishing guidelines for lifing of composite repairs. The long-term performance of composites under oilfield conditions is still not yet well established. Long-term assessment through accelerated testing is both expensive and unreliable unless field experience is available to corroborate the test results. To make matters worse, laminate properties are highly skill-dependent and they are also highly affected by the environments under which the laminate is fabricated. This not only has a bearing on the reliability of a repaired asset, but it also dictates the required frequency of inspection throughout the life of the repair in the field.

Overall, composite repairs are a cost competitive solution that have gained strong acceptance by the O&G industry, as evident by the advent of newer and better products over the years. Gradually, end users have become more accustomed to this class of pipeline repair solution as they gain a better understanding of composite materials. This trend is expected to grow with field experience and as new innovations come to the fore, whereby current limitations are removed and better features are introduced.

Acknowledgements

The authors are grateful to colleagues and associates of their respective organizations, especially to Dr P.J. Falzon, M. Stoessiger, Wayne D. Hillier and Timothy W. Eccleshall of the Cooperative Research Centre for Advanced Composites Structures Ltd (CRC−ACS) and ACS Australia Pty Ltd, and to A.Y.L. Leong, Y.C Tan and M.A. Mahtar of PETRONAS Research, for useful discussions and technical contributions towards the development of the ProAssure™ products described in this chapter. A portion of the development work on the ProAssure™ Clamp described in this chapter has been undertaken as part of a CRC−ACS research program, established and supported under the Australian government's Cooperative Research Centres Program.

References

Alexander, C., Ochoa, O.O., 2010. Extending onshore pipeline repair to offshore steel risers with carbon-fibre reinforced composites. Composite Structures 92, 499−507.

A574−13, 2013. Standard Specification for Alloy Steel Socket-Head Cap Screws. ASTM International.

A194−13, 2013. Standard Specification for Carbon and Alloy Steel Nuts for Bolts for High Pressure of High Temperature Service, or Both. ASTM International.

A36 − Standard Speci ASTM A36. Standard Specification for Carbon Structural Steel.

Coley, D., Caraballo, A., 2011. Practical aspects for the development of rehabilitation systems for ageing onshore pipelines: a case study. In: Pipeline Technology Conference, Hannover Messe, Germany.

ASME PCC-2, 2011. Repair of Pressure Equipment and Piping. American Society for Mechanical Engineers.

D'Mello, C., Boswell, L.F., May 30−June 4, 1999. The use of grout for the repair and strengthening of steel tubular members. In: Proceedings of the Ninth (1999) International Offshore and Polar Engineering Conference, Brest, France.

Djukic, L.P., Leong, A.Y.L., Falzon, P.J., Leong, K.H., 2014. Qualification of a composite system for pipeline repairs under dry, wet, and water-submerged conditions. Journal of Reinforced Plastics and Composites 33 (6), 566−578.

Duella, J.M., Wilsona, J.M., Kessler, M.R., 2008. Analysis of a carbon composite overwrap pipeline repair system. International Journal of Pressure Vessels and Piping 85 (11), 782−788.

Djukic, L.P., Sum, W.S., Leong, K.H., Hillier, W.D., Eccleshall, T.W., Leong, A.Y.L., 2015. Development of a fibre reinforced polymer composite clamp for metallic pipeline repairs. Materials and Design 70, 68−80.

Djukic, L.P., Sum, W.S., Leong, K.H., Leong, A.Y.L., Hillier, W.D., Eccleshall, T.W., Falzon, P.J., 2014. A novel high pressure composite clamp for pipeline repair. In: Element Oilfield Engineering with Polymers 2014.

ASTM D1599−99, 1999. Standard Test Method for Resistance to Short-Time Hydraulic Pressure of Plastic Pipe, Tubing, and Fittings. ASTM International.

D5229-92 − Standard ASTM D5229-92. Standard Test Method for Moisture Absorption Properties and Equilibrium Conditioning of Polymer Matrix Composite Materials.

D1141-98 − Standard, 1141 ASTM D1141-98. Standard Practice for the Preparation of Substitute Ocean Water.

D4417-03 − Standard ASTM D4417-03. Standard Test Methods for Field Measurement of Surface Profile of Blast Cleaned Steel.

Frassine, R., 1997. Long-term performance of a polymer composite repair system for gas pipelines. Advances in Polymer Technology 16 (1), 33−43.

Gibson, A.G., Linden, J.M., Elder, D., Leong, K.H., 2011. Non-metallic pipe systems for use in oil and gas. Plastics, Rubber and Composites 40 (10), 465−480.

Goertzen, W.K., Kessler, M.R., 2007. Dynamic mechanical analysis of carbon/epoxy composites for structural pipeline repair. Composites Part B: Engineering 38 (1), 1−9.

Islam, M.S., 2014. The University of Sydney/Cooperative Research Centre for Advanced Composite Structures Ltd, Unpublished work.

Klein, D.H., 1991. Cold curing epoxy systems for protection against heavy corrosion. Anti-Corrosion Methods and Materials 38 (3), 4−10.

Leong, K.H., Leong, A.Y.L., Ramli, S.H., Tan, Y.C., Johar, R.M., Chia, M.T., Hassan, H.A., 2009. Testing grouted sleeve connections for pipelines repairs. In: 3rd International Conference on Integrity, Reliability & Failure (IRF 2009), Porto, Portugal, pp. 20−24.

Leong, A.Y.L., Leong, K.H., Tan, Y.C., Liew, P.F.M., Wood, C.D., Tian, W., Kozielski, K.A., 2011. Overwrap composite repairs for offshore risers at topside and splash zone. In: 18th International Conference on Composite Materials, Korea.

Liu, X.L., Leong, A.Y.L., Leong, K.H., Falzon, P.J., Tan, Y.C., March 2014. Heat transfer analysis and cure modelling of composite repairs for pipelines. Journal of Reinforced Plastics and Composites 33, 586−597.

McGeorge, D., Echtermeyer, A.E., Leong, K.H., Melve, B., Robinson, M., Fischer, K.-P., 2009. Repair of floating offshore units using bonded fibre composite materials. Composites Part A: Applied Science and Manufacturing 40 (9), 1364−1380.

Ochoa, O.O., Salama, M.M., 2005. Offshore composites: transition barriers to an enabling technology. Composites Science and Technology 65 (15−16), 2588−2596.

ISO/TS 24817, 2006. Petroleum, Petrochemical and Natural Gas Industries − Composite Repairs for Pipework − Qualification and Design, Installation, Testing and Inspection. International Organisation for Standardization.

ISO 14692-2, 2002. Petroleum and Natural Gas Industries − Glass-reinforced Plastics (GRP) Piping − Part 2: Qualification and Manufacture. International Organisation for Standardization.

Recommended Practice DNV-RP-C301, 2012. Design, Fabrication, Operation and Qualification of Bonded Repair of Steel Structures. Det Norske Veritas.

Sum, W.S., Leong, K.H., 2014. Numerical study of annular flaws/defects affecting the integrity of grouted composite sleeve repairs on pipelines. Journal of Reinforced Plastics and Composites 33 (6), 556−565.

Shamsuddoha, M., Islam, M.M., Aravinthan, T., Manalo, A., Lau, K.T., 2013a. Effectiveness of using fibre-reinforced polymer composites for underwater steel pipeline repairs. Composite Structures 100, 40−54.

Shamsuddoha, M., Islam, M.M., Aravinthan, T., Manalo, A., Lau, K.T., 2013b. Characterisation of mechanical and thermal properties of epoxy grouts for composite repair of steel pipelines. Materials and Design 52, 315−327.

Shamsuddoha, M., Islam, M.M., Aravinthan, T., Manalo, A., Lau, K.T., 2012. Fibre composites for high pressure pipeline repairs, in-air and subsea − an overview. In: 3rd Asia-Pacific Conference on FRP in Structures (APFIS 2012), Sapporo, Japan.

Standard DNV-OS-C501, 2013. Composite Components. Det Norske Veritas.

Tavakkolizadeh, M., Saadatmanesh, H., 2001. Galvanic corrosion of carbon and steel in aggressive environments. Journal of Composites for Construction 5, 200−210.

Varma, I.K., Gupta, V.B., 2000. Thermosetting resin − properties. Comprehensive Composite Materials 2, 1−56.

This page intentionally left blank

Fiber-reinforced polymer (FRP) repair systems for corroded steel pipelines

13

C.S. Sirimanna[1,2], A.C. Manalo[1,2], W. Karunasena[1], S. Banerjee[1], L. McGarva[2,3]
[1]University of Southern Queensland, Toowoomba, QLD, Australia; [2]Cooperative Research Centre for Advanced Composite Structures, Port Melbourne, VIC, Australia; [3]Advanced Composite Structures Australia Pty Ltd, Port Melbourne, VIC, Australia

13.1 Introduction

With over 1.7 million kilometeres of gas, crude oil and petroleum product pipelines throughout the world (Mohitpour et al., 2003), the transportation of oil and gas through steel pipelines obviously plays a vital role in the supply of growing energy demands. Many of these pipelines have been in operation since the 1940s and 1950s (Chapetti et al., 2001). A wide range of temperature variations (−50−130 °C), high pressure and chemical erosion are the major factors that cause corrosion in transmission pipelines (Palmer-Jones and Paisley, 2000). Corrosion can cause both external and internal defects in pipelines, rapidly leading to leakage or rupture. Consequently, in the United States alone, between $2.0 and $3.3 billion is lost every year repairing and replacing corroded gas and petroleum pipelines (Koch et al., 2001). This ultimately results in an increase in the cost of energy.

The exceptional advantages of fibre composites have motivated the oil and gas industry to consider these materials for internal repair and rehabilitation. The use of fibre composite materials in the development of new piping systems, pressure vessels and other structural components is continually growing (Price, 2002). Compared with traditional repair systems like the cutting of damaged pipelines, welding, and so on, composite repair systems are more reliable and cost-effective. The high performance of glass, carbon or aramid fibres for reinforcing plastics is particularly suitable for pipeline systems carrying high corrosive fluids and can be used both onshore and offshore (Lursen, 2001). In addition, composites can be used to rehabilitate externally and internally corroded pipeline to prevent further corrosion, leading to an increase in the lifetime of pipeline. The high tensile strength, lightweight, durability and versatility of fibre composites make them the material of choice for many repair and rehabilitation projects in pipelines (Elsani, 2009). These properties, combined with directional dependency, allow the material to be inserted into the pipe and then reshaped and placed against the wall in the area where repair is required (Bruce et al., 2006). Moreover, pipe diameter is not excessively decreased and the flow capacity has been known to increase in some cases due to the smooth final coating that causes less friction than some pipe materials, such as concrete (Toutanji and Dempsey, 2001).

Rehabilitation of Pipelines Using Fiber-reinforced Polymer (FRP) Composites. http://dx.doi.org/10.1016/B978-0-85709-684-5.00013-8

The choice of pipeline rehabilitation methods is driven by factors like economics, urgency and engineering considerations (Palmer-Jones and Paisley, 2000). The majority of the remediation work using composites is focused on the external repair of pipelines to restore hoop strength due to the loss of localised wall thickness in steel (Alexander and Ochoa, 2010). The details of this repair system are presented in Chapters 11 and 12. For the internal repair of pipeline leaks, fibre composites are also becoming a suitable option as they can be designed to restore the original pipe strength. Using advanced composites for internal repair and rehabilitation of pipelines does not require soil excavation or the removal of existing pipe and has the advantages of easy mobility, improved tailorability and rapid installation.

However, most internal repair methods are used for low operating pressure pipelines and only to restore leak tightness (Toutanji and Dempsey, 2001). Also, these internal repair systems are considered to cause reductions in the inside diameter of pipelines that may hinder the ability to clean and inspect them using traditional tools. Thus, the use of composite materials for internal repair of pipes presents a number of difficulties that have yet to be fully explored.

A limited number of studies have been conducted on the internal repair of steel pipelines using composite material systems. As a consequence, only a few industries have used composite technologies for internal repair. In their report, Bruce et al. (2006) indicated that internal repair would have the best economics for underwater repair locations as it reduces out-of-service time and does not require divers and habitats. Such economics arise because the majority of the gas transmission line companies in the United States consider the ability of the pipeline to remain in service during internal repair to be very important. Moreover, they would consider internal repair, even if the pipeline needs to be out of service (no flow), only if the pipeline remains pressurised and the line can still be inspected by a pipe inspection gauge after repair. However, these companies have indicated that they would consider performing a repair from inside the pipe once a proven and accepted internal repair system becomes available. Thus, the selection of the most appropriate technique of renovation, particularly on the internal repair of high-pressure and deep water pipeline applications, is a critical and ongoing issue.

This chapter reviews technologies available for the internal repair of steel pipelines using fibre composite materials. It focuses on bonded and unbonded internal repair systems, both rigid and flexible. These have great potential for use in the internal repair of steel pipelines used in the oil and gas industry. The chapter includes an extensive review of the different composite repair technologies, repair materials and installation methods. Evaluation of these available composite technologies against performance requirements, such as maximum allowable operating pressure and service temperature, is also conducted to help identify existing technology gaps. Areas that require further investigation relating to the internal repair of steel pipelines with composites are included in the chapter.

13.2 Internal corrosion defect types

Damage to pipelines can be the result of degradation over time, accidental impact or extreme environmental conditions, all of which adversely affect the integrity of the pipeline. The types of consequences due to damage or deterioration are listed in Table 13.1.

Table 13.1 Basic damage categorisation of pipelines

Physical damage to pipe wall	Overstressing or fatigue damage	Exterior coating damage or deterioration	Damage or failure of components
1. Corrosion (internal and external) 2. Gouge, groove or notch 3. Puncture 4. Rupture 5. Cracking	1. Severe bending without buckling 2. Fatigue damage 3. Overpressure	1. Anticorrosion coating damage 2. Weight coating damage 3. Anode damage, loss or depletion	1. Valve damage, failure or leakage 2. Flange damage or leakage 3. Connector damage or leakage

Conveying fluids within piping systems, particularly for oil, gas and petrochemical applications, can present problems of corrosion or erosion, or a combination of these two. Corrosion is the deterioration or destruction of the pipeline material through electro-chemical reaction with its environment. For corrosion to occur some form of conductive solution, that is electrolyte, must be present. Generally, corrosion occurs due to the corrosivity of the transported fluid in association with the composition of the steel and application of measures unable to inhibit or guard against the corrosion. Sweet corrosion, sour corrosion and sulphate-reducing bacteria (Palmer-Jones and Paisley, 2000) are the three most common corrosion categories in steel pipelines. The rate of corrosion is affected by temperature, pressure, concentration of carbon dioxide and the flow rate of the oil and gas. Carbon dioxide and water are the major contributing factors to sweet corrosion. When carbon dioxide and water simultaneously exist in pipelines, the carbon dioxide dissolves in water to form carbonic acid which erodes the steel walls of pipelines. When uncovered steel keeps in contact with carbonic acid, sweet corrosion develops quickly. If the fluid contains water and hydrogen sulphide, sour corrosion occurs in the pipelines. This hydrogen sulphide causes metal loss corrosion, a mechanism similar to carbon dioxide corrosion.

The corrosion mechanism of microbial metabolism is less understood and needs further investigation. A number of bacterial types live in oil and gas production facilities. Sulphate-reducing bacteria is believed to be associated with corrosion. The acidic by-products of their metabolism are thought to be the primary cause of microbial-induced corrosion.

Axisymmetric, trench and spot defects are three basic forms of internal corrosion (Cosham and Hopkins, 2004; Meniconi et al., 2002). Figure 13.1 illustrates a free body diagram for a rigid bonded internal repair system for an internal axisymmetric corrosion defect. Thermal loading, caused by temperature variation, and mechanical loadings are two major loadings generally applied to pipelines. Further mechanical loading can be classified as some mixture of an internal pressure P, axial force F, torque T and bending moment M. In Figure 13.1, t_p is the thickness of a pipe and t_s is the pipe thickness of the corroded region. The traditional repair of a pipeline with this type of defect is to weld a steel sleeve. However, fibre-reinforced composite

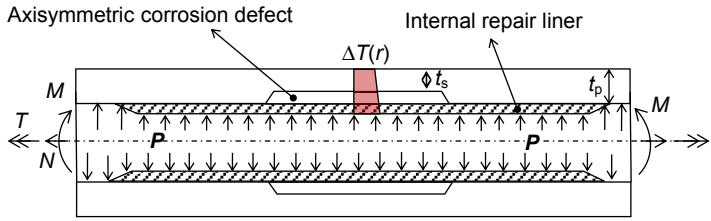

Figure 13.1 Internal bonded and unbonded composite repair for a pipeline subjected to internal pressure P, axial force N, torque T, bending moment M and thermal loading $\Delta T(r)$.

repairs are becoming widely used as an alternative to the installation of welded, full-encirclement sleeves for the repair of gas transmission pipelines (BS EN ISO-14692-4-2002). When the corrosion causes pipelines to develop trench and spot internal defects, the bonded internal composite repair technique can also be adopted.

13.3 Classifications of internal repair systems for steel pipelines

Generally three classes of internal composite repairs are considered, namely rigid bonded, rigid unbonded and flexible unbonded repair (ASME PCC-2, 2008), as illustrated in Figure 13.2. As shown in Figure 13.2(a), for the rigidly bonded composite repair, the internal pipeline surface is cleaned and the composite materials are cured onto the pipe internal wall. The cured interface layer is very thin so there is no relative deformation at the interface between the composite liner and steel pipe. That is, the adhesive bonding is 'rigid', and the composite liner and pipe act as one structural component. There is load transfer between the internal composite pipe and the external steel pipe, resulting in the internal pressure stress being transferred to the host pipe. Bending and other external loads are carried by both the internal composite pipe and the external steel pipe working in unison.

Rigid unbonded repair can be achieved by either inserting a cured composite pipe into a steel pipeline or alternatively curing a composite repair into a pipe while

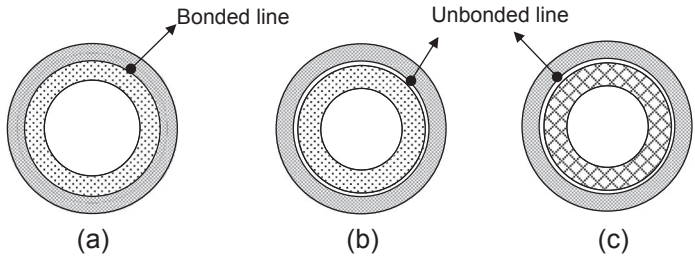

Figure 13.2 Unbonded and bonded pipeline repairs: (a) rigid bonded repair; (b) rigid unbonded repair; and (c) flexible unbonded repair.

preventing any form of bonding to the inside of the pipeline (Figure 13.2(b)). For this situation, the pipe is used as an external mould. There is no load transfer between the internal composite pipe and the external steel pipe. Therefore, the composite pipe must be capable of carrying the full internal pressure load. The rigid liner can carry bending and other external loads.

As illustrated in Figure 13.2(c), the third alternative is a flexible unbonded composite repair. In this case, the repair material is a reinforced unimpregnated membrane which remains flexible. For both unbonded liners (as illustrated in Figure 13.2(b) and (c)), there is no load transfer between the internal composite liner and the external steel pipe. The self-supporting internal liner carries the full working pressure. The flexible liner cannot carry a bending load and relies on the steel pipeline for this.

13.4 State-of-the-art composite technologies for internal repair

A number of innovations and new composite technologies are now available for pipeline repair in deep water projects in the oil and gas industry (Stringfellow et al., 2006). Generally, composite pipes for gas distribution systems are classified based on the maximum allowable operating pressure (Beech, 2009), as listed in Table 13.2.

The following three technologies are used for the internal repair of the liner of pipelines to prevent further corrosion (Palmer-Jones and Paisley, 2000). Heavens and Gumbel (2004) reviewed different installation technologies for pressure pipe lining and renovation. According to them, these renovation technologies are categorised as cured-in-place pipe and unbonded inserted hoses, including fold-and-form liners and slip liners:

- Cured-in-place: A bonded internal repair system using a thin and flexible reinforced textile liner with the outermost layer coated with polyethylene and the inside diameter saturated with liquid thermosetting resin. The liner is usually installed by using water pressure to propel the liner through the pipe and turn it 'inside out' so that the saturated resin side is pressed tightly against the host pipe section to be repaired (Rusch, 2004).

Table 13.2 Classification of gas line based on maximum allowable operating pressure (Beech, 2009)

Pressure (bar)	Type of line
Less than 2	General service lines
7–10	Low-pressure distribution lines
Less than 40	Local transmission lines (medium pressure)
60–85	High-pressure grid lines
Greater than 100	Source feed lines

- Fold-and-form liners: This is a flexible and unbonded composite repair system which is usually made up of thermoplastic pipe folded into a U or C shape, and after being rolled inside the pipe, expanded with pressure and heat. This type of repair system can be either bonded or unbonded, and the process is typically limited to liners less than 450 mm in diameter.
- Slip liners: This is a rigid and unbonded type of repair system which entails pushing or pulling a new pipeline into the old one. In some types, a pressure pipe of smaller diameter than the host pipe is inserted and expanded using heat and pressure to form a close-fit liner.

Some of the above repair systems were originally designed to repair low-pressure pipelines. But with further development, it is possible that these systems could be applied to the internal repair of high-pressure steel pipelines. These technologies are discussed subsequently, together with installation technologies, applications, advantages and disadvantages.

13.4.1 Cured-in-place pipe technologies

The cured-in-place pipe (CIPP) technology has been employed worldwide for more than 30 years and is one of many options available for rehabilitating and upgrading underground municipal and industrial pipe infrastructure. CIPP is a bonded repair system and a trenchless rehabilitation technique for lining the interior of a pipe with internal pitting corrosion, erosion and/or general degradation. CIPP has been used in the rehabilitation of pipelines in low-pressure applications, such as sewerage, drainage, water and gas mains and culverts. Presently, fully structural CIPP liners are available in the diameter range of 100−1000 mm.

Rehabilitation of pipes by CIPP, with thermoset polyester resins and polyester felt, usually requires satisfying predetermined specifications for both materials and installation. With CIPP, a tubular liner is saturated with a resin, which is then inserted into the damaged pipe and cured via heat and/or ambient or ultra violet light. The pipe defect is initially identified and located, usually by means of a closed circuit television survey or PIG. The resin saturated liner is then inserted into the pipe and inflated against the wall of the pipe by air or water pressure. The resin cures and hardens into a smooth structure and a new composite pipe is created within the old pipe. The materials used to manufacture the components are chosen to suit the function of the repaired pipeline. The combination of the liner, resin, the method of installation and the chosen curing method will determine the overall quality of the end product.

13.4.1.1 Liners

The flexible, tubular liner of a CIPP is typically made of polyester fabric that is a needled, woven or knitted reinforced fibre sheet using carbon, glass or aramid fibres or a combination of both. Depending on its application, the liner is coated with an impervious film such as polyethylene for the transport of drinking water or polyester for gas pipes. Other coatings include urethane and polyvinyl chloride (PVC). The final smooth surface reduces the surface friction and provides an additional corrosion barrier for the pipe. Liner tube sizes range from 100 to 2500 mm in diameter with

thicknesses of 3−58.5 mm, depending on the application. Continuous pipe lengths of up to 825 m have reportedly been installed with greater lengths feasible (Oxner and Allsup, 1999).

13.4.1.2 Resins

The typical resin types used in CIPP applications are given in Table 13.3. A flexible resin is preferred to ensure perfect adherence of the liner to the host pipe and, at the same time, to provide sufficient elasticity for settlement and pipe deflections.

13.4.1.3 Liner saturation

The liner is custom manufactured depending on application requirements, and the production technique depends on the CIPP installation method (such as inversion or pull-in-place). For installation by the inversion method, the liner is subjected to a vacuum to remove air from the tube. Resin, with dye, is pumped into the liner and displaces the evacuated air, saturating the inside of the liner. All excess resin is then removed by pulling the liner through a specially designed set of rollers (Muenchmeyer and Gemora, 2007). For CIPP installation by the pull-in-place method, the outside of the liner tube is saturated with resin. Depending on the resins used, the saturated liner can be stored for up to 6 months until installation into the host pipe.

13.4.1.4 Installation

Inversion is a more common technique for CIPP installations. Here, the resin-impregnated tube is clamped around an inversion ring and turned inside out or inverted down the length of the pipe using air or water pressure. This inversion process results in no relative movement between the tube and the deteriorated existing pipe wall, thereby minimising trauma and potential damage to the flexible tube material (Oxner and Allsup, 1999). Once cured in place, the end and connection points are trimmed to allow for flow. Figure 13.3 shows a CIPP installation by air or water inversion.

The pull-in-place (PIP) method is the second CIPP installation technique. Here the liner is pulled into the old pipe through an existing access or manhole structure and cured in place. In some applications, the PIP technique includes using a slip sheet

Table 13.3 Resin options for CIPP applications

Resin type	Application
Polyester	Typical sewerage pipes, inexpensive standard resin
Vinyl ester	Industrial or special waste/chemical applications, higher corrosion resistance, pressure applications
Epoxy	Industrial and potable water applications, pressure applications, higher temperature applications, suitable for saturation on site

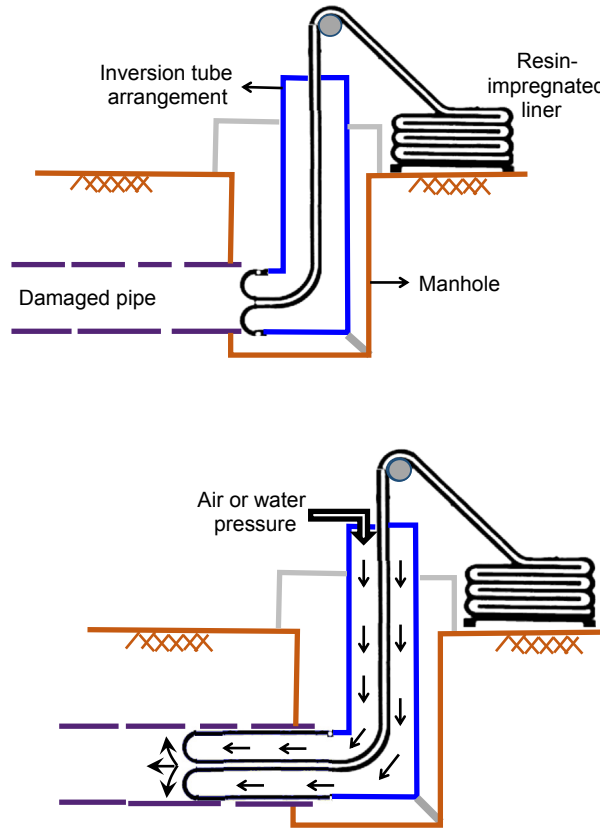

Figure 13.3 Resin-impregnated liner inserted into a pipe by an inversion process: (a) inversion apparatus; (b) inversion process.

to protect the resin-impregnated liner as the liner is winched into place (Reinforced Plastics, 2010). With the ends of the liner sealed, the liner is expanded by air and/or steam pressure for curing of the composite. Pressure is maintained until the liner cure is completed. The greatest advantage of the PIP method versus the inversion method is its ability to line at 45° and 90° angles and the option to line specific sections of pipe without lining the entire length (Nu Flow, 2010).

13.4.1.5 Advantages and disadvantages

Compared to other methods, the main reported advantage of CIPP is that being a trenchless technology, no excavation is required to rehabilitate the pipeline. The overall average cost of CIPP is USD 0.93 per mm diameter per m length of pipe repair compared to an open cut method of USD 2.60 per mm diameter per m length (Zhao et al., 2002). The technology also results in a minimal reduction of the cross section due to its thin liner. CIPP provides a smooth interior and no joints. CIPP technology can be accommodated in noncircular sections, bends, different crosssections, all pipe

materials and various loading conditions (Trenchless International, 2009). Long lengths over several thousand feet can be installed in a continuous jointless section (Muenchmeyer and Gemora, 2007).

The main disadvantage of CIPP is the requirement to take the host pipe out of service during installation and curing. Flow diversion or bypass pumping adds to the project cost and, as a result, may not be cost-effective for large-diameter pipes (Singh, 2001). Most of the resins used in CIPP contain styrene, which produces a pungent odour and may be a cause for concern to workers and the public (Bauer and McCartney, 2004). Most CIPP applications are for gravity or low-pressure pipelines, and there are no reports of its use for rehabilitating high-pressure pipelines such as those in the oil and gas industry. Salam and Christoph (2009) identified four major problems in CIPP technology which occur after the curing: bottom lift-ups, ribs, pinhole and fins and wrinkles. Bottom lift-up and rib problems occur due to water infiltration through the broken pipe joints. Pinholes normally develop from a pre-existing hole in the felt tube which was not covered by resin during curing. The hole may also have developed during storage and handling of felt tube and/or resin impregnation. Fins and wrinkles result from shape mismatch between the host pipe and the liner tube.

13.4.2 Unbonded composite repair technologies

Unbonded composite repair systems provide internal repair of steel pipeline solutions with broad applicability and efficiency. Because they are not bonded to the pipe wall and constructed of composite materials, these systems have the potential to provide a structure that can be quickly installed, variably configured and designed to adapt to a great range of system movements and environmental loads. This type of structure can withstand significant flexure while maintaining the required axial strength and pressure integrity for deep water applications (Kraincanic and Kebadze, 2001).

The unbonded composite repair system can be either rigid or flexible. A rigid composite pipe is installed and cured inside the corroded steel pipe, using the damaged pipe as a form or mould, but is not bonded to the pipe. In this system, the internal composite liner acts as the pipe, with no or minimal contribution from the original pipe. There is no load transfer between the internal composite pipe and the external steel pipe. Therefore, the composite pipe must be capable of carrying the full internal pressure load as well as bending and other external loads.

In the case of flexible systems, they are loose fitting and pulled into the damaged pipe, serving as a routing conduit. The self-supporting internal liner carries the full working pressure while the repair system relies on the steel pipeline to carry the bending load. Flexible liners are available for gas, water or oil applications in nominal sizes of 150−500 mm with a maximum working pressure of up to 40 bar. Installation lengths of 2000 m can typically be achieved, with laying speeds of up to 400 m per hour. There is no load transfer between the internal composite liner and the external steel pipe.

Unbonded repair systems for internal pipelines using composite technologies are discussed, by Heavens and Gumbel (2004), on the basis of installation processes, which are the fold-and-form and the slip liner processes.

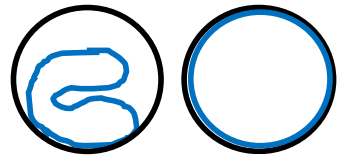

Figure 13.4 Installation of through fold-and-form process: (a) liner in C shape and (b) liner is expanded.

13.4.2.1 Fold-and-form liners

This type of internal repair system is normally a circular woven hose which is factory impregnated with polyethylene and is folded into a C shape for delivery to the site, as shown in Figure 13.4 (Heavens and Gumbel, 2004). The liner is pulled into the host pipe and re-rounded/expanded using air or steam. The product is classified as fully structural on the basis of long-term internal pressure tests. The liner does not adhere to the host pipe and has low ring stiffness. Carbon steel piping with inserted composite hoses offer a cost-effective alternative repair method by eliminating corrosion (Savino et al., 2009). Thermoplastic liners offer the combination of corrosion resistance and mechanical strength, which are unachievable with singular materials. Under pressure conditions, the liner is fully supported by the metalwork, while under vacuum conditions, the liner must be thick enough along with the venting system to withstand the collapsing forces created by the negative pressure.

13.4.2.2 Slip liner

The slip liner is a type of internal repair system which entails pushing or pulling a new pipeline into the existing pipe. In most cases, these composite liners are rigid and used in the repair of straight pipelines. Some of them are also categorised as close-fit systems when the liner which is inserted into a pressure pipe has a smaller diameter than the host pipe. The insertion is followed by expansion using heat and pressure to form a close fitting liner (Heavens and Gumbel, 2004). The expansion process increases the hoop tensile strength of the repair system. Currently available close-fit PVC products possess diameter and pressure ratings ranging from 50 to 1600 mm and 0.35−1.6 MPa, respectively. All available slip liner products operate in lower pressure regions.

13.5 Evaluation of composite technologies for internal repair

Around 24 internal repair technologies were reviewed and represented in symbolic form, from 1 to 24. Performance measures, such as maximum allowable working pressure (MAWP) and maximum service temperature, of the various internal repair technology products are identified and plotted in Figures 13.5 and 13.6, respectively.

Based on these performance requirements, an upper and lower bound working pressure was established for the three different pipe diameters which are plotted in

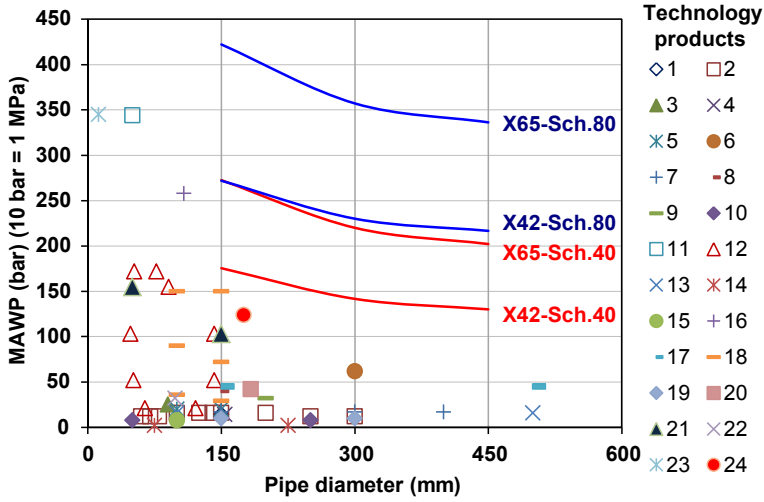

Figure 13.5 Comparison of MAWP with pipe diameter for different technologies.

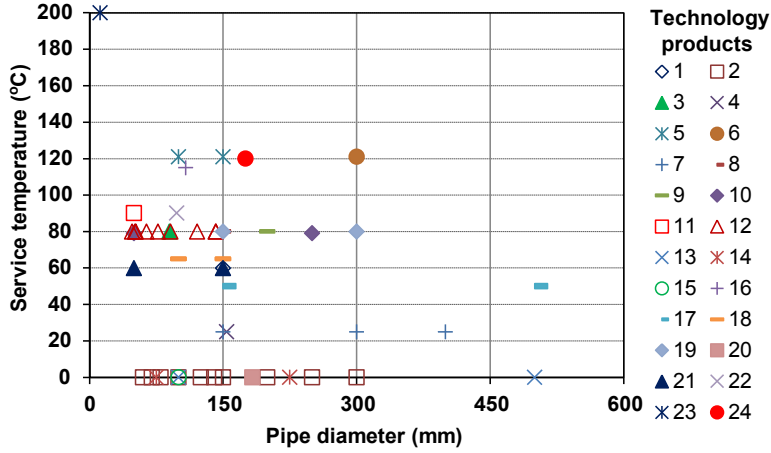

Figure 13.6 Comparison of service temperature with pipe diameter for different technologies.

Figure 13.5. The upper bound is based on a Schedule 80 X65 pipe while the lower bound is based on a Schedule 40 X42 pipe. It should be noted that upper and lower bound working pressure was calculated based on the yield strength of the steel and pipe geometry but does not take into account allowances for fatigue and corrosion, which will reduce the allowable working pressure of the pipe. These factors alone can reduce the working pressure by 30%.

As can be seen from the comparison shown in Figure 13.6, most of the technologies currently in use are limited to pipe diameters of 200 mm or less. With regards to the working pressure, only a small number of technologies are able to meet or get close to the capability of an X42 pipe, while none of the present technologies can achieve

the performance needed for an X65 pipe. Also note that only a few internal technology products are available for large-diameter pipes greater than 200 mm, and working pressures are limited to less than 5 MPa.

MAWP can be enhanced in all of the technologies by increasing the amount of reinforcing layers being used in the technology. There is potential to increase the capacity by adding additional layers. What needs to be determined is the reinforcing layer thickness for the respective technology, the identification (from the technology providers) of any limitations in how the current solutions are manufactured and the practicalities of increasing the reinforcing layer thickness. When reviewing the internal repair technologies, only small diameter (less than 150 mm) internal repair technological products can accommodate higher burst pressure. For the large diameter pipes, none of the internal repair technologies are capable of accommodating burst pressure greater than 20 MPa (see Figure 13.5). The majority of the current technologies are used in applications where the pipe diameter is no greater than 200 mm. Increasing the pipe diameter is, in principle, not anticipated to be difficult, although there may be limitations with the current manufacturing methods used in the technologies. Another aspect that needs to be considered for the flexible pipe technologies is their ability to be spooled or rolled easily, especially for large-diameter and high-pressure applications as this is an important consideration in the handling and installing process.

Examining the service temperature capabilities of the different technologies, it can be seen that the majority of technologies fall into the 80 °C temperature zone and a few technologies can accommodate up to a 120 °C limit. The service temperature for the various technologies is primarily limited by the polymer(s) used in the construction. Depending on the technology, there may be up to three different polymers being used, including a thermoplastic outer casing, thermoplastic inner lining and a thermoplastic or thermoset for the reinforcing layer. By selecting a suitable polymer, there is potential to increase the service temperature of each of the technologies.

In summary, these performance limitations of the currently available composite technologies can potentially be overcome by addressing the existing weaknesses. Increasing the thickness and identifying proper orientation of the reinforcing layers or changing the fibre type to a stiffer fibre will enhance the pressure carrying capacity of the technology. As a follow-up step, developing numerical and analytical models will help to identify the behaviour of internal repairs and identify some solutions to improve existing systems. Some novel analytical methods for internal composite repair designs are presented next.

13.6 Analytical methods for design of internal composite repairs

Analytical methods are important for internal composite repair systems to ensure that damaged pipelines are properly analysed to evaluate the system against performance measures. Existing methods specifically focus on external repairs of pipelines with internal repairs still unexamined, even though the concept could potentially be applied to internal repairs. Therefore, the concepts and approaches that could be adopted for analysing unbonded and bonded repairs are considered below.

13.6.1 Thin- and thick-walled cylinder analyses

Thin-walled and thick-walled cylinders are forms of pipeline primarily used in the offshore industry to transport gas and liquid under pressure. Cylindrical pipes are also used as a structural load bearing member to restrain the motion of a platform, for example, in response to wind, waves and currents (to within a specified limit). When a pipe is exposed to a combination of internal and external pressure, the pipe material will be subjected to pressure loading and, as a result, will develop stresses in all directions. The resulting normal stresses induced by the pressure loading are functions of the pipe diameter, wall thickness and cylindrical shell boundary conditions (open-ended cylinder or closed-ended cylinder) (Kashani and Young, 2008).

Two types of analytical models are available for dealing with cylindrical pressure pipes. The thin wall method is the most commonly adopted solution. It is based on a simple mechanics approach and is only applicable to vessels having a diameter-to-wall-thickness ratio of greater than 20 (Hearn, 1997). Using the thin wall method for an unconstrained, closed-end thin wall cylindrical pressure vessel, the circumferential hoop stress and longitudinal axial stress can be shown to take the form:

$$\sigma_\theta = \frac{1}{2}\left(\frac{D}{t}\right)P_\mathrm{i} \tag{13.1}$$

$$\sigma_\mathrm{a} = \frac{1}{4}\left(\frac{D}{t}\right)P_\mathrm{i} \tag{13.2}$$

where D is the cylindrical vessel's outside diameter, σ_θ is stress in the circumferential hoop direction and σ_a is the longitudinal axial stress. The variable P_i is a measure of the applied internal pressure. It is interesting to note that the magnitude of hoop stress, as shown in Eqn (13.1), is twice the magnitude of the longitudinal stress. It is for this reason that, during a typical pressure test, a failure mode in the form of longitudinal burst often occurs.

The second method is the Lame approach (Kashani and Young, 2008), which is based on displacement differential equations and is applicable to any cylindrical vessel with any diameter-to-wall-thickness ratio. The Lame method is often referred to as the solution for thick wall cylindrical pressure vessels. Equations for the hoop stress and radial stress in a thick-walled cylinder were developed by Lame in the early nineteenth century (Timoshenko and Goodier, 1969):

$$\sigma_\mathrm{h} = A + \frac{B}{r^2} \tag{13.3}$$

$$\sigma_\mathrm{r} = A - \frac{B}{r^2} \tag{13.4}$$

where A and B are constants which depend on boundary conditions.

These equations are associated with the assumption that any section of thick cylinder will remain plane before and after the application of pressure. This assumption

means that the strain along the axis or length remains constant. The above theory was developed for isotropic materials and some assumptions need to be considered when applying it to internal orthotropic composite repair systems. The inner composite layer needs to be biaxial lamina, having $E_1 = E_2$ where E_1 and E_2 are stiffness along the hoop and axial directions.

For the analysis, only the positive internal pressure (P_i) is considered and a positive pressure gradient is maintained from the inner to outer radius. Hence, stress in the radial direction is always in compression and is insignificant compared to the magnitude of hoop and axial stresses. As a result, hoop and axial stresses govern the design. Therefore, for approximate analysis, the assumption $E_1 = E_2 = E_3$ is made and Lame's approach for an isotropic material can be used, wherein E_3 is stiffness along the radial direction.

13.6.2 Modified version of Lame's equations (MVLE)

To overcome the limitations in the Lame theory when applying to orthotropic composite repair systems, a new modified version of Lame's equations (MVLE) was developed by the authors to undertake the analysis of infinitely long orthotropic cylinders subjected to internal and/or external pressure. The hoop and radial stresses at any point in the wall cross section of an orthotropic cylinder at radius r are given by the following equations:

$$A^* = \left[\frac{2 + \vartheta_{\theta r} + (\vartheta_{ar} - 2\vartheta_{a\theta})\vartheta_{\theta a}}{E_\theta}\right], B^* = \left[\frac{-1 - 2\vartheta_{r\theta} + (\vartheta_{ar} - 2\vartheta_{a\theta})\vartheta_{ra}}{E_r}\right]$$

$$C^* = \left[\frac{(1 - \vartheta_{a\theta}\vartheta_{\theta a})}{E_\theta}\right], D^* = \left[\frac{(-\vartheta_{r\theta} - \vartheta_{a\theta}\vartheta_{ra})}{E_r}\right] \tag{13.5}$$

where A^*, B^*, C^* and D^* are constants that depend on the orthotropic material properties. Modified Lame's coefficients α and β are expressed as the real roots of the following quadratic equation:

$$\left[C^* D^2 + D(A^* + B^*) + (A^* + B^* - C^* - D^*)\right] = 0 \tag{13.6}$$

Roots are α and β, if:

1. $\alpha \neq \beta$ then

$$\sigma_r = C_1 r^\alpha + C_2 r^\beta \tag{13.7}$$

$$\sigma_\theta = C_1(1 + \alpha) r^\alpha + C_2(1 + \beta) r^\beta \tag{13.8}$$

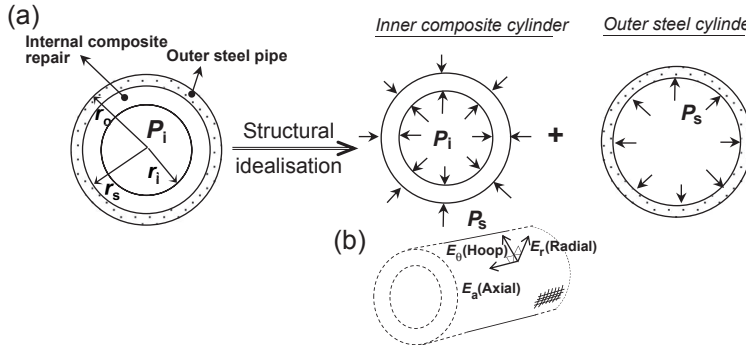

Figure 13.7 (a) Internal composite repair components and (b) structural idealisation and composite material axis system.

2. $\alpha = \beta$ then

$$\sigma_r = C_1 r^{\alpha} + C_2 \log_e r r^{\alpha} \tag{13.9}$$

$$\sigma_\theta = C_1(1+\alpha)r^{\alpha} + C_2 r^{\alpha}\left(1 + \log_e r + \log_e r\alpha\right) \tag{13.10}$$

The modified Lame's coefficients and the corresponding MVLE for common available orthotropic material cylinders were studied, and it was concluded that, for currently available orthotropic materials, the values of α and β are not equal to each other. For isotropic materials, α and β are equal to 0 and -2, and Eqns (13.7) and (13.8) convert to Isotropic Lame's form as Eqns (13.3) and (13.4). Internal composite repair systems can be split into two cylinders using contact pressure, as depicted in Figure 13.7. Then the system can be analysed by considering strain compatibility at the composite−steel interface and appropriate boundary conditions.

13.7 Studies on internal repair of steel pipe rehabilitations

There are currently limited studies conducted on the internal repair of steel pipelines using composite material systems. Similarly, there is a dearth of printed material on the usage and results from such repair applications. Consequently, there are only a few industries that have used composite technologies for internal repair.

Internal repair systems using carbon and glass fibre (GF) composites were reviewed and evaluated by Bruce et al. (2006). Carbon fibre (CF) liner repair was seen as the more promising process, having better strength and stiffness characteristics than GF liners. However, the developed and investigated CF liner systems were patch repair only (sectional liners) and bonded to the steel pipelines. The details of these tests are discussed in the following sections.

13.7.1 Glass fibre liner repair

In their test programme, Bruce et al. (2006) investigated the bonding behaviour of glass high-density polyethylene to steel. Defects (damages) with different geometries were created in a virgin pipe to simulate a 30% reduction in burst strength. The results revealed that the actual bursting pressure of long shallow damaged pipe was only 1% greater than the unrepaired pipe section and 38% lower than that of the virgin pipe, while short deep damaged pipe is 7% greater than the unrepaired section and 28% lower than the virgin pipe. This clearly indicates that GF liner repair is only marginally effective in restoring the pressure containing capabilities of pipeline. This is due to the fact that the difference in the modulus of elasticity between the steel and the liner material prevents the liner from carrying its share of load. The GF composite liners were consequently dropped from their testing programme but they concluded that these initial results opened the door for exploring higher modulus fibre-reinforced materials for internal liners of pipelines.

13.7.2 Carbon fibre liner repair

Carbon fibre has a modulus of elasticity almost similar to that of steel, thus has greater potential for internal repair of steel pipelines. Bruce et al. (2006) tested a section of 508-mm diameter and 6.35-mm-thick API 5L X52 pipe with a simulated corrosion defect. A defect was introduced to the pipe to represent a 25% reduction in burst strength. The CF fabric used for the internal repair had a modulus of 241 GPa.

The results of a solid/half-round/radial 11.42-mm-thick CF patch in short and deep damaged pipe revealed a 4% higher burst pressure than the unrepaired pipe and only 6% lower than the actual burst pressure for virgin pipe, while a thin radial 11.42-mm-thick CF patch short/deep damage showed a 2% improvement over the performance of the unrepaired pipe and 16% lower than the virgin pipe. The repaired pipe in a thin radial 7.11-mm-thick CF patch in short and deep damage had a 17% higher bursting strength than the unrepaired pipes but 18% lower than the virgin pipe. Thick, axial 7.62-mm-thick CF patch in long and shallow damage was much less effective at restoring the pressure containing capability of a pipeline as compared to other tests. The repaired pipe had essentially the same measured performance of the unrepaired pipe and 30% lower than the virgin pipe. This is due to the thickness of the simulated liner being limited to less than 12.7 mm to allow subsequent examinations of the repaired pipeline by internal inspection devices. The test results also indicated that the CF liner repair provided a marginally improved capability to restore the pressure capability of a pipeline as compared to the measured performance of a GF liner repair.

13.8 Summary

This chapter reviewed the available literature and technologies applicable to the internal repair of corroded steel pipelines using FRP composite materials. Rigid bonded,

rigid unbonded and flexible unbonded FRP repair technologies, installation methods, advantages and disadvantages have been discussed. The performance of commercially available internal repair technological products was evaluated in terms of MAWP and maximum service temperature and a number of issues were identified for these technologies to become suitable alternative repair systems for oil and gas pipelines. For example, increasing the thickness of the reinforcing layer or changing the fibre type to a stiffer fibre will enhance the pressure carrying capacity of some of the available composite technologies. Modifying or replacing polymers currently being used in the technologies will help to improve the service temperature. However, in order to make such changes, the practicalities of doing so will also need to be considered. This will include the ability to spool larger diameter products, the reduction in pipe cross section with increased wall thickness and the ability to manufacture with different reinforcements, polymers and geometries.

Some novel analytical methods that can be used to effectively design composite materials for internal repair were presented. Finally, available experimental studies conducted on internal FRP repair rehabilitation systems for steel pipe were discussed, demonstrating the high potential of composite materials for restoring the pressure capability of damaged pipelines.

Acknowledgements

This work was undertaken as part of a CRC−ACS research programme, established and supported under the Australian government's Cooperative Research Centres Program.

References

Alexander, C., Ochoa, O., 2010. Extending onshore pipeline repair to offshore steel risers with carbon-fibre reinforced composites. Composite Structures 92, 499−507.

ASME, 2008. Repair of Pressure Equipment and Piping, ASME PCC-2. The American Society of Mechanical Engineers, New York.

Bauer, G., McCartney, D., 2004. Odour control − more than sewage when installing cured-in-place sewer pipe liners. In: North American No-dig Conference, North American Society for Trenchless Technology (NASTT).

Beech, S.B., 2009. Plastic pipes − a lock into future. In: 7th European Forum Gas, Madrid, Spain.

Bruce, B., Boring, M., Porter, N., Ritter, G., Harwig, D., Harris, I., Dierksheide, J., Mohr, B., Lozev, M., Gordon, R., Neary, C., Sullivan, M., 2006. Internal Repair of Pipelines Final Technical Report. EWI Project No. 46211GTH. Edison Welding Institute, Columbus, Ohio, p. 202.

Chapetti, M.D., Otegaui, J.L., Manfredi, C., Martins, C.F., 2001. Full scale experimental analysis of stress states in sleeve repairs of gas pipelines. International Journal of Pressure Vessels and Piping 379, 78−87.

Cosham, A., Hopkins, P., May 2004. The assessment of corrosion pipelines − guidance in the pipelines defect assessment manual. In: Pipeline Pigging and Integrity Management Conference, Amsterdam, The Netherlands.

Elsani, M., 2009. FRP Super Laminates Present Unparalleled Solutions to Old Problems. Reinforced Plastics, pp. 40–45. Website: www.quakewrap.com/Brochure/FRP%20Super Laminates.pdf.

Hearn, E.J., 1997. Mechanics of Materials 2, Third Edition – The Mechanics of Elastic and Plastic Deformation of Solids and Structural Materials, ISBN-10: 0750632666.

Heavens, J.W., Gumbel, J.E., 2004. Gravity and Pressure Pipe Liner Design Issues. North American Society of Trenchless Technology (NASTT), New Orleans, Louisiana.

ISO, Petroleum and Natural Gas Industries-Glass-reinforced Plastics Piping, Part IV: Fabrication, Installation and Operation, BS EN ISO-14692-4-2002.

Kashani, M., Young, R., 2008. Hoop stress approximation in offshore design codes. Marine Structures 21, 224–239.

Koch, G.H., Brongers, M.P., Tompson, N.G., Virmani, Y.P., Payer, J.H., 2001. Corrosion Cost and Preventative Strategies in the United States. Federal Highway Administration, Office of Infrastructure Research and Development, pp. 260–311.

Kraincanic, I., Kebadze, E., 2001. Slip initiation and progression in helical armouring layers of unbonded flexible pipes and its effect on pipe bending behaviour. Journal of Strain Analysis 36 (3), 265–275.

Lursen, H., 2001. Reinforced thermoplastic pipes – state of development, situation on the world market and system introduction in Germany. 3R International Special Plastic Pipes 40, 46–49.

Meniconi, L.C.M., Freire, J.F.L., Vieira, R.D., Diniz, J.L.C., September 29–October 3, 2002. Stress analysis of pipelines with composite repairs. In: Proceedings of IPC2002, 4th International Pipeline Conference, Alberta, Canada. IPC02–27372.

Mohitpour, M., Golshan, H., Murray, A., 2003. Pipeline Design and Construction: A Practical Approach, second ed. ASME Press, New York, NY. pp. 499–518.

Muenchmeyer, G.P., Gemora, I., 2007. Mainline Pipe Rehabilitation Using Cured-in-place Pipe (CIPP) & Folded Pipe Technology (accessed 23.09.14.). muenchmeyerassoc.com/pdf/cipp01.pdf.

Nu Flow, 2010. Structural Lining (accessed 23.09.14.). http://www.nuflowtech.com/products/structurallining.aspx.

Oxner, K.B., Allsup, T., 1999. Advances in Cured-in-place Pipe Rehabilitation for Pressurized Piping Systems (accessed 16.09.14.). www.insituform.com/mm/files/Adnvances_incured.pdf.

Palmer-Jones, R., Paisley, D., September 2000. Repairing internal corrosion defects in pipelines—a case study. In: 4th International Pipeline Rehabilitation and Maintenance Conference, Prague.

Price, J.C., 2002. The state-of-the-art in composite development and applications for the oil and gas industry. In: Proceedings of the 12th International Offshore and Polar Engineering Conference, Kitakyushu, Japan, pp. 125–131.

Reinforced Plastics, 2010. Cured in Place Pipe Aids Restoration Project (accessed 23.09.14.). http://www.reinforcedplastics.com/view/4177/cured-in-place-pipe-aids-restoration-project/.

Rusch, D.W., 2004. Internal repair of pipeline leaks using pressure-activated sealants. In: Proceedings of the Society of Petroleum Engineer (SPE) Eastern Regional Meeting, West Virginia, 10 pp.

Salam, K.P., Christoph, D.P., 2009. Trouble shooting for trenchless liner installation during sewer line rehabilitation. Journal of Adhesion Science and Technology 23 (13–14), 1827–1844.

Savino, V., Mehdi, M., Al-Dossary, A., 2009. Thermoplastic Liners for Rehabilitation of Oil Flowline and Water Injection Lines, Integrity and Service Life p.8. Website: www.ndt.net/article/mendt2009/papers/Vincenzo-1.pdf.

Singh, A., 2001. Creative Systems in Structural and Construction Engineering. Taylor & Francis, 1040 pages.

Stringfellow, W.D., Catha, S.C., Bethel, K., Kanninen, M.F., Mortenson, T.C., Ekelund, A., Gallagher, J.L., Cahrbonneau, K.R., Mandich, I., 2006. An innovative self-monitoring pipe lining system allows restoration of degraded pipelines. In: 2005 Subsurface Solutions Conference and Expo, Amsterdam, p. 23.

Timoshenko, S.P., Goodier, J.N., 1969. Theory of Elasticity, third ed. McGraw-Hill, New York.

Toutanji, H., Dempsey, S., 2001. Stress modelling of pipelines strengthened with advanced composite materials. Thin-walled Structures 39, 153−165.

Trenchless International, 2009. CIPP − a Cure for Damaged Pipes (accessed 13.08.14.). http://trenchlessinternational.com/news/cipp_a_cure_for_damaged_pipes/004599/.

Zhao, J.Q., Rajani, B., 2002. Construction and rehabilitation costs for buried pipe with a focus on trenchless technology. In: Research Report No.101, Institute for Research in Construction, National Research Council, Canada.

This page intentionally left blank

Index

Note: Page numbers followed by "f" and "t" denote figures and tables, respectively.